Protein Phosphatase 2A in Alzheimer's Disease Pathogenesis, Memory and Development

Dissertation

zur
Erlangung der naturwissenschaftlichen Doktorwürde
(Dr. sc. nat.)

vorgelegt der
Mathematisch-naturwissenschaftlichen Fakultät
der
Universität Zürich

von

Andreas SCHILD

von Brienz BE

Promotionskomitee

Prof. Dr. Peter Sonderegger (Vorsitz)

PD Dr. Jürgen Götz (Leitung der Dissertation)

Prof. Dr. Roger M. Nitsch

Zürich, 2005

To

My girlfriend, Sibylle, who encouraged me,

My parents, Annelis and Jürg, who enabled me, and

My sister and brother, Katrin and Klaus, who put up with me.

1 TABLE OF CONTENTS

2 ACKNOWLEDGEMENTS

First of all, I am extremely grateful to PD. Dr. Jürgen Götz for being a very helpful doctoral thesis supervisor and mentor. I particularly appreciated his respect and patience towards young researchers, introducing me to diverse aspects of biological science while leaving me with much responsibility.

I am very thankful to Prof. Roger M. Nitsch, Director of the Division of Psychiatry Research and member of the thesis steering committee, for offering me and contributing to a research environment in the field of Alzheimer's disease that has been very motivating. Also I appreciated his effort for a new interdisciplinary brain symposium and support for running and social events, which have made my training at his department worthwhile in many ways.

Special thanks belong to Prof. Peter Sonderegger, head of the Department of Biochemistry, for accepting to be my external doctoral advisor and chair of my thesis steering committee.

I am particularly obliged to Eva Moritz for excellent technical assistance in regard to immunohistochemistry, and to Daniel Schuppli, who was a most helpful colleague in producing transgenic and knockout mice.

Special thanks belong to Prof. Hans-Peter Lipp and Dr. David Wolfer at the Institute of Anatomy, for letting me use their animal behavior facilities and software (Wintrack), and to Dr. Birgit Ledermann and her group at the Institute of Laboratory Animal Research for their ES-cell work and helpful advice in creating knockout mice.

Also I am indebted to Dr. Lars Ittner at the Research Laboratory for Calcium Metabolism, Orthopedic University Hospital Balgrist, Zurich, for his interest in my work and for being of immense scientific help in many ways.

Further collaborators in Zurich and abroad have assisted me with their techniques and knowledge and shall receive my thanks: Drs. Brian A. Hemmings and Karsten Schmidt at the Friedrich Miescher Institute, Basel, Dr. Charlotte Remé and coworkers at the Laboratory of Retinal Cell Biology, Eye Clinic, University Hospital Zurich, Drs. Mathias Seeliger, Naoyuki Tanimoto and Felix Tonagel at the Department of Pathophysiology of Vision and Neuroophthalmology, University of Tübingen, Germany, Drs. Stefan Isenmann and Alexandra Kretz at the Department of Neurology, University of Jena Medical School, Germany, and Dr. Egon Ogris at the Department of Medical Biochemistry, Medical University of Vienna, Austria.

I am thankful for antibodies by Drs. Brian A. Hemmings, Peter Davies, Peter Seubert, Chantal Mourton-Gilles, and André Delacourte, and for support by grants from the EMDO Foundation, the Olga Mayenfisch Foundation, the Kurt und Senta Herrmann Foundation, the NCCR on Neural Plasticity and Repair, and the Swiss National Science Foundation to J.G.

I would like to thank my colleagues at the Division of Psychiatry Research for the numerous scientific, but also political discussions, in particular Fred Hoerndli, Marlen Knobloch, Bernhard Kohli and Della David. Many coworkers at our department have been fun to work with and spend spare time with, and have therefore helped a lot to make my Ph.D. training a pleasant experience.

I owe my thanks to Jay Tracy and Zoë Goodger for helping me to spruce up my scientific English.

The Center for Neuroscience Zurich (ZNZ) has provided an extensive training program and financial support for graduate students and I am thankful to everyone who has contributed to a great instructive neuroscience program.

Last but not least, my special thanks belong to my family and girlfriend, Sibylle. They have been patient in many instances and have been very supportive and encouraging throughout my doctoral studies.

3 CURRICULUM VITAE

Family name:	**Schild**
First name:	**Andreas**
Date of birth:	February 25, 1974
Place of birth:	Zweisimmen, Switzerland
Nationality:	Swiss
Work address:	University of Zurich Division of Psychiatry Research August Forel Strasse 1 CH-8008 Zurich, Switzerland
Phone/Fax numbers:	+41-1-634-8886/ +41-1-634-8874
Permanent address:	Höhenweg 11 CH-8032 Zurich, Switzerland
Phone number:	+41-43-499-8247
Email:	schild@bli.unizh.ch

Education/ Studies

1995 Maturitaet Typus C (equivalent to A-levels)

1995-1997 Vordiplom in Biology/ Microbiology (a two-year undergraduate degree) at the University of Berne, Switzerland.

1997-2000 Preparation of the three year bioengineer's degree in Biotechnology (equivalent of MS in Biotechnology) at the Ecole Superieure de Biotechnologie de Strasbourg, ESBS (European School of the Higher Rhine Universities), Louis Pasteur University, Strasbourg, France.

2001-2005 Ph.D. student at the Division of Psychiatry Research, University of Zurich, Switzerland, with participation in the Ph.D. student program of the Center for Neuroscience (ZNZ) in Zurich.

Work experience

- Summer Internship 1998 (4 weeks at the High Technology Center, University of Bergen, Norway; Supervisor: Prof. L. Haaheim): Antigenic sin; Influenza virus antibodies and interleukins in sera of MMR vaccinated children.
- Summer Internship 1999 (4 weeks at the Institute of Plant Molecular Biology, Strasbourg, France; Supervisor: Dr. D. Gilmer): Cellular localization of proteins P25 and N, encoded by the RNA 3 of the Beet Necrotic Yellow Vein Virus, using proteins fused to GFP.
- Diploma thesis 2000 (8 months at the University of Michigan, USA; Supervisor: Prof. M.J. Imperiale): Development and production of recombinant Adeno-associated virus vectors for the gene therapy of motor neuron diseases.
- Ph.D. thesis 2001-2005 at the Division of Psychiatry Research, University of Zurich, Switzerland; Supervisor: Dr. J. Götz: Generation and analysis of protein phosphatase 2A transgenic and knockout mice to study neuronal functions and implications for Alzheimer’s disease.
- Teaching of Biology and Medicine students in Biochemistry practical training at the Department of Biochemistry, University of Zurich, Switzerland (2002-2004).

Training periods 1998-1999

- Microbiological genetics (4 weeks; Department of Applied Microbiology, University of Basel, Switzerland).
- Microbiological breeding techniques and growth physiology, characterization of continuous cultures (2 weeks; Swiss Federal Institute for Environmental Science and Technology EAWAG, Duebendorf, Switzerland).
- Molecular biology of plants (6 weeks; Department of Plant Physiology, University of Freiburg, Germany).
- Genetic engineering and molecular biology, bioinformatics and molecular modeling (5 weeks); mammalian cell cultures, immunology and protein purification (4 weeks); biochemistry, protein biosynthesis, enzymology and biophysics (4 weeks; European School of the Higher Rhine Universities ESBS, Strasbourg, France).
- Process technology (2 weeks; Institute of Mechanical Process Engineering and Mechanics, University of Karlsruhe, Germany)

Computer science

Good knowledge of standard software of PC and Macintosh computers (Windows, Office, Corel Draw, Adobe Photoshop and Illustrator, ImageJ, SPSS statistics); computer aided sequence and homology analysis (GCG, SRS, DNAstar, VectorNTI); basic knowledge of molecular modeling (RasMol, Quanta, Charmm, Modeller, MCSS); UNIX, C++ and assembler programming.

Languages

German:	native language
English:	fluent, written and spoken (International Proficiency score in TOEIC '99)
French:	fluent, written and spoken

Miscellaneous

1992	Exchange year with Youth for Understanding (YFU) in Geelong, Australia. Year 12 at Geelong High School with VCE-leaving certificate.
1993-1997	Part time job as night watch in the old people's home Lorraine in Berne.
1995	15 weeks of military service as a specialist of electronic warfare.
1996-	Clean driver's license
1997	Advanced diver certificate
1992-2003	Concerts with University- and Youth Orchestras in Switzerland, France, Germany, Australia, Japan, and the USA as a cellist.
2004	Olympic distance Triathlon in 2:21, Zurich Marathon in 2:58
2002-2005	Member of the Society for Neuroscience, Washington DC.

4 PUBLICATIONS AND PUBLIC PRESENTATIONS

4.1 Original, peer-reviewed papers

Schmidt, K., Kins, S., **Schild, A.**, Nitsch, R.M., Hemmings, B.A. and Gotz, J. (**2002**) Diversity, developmental regulation and distribution of murine PR55/B subunits of protein phosphatase 2A. *Eur J Neurosci, 16, 2039-2048.*

Hoerndli, F., Toigo, M., **Schild, A.**, Gotz, J. and Day, P. (**2004**) Reference genes identified in SH-SY5Y cells using custom-made gene arrays with validation by quantitative polymerase chain reaction. *Anal Biochem. Dec 1;335(1):30-41.*

Schild, A., Schmidt, K., Hemmings, B.A. and Gotz, J. (**2005**) Protein phosphatase 2A regulatory subunit B/PR55 levels in undifferentiated and neuronally differentiated cells. *submitted.*

Schild, A., Isenmann, S., Tanimoto, N., Tonagel, F., Seliger, M., Ittner, L.M., Kretz, A., Ogris E., and Gotz, J. (**2005**) Role for protein phosphatase 2A in the development of the Harderian gland revealed in transgenic mice. *submitted.*

4.2 Reviews and book chapters

Chen, F., Ferrari, A., **Schild, A.**, Kurosinski, P., David, D., Hoerndli, F., Pennanen, L., Kins, S., van Dorpe, J., Nitsch, RM., Gotz, J. (**2003**) Amyloid-induced neurofibrillary tangle formation. *In: Alzheimer's disease and related disorders: Research advances (editors: K. Iqbal, B. Winblad; Ana Aslan International Foundation), p. 343-354 (chapter 30).*

Gotz, J. and **Schild, A.** (**2003**) Transgenic and knockout models of PP2A. *Methods Enzymol, 366, 390-403.*

Gotz, J., Streffer, J.R., David, D., **Schild, A.**, Hoerndli, F., Pennanen, L., Kurosinski, P. and Chen, F. (**2004**) Transgenic animal models of Alzheimer's disease and related disorders: histopathology, behavior and therapy. *Mol Psychiatry, 9, 664-683.*

Gotz, J., **Schild, A.**, Hoerndli, F. and Penannen, L. (**2004**) Amyloid-induced neurofibrillary tangle formation in Alzheimer's disease: Insight from transgenig mouse and tissue culture models. *Int. J. of Devl Neuroscience, 22, 453-465.*

4.3 Poster presentations

A. Schild, S. Kins, A. Crameri, D.P. Wolfer, H.P. Lipp, R.M. Nitsch, J. Götz: Hyper-phosphorylation Of Tau And Learning Deficits In PP2A-Mutant Mice. ***Center for Neuroscience (ZNZ) Symposium, Zurich (2001).***

A. Schild, S. Kins, A. Crameri, P. Sonderegger, D.R.H. Evans, B.A. Hemmings, R.M. Nitsch, and J. Götz: Hyperphosphorylation Of Tau And Learning Deficits In PP2A-Mutant Mice. ***Society for Neuroscience Meeting, San Diego, USA (2001).***

A. Schild, P. Kurosinski, K. Schmidt, B. Hemmings, S. Kins, R.M. Nitsch, and J. Götz: Protein phosphatase 2A in the brain: Distribution of murine PR55/B subunits and activation of the ERK and JNK signaling pathways in PP2A deficient neurons. ***Center for Neuroscience (ZNZ) Symposium, Zurich (2003).***

A. Schild, R.M. Nitsch, and J. Götz: Hyperphosphorylation and altered compartmentalization of tau, and a progressive eye phenotype in mice expressing the L309A mutant catalytic subunit of PP2A. ***Society for Neuroscience Meeting, New Orleans, USA (2003).***

A. Schild, R.M. Nitsch, and J. Götz: Tau hyperphosphorylation and modified cell adhesion proteins in transgenic mice with altered protein phosphatase 2A composition. ***Center for Neuroscience (ZNZ) Symposium, Zurich (2004).***

A. Schild, S. Isenmann, E. Ogris, R.M. Nitsch, and J. Götz: Altered protein phosphatase 2A composition modifies cell adhesion and cytoskeletal proteins in transgenic mice. ***Society for Neuroscience Meeting, San Diego, USA (2004).***

4.4 Talks

"From Alzheimer's Disease To Protein Phosphatase 2A (PP2A)", ***Ph.D. Retreat Valens, Switzerland (2001).***

"Protein Phosphatase 2A Deficits Are Jointly Responsible For Alzheimer's Disease Pathology And Loss Of Cell Adhesion", ***Department of Cell Biology, Harvard Medical School, Boston, USA (2004).***

"PP2A Deficits Are Jointly Responsible For AD Pathology And Loss Of Cell Adhesion – A PP2A Mouse Model", ***1st Winter Brain Symposium, Sils, Switzerland (2005).***

5 SUMMARY

Background: Of all forms of dementia, Alzheimer's disease is the most prevalent and affects nearly half of the population above 85 years. It is histopathologically characterized by β-amyloid-containing plaques, protein tau-containing neurofibrillary tangles, reduced synaptic density and neuronal loss in selected brain areas. In a related disorder termed frontotemporal dementia (FTD), which is characterized by tangles in the absence of β-amyloid deposition, mutations in tau have been identified which also lead to neurodegeneration and dementia. In both, AD and FTD, tau is hyperphosphorylated, detaches from the microtubules and forms filaments. Tau is a substrate of protein phosphatase 2A (PP2A). PP2A is a family of heterotrimeric enzymes with diverse functions under physiologic and pathologic conditions. In brains of AD patients, mRNA levels of individual subunits of PP2A have been found to be reduced and to affect PP2A activity, which correlated with tangle load. Since specific inhibition of PP2A *in vivo* is not possible chemically, we have designed dominant negative transgenic mouse models with altered PP2A composition and/or activity, by overexpression of the mutant catalytic subunits L199P and L309A. Leucine 199 of the catalytic subunit Cα is in the catalytic core while the carboxyterminal leucine 309 plays a crucial role in the recruitment of regulatory subunits into the complex *in vitro*, a process that determines substrate specificity of PP2A.

Results: As PP2A is abundant in brain, we determined the distribution and expression levels of the four members of the regulatory subunit family PR55/B in murine brain and human cell lines. PR55α levels were highest in both HEK-293 and SH-SY5Y neuroblastoma cells, whereas PR55β levels were lowest. In contrast, differentiation of neuroblastoma cells caused the selective upregulation of PR55β, implying an important role of this regulatory subunit in neuronal differentiation. Chronic inhibition of PP2A activity by expressing Cα L199P was sufficient to induce tau hyperphosphorylation and relocalization to the somatodendritic compartment in neurons, as well as impairment in memory and learning. Cα L309A expressing mice revealed a reduced recruitment of the regulatory subunits PR55α and PR61ε, and an increased recruitment of PR61γ and PR59 into the complex, demonstrating a role for the carboxyterminal leucine of Cα in regulating holoenzyme assembly *in vivo*. This was associated with an increased phosphorylation of tau in brain and a reduced capability to dephosphorylate vimentin. In addition we observed a delayed and impaired postnatal development of the Harderian and lacrimal glands, causing a depression of the eyeball within the orbit (enophthalmos). In these glands PP2A dysfunction brought about a pronounced inactivating phosphorylation of the cadherin-directed glycogen synthase kinase-3β (GSK-3β) at Ser-9. Cadherin and β-catenin were reduced and shifted from the membrane to the cytosol, demonstrating a role for distinct PP2A regulatory subunits in cell adhesion.

Significance: Our novel transgenic mouse models, together with the consolidated findings from the present studies on the distribution of PR55/B subunits and their abundance in mice and human cell lines, provide valuable tools to study the role of PR55/B regulatory subunits in PP2A specificity and activity. Our results have thereby facilitated the development and analysis of *in vivo* models of PP2A function in the brain, have contributed to the understanding of PP2A composition and specificity as well as the development of the lacrimal system, and have further revealed an involvement of PP2A activity in memory retrieval of mice.

6 ZUSAMMENFASSUNG

Hintergrund: Die Alzheimer-Erkrankung ist die häufigste Form der Demenz und erfasst fast die Hälfte aller Menschen über 85 Jahren. Sie ist histopathologisch charakterisiert durch β-Amyloid enthaltende 'Plaques', Tau enthaltende neurofibrilläre 'Tangles', verminderte Synapsendichte sowie den Verlust von Neuronen in bestimmten Hirnregionen. Bei einer verwandten Krankheit, der Frontotemperalen Demenz (FTD), welche charakterisiert ist durch Tangles ohne β-Amyloid Ablagerungen, wurden Mutationen in Tau gefunden, welche ebenfalls zu Neurodegeneration und Demenz führen. In Alzheimer und FTD ist Tau überphosphoryliert und bindet dadurch weniger gut an Mikrotubuli, was die Bildung von Filamenten begünstigt. Tau ist ein Substrat der Protein Phosphatase 2A (PP2A). PP2A ist eine Familie von heterotrimeren Enzymen mit verschiedensten Funktionen unter physiologischen und pathologischen Bedingungen. In Gehirnen von Alzheimerpatienten sind verminderte mRNA Mengen bestimmter PP2A Untereinheiten und eine reduzierte PP2A Aktivität gefunden worden, welche mit der Anzahl Tangles korrelierte. Da eine spezifische Inhibierung von PP2A *in vivo* chemisch nicht möglich ist, haben wir dominant negative transgene Mäuse mit veränderter PP2A Zusammensetzung und/oder Aktivität entwickelt, welche die mutierten Cα Untereinheiten L199P und L309A überexprimieren. Leucin 199 der katalytischen Untereinheit Cα ist wichtig für die Aktivität von PP2A, während Leucin 309 *in vitro* eine entscheidende Rolle beim Rekrutieren von regulatorischen Untereinheiten in den Komplex spielt, ein Prozess, der die Substratspezifität von PP2A bestimmt.

Resultate: Da PP2A reichlich im Hirn vorhanden ist, haben wir die Verteilung und Expression der PR55/B Familie seiner regulatorischen Untereinheiten in Mäusehirnen und menschlichen Zelllinien bestimmt. PR55α war sowohl in HEK-293 als auch in SH-SY5Y Neuroblastom Zellen stark vertreten, während PR55β kaum vorhanden war. Wurden Neuroblastom Zellen hingegen differenziert, kam es zu einer selektiven Hochregulation von PR55β, was auf eine wichtige Rolle dieser Untereinheit in der neuronalen Differenzierung hindeutet. Chronische Inhibierung der PP2A Aktivität durch das Exprimieren von Cα L199P war ausreichend, um eine Überphosphorylierung von Tau und Umverteilung ins somatodendritische Kompartiment in Neuronen sowie Defizite im Lernen und Erinnern zu erreichen. Cα L309A exprimierende Mäuse zeigen eine verstärkte Rekrutierung der regulatorischen Untereinheiten PR61γ and PR59 auf Kosten von PR55α und PR61ε in den PP2A Komplex, was eine Rolle für das carboxy-terminale Leucin von Cα beim Zusammenfügen von Holoenzymen *in vivo* demonstriert. Dieselben Mäuse zeigen eine verstärkte Phosphorylierung von Tau im Gehirn und ein vermindertes Potenzial, Vimentin zu dephosphorylieren. Zudem haben wir eine verzögerte und beeinträchtigte postnatale Entwicklung der Harder'schen und der Tränendrüse beobachtet, welche ein Zurücksinken des Auges in der Orbita (Enophthalmus) zur Folge hatte. Die PP2A Fehlfunktion bewirkte ausserdem eine starke inaktivierende Phosphorylierung der Cadherin-gerichteten Glycogen Synthase Kinase-3β (GSK-3β) an Ser-9. Cadherin und β-Catenin waren dadurch verringert und von der Membran ins Cytosol umgelagert, was eine Rolle von spezifischen Untereinheiten von PP2A in der Zelladhäsion erkennen lässt.

Signifikanz: Unsere neuen transgenen Maus-Modelle, zusammen mit den Erkenntnissen aus den vorliegenden Studien über die Verteilung von PR55/B Einheiten und deren Vorkommen in Mäusen und humanen Zelllinien, sind wertvolle Hilfsmittel, um den Einfluss von PR55/B auf die Spezifität und Aktivität von PP2A zu erforschen. Unsere Resultate haben damit die Entwicklung und Analyse von *in vivo* Modellen der Funktion von PP2A im Gehirn vereinfacht, haben Beiträge zum Verständnis der PP2A Zusammensetzung und Aktivität sowie der Entwicklung des Tränendrüsensystems geleistet, und haben ausserdem eine Funktion von PP2A beim Erinnern in Mäusen aufgezeigt.

7 INTRODUCTION

7.1 Alzheimer's disease

Initially described in 1907 by Alois Alzheimer, this condition, which now bears his name, describes a fatal neurodegenerative disorder that starts with mild memory impairment and poor judgment but progresses to apraxia, aphasia, and agnosia (Alzheimer, 1907; Kimberly et al., 2001). The latter stages are often characterized by complete debilitation, requiring constant intensive supervision. Following initial diagnosis, the course of the disease varies from a few years to over 20 years, with an average of 4 to 8 years. Rare cases of AD, particularly those of early onset in the second and third decades of life, are familial and inherited as autosomal dominant disorders (Price and Sisodia, 1998; Rossor et al., 1996; Squire and Zola, 1998); however, the vast majority of patients are over the age of 60 such that, within industrialized countries, 10% of the population older than 65 years and as many as 47% of those older than 85 years are afflicted (Bierer et al., 1995; Lobo et al., 2000).

Clinically diagnosed Alzheimer's disease is a common condition and its public health impact will continue to increase with increasing longevity of the population. With up to 85% of moderate or severe cognitive impairments due to AD, it is the leading cause of dementia in the elderly, with stroke and atherosclerosis being the second most common cause and dementia associated with Parkinson's disease being the third (Evans et al., 1989). As suggested by data from 1995 (Ewbank, 1999) and more recent data from the World Health Organization (WHO), AD is the fourth leading cause of death in developed nations (after heart disease, cancer, and stroke). WHO estimates that by the year 2025 more than 22 million people worldwide will have Alzheimer disease, which will cause enormous costs as already in 2000, the annual social cost of AD for the United States was approaching $100 billion. Besides memory loss, Alzheimer's patients show dramatic personality changes, disorientation, declining physical coordination, and an inability to care for themselves. In the final stages, victims are bedridden, lose urinary and bowel control, and suffer epileptic attacks. Death is usually due to pneumonia, bedsores or urinary tract infection.

7.1.1 Genetics and risk factors for AD

Alzheimer disease is a genetically complex and heterogeneous disorder. Causal mutations leading to predominantly early onset of FAD have been characterized in three genes: APP on chromosome 21 (APP), presenilin 1 on chromosome 14 (PSEN1) and presenilin 2 on chromosome 1 (PSEN2). These mutations are inherited in an autosomal dominant manner with nearly 100% penetrance (Kimberly et al., 2001). However, mutations in these genes account for less than 5% of the total number of AD cases. The remaining 95% are mostly sporadic late-onset cases (SAD) with no recognizable pattern of classical Mendelian inheritance. Although there is a strong body of evidence for alpha-2 macroglobulin (α-2M, gene A2M) and the low-

density lipoprotein receptor related protein (LRP, gene LRP), none of the more than three dozen putative AD loci proposed to date have been consistently replicated (Bertram and Tanzi, 2004). The ε4 allele of the apolipoprotein E (ApoE) gene is the only genetic risk factor that has been established and verified in multiple genetic analyses of different human populations (Cherny et al., 2001; Rocchi et al., 2003). Studies implicating the ApoE gene as an AD susceptibility locus derived from several intersecting lines of investigation; Linkage analysis on late-onset AD families, ApoE immunoreactivity in senile plaques and neurofibrillary tangles (NFTs) of patient with AD, and ApoE binding to Aβ (Irizarry et al., 2004; Kang et al., 2000). Association studies revealed that inheritance of the ε4 allele (ApoE4, C112R) is associated with a copy-number-dependent increase in risk of both sporadic and late onset FAD and with a decrease in the age of onset in late-onset AD. Conversely, the ε2 allele confers a protective effect against late-onset AD. However, it seems that the inheritance of the ε4 allele may be neither necessary nor sufficient by itself to cause AD. In Down syndrome, where the triplication leads to overexpression of chromosome 21 resident genes, including the APP gene, neuropathological changes similar to AD can be found as early as at the age of 40 years. At 20-30 years, there is already formation of amyloid plaques and later neurofibrillary tangles (Andersson and Porath, 1986). Yet, as presented above, the most important risk factor for AD is age (Bierer et al., 1995).

7.1.2 Pathology

The distinctive brain lesions, senile plaques and neurofibrillary tangles, used by Alois Alzheimer together with the clinical deficits to describe the disease, are still used today as the defining features for diagnosis (Figure 1) (Haass et al., 1991; Itagaki et al., 1989). In addition to these striking changes, there is variable cerebral cortical atrophy and associated ventricular dilation, both of which are consequences of the neuron loss and astrocyte proliferation in affected regions. The progressive neuronal loss in AD is initiated in the medial temporal lobe (i.e. enthorinal cortex, hippocampus and subiculum). At later stages it extends to other neocortical regions, particularly association areas, the basal brain cholinergic system and several brain stem monoaminergic nuclei (Braak et al., 1999; Price and Sisodia, 1998). This sequentially destructive process is macroscopically characterized by shrinkage of the gyri, a widening of the sulci and an enlargement of the ventricles. The microscopical changes are manifested by neuronal loss and marked gliosis throughout the hippocampus and cerebral cortex, as well as synaptic alteration (Braak and Braak, 1995; Buee and Delacourte, 1999).
Both neurofibrillary tangles and senile plaques are found in normal aged persons, but it is their quantitative increase that defines the pathologic diagnosis of AD.

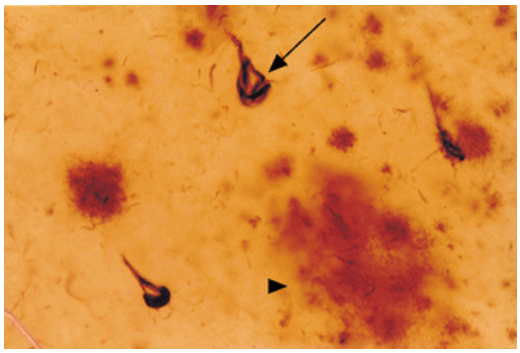

Figure 1:
Light micrograph of AD neuropathology. Section from the cortex of a patient with AD. The intraneuronal tangle (arrow) is stained dark brown with an antibody that specifically targets paired helical filaments. These filaments are also seen as the dense brown material (dystrophic processes) embedded in the extracellular plaque (arrowhead). The lighter reddish staining of the plaque is from another antibody directed specifically against β-amyloid. From Dr. J. Price (Encyclopedia of life sciences).

7.1.3 Neurofibrillary tangles

Neurofibrillary tangles (NFT) consist of abnormal 20-nm wide helical filaments with an 80-nm half-periodicity, termed paired helical filaments (PHF), and 12- to 15-nm straight filaments. Paired helical and straight filaments occur not only in neuronal perikaryon as neurofibrillary tangles, but also within dendrites and axons as neuropil threads, and within synaptic terminals of the large dystrophic neurites surrounding the β-amyloid deposits of senile plaques (Figure 1) (Braak et al., 1999). A series of studies have focused on the formation and composition of the PHF and how they might contribute to neuronal death. PHF is shown to be a highly organized structure. Both immunocytochemical and chemical analysis indicate that microtubule-associated protein tau in hyperphosphorylated form (Goedert et al., 1992; Grundke-Iqbal et al., 1986), ubiquitin (Mori et al., 1987), fatty acid and carbohydrate (Goux et al., 1995) are the components of PHF (Figure 2). Tau protein normally consists of a family of soluble, basic proteins that not only bind to microtubules but also stabilize them. The binding to microtubules is partly determined by the number of phosphates attached to it. Highly phosphorylated forms of tau proteins accumulate in AD and therefore it has been suggested that there is an imbalance between the activities of tau-directed kinases and phosphatases in AD (Trojanowski and Lee, 1995). Some phosphatases, enzymes that remove phosphate groups from tau, are suppressed in neurons of AD patients, resulting in accumulation of extra phosphates in the system (this is discussed in more detail in section 7.2 "Phosphorylation as a regulatory principle"). Abnormal phosphorylation or hyperphosphorylation of tau disturbs its binding ability to microtubules and tau subsequently precipitates in the somatodentritic compartment and could finally lead to the formation of PHF-tau (Gotz, 2001). This alteration of microtubule stability by tau modifications may disrupt intracellular transport, cellular geometry and neuronal viability, harming and killing the nerve cells (Price and Sisodia, 1998; Roush, 1995). Tau is also released into cerebrospinal fluid (CSF). Elevated tau in CSF of AD subjects can be measured by an enzyme-linked immunosorbent assay (ELISA) (Jensen et al., 1995) or by ELISA using phosphorylation-independent and sequence-specific antibodies (Mori et al., 1995). Comparable markers may provide an aid for AD diagnosis (Mehta et al., 1996). Following the complete degeneration of the affected neurons, the highly insoluble NFTs remain in the extracellular space (Vickers et al.,

1992). NFTs are also found in other neurodegenerative diseases such as corticobasal degeneration, argyrophilic grain disease, progressive nuclear palsy and frontotemporal dementia with Parkinsonism (Goedert et al., 1998).
There is now a considerable effort to understand how the two identified posttranslational modifications of NFT, phosphorylation and glycation, mediate the transformation of soluble tau into insoluble PHF.

7.1.4 Amyloid plaques and amyloid-β precursor protein

Understanding of the pathogenesis of amyloid-β (Aβ) deposition was greatly advanced by the sequencing of Aβ by G. Glenner and C. Wong in 1983 (Glenner and Wong, 1984). Subsequent cloning showed that Aβ is a 39- to 42-amino acid fragment of a larger 695- to 770-amino-acid, membrane-spanning glycoprotein, termed amyloid-β precursor protein (AβPP or APP) (Kang et al., 1987; Masters et al., 1985). The gene for APP resides as a single copy on the long arm of chromosome 21 and is comprised of 18 exons spanning a genomic region of about 400 kb (Lamb et al., 1993; Robakis et al., 1987).
The importance of APP in the primary etiology of AD is fairly well established, with FAD associated with a number of mutations in the APP gene on chromosome 21. Some of the mutations in APP leading to AD have been related to Aβ processing, yielding more of the longer form of Aβ ($A\beta_{42}$), which has a greater propensity to form Aβ fibrils (Figure 2). Additional support for the importance of APP in the pathogenesis of AD comes from Down's syndrome, in which an extra copy of chromosome 21 leads at mid-life (20 - 30 years) to a similar spectrum of pathologic changes as found in AD, amyloid plaques and neurofibrillary tangles (Andersson and Porath, 1986).

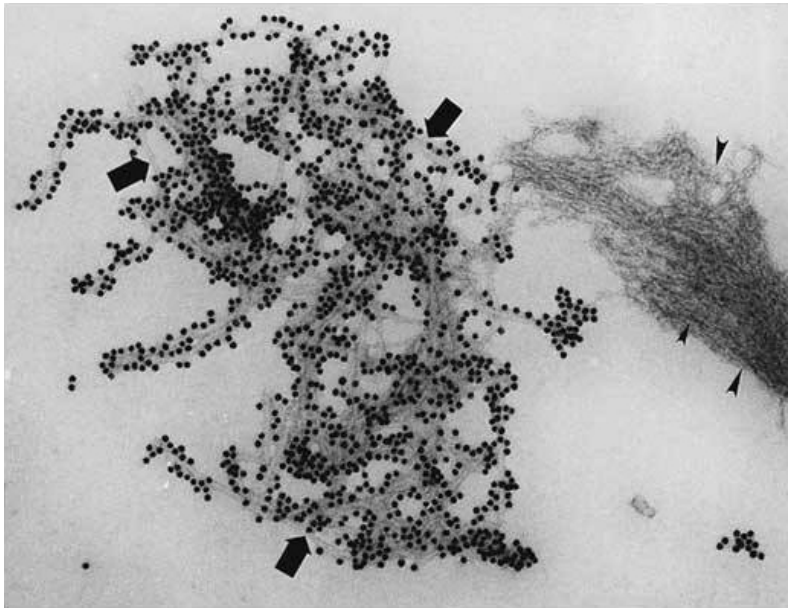

Figure 2:
Structural and antigenic differences between paired helical filaments (large arrows), and Aβ filaments (arrowheads) are readily apparent in this negatively stained preparation. Heavy subunits of neuro-filaments are localized by colloidal gold to paired helical filaments but not to Aβ filaments. (× 105,000), from Encyclopedia of Neuroscience, Elsevier.

APP is conserved across vertebrates and invertebrates and is part of a multi-gene super family from which sixteen amyloid precursor–like proteins (APLP) and APP species homologs have been isolated and characterized (Coulson et al., 2000).

APP is trafficked through the constitutive secretory pathway where it undergoes posttranslational processing including a variety of proteolytic cleavage events. The signal peptide is cleaved after co-translational translocation to the membrane of the endoplasmic reticulum (ER). Both during and after its transport through the secretory pathway to the cell surface, a subset of APP molecules undergoes specific endoproteolytic cleavage by α-, β- and γ-secretases (Figure 3). The degradation of APP can occur by two different pathways: Either the non-amyloidogenic α-secretase pathway or the amyloidogenic β-secretase pathway (Baker et al., 1997), whereas the preceding cleavage of APP by either α- or β-secretase is a prerequisite for γ-secretase cleavage (Figure 3).

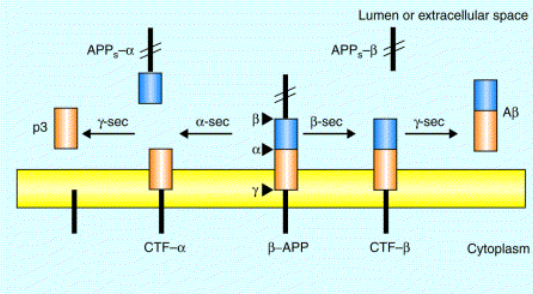

Figure 3:
Proteolytic processing of APP. APP can be cleaved by α-secretase (α-sec) in the Aβ domain (in blue and red) to generate soluble APP_S-α and a membrane-bound CTF-α. Alternatively, β-APP can be cleaved by β-secretase (β -sec) producing APP_S-β and CTF-β bearing the total Aβ domain. Both CTF-α and CTF-β are substrates for an intra-membranous cut by γ-secretase (γ-sec), resulting in the generation of p3 (red) and of Aβ (blue-red), respectively (Ruediger et al., 2001).

Under normal conditions, the α-secretase pathway is predominant, precluding the formation of Aβ (Esch et al., 1990; Kimberly et al., 2001). A smaller proportion of APP is processed by the amyloidogenic pathway, which takes place intracellularly in the secretory pathway or following internalization of cell surface bound APP into the endosomal-lysosomal compartment. β-secretase releases a truncated form of soluble APP (APPS-β) from the cell surface (Schubert et al., 1989), leaving a 99 amino acid CTF-β in the membrane, which is subsequently cleaved by the γ-secretase at either residue 711 or 713 to create either $Aβ_{40}$ or $Aβ_{42}$ (Baker et al., 1997; Di Rosa et al., 2002).

The so-called Swedish mutation in APP (APPswe, K595N and M596L) or the London mutation (V717I) located close to the β- and γ-secretase sites, respectively, cause enhanced production of Aβ (Cai et al., 2001; Citron et al., 1994; Goate et al., 1991; Mullan et al., 1992; Suzuki et al., 1994), specifically the highly pathogenic $Aβ_{42}$ (Di Rosa et al., 2002; Steiner et al., 1999).

The Aβ of senile plaques consists of 7- to 10-nm helical filaments (Figure 2) that share with paired helical filaments the ability to bind the dye Congo red. *In vitro*, the soluble peptides (dimers) precipitate and adopt a β-sheet structure (Hilbich et al., 1991). This formation of insoluble aggregates has been considered to be a key element in the neurotoxic mode of action of Aβ (Pike et al., 1993; Pike et al., 1991). Although the $Aβ_{42}$ isoform contributes to only 10% of the total Aβ secreted by cells in culture as well as in human brain, it is the most toxic species as it aggregates promptly and acts as a seed for subsequent aggregation of $Aβ_{40}$ species (Asami-

Odaka et al., 1995; Jarrett and Lansbury, 1993). Moreover, intracellular $A\beta_{42}$ induces neuronal death (Kienlen-Campard et al., 2002).

Two different types of amyloid plaques are found in the brain parenchyma of AD patients: Neuritic or mature plaques and diffuse deposits. Neuritic plaques have a dense fibrillar amyloid core consisting mainly of $A\beta_{42}$, but also containing of $A\beta_{40}$ (Kimberly et al., 2001). They are surrounded by dystrophic neurites, activated astrocytes and microglia (Cummings et al., 1998; De Strooper and Annaert, 2000). In contrary, diffuse plaques are amorphous and solely consist of $A\beta_{42}$. They do not contain degenerated axons or dendrites and lack activated microglia and astrocytes (Kimberly et al., 2001).

Various sources for the Aß found in senile plaques have been considered: neuronal, glial or vascular. $A\beta_{40}$ and $A\beta_{42}$ are constitutively secreted by a multitude of different cell types and can be detected in conditioned cell culture medium and human cerebrospinal fluid (Haass et al., 1992; Seubert et al., 1992). Presently, a neuronal origin for Aβ is supported by the high level of APP mRNA and protein in neurons. The accumulation of APP in neurites surrounding Aβ in senile plaques suggests that neurites may be the source of Aβ for senile plaques. In normal neurons, most APP is associated with vesicles, outer mitochondrial membranes, and a subclass of microtubules, whereas in AD it additionally accumulates in secondary lysosomes, termed dense bodies, and PHF. Nonneuronal cells such as microglia and astrocytes are probably not important in APP synthesis; however, those cells, found in the vast majority of senile plaques, may play a role in proteolytic processing of APP to Aβ. The nature of the neuronal abnormality responsible for an increased level of APP in AD is unknown, although a number of physiologic perturbations, such as apoxia, oxidative stress, and cell injury, do increase the level of APP. Aβ deposition is not only observed in brains of AD patients, but diffuse plaques can also be found in brains of healthy aged individuals, suggesting that the formation of plaques might be inevitable to some degree (Davies et al., 1988).

7.1.5 Relationship between plaques and tangles

As outlined above, Aβ plaques and NFTs are the defining neuropathological hallmarks of AD, but their pathophysiological relation is still not fully elucidated. The finding that neurons are primarily responsible for APP production and also contain NFT highlights a key issue in AD, the relationship of Aβ plaques to NFT. Recent studies demonstrated a direct high-affinity interaction between tau and APP.

Several mechanisms for Aβ-induced neurotoxicity have been proposed, including oxidative stress, free radical formation, disrupted calcium homeostasis, induction of apoptosis, neuritic damage, chronic inflammation and formation of amyloid pores (Di Rosa et al., 2002; Lashuel et al., 2002; Pratico, 2002). Based on genetic findings in FAD and observations in Down's syndrome, the "amyloid cascade hypothesis" has been postulated which claims that a dysregulation in APP processing, resulting in increased production of Aβ or failure to clear the peptide leads to AD primarily through amyloid deposition. The aggregated Aβ in turn is then supposed to induce all subsequent pathology, including tau hyperphosphorylation, tangle

formation, neuronal cell death and memory impairment (Haass et al., 1991; Hardy and Higgins, 1992). This is supported by the fact that human carriers of pathogenic mutations in the APP gene ultimately develop both Aβ plaques and NFT.

Nevertheless, the amyloid cascade hypothesis was challenged because several findings suggested that Aβ was not the sole cause for AD, for example that tau-containing neurofibrillary tangles were involved in several other neurodegenerative diseases in absence of Aβ deposits. Also mutations in the APP gene as well as in the closely related presenilin 1 and 2 genes account for less than 5% (familial) of the total number of AD cases, which are mostly sporadic late-onset cases (SAD) (see section 7.1.1). Furthermore, the frequency of NFT correlates to dementia better than does that of senile plaques (Arriagada et al. 1992), with the degree of dementia not correlating with the number of Aβ plaques (Terry, 1996), and neurofibrillary tangle formation seems to predate plaque formation (Braak et al., 1996). In addition, transgenic mice over-expressing APP develop little if any neurodegeneration, even with extensive amyloid deposition (Hsiao et al., 1996). Therefore, it is not surprising that disorders leading to hyperphosphorylated tau accumulation are associated with dementia.

Nevertheless, a large body of genetic and cell biological evidence from recent studies strongly argues for pathogenic and inductional activities of Aβ in the formation of neurofibrillary tangles (Ferrari et al., 2003; Gotz et al., 2001; Lewis et al., 2001; Oddo et al., 2003). It has been shown in triple transgenic mice (APPswe, presenilin1 (PS1M146V), and tauP301L), that anti Aβ antibodies administered to the hippocampus reduce not only extracellular and intracellular Aβ accumulations but also lead to a clearance of an early tau pathology (Oddo et al., 2004). Further, the amyloid cascade hypothesis has gained strength through the observation that AD-causing mutations identified in APP and the presenilin genes alter APP metabolism causing increased production of $A\beta_{42}$. Furthermore, stereotactic injection of $A\beta_{42}$ fibrils into the brain of a tau transgenic mouse line caused fivefold increase in the number of NFTs in cell bodies within the amygdala (Gotz et al., 2001). In related experiments, it was shown that tau filament formation in cells expressing mutant tau can be induced by a treatment with pre-aggregated Aβ (Ferrari et al., 2003).

The pathogenic relationship of the two major lesions of AD and their relative contribution to the clinical features of the disease are a long-standing matter of debate. This has major implications for the development of treatment strategies. An Aβ-directed treatment would only reduce NFT formation if NFT formation were downstream of Aβ, while it would have no effect on NFT numbers if the formation of the two lesions were caused by an upstream pathogenic signal.

NFT develop in specific predilection sites and spread in a predictable, non-random manner across the brain. This sequence of the tau pathology provides a basis for distinguishing six stages of disease progression (Braak and Braak, 1991; Braak and Braak, 1995): the transentorhinal stages I-II representing clinically silent cases; the limbic stages III-IV of incipient AD; and the neocortical stages V-VI of fully developed AD.

A comparative study of the Aβ-associated pathology defined five phases. These differ markedly from the stages which define the spreading of NFT: The neocortical phase 1 is followed by the allocortical phase 2. In phase 3, the diencephalic nuclei, the striatum and the cholinergic nuclei of the basal forebrain develop Aβ deposits, and in phase 4, several brainstem nuclei become

additionally involved. Finally, phase 5 is characterized by cerebellar Aβ-deposition. These findings suggest that Aβ-deposition expands anterogradely into regions that receive neuronal projections from regions already exhibiting Aβ (Everett et al., 2002).

Numerous correlation studies failed to demonstrate a clear relationship between the severity of dementia and Aβ deposition in human AD brain whereas a correlation between NFT numbers and severity of dementia has been reported (Arriagada et al., 1992; Bierer et al., 1995; Crystal et al., 1988; Morrison and Hof, 1997; Nagy et al., 1996). It was shown that total NFT counts in specific brain areas such as the entorhinal and frontal cortex, as well as neuron numbers in the CA1 region of the hippocampus were the best predictors of cognitive deficits in brain aging and AD (Bussiere et al., 2003; Giannakopoulos et al., 2003). Delacourte and coworkers however proposed a synergistic interaction between the APP- and tau-related pathology, despite a different spatiotemporal distribution of plaques and NFT (Buee and Delacourte, 1999; Delacourte et al., 2002). They also found that whenever Aβ aggregates were detected, tau pathology was found, at least in the entorhinal cortex. The opposite was not true as cases were found with an advanced tau pathology and no traces of Aβ aggregates (Delacourte et al., 2002).

7.1.5.1 Neuronal damage

In AD, only around 85% of the neuronal loss can be explained by NFT formation (Bussiere et al., 2003; Gomez-Isla et al., 1997). This implies that non-NFT-related mechanisms of neurodegeneration may also compromise vulnerable subsets of neurons. A quantitative analysis of NFT in human brain revealed that a substantial number of pyramidal cells may persist either unaffected or in a transitional stage of NFT formation. Whereas it is not possible to assess whether such transitional neurons are fully functional, these affected neurons might respond positively to therapeutic strategies aimed at protecting the cells that are prone to neurofibrillary degeneration in AD (Bussiere et al., 2003).

As plaques and NFT are not only the histopathological hallmarks of FAD, but also sporadic AD (SAD), it will be important to know what triggers their formation and how they are functionally related. Some insight may be gained by an analysis of adult lifestyle risk factors combined with the evidence of a genetic predisposition (as determined by the inheritance of risk alleles of susceptibility genes), which together may cause SAD (Holness et al., 2000).

Although the etiology of FAD and SAD differ, the clinical picture and the morphological end stage in the brain appear to be the same. Such a constellation, which combines heterogeneity in origin with homogeneity in clinical appearance and morphology of disease is, although rare, not unknown. A good example for this pattern is diabetes mellitus: In type I diabetes, insulin production is deficient, whereas in type II the function of the insulin receptor is impaired. Analogous to diabetes, one may subdivide AD into type I AD (the inherited forms of FAD) and type II AD (the sporadic forms of AD, SAD) (Hoyer, 2002).

Beyond this mere analogy, glucose levels themselves have been claimed to play a role in the pathogenesis of SAD. There is evidence that SAD may be caused by a reduced neuronal activity due to reductions in both insulin and ATP, which would lead to the formation of both Aβ plaques and NFT (Salehi et al., 1995; Salehi et al., 1994; Salehi et al., 1996; Swaab et al., 1998).

Insulin and ATP have both been shown to regulate the phosphorylation status of tau by influencing the activities of kinases. A reduction in ATP activates the external signal-regulated kinase ERK whereas reduced insulin levels lead to an increased activity of glycogen synthase kinase-3 (GSK-3), both of which are candidate kinases for the process of tau aggregation and NFT formation (Baumann et al., 1993; Chen et al., 2004; Hong et al., 1997; Roder and Ingram, 1991). Obviously, the glucose hypothesis does not place Aβ upstream of tau, as both tau and APP/Aβ would be substrates of metabolic dysfunction.

Neuronal damage in SAD could further be caused by oxidative stress and lipid peroxidation, which is thought to be a prominent and especially deleterious form of oxidative damage in the brain due to this organ's relative enrichment in polyunsaturated fatty acids. Interestingly ApoE, which is involved in the transport of lipids and in particular cholesterol, represents the strongest genetic risk factor for SAD (see section 7.1.1) (Rocchi et al., 2003). A wide range of studies suggest that brain cholesterol metabolism is central to the AD pathophysiology by affecting APP processing and Aβ formation (Bassett and Montine, 2003; Poirier, 2003). Yet in the tau transgenic mice, the role of cholesterol has not been addressed so far.

A further hypothesis proposes mitotic failure as a cause of the neuronal degeneration in AD (Arendt, 2003; Arendt et al., 2000; Bowser and Smith, 2002). Non-neuronal cells use morphoregulatory cues and internal signaling pathways to control proliferation and differentiation in the process of tissue repair and regeneration, after development is completed. In neuronal cells, synaptic plasticity is controlled by the same cues and signaling pathways, which have been developed primarily to control proliferation. As postmitotic neurons are capable of using these molecular mechanisms, according to the mitotic failure theory, this puts a neuron at risk to erroneously convert signals which are derived from plastic synaptic changes into positional cues that will activate the cell cycle. This cell cycle activation potentially links synaptic plasticity to cell death, as signaling cascades are activated which could lead to the accumulation of tau and β-amyloid. This would mean that preventing cell cycle activation of neurons might be crucial to prevent neurodegeneration (Arendt, 2003). To be able to test this and the other hypotheses mentioned above, the development of sophisticated transgenic animal models together with a thorough histopathological analysis of early stages of human AD would be required.

7.1.6 Interaction of β-amyloid and tau in animal models

Before NFT formation had been achieved in tau transgenic mice, the relationship of plaques and NFT in AD was addressed in different non-transgenic species such as rats and monkeys (Geula, 1998). Intracerebral injection of plaque-equivalent concentrations of fibrillar, but not soluble, Aβ resulted in profound neuronal loss, tau phosphorylation and microglial proliferation in the aged rhesus monkey cerebral cortex. In contrast, the same preparations were not toxic in the young adult rhesus brain, indicating a role for age in Aβ toxicity. This toxicity was also highly species-specific as it was neither observed in young nor in aged rats (Geula, 1998). These results

suggested that Aβ neurotoxicity *in vivo* is a pathological response of the aging brain, which is most pronounced in higher order primates.

In transgenic mice, the presence of the P301L mutation appeared to accelerate tau filament formation at a younger age, while transgenic mice with high expression levels of human tau developed NFT only at high age (DeTure et al., 2000; Gotz, 2001; Ishihara et al., 2001). P301L mutant mice are therefore suitable models to determine whether β-amyloid affects the tau pathology in these mice. Synthetic preparations of fibrillar $A\beta_{42}$ were stereotaxically injected into the somatosensory cortex and the hippocampus (CA1 region) of P301L and wild-type human tau transgenic mice and non-transgenic littermate controls, causing a fivefold increase of NFT in the amygdala of P301L transgenic, but not wild-type tau transgenic or control mice, eighteen days following the injections (Gotz, 2001). In contrast, when the reversed peptide $A\beta_{42\text{-}1}$ was injected, levels of NFT were not affected (Figure 4) (Gotz et al., 2004). NFT formation in the $A\beta_{42}$-injected P301L mice was tightly correlated with the pathological phosphorylation of tau at S422 and the epitope AT100 (T212/S214), but not AT8 (S202/T205). The finding that $A\beta_{42}$ was not capable of inducing NFT formation in non-NFT-forming wild-type tau transgenic mice may reflect species differences between mice and men. Alternatively, it may imply that, at least in mice, $A\beta_{42}$ can not induce NFT formation de novo, which would be in disagreement with the amyloid cascade hypothesis. Interestingly, in cultured murine hippocampal neurons, toxicity of $A\beta_{42}$ has been shown to be dependent on the presence of tau (Di Rosa et al., 2002).

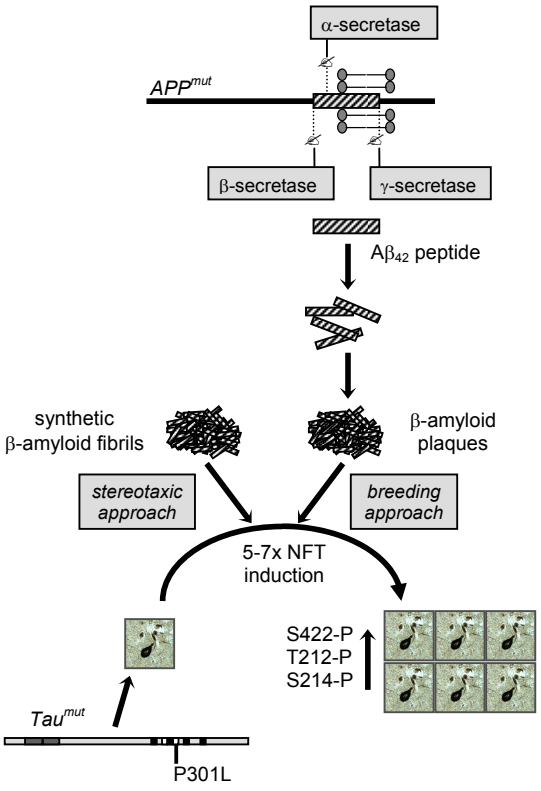

Figure 4:
APP can be proteolytically cleaved by the membrane-associated α-secretase, which cleaves APP within the Aβ domain. This pathway is non-amyloidogenic, as this cleavage precludes the formation of Aβ. Alternatively, cleavage may occur in the endosomal-lysosomal pathway, first by the β-secretase and then by the γ-secretase generating the Aβ peptide. Aβ is deposited around meningeal and cerebral vessels, and in the gray matter as β-amyloid plaques. To determine the relationship between Aβ and the NFT/tau pathology in AD, two alternative approaches were pursued. One involved the intercrossing of APP and Tau mutant mice with a plaque and NFT pathology (breeding approach), the other the stereotaxic injection of fibrillar preparations of $A\beta_{42}$ into mutant tau transgenic brains (stereotaxic approach). Both resulted in increased NFT formation, which was associated with phosphorylation of tau at the phospho-epitopes Thr212/Ser214 and Ser422.

J. Götz, A. Schild, F. Hoerndli, and L. Pennanen (2003), Int. J. of Devl Neuroscience, 22, 453-465.

An alternative approach was chosen by Lewis and coworkers who crossed Aβ-producing APP-mutant Tg2576 mice with their PrP promoter-driven P301L tau mutant mice (Lewis et al., 2001). Double transgenic mice showed a more than sevenfold increase in NFT numbers in the olfactory bulb, the entorhinal cortex and the amygdala compared to P301L single transgenic mice, whereas plaque formation was unaffected by the presence of the tau lesions (Figure 4).
When both approaches are taken together, they imply that not all brain areas are similarly susceptible to Aβ-mediated NFT induction. In both studies, the amygdala is a hot spot of NFT induction. Unless tau levels are particularly high in the amygdala compared to other brain areas such as the hippocampus or cortical areas, a different transcriptional profile may account for the observed differences. A following study of amygdala-specific gene expression provided a list of genes, some of which may confer an increased tau-related vulnerability of amygdaloid neurons to $A\beta_{42}$ (Zirlinger et al., 2001). Alternatively, it may be the nerve terminals which are susceptible to $A\beta_{42}$, whereas direct exposure of the cell body or neurites may not pose a risk to the tau-expressing neuron. Whether Aβ is taken up by a receptor-mediated mechanisms or whether it forms pores is still a matter of debate (Lashuel et al., 2002; Verdier and Penke, 2004) (Figure 4). A recent study with double transgenic mice expressing the amyloid precursor protein, bearing the Swedish mutations, and expressing tau protein containing three of the mutations present in frontotemporal dementia linked to chromosome 17 (FTDP-17), suggested that Aβ could facilitate the phosphorylation of tau at a site not directed by proline, such as serine 262, and that modification could facilitate tau aberrant aggregation (Perez et al., 2005).

Together with a study showing that aggregated synthetic $A\beta_{42}$ caused a decreased solubility of tau along with the generation of PHF-like tau containing filaments in a human tissue culture system (Figure 4) (Ferrari et al., 2003; Gotz et al., 2004), the above experiments demonstrate pathological interactions between Aβ and tau that lead to increased NFT formation. Moreover, the region-specific induction of Aβ-mediated NFT formation in P301L tau transgenic mice mirrors, to some extent, the regional vulnerability observed in AD brains. For a complete review, see the recent article by Götz, Schild, Hoerndli, and Pennanen (Gotz et al., 2004).

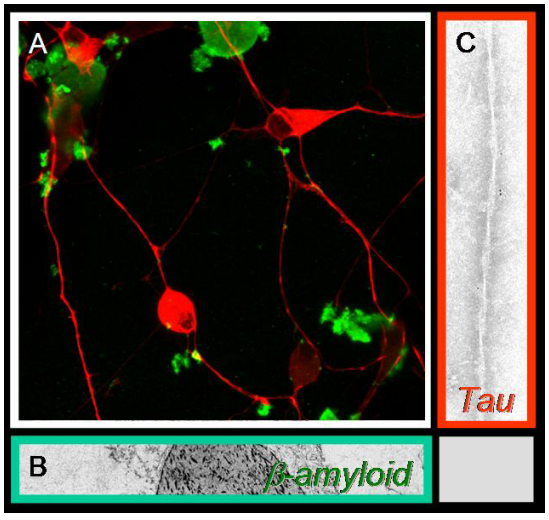

Figure 5:
Stably expressed human tau in neuronally differentiated human SH-SY5Y cells (A, in red), exposed to aggregated synthetic β-amyloid peptide ($A\beta_{42}$) (A, in green). Electron-micrograph of the fibrillar preparations of $A\beta_{42}$ (B). $A\beta_{42}$ caused the generation of PHF-like tau containing filaments that were 20 nm wide and had periodicities of 130 to 140 nm in the presence of P301L mutant tau, or 150 to 160 nm in the presence of wild-type tau (C).

J. Götz, A. Schild, F. Hoerndli, and L. Pennanen, Int. J. of Devl Neuroscience, 22, 453-465.

7.1.7 Histopathology of tau transgenic mouse models

In one of the first tau transgenic mouse models, the longest human 4R brain tau isoform was expressed neuronally without any pathogenic mutation (Goedert et al., 1995). Despite the lack of an NFT pathology, these mice modeled aspects of human AD, such as somatodendritic localization and hyperphosphorylation of tau and, therefore, represented an early pre-NFT phenotype. The use of stronger promoters to drive transgene expression caused a more pronounced phenotype (Gotz et al., 2000; Ishihara et al., 1999; Moechars et al., 1999). Due to a high expression level of the transgene in motor neurons, large numbers of pathologically enlarged axons with neurofilament- and tau-immunoreactive spheroids were present, a neuropathological characteristic of most cases of amyotrophic lateral sclerosis (ALS), where they are believed to impair slow axonal transport (Hirano et al., 1984; Munoz et al., 1988; Rouleau et al., 1996). Tau protein extracted from transgenic brain and spinal cord has been shown to become increasingly insoluble as the mice became older. Despite the decreased solubility of tau, NFT did not form, unless the mice reached a very old age (Ishihara et al., 2001). Taken together, these findings demonstrated that overexpression of human tau can lead to an axonopathy resulting in nerve cell dysfunction and amyotrophy (Chen et al., 2004; Gotz, 2001).

With the identification of pathogenic tau mutations in FTDP-17 in 1998, several groups achieved NFT formation both in neurons (Allen et al., 2002; DeTure et al., 2000; Gotz, 2001; Tanemura et al., 2001; Tatebayashi et al., 2002) and in glial cells of transgenic mice (Gotz, 2001; Higuchi et al., 2002). The P301L mutation was one of the first FTDP-17 mutations that had been identified in human patients (Grover et al., 1999). This mutation was shown *in vitro* to cause both an accelerated aggregation of tau into filaments and a marked reduction in the ability of tau to promote microtubule assembly (Barghorn et al., 2000; Hasegawa et al., 1998; Ko et al., 1999). Also, the P301L mutation is quite frequent as it has been detected in 11% of familial cases of frontotemporal dementia (FTD) (Sobrido et al., 2003) and therefore, made it a fitting choice to be expressed in transgenic mice.

When a human tau isoform lacking the two amino-terminal inserts was expressed together with the P301L mutation under the control of the murine PrP promoter (DeTure et al., 2000), 90% of the mice developed severe motor and behavioral disturbances by 10 months of age. These were more pronounced than reported in the previously published wild-type tau transgenic mouse models (Gotz et al., 2000; Ishihara et al., 1999; Moechars et al., 1999). Importantly, NFT were identified by Gallyas silver stainings and thioflavin S-fluorescent microscopy both in brain and spinal cord, and motor neurons were reduced twofold in the spinal cord (DeTure et al., 2000). The same mutation was expressed using the longest human tau isoform containing both amino-terminal inserts. The mThy1.2 promoter was chosen instead of the PrP promoter, which may account for different expression patterns in these mice (Gotz, 2001). Again, NFT were identified. In addition, tau filaments were revealed by immuno-electron microscopy of sarcosyl extracts using phospho-tau-specific antibodies. Due to low expression levels in motor neurons of the spinal cord, no motor phenotype was observed.

The P301S mutation is an aggressive mutation that causes clinical signs of FTDP-17 already in the third decade of life (Bugiani et al., 1999). When P301S mutant tau was expressed under the control of the mThy1.2 promoter, massive NFT formation was found (Allen et al., 2002). To address the role of distinct tau phospho-epitopes in tau filament formation, tau was analyzed in both the soluble and insoluble fraction. Perchloric-acid soluble tau was phosphorylated at many phospho-epitopes of tau, with the exception of the AT100 phospho-epitope S214, whereas sarkosyl-insoluble tau was strongly immunoreactive with all antibodies including AT100. Interestingly, this site has been shown, together with S422, to be linked to NFT formation in P301L mice (Gotz, 2001). Together, this indicates that immunoreactivity for phospho-S214 closely mirrors the presence of tau filaments, suggesting that phosphorylation of this site occurs in the course of, or after, filament assembly.

The first tau transgenic mouse models dealt with neuronal tau and its assembly into NFT. To address the tau pathology in glial cells, G272V mutant tau was expressed by combining a PrP-driven expression system with an autoregulatory transactivator loop that resulted in high expression in a subset of neurons and oligodendrocytes. Electron microscopy established filament formation associated with hyperphosphorylation of tau. Thioflavin S-positive fibrillary inclusions were identified in oligodendrocytes and motor neurons in spinal cord (Gotz, 2001). The clinical phenotype of these mice was subtle. In contrast, when human wild-type tau was over-expressed in neurons and glial cells using the mouse Tα1 α-tubulin promoter, a glial pathology was found resembling the astrocytic plaques in CBD and the coiled bodies in CBD and PSP (Higuchi et al., 2002).

The role of glucose and insulin levels in NFT formation has not been addressed in the tau transgenic models. Of the many kinases implicated in the mitotic failure hypothesis (Arendt, 2003), the wnt signaling pathway component GSK-3, and the activator p25 of the cyclin-dependent kinase cdk-5 have been co-expressed with tau. Unexpectedly, co-expression of GSK-3β with wild-type human tau reduced the number of axonal dilations and alleviated the motor phenotype that was typical for single human tau transgenic mice, whereas co-expression of p25 with P301L tau was accompanied by increased numbers of NFT (Chevallet et al., 2003; Moechars et al., 1999; Spittaels et al., 2000).

7.2 Phosphorylation as a regulatory principle

During a lifetime, a cell has to fulfill many tasks. In order for cellular processes to function properly there has to be a tight regulation of all procedures involved. Today, centuries after the first discovery of phosphorylated proteins and the demonstration that enzyme activity can be regulated through its phosphorylation, as shown for the glycogen phosphorylase (Fischer and Krebs, 1955; Sutherland and Wosilait, 1955), the outstanding role of reversible protein phosphorylation in cell regulation is undisputable. Reversible phosphorylation of Ser, Thr, and Tyr residues occurring through the concerted action of protein kinases and protein phosphatases affects about one-third of eukaryotic proteins and represents the most frequent and general mechanism by which nearly all biological functions are regulated. The fundamental biological

importance of protein phosphorylation is underlined by the existence of more than 600 protein kinase genes and slightly less than 100 protein phosphatase genes within the human genome. Much of the specificity of protein phosphorylation resides in the kinases responsible for transferring the phosphate group from ATP to the target proteins, as witnessed by the rich diversity of cellular kinases. In *Drosophila melanogaster*, *Saccharomyces cerevisiae* and *Caenorhabditis elegans* protein kinases belong to the protein families with the most members. In all three organisms, they represent 2% of the total proteome (Rubin et al., 2000). In principle, protein phosphatases play an equally important role in the regulation of protein phosphorylation, but there are relatively few different protein phosphatase enzymes. In mammalian cells, two closely related phosphoprotein phosphatases, PP1 and PP2A, account for >90% of the total phosphatase activity (Depaoli-Roach et al., 1994). This figure by itself, in conjunction with the observation that protein phosphatases operate on a minority of potential phosphoacceptor residues preselected by protein kinases, would indicate that the specificity of phosphatases needs to be less stringent than that of protein kinases. This is especially true of site specificity, i.e. the ability to recognize consensus sequences defined by local structural features surrounding the phosphoacceptor amino acid. This is a prominent feature of most protein kinases, with special reference of Ser/Thr specific ones, and has been exploited for the design of hundreds of specific peptide substrates. These proved useful for the selective monitoring of individual kinases or classes of kinases, whose structural features responsible for site specificity in many instances have been disclosed by mutational and structural analyzes. In contrast many attempts to define consensus sequences recognized by individual protein phosphatases were less rewarding consistent with the notion that residues surrounding the phospho-amino acid may play a marginal role in substrate recognition, which is mainly mediated by targeting subunits and/or structural modules outside the catalytic core of the phosphatase (Shibasaki et al., 1996; Song et al., 2001).

Protein kinases catalyze the transfer of the γ-phosphoryl group of ATP to the hydroxyl group of Ser, Thr, and Tyr residues within specific protein substrates. Protein phosphatases are hydrolytic enzymes that remove the phosphoryl group from the phosphorylated residue(s). Unlike protein kinases, where tyrosine specific and serine/threonine specific kinases share substantial sequence identity, the protein phosphatase can be divided into two unrelated large families: protein serine/threonine phosphatases, which remove the phosphoryl group from serine/threonine residues, and protein tyrosine phosphatases (PTPs), which hydrolyze phosphotyrosine.

In contrast to protein kinase activation, which tends to be associated with cell growth and proliferation, PP2A phosphatase activity is associated with growth inhibition and cell cycle arrest, and abnormal phosphorylation is one of the causes or consequences of frequent diseases like cancer, diabetes, Alzheimer's disease and rheumatic arthritis (Cohen, 2000). Protein phosphatases play critical roles in the timing, extent and localization of protein phosphorylation and in regulating those cellular processes modulated by phosphorylation. Therefore, specificity also comes from protein phosphatases, whose complexity, achieved in part through combinatorial subunit interactions, equals that of protein kinases (Virshup, 2000). The phosphorylation of a protein can alter its behavior in almost every conceivable way, and

multisite phosphorylation can enable several such effects to operate in the same protein (Cohen, 2000). In many cases phosphorylation regulates the intrinsic biological activity of enzymes (Gabrielli et al., 1997; Sugiura et al., 1999; Davis, R. J., 2000). Also phosphorylation affects stability (Brondello et al., 1999; Nosworthy et al., 1998; Szilak et al., 1997), interaction with other proteins (Di Paolo et al., 1997; Kann et al., 1999) or DNA (Steegenga et al., 1996), binding of metallic ions (Taborsky, 1991), and translocation between cellular compartments (Jans, 1995; Petersen et al., 1999). There are several proteins and protein domains known that recognize their binding partners within cellular signal cascades only when phosphorylated (Yaffe and Cantley, 1999; Yaffe and Elia, 2001).

Examples for such specific modules are SH2 (src homology 2) domains (Schaffhausen, 1995), WW domains (Lu et al., 1999), forkhead-associated (FHA) domains (Durocher et al., 2000) and 14-3-3 proteins (Aitken, 1996; Yaffe et al., 1997). The phosphorylation sites in eukaryotes are most frequently found at serine/threonine or tyrosine side chains. Dephosphorylation thereof follows one of two distinct mechanisms (Barford et al., 1998; Denu et al., 1996). Tyrosin phosphatases form a covalent phospho-enzyme intermediate at the phosphor atom, after nucleophilic attack of a thiolat anion from a cystein side chain (Denu et al., 1996). In contrary, with serine/threonine-specific protein phosphatases, there is no temporary transfer of phosphate to the enzyme as the nucleophilic attack at the phosphor atom is caused by a water molecule, activated by two metallic ions (Egloff et al., 1995). Protein phosphatase 2A (PP2A), together with PP1, PP2B (calcineurin), PP4 and PP5, belongs to the PPP family of protein Ser/Thr phosphatases. Members of this family have no sequence homology to the PPM family, to which belongs the Mg^{2+} dependent PP2C (Barford, 1996; Wera and Hemmings, 1995; Zolnierowicz, 2000).

7.2.1 Protein phosphatase 2A (PP2A)

PP2A is a highly abundant and ubiquitously expressed serine/threonine-specific protein phosphatase with important roles in embryonic development and differentiated tissues (Mayer-Jaekel and Hemmings, 1994; Goldberg, 1999; Janssens and Goris, 2001; Millward et al., 1999; Sontag, 2001; Virshup, 2000). PP2A is tightly controlled by association with regulatory subunits, post-translational modification and the interaction with cellular proteins.

The PP2A holoenzyme is a heterotrimer made of a scaffolding A, a regulatory B, and a catalytic C subunit. The catalytic C subunit with a molecular weight of 36 kDa has so far been found as two isoforms, α and β, which differ only in eight out of a total of 309 amino acids (Stone et al., 1987). Both are expressed ubiquitously in all tissues, though the isoform α is found at higher concentrations (Khew-Goodall and Hemmings, 1988) and it has been shown to be an essential protein despite a high sequence homology to the isoform β. A Cα-/- knock-out can not be compensated by Cβ and therefore the deletion of Cα is embryonically lethal in mice (Gotz et al., 1998), possibly due to a different subcellular localization of both C isoforms (Gotz et al., 2000). The catalytic subunit of PP2A belongs to the proteins that have been the most highly conserved during evolution, as shown in sequence comparisons with lower eukaryotes as *Saccharomyces*

cerevisiae (Sneddon et al., 1990), *Schizosaccharomyces pombe* (Kinoshita et al., 1990), *Xenopus laevis* (Van Hoof et al., 1995), *Drosophila melanogaster* (Orgad et al., 1990) or plants as *Arabidopsis thaliana* (Perez-Callejon et al., 1998) and *Brassica napus* (MacKintosh et al., 1990). PP2A is a metallo-enzyme with Fe^{2+} and Zn^{2+} in the active site (Nishito et al., 1999; Nishito et al., 1999).

The A subunit is a 65 kDa protein (also called PR65) that associates with the catalytic subunit to form a core dimer (Groves et al., 1999; Kamibayashi et al., 1992; Kremmer et al., 1997). The apparent dissociation constant of this interaction has been determined at approximately 85 pM (Turowski et al., 1997). As well as for C, there are two isoforms of the scaffolding subunit A in mammals, which show a sequence homology of 87% (Hemmings et al., 1990). The three dimensional structure of A has been studied in much detail (Groves et al., 1999). It contains an array of 15 HEAT motifs consisting of 39 amino acids each. HEAT (huntingtin/ elongation/ A subunit/ target of rapamycin) motifs have been named after the first proteins, in which they have been discovered (Andrade and Bork, 1995; Groves et al., 1999). Such motifs of 37-43 amino acids length are found in proteins in repeats of 3 to 22. All 15 HEAT motifs in the A subunit of PP2A build an alike structure, namely two antiparallel helices forming something like a double layer of α-helices. The loops between both helices of a motif contain conserved amino acids and exposed hydrophobic surfaces, thereby providing docking sites for both catalytic and regulatory subunits. Yet only A subunits in the core dimer can assemble with various regulatory B subunits to form heterotrimers with distinct localization and substrate specificity (McCright et al., 1996; Moreno et al., 2000; Strack et al., 1998; Tehrani et al., 1996).

Four B subunit families with no sequence homologies have been identified so far, termed B/PR55, B'/PR56/PR61, B''/PR59/PR72/130 and B'''/PR93/PR110 (Janssens and Goris, 2001). In contrast to Drosophila, where each subunit is encoded by a single gene, mammals express at least two A (α and β), two C (α and β), four B, at least five B', four B'', and two B''' isoforms. As a result, a total of more than 72 PP2A holoenzymes can be generated. Taking into account the different splice variants, this number may be even higher (Martens et al., 2004; Schmidt et al., 2002). Heterotrimers with PR55 subunits are often named PP2A1, whereas trimers including PR61 subunits are referred to as PP2A0, not to be confounded with PP2AD for the dimeric form. The four isoforms of the B/PR55 family are expressed in a tissue specific manner (Mayer et al., 1991; Schmidt et al., 2002; Strack et al., 1999; Zolnierowicz et al., 1994) and contain six WD repeats (Neer et al., 1994). These weakly conserved sequence motifs of approximately 40 amino acids probably conduce to the interaction with other proteins (Smith et al., 1999). PR55α for example associates with the type I transforming growth factor beta (TGF-beta) receptor, resulting in the phosphorylation of PR55α by the receptor kinase (Griswold-Prenner et al., 1998).

The B'/PR61 family consists of at least five distinct gene products (Csortos et al., 1996; McCright and Virshup, 1995; Tehrani et al., 1996). All PR61 family members contain a highly conserved central region, which is very likely required for the interaction with the A and possibly the C subunit (Zolnierowicz et al., 1996). They are almost exclusively phosphoroteins (McCright et al., 1996) and the different isoforms are expressed in a tissue-specific manner (Csortos et al., 1996; McCright and Virshup, 1995; Tehrani et al., 1996).

The B" family comprises the two related proteins, PR72 und PR130, possibly two splice variants of the same gene product (Hendrix et al., 1993), and the proteins PR59 and PR48 (Voorhoeve et al., 1999; Yan et al., 2000). PR59 shares 56% identity and 65% similarity with PR72, but its expression pattern differs completely form that of PR72 (Voorhoeve et al., 1999). PR48 shares 68% homology with PR59 and was identified as an interaction partner of Cdc6, a protein required for the initiation of DNA replication (Yan et al., 2000).
The members of the fourth and last family of regulatory subunits described until now, B''', have in common a conserved epitope that they share with B' subunits. Striatin (PR110) and S/G2 nuclear autoantigen (SG2NA; PR93) contain WD-40 repeats and interact with PP2AD and additional proteins, suggesting a function as scaffolding proteins in Ca^{2+}-dependent signaling (Moreno et al., 2000).

7.2.1.1 Post-translational modifications of the catalytic subunit

PP2A not only appears to integrate signals within phosphorylation cascades but also to be the focal point of a distinct post-translational modification system. The C-terminal sequence of the catalytic subunit is extremely well conserved, and several of its amino acids within it are important for binding of the third subunits to the PP2A core dimer. Recruitment of regulatory subunits into the PP2A complex is therefore determined by post-translational modifications of the C subunit at its carboxy-terminus, which contains a highly conserved DYFL motif at position 306-309 (Ogris et al., 1997). The modifications include at least three post-translational modifications: methyl esterification of the C-terminal leucine 309, phosphorylation of a conserved tyrosine located two residues from the C-terminus and phosphorylation of an as yet unidentified threonine (Tolstykh et al., 2000; Turowski et al., 1995; Wu et al., 2000; Yu et al., 2001; Zukerberg et al., 2000). Leucine 309 is reversibly methylated by a new type of methyltransferase (LCMT, leucine carboxyl methyltransferase), and demethylated by a specific methylesterase (PME-1, phosphatase methylesterase). In addition to its esterase function, PME-1 stabilizes an inactive conformation of PP2A that can be reactivated by the PP2A activator (PTPA) (Fellner et al., 2003; Longin et al., 2004), a PP2A-interacting protein essential for cell survival (Van Hoof et al., 2000).
Despite the fact that post-translational modifications to the catalytic regulatory subunits have been described, the biochemical basis for such dynamic regulation is not known. The C subunit is the target for inactivating phosphorylations on some of its tyrosine and threonine residues so that phosphorylation of either the Tyr or the Thr site inhibits phosphatase activity *in vitro* (Janssens and Goris, 2001), and most of the PR61 proteins (except PR61γ) are phosphoproteins *in vivo* (McCright et al., 1996). On the other hand, carboxyl methylation of the C subunit does not affect phosphatase activity *in vitro* (Tolstykh et al., 2000). However, purified PP2A carboxyl methyltransferase methylates the C subunit only in the context of an AC dimer and the resulting dimer containing the methylated C subunit has a higher affinity for a B regulatory subunit than does a dimer with an unmethylated C subunit (Tolstykh et al., 2000). Consistent with this observation, a tagged version of a mammalian PP2A C subunit containing a mutation of the

conserved C-terminal leucine showed reduced participation in ABC heterotrimers *in vivo* but normal participation as an AC heterodimer (Chung et al., 1999). These observations suggest that carboxyl methylation could affect the association of the C subunit with regulatory subunits *in vivo* and, as a result, alter targeting of the phosphatase towards certain substrates relevant for its normal biological activity. When negatively charged amino acids were introduced at threonine 304 or tyrosine 307 to mimic phosphorylation, the A, but not the B subunits, were bound by mutant C in transfected NIH3T3 cells (Ogris et al., 1997). Similar findings were obtained with mutants Y307F and L309Q, demonstrating the importance of the carboxy-terminal residues for heterotrimer assembly (Chung et al., 1999). More specifically, it was shown that the L309A mutant was defective in binding distinct subunits, such as B/PR55α, *in vitro* (Bryant et al., 1999).

Comparable findings were obtained in *S. cerevisiae*. Removal of the carboxy-terminal leucine or substitution by alanine did not inhibit general PP2A activity, but abolished binding of B/PR55. Binding of B'/PR61 was assumed to be retained as judged from a cell growth inhibition assay (Evans and Hemmings, 2000). These data support the notion that B/PR55 and B'/PR61 compete for binding to the core dimer. The kinase–phosphatase relationship is more intimate than previously thought on the basis of the general antagonism between both classes of enzymes. Indeed, signal transduction 'cassettes' have been discovered in which a protein kinase and PP2A directly interact, or in which the kinase and PP2A are linked via a common anchoring protein. PP2A controls the activity of at least 50 different kinases (Millward et al., 1999). Understanding the regulation of these kinase–phosphatase couples will be of importance to gain deeper insights into the signaling pathways in which they are involved.

7.2.2 PP2A in human disease

PP2A holoenzymes have been shown to play an important role in human disease. The structural subunit A, for instance, has been identified as a tumor suppressor. It is mutated in melanomas and carcinomas, as well as tumor-derived cell lines (Calin et al., 2000; Ruediger et al., 2001; Wang et al., 1998). In addition, an expanded CAG repeat was found immediately upstream of the B/PR55β gene in humans with spinocerebellar ataxia, indicating that deregulation of PR55 may have functional consequences in neurodegenerative disorders (Holmes et al., 1999). Finally, PP2A dysfunction has been implicated in neurodegenerative disorders such as Alzheimer's disease (AD) and frontotemporal dementia (FTD) (Gong et al., 1995; Gotz and Schild, 2003). These disease entities collectively termed tauopathies are characterized by neurofibrillary tangles (NFT), which are composed of hyperphosphorylated isoforms of the microtubule-associated protein tau (Gotz et al., 2004). *In vitro* PP2A is the most powerful enzyme able to dephosphorylate tau , and ABαC, a major form of PP2A in brain, binds tightly to tau protein (Gong et al., 1994; Grundke-Iqbal et al., 1986; Sontag et al., 1999; Wang et al., 1995). Intronic mutations in the tau gene cause frontotemporal dementia and parkinsonism linked to chromosome 17 (FTDP-17). *In vitro* as well as *in vivo* the FTDP-17 mutations G272V, ΔK280, P301L, P301S, S305N, V337M, G389R, and R406W inhibit by 20-95% the binding of

recombinant three-repeat and four-repeat tau isoforms to the ABαC holoenzyme and the AC core enzyme of PP2A (Goedert et al., 2000). These results indicate that altered protein-protein interactions between PP2A and tau may contribute to FTDP-17 pathogenesis (Goedert et al., 2000). Tau could be modified in different tauopathies by PP2A dephosphorylation, but different phosphatases and kinases and other agents that could induce tau phosphorylation are also under investigation (see section 7.2.2.2 "Other agents that could induce tau phosphorylation in tauopathies").

7.2.2.1 PP2A in Alzheimer's disease

In Alzheimer's disease brain, tau can be isolated from a cytosolic fraction, from soluble abnormally phosphorylated tau (P-tau), and as a component of PHF (PHF-tau) (Kopke et al., 1993). A pool of soluble non-PHF but abnormally hyperphosphorylated tau suggests that the aberrant phosphorylation of tau precedes its polymerization into PHF. Thus, the cellular mechanisms by which tau becomes abnormally hyperphosphorylated and assembles into PHF should provide profound insights into the pathogenesis of the disease. Therefore, any factor that causes the up-regulation of protein kinases or/and the down-regulation of protein phosphatases (PPs) is likely to position tau into an abnormally phosphorylated state.

Since the first discovery that activities of PP2A, PP2B, and PP1 are significantly decreased in AD brain (Gong et al., 1993), increasing data both *in vitro* and *in vivo* have suggested the involvement of a decreased phosphatase activity (Gong et al., 2000; Kim et al., 1999; Merrick et al., 1997; Planel et al., 2001). While it is still possible that there is an involvement of PP2B and PP1, several studies have demonstrated that PP2A is a major tau phosphatase (Goedert et al., 1995; Gong et al., 1994; Sontag et al., 1996). By using okadaic acid as a selective suppressor of PP2A, studies on cell lines (Arendt et al., 1998; Favre et al., 1997; Merrick et al., 1997; Tanaka et al., 1998), primary cultured hippocampal neurons (Gong et al., 2001; Kim et al., 1999; Malchiodi-Albedi et al., 1997), metabolically active rat brain slices (Bennecib et al., 2000; Gong et al., 2001; Gong et al., 2000; Mudher et al., 1999), chronic intraventricular microinfusion (Arendt et al., 1998) and acute injection into rat hippocampus unilaterally (Lee et al., 2000) all came to the point that PP2A inhibition was sure to cause tau hyperphosphorylation. In addition to hyperphosphorylation, injection of OA causes amyloid deposition, neurodegeneration, and memory impairment in rat (Arendt et al., 1995; He et al., 2001; Tapia et al., 1999). Since OA in part also inhibits PP1, it was important to see that specific inhibition of PP2A in cultured cells by SV40 small t protein, as well as in a transgenic mouse line by the dominant negative mutant L199P of PP2AC is sufficient to induce PHF-like tau hyperphosphorylation (Kins et al., 2001; Sontag et al., 1996; p. 28 and Fig. 2 p. 32). In the mouse model, tau was not only abnormally hyperphosphorylated, but compartmentalized and ubiquitinated as observed in AD in the presence of a decreased PP2A activity (Kins et al., 2001). In addition to these data from *in vitro* experiments and transgenic mice, there is a growing body of evidence demonstrating a reduced abundance and activity of PP2A in AD patients. In AD brains, PP2A activity was decreased by 30% compared with controls (Gong et al., 1995). One

explanation for this decrease could be the downregulation of one or more PP2A subunits. Indeed, microarray analyses have revealed that the expression of the catalytic subunit gene decreases in mice hippocampus as a result of aging (Jiang et al., 2001) and is downregulated in early AD (Loring et al., 2001). In the hippocampus of AD patients, of five subunits analyzed, Cα, B/PR55γ, and B'/PR61ε mRNA expression was quantitatively decreased (Vogelsberg-Ragaglia et al., 2001). In addition, reduced expression levels of ABαC were recently reported in frontal and temporal cortices in AD. These affected PP2A activity, which was correlated with NFT load, suggesting that PP2A dysfunction contributes to the tau pathology in AD (Sontag et al., 2004). Therefore PP2A is considered to be the crucial tau phosphatase *in vivo*. In addition, PP2A might be the key phosphatase of other high-molecular-weight microtubule-associated proteins such as MAP1 and MAP2 (Gong et al., 2000).

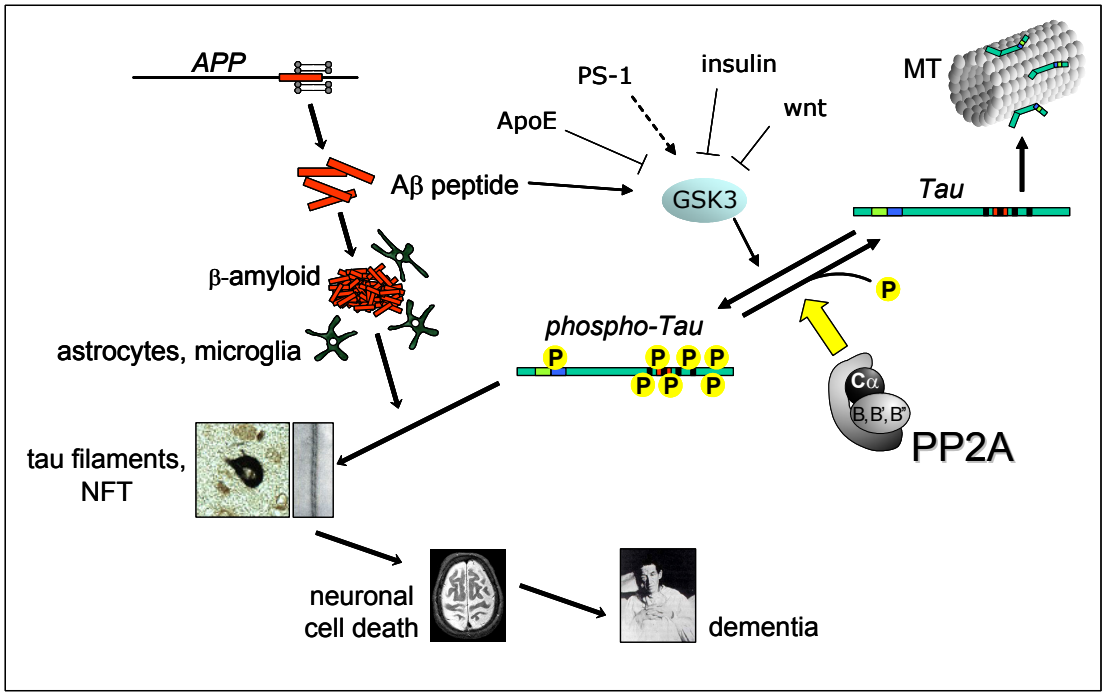

Figure 6: Involvement of PP2A in Alzheimer's disease. PP2A is the major phosphatase to dephosphorylate the microtubule (MT) binding protein tau. As indicated by the name tau normally binds to and stabilizes the MT system. Abnormally phosphorylated tau is released from MTs and can form filaments and neurofibrillary tangles (NFT) in the soma of the neuron. This process is accelerated by aggregated amyloid β *in vitro* and possibly in AD brain. Interestingly, Aβ peptides are also a cofactor to activate glycogen synthase kinase-3 (GSK-3), which in turn phosphorylates tau. NFT has been shown to be directly related to neuronal cell death and dementia.

Yet another involvement of PP2A in AD has been proposed. It is known that *S*-Adenosylmethionine-dependent carboxyl methylation is essential for the assembly of PP2A heterotrimers, and epidemiological evidence indicates that elevated plasma homocysteine is an independent risk factor for AD. The PP2A methylation system could therefore be the link relating elevated plasma homocysteine to AD since homocysteine is a key intermediate in the methyl

cycle and elevated plasma homocysteine results in a global decrease in cellular methylation (Vafai and Stock, 2002).

7.2.2.2 Other agents that induce tau phosphorylation in tauopathies

In contrast to PP2A, few data are available concerning pure PP1 regulation on tau phosphorylation, partly due to the lack of a specific suppressor because of its diffuse intracellular distribution and poor knowledge of its structures and functions. Calyculin (CA) and OA are well-documented tools used in studies focusing on PPs. As an inhibitor CA strongly yet incompletely inhibits activities of PP2A and PP1 simultaneously at nanomolar concentrations while higher concentrations of OA are required to inhibit PP1 besides PP2A (Favre et al., 1997). Tau links PP1 to microtubules and might therefore be dephosphorylated by PP1 (Liao et al., 1998). Yet *in vitro* PP1 has a much weaker potential than PP2A to dephosphorylate AD P-tau, and PP1 was reported to cause tau hyperphosphorylation only when it was inhibited together with PP2A (Yamamoto et al., 1995). Apart from direct phosphorylation on tau when PP2A and PP1 are inhibited, an indirect pathway by promoting kinase activity cannot be excluded. By using metabolically living brain slices, it has been shown that PP1 up-regulates tau phosphorylation indirectly by regulating the activities of protein kinases (Bennecib et al., 2000). In SY5Y cells treated with OA, the activity of mitogen-activated protein kinase (MAPK) and cyclin-dependent kinase (Cdk) increased as PP2A and PP1 activity was inhibited (Tanaka et al., 1998) There is much evidence that PP2A controls the activities of more than 30 kinases of several major protein kinase families in the cell, and that several kinases form stable complexes with PP2A (Millward et al., 1999) This includes the calmodulin-dependent protein kinase II (CaMKII) activity, which seems to be the major tau Ser 262/356 kinase in brain (Bennecib et al., 2001), and MAPK cascades (Anderson et al., 1990; Gomez and Cohen, 1991; Millward et al., 1999; Silverstein et al., 2002). MAPKs include the extracellular signal-related kinases (ERKs), which are activated by mitogenic stimuli including growth factors, the c-Jun N-terminal kinases (JNKs) and p38 MAPKs. *In vitro* studies suggest that PP2A plays a major role in the down-regulation of the ERK pathway at several stages (Millward et al., 1999). MAPK dephosphorylation has been attributed to PP2A, in addition to a unique family of dual specificity phosphatases called MAP kinase phosphatases (MKPs) (Alessi et al., 1995; Chung and Brautigan, 1999; Guan and Butch, 1995; Hirsch and Stork, 1997). Inhibition of PP2A by OA or by a dominant negative mutation of PP2AC has lead to the activation of ERK and JNK signaling pathways *in vivo* (Kins et al., 2003; Sonoda et al., 1997), and activation of PP2A inhibited JNK activity (Shanley et al., 2001), suggesting an additional indirect role of PP2A in tau hyperphosphorylation.

In AD it has been suggested that Aβ could increase tau phosphorylation possibly by GSK-3 activation (Alvarez et al., 1999; Yankner, 1996) and it has been suggested that Aβ could act as an antagonist for the insulin receptor (Xie et al., 2002). Thus, protein kinase B (PKB/Akt) should be inactivated and as a consequence of that, GSK-3 could be more active. In addition the stress kinase, p38, is also activated in AD (Hensley et al., 1999; Zhu et al., 2000) and in other

tauopathies (Ferrer et al., 2001; Hartzler et al., 2002) and can phosphorylate tau on residues that are modified in AD (Anderton et al., 2001; Gomez-Ramos et al., 2003). This is particularly interesting since p38 could be activated in stress conditions (Anderton et al., 2001) and oxidative stress has been implicated in AD and other tauopathies like progressive supranuclear palsy (PSP) (Nunomura et al., 2001; Odetti et al., 2000; Smith et al., 1996). This suggests that oxidative stress could facilitate tau phosphorylation through the activation of p38. Another consequence of stress is lipid peroxidation causing the modification of arachidonic acid and yielding compounds like 4-hydroxynonenal (HNE) or acrolein (Sayre et al., 1997; Uchida et al., 1998). Both compounds are present in the brain of AD patients and colocalize with NFT (Lovell et al., 2001; Sayre et al., 1997). While HNE inhibits tau dephosphorylation and allows the *in vitro* formation of tau filaments (Mattson et al., 1997; Perez et al., 2000; Perez et al., 2002), acrolein favors tau phosphorylation by the stress kinase p38 (Gomez-Ramos et al., 2003). Consequently, tau could be modified by phosphorylation in different tauopathies by different kinases and, as a consequence of that phosphorylation, tau could change its conformation and increase its capacity to assemble into aberrant polymers (Takeda et al., 2000).

7.2.3 PP2A modification in the mouse

The following paper (Gotz and Schild, 2003) outlines the current state of transgenic and knock-out models of PP2A. It should give an overview about different experimental approaches to better understand PP2A function *in vivo*. Limitations of these methods are discussed as well as their implications for the understanding of human disease.

[29] Transgenic and Knockout Models of PP2A

By JÜRGEN GÖTZ and ANDREAS SCHILD

Introduction

Protein phosphatase 2A (PP2A) is a serine/threonine-specific protein phosphatase with important roles in cell growth, embryonic development, and human disease. All PP2A holoenzymes have in common a catalytic subunit C36 and a structural scaffolding subunit A65. These core subunits assemble with various regulatory B subunits to form heterotrimers with distinct functions in the cell.

Four families of B subunits have been identified so far, termed B/PR55, B′/PR56/PR61, B″/PR72 and B‴/PR93/PR110.[1] In contrast to *Drosophila*, where each subunit is encoded by a single gene, mammals express at least two A, two C, four B, at least eight B′, four B″, and two B‴ isoforms. Thus, a total of about 75 PP2A holoenzymes can be generated. Taking the different splice variants into account, even more holoenzymes can be formed.[2] This complexity, in addition to posttranslational modifications, including phosphorylation and methylation of the C subunits, provides a vast variety of possibilities for the regulation of PP2A activity.[1]

Despite the identification of an increasing number of *in vitro* substrates of PP2A, the specific PP2A holoenzymes involved in dephosphorylation are unknown for most substrates. Even more so, it is far from being understood how substrate specificity is achieved *in vivo*, and how the vast variety of PP2A holoenzymes is regulated. In the light of the accumulating evidence that distinct holoenzymes are involved in human disease, understanding the

[1] V. Janssens and J. Goris, *Biochem. J.* **353**, 417 (2001).
[2] K. Schmidt, S. Kins, A. Schild, R. M. Nitsch, B. A. Hemmings, and J. Gotz, *Eur. J. Neurosci.* **16**, 2039 (2002).

METHODS IN ENZYMOLOGY, VOL. 366
0076-6879/2003 $35.00

function and regulation of the individual subunits may eventually help to combat human disease. The structural subunits A/PR65α and A/PR65β, for example, have been identified as tumor suppressors. Their genes are mutated in melanomas and carcinomas, as well as tumor-derived cell lines.[3–5] Then, in humans with spinocerebellar ataxia, an expanded CAG repeat has been identified immediately upstream of the B/PR55β gene, indicating that dysregulation of PR55 may have functional consequences in neurodegenerative disorders.[6] Finally, PP2A dysfunction has been implicated in Alzheimer's disease (AD). The microtubule-associated protein tau is a substrate of PP2A,[7] and hyperphosphorylated forms of tau form insoluble intracellular deposits in several human neurodegenerative diseases, including AD.[8] In AD brain homogenates, PP2A activity is 30% reduced compared with controls,[9] and in the hippocampus of AD brains, of five subunits analyzed, Cα, B/PR55γ and B′/PR61ε mRNA expression is quantitatively decreased.[10]

In this chapter we review different experimental approaches in mice aimed to dissect PP2A function *in vivo*. The limitations of these approaches are discussed, as well as their implications for the understanding of human disease.

Classification of Transgenic Approaches

Transgenic approaches to address PP2A function in mice can be classified as follows: (1) complete or inducible versus tissue-specific knockouts of the catalytic, regulatory, or structural subunits of PP2A, (2) transgenic overexpression of regulatory subunits, and (3) dominant negative mutant approaches using either the structural subunit A or the catalytic

[3] S. S. Wang, E. D. Esplin, J. L. Li, L. Huang, A. Gazdar, J. Minna, and G. A. Evans, *Science* **282**, 284 (1998).
[4] G. A. Calin, M. G. di Iasio, E. Caprini, I. Vorechovsky, P. G. Natali, G. Sozzi, C. M. Croce, G. Barbanti-Brodano, G. Russo, and M. Negrini, *Oncogene* **19**, 1191 (2000).
[5] R. Ruediger, H. T. Pham, and G. Walter, *Oncogene* **20**, 10 (2001).
[6] S. E. Holmes, E. E. O'Hearn, M. G. McInnis, D. A. Gorelick-Feldman, J. J. Kleiderlein, C. Callahan, N. G. Kwak, R. G. Ingersoll-Ashworth, M. Sherr, A. J. Sumner, A. H. Sharp, U. Ananth, W. K. Seltzer, M. A. Boss, A. M. Vieria-Saecker, J. T. Epplen, O. Riess, C. A. Ross and R. L. Margolis, *Nat. Genet.* **23**, 391 (1999).
[7] C. X. Gong, I. Grundke-Iqbal, Z. Damuni, and K. Iqbal, *FEBS Lett.* **341**, 94 (1994).
[8] J. Gotz, *Brain Res. Brain Res. Rev.* **35**, 266 (2001).
[9] C. X. Gong, S. Shaikh, J. Z. Wang, T. Zaidi, I. Grundke-Iqbal, and K. Iqbal, *J. Neurochem.* **65**, 732 (1995).
[10] V. Vogelsberg-Ragaglia, T. Schuck, J. Q. Trojanowski, and V. M. Lee, *Exp. Neurol.* **168**, 402 (2001).

TABLE I
PHENOTYPE OF PP2A TRANSGENIC AND KNOCKOUT MICE

Genotype	Transgene expression	Phenotype	Reference
PP2A $C\alpha^{-/-}$ (knockout)		Embryonic lethality, no mesoderm induction	Gotz, 1998 and 2002[14,15]
PP2A A/PR65 mutant Δ5 (transgenic)	Muscle	Form of dilated cardiomyopathy (often premature death)	Brewis, 2000[27]
PP2A B′/PR56γ (transgenic)	Lung	Neonatal death, small lungs, absence of β-catenin	Everett, 2002[17]
PP2A Cα mutant L199P (transgenic)	Postnatally in neurons	Hyperphosphorylation and aggregation of tau	Kins, 2001[22]
PP2A Cα mutant L309A (transgenic)	Postnatally in neurons	Hyperphosphorylation and aggregation of tau	Schild, 2003[24]

subunit C as template. All of these three approaches have been pursued (Table I). The advantages and limitations of the different approaches are discussed.

Animal Models: PP2A Knockout Mice

The high degree of homology of the two catalytic subunits Cα and Cβ in mice[11] implies that deletion of one subunit (Cα) would be compensated by upregulation of the second subunit (Cβ) resulting in a very moderate phenotype. The A and B subunits are less homologous than C, but the degree of homology is still quite high,[2] meaning that targeting of these subunits should result in a more robust phenotype.

PP2A Cα Knockout Mice

The PP2A Cα gene has a short promoter so that deletion of 0.5 kb immediately upstream of the transcription start site of the rat Cα gene abolishes expression in the chloramphenicol acetyltransferase (CAT) assay.[12] We are able to confirm this in embryonic stem cells and eventually in mice by replacing more than 0.5 kb of the Cα promoter, exon 1, and 0.3 kb of intron 1 by a neomycin resistance cassette constitutively transcribed from a phosphoglycerate kinase promoter inserted in opposite transcriptional orientation. Electroporation of the embryonic stem cell line GS1 with a

[11] J. Gotz and W. Kues, *Biol. Chem.* **380**, 1117 (1999).
[12] Y. Kitagawa, H. Shima, K. Sasaki, and M. Nagao, *Biochim. Biophys. Acta* **1089**, 339 (1991).

targeting construct in which the neomycin cassette is flanked by 1 kb and 6 kb of Cα sequences, respectively, allows to isolate homologously targeted clones at a frequency of at least 3 in 100. To obtain homologous recombinants, a plate with embryonic stem cells is grown to subconfluency. The cells are washed with 10 ml CMF-PBS and incubated with 2 ml/plate of a trypsin/EDTA solution (Gibco BRL) for 5 min at 37°C. The cells are disaggregated by trituration, washed once in CMF-PBS, and resuspended at 5×10^6 in 0.8 ml CMF-PBS. This cell suspension is transferred to a 0.4 cm wide electroporation cuvette containing 30 μg of linearized targeting construct. A single pulse of 240 V and 500 μF is applied using the BioRad gene pulser. For other instruments, the optimal conditions have to be determined experimentally. The cells are transferred into a 50-ml tube containing 30 ml of embryonic stem cell medium. Cell viability is determined and the cells are distributed onto six 6-cm plates containing a layer of neomycin-resistant murine embryonic fibroblasts.[13] Selection with G418 (geneticin) is initiated after 24 hr and neomycin-resistant clones become visible after 10 days. These clones are picked and screened by PCR to determine homologous recombinants.

By this approach, we are able to identify several independent embryonic stem cell clones of which, in a recent experiment, two allowed germ line transmission of the mutated allele upon injection of the targeted cells into blastocysts. By this, we are able to establish two mouse strains with identical phenotypes. Analysis of both strains shows that no Cα RNA is transcribed from the mutant allele. $C\alpha^{-/-}$ embryos develop normally until post-implantation (around embryonic days 5.5–6.0). When they start degenerating, while no Cα protein is expressed in $C\alpha^{-/-}$ embryos, we find unaltered levels of total PP2A C. Degenerated embryos can be recovered even at day E13.5, indicating that the embryonic tissue is still capable of proliferating without Cα but that its normal differentiation is significantly impaired. Here, the primary germ layers ectoderm and endoderm are formed, but mesoderm formation is absent in degenerating $C\alpha^{-/-}$ embryos.[14] Using a blastocyst culture system (as described below) we are able to show that during normal early embryonic development, Cα is predominantly present at the plasma membrane whereas the highly homologous isoform Cβ is localized in the cytoplasm and nucleus. This shows us that Cβ cannot compensate for vital functions of Cα in $C\alpha^{-/-}$ embryos. Cα is found in a

[13] B. Hogan, R. Beddington, R. Constantini, and E. Lacy, "Manipulating the Mouse Embryo: A Laboratory Report," Cold Spring Harbor Laboratory Press, Plainview, NY, 1994, pp. 253–290.
[14] J. Gotz, A. Probst, E. Ehler, B. Hemmings, and W. Kues, *Proc. Natl. Acad. Sci. U.S.A.* **95**, 12370 (1998).

complex containing E-cadherin and β-catenin. In $C\alpha^{-/-}$ embryos, E-cadherin and β-catenin are redistributed from the plasma membrane to the cytosol, and cytosolic concentrations of β-catenin are low. Our results suggest that Cα is required for stabilization of E-cadherin/β-catenin complexes at the plasma membrane.[15]

Regulatory Subunit Knockout Mice

No reports of a PP2A regulatory subunit knockout mouse have been published so far. As the promoters are not as extensively characterized and splice variants have been identified with variable first exons more than 50 kb apart from each other,[2] a targeting approach, as outlined above for Cα, is not feasible. We have initiated targeting of the B/PR55γ subunit based on the following strategy: B/PR55γ has nine coding exons.[2] Exon 1 ends with the first nucleotide of an amino acid-encoding triplet, exon 2 ends with the third, exon 3 with the first and exon 4 again with the third nucleotide (Fig. 1). This has significant consequences for the design of the targeting construct. Replacing exon 2 by a neomycin resistance gene could, by read-through transcription and splicing out exons 2 and 3, restore the open reading frame and result in a truncated protein encoded by exons 1 and 4 through 9. Similarly, replacing exon 3 could, by splicing out exons 3 and 4, result in a protein encoded by exons 1, 2, and 5 through 9. Similar splicing artifacts have been reported. Instead of a phenotype caused by the null mutation, it may in fact be caused by an aberrantly spliced protein.[16] To exclude this artifact, a neomycin resistance gene (neo^R) cassette is best inserted so that only the 5′ portion of exon 3 and the 3′ portion of exon 4 are retained (Fig. 1). As an additional measure of precaution, three stop codons, one for each reading frame, are included. The neo^R gene is under the transcriptional control of the herpes simplex virus-thymidine kinase (*HSV-tk*) promoter, inserted in an antisense orientation. As the neomycin resistance cassette is flanked by two *lox*P sites, it can be removed subsequently by Cre-mediated recombination (Fig. 1).

Animal Models: PP2A Regulatory Subunit Transgenic Mice

Of the many regulatory subunits of PP2A, only B′/PR56γ has been expressed in transgenic mice so far. In the developing mouse embryo, PR56γ is present in the lung, and protein levels reach maximal levels at embryonic

[15] J. Gotz, A. Probst, C. Mistl, R. M. Nitsch, and E. Ehler, *Mech. Dev.* **93**, 83 (2000).
[16] U. Muller, N. Cristina, Z. W. Li, D. P. Wolfer, H. P. Lipp, T. Rulicke, S. Brandner, A. Aguzzi, and C. Weissmann, *Cell* **79**, 755 (1994).

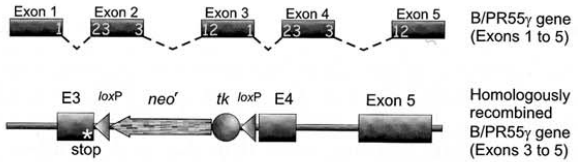

FIG. 1. Gene targeting of B/PR55γ in mice. As the open reading frame is disrupted at the intron/exon boundaries, this has significant consequences for the design of the targeting construct. A simple replacement of 5′ exons by a neomycin resistance cassette could result in splicing artifacts that have been reported. Instead of a null mutant, one might in fact observe a phenotype that is caused by an aberrantly spliced protein. To circumvent this, the 5′ portion of exon 3 and the 3′ portion of exon 4 is fused to a neomycin resistance cassette (neo^R) that is under the transcriptional control of the herpes simplex virus-thymidine kinase (*HSV-tk*) promoter, inserted in an antisense orientation. As the neo^R cassette is flanked by two *lox*P sites, it can be removed subsequently by Cre-mediated recombination. Three stop codons, one for each reading frame, are introduced as an additional measure of precaution.

day E17.[17] To develop mice that overexpress PR56γ in the lung, the full length PR56γ human cDNA is best cloned into an expression vector that contains both the 3.7 kb long lung-specific human surfactant protein promoter and an SV40 small T-antigen poly A/splice cassette. Indeed, pronuclear injection of the linearized construct allows the production of transgenic mice that express PR56γ specifically in lung. Mice obtained by this approach die neonatally, and lack a normal peripheral lung structure. In lung tissue of PR56γ transgenic embryos, β-catenin, a major component of the wnt signaling pathway, is absent, suggesting a role of PR56γ in wnt signaling during lung airway morphogenesis.

Animal Models: PP2A Cα Dominant Negative Mutant Mice

Mutations in the catalytic subunit fall into two categories: (1) When they are introduced into the carboxy-terminus, a region known to modulate the binding of regulatory subunits, the catalytic activity is unaffected, but either no or only a subset of heterotrimers are assembled. (2) Mutations in the catalytic site of Cα reduce or abolish the catalytic activity without affecting holoenzyme assembly. The expression of mutant Cα occurs at the expense of the endogenous Cα as the catalytic subunit is subject to a potent autoregulatory mechanism that keeps total levels of Cα constant.[18] We are able to express these two types of mutant forms of Cα in neurons of transgenic mice, as outlined below.

[17] A. D. Everett, C. Kamibayashi, and D. L. Brautigan, *Am. J. Physiol. Lung Cell Mol. Physiol.* **282**, L1266 (2002).
[18] Z. Baharians and A. H. Schonthal, *J. Biol. Chem.* **273**, 19019 (1998).

The Dom1 Line

By mutagenesis of human Cα in *Saccharomyces cerevisiae* a number of mutants can be studied *in vivo*. One of them, L199P, is catalytically impaired, probably due to a disruption of metal- or substrate-binding implicated in catalytic function rather than due to a disturbed subunit interaction through misfolding.[19]

The cDNA of the human Cα mutant L199P, which we used to generate transgenic mice, is derived from the yeast plasmid YEpDE2.5.12 that carries a 978 bp *Hin*dIII/*Bam*HI fragment encoding the HA-PP2ACα-2512 mutant allele. To be able to discriminate mutant Cα from the highly homologous endogenous murine Cα, it is advantageous to epitope tag the mutant cDNA. As the highly conserved carboxy-terminus contains a leucine at position 309 that is methylated, the tag is better fused to the aminoterminus immediately downstream of the start codon. The HA (hemagglutinin)-PP2ACα-2512 allele contains the t196→c transition mutation encoding an L199P amino acid substitution (numbering is for the untagged Cα).[19] The 978 bp fragment is subcloned into the neuron-specific murine Thy1.2 expression vector.[20,21] 20 μg of plasmid DNA are digested with appropriate restriction enzymes to remove the prokaryotic vector sequences. To preclude damage of the DNA by UV light, the DNA in the preparative agarose gel is not stained with ethidium bromide. Instead, the DNA is visualized by the addition of 2 μg/ml crystal violet (Sigma) to the gel, without the requirement of UV light. The DNA fragment for microinjection is cut out and purified with the PrepAGene DNA purification kit (BioRad). The DNA is further purified, to remove residual agarose, by spinning through a Millipore Ultrafree-MC 0.45 μm filter unit at 5000*g*. The DNA is eluted with microinjection buffer (8 m*M* Tris pH 7.4, 0.15 m*M* EDTA) and adjusted to 2–3 ng/μl. Before final use, the DNA is again purified using a Millipore Ultrafree-MC 0.22 μm filter unit. Transgenic mice are produced by pronuclear microinjection of B6D2F1 × B6D2F1 embryos cultured in Hepes-buffered M2 medium (Sigma). Founder animals are typically intercrossed with C57BL/6 mice to establish lines. Continuous backcrossing (up to 10 times) allows to obtain mice with the transgene expressed on a virtually pure C57BL/6 background that is suitable for behavioral studies. To test the role of the PP2A transgene

[19] D. R. Evans, T. Myles, J. Hofsteenge, and B. A. Hemmings, *J. Biol. Chem.* **274**, 24038 (1999).
[20] A. Luthi, H. Putten, F. M. Botteri, I. M. Mansuy, M. Meins, U. Frey, G. Sansig, C. Portet, M. Schmutz, M. Schroder, C. Nitsch, J. P. Laurent, and D. Monard, *J. Neurosci.* **17**, 4688 (1997).
[21] A. Probst, J. Gotz, K. H. Wiederhold, M. Tolnay, C. Mistl, A. L. Jaton, M. Hong, T. Ishihara, V. M. Lee, J. Q. Trojanowski, R. Jakes, R. A. Crowther, M. G. Spillantini, K. Burki, and M. Goedert, *Acta Neuropathol. (Berl.)* **99**, 469 (2000).

in lesion paradigms, it is more appropriate to backcross onto an FVB background that is susceptible to kainic acid or pilocarpine lesions.

By this approach we are able to obtain transgenic mice with a chronic reduction of PP2A activity in brain. Our results also show that reduced PP2A activity is associated with altered compartmentalization, hyperphosphorylation and ubiquitination of tau, resembling a key pathological finding in AD.[22]

The Dom5 Line

The C-terminal leucine residue of Cα modulates the binding of the B/PR55 subunits through reversible methylation. In *S. cerevisiae*, mutation of Pph22p Leu-377, the equivalent to human Cα Leu-309, to alanine inhibits PP2A activity *in vitro* by preventing the binding of the B/PR55 regulatory subunits to the core dimer of PP2A.[23]

In order to produce transgenic mice that express Cα L309A under the control of a neuron-specific promoter, a yeast plasmid containing a 978 bp *Hin*dIII/*Bam*HI fragment encoding the Cα wild-type allele is fused to a single hemagglutinin epitope located immediately downstream of the start codon. To obtain the L309A amino acid substitution in Cα, the CTG triplet at position 309 is changed to GCG using the QuickChange site-directed mutagenesis kit from Stratagene. The mutated fragment is subcloned into the neuron-specific murine Thy1.2 expression vector.

As for Dom1, the HA-tagged cDNA under the control of the mThy1.2 promoter allows to obtain transgenic mice showing high levels of transgene expression in neurons. In these mice, similar to the Dom1 mice, tau is hyperphosphorylated and translocated to the somatodendritic domain of neurons, suggesting a role of the B/PR55 family in the tau pathogenesis of AD.[24]

Animal Models: PP2A PR65 Dominant Negative Mutant Mice

The scaffolding subunit A/PR65 consists of 15 nonidentical repeats. The first ten repeats bind the regulatory B subunits whereas the remaining are required for binding of the C subunit. The B subunits can only be recruited into the complex when the C subunit is already bound to A.[25] *In vitro* and

[22] S. Kins, A. Crameri, D. R. Evans, B. A. Hemmings, R. M. Nitsch, and J. Gotz, *J. Biol. Chem.* **276**, 38193 (2001).
[23] D. R. Evans and B. A. Hemmings, *Genetics* **156**, 21 (2000).
[24] A. Schild, R. M. Nitsch, and J. Götz (2003), in preparation.
[25] R. Ruediger, M. Hentz, J. Fait, M. Mumby, and G. Walter, *J. Virol.* **68**, 123 (1994).

in vivo studies demonstrated that the mutant AΔ5 lacking repeat 5 binds the C subunit, but not the regulatory B subunits.[25,26]

To generate transgenic mice that express high levels of the dominant negative mutant form of A, AΔ5, in heart, skeletal and smooth muscle, a nine amino acid epitope tag (EE) is introduced by PCR at the 3′ end of the human A subunit-cDNA open reading frame. The cDNA is subcloned into a vector that contains the CMV enhancer, the chicken β-actin promoter, and the rabbit β-globin polyadenylation signal to yield high gene expression in muscle tissue. The DNA is purified from the gel using the DNA purification kit from Qiagen. It is concentrated with an Elutip column (Schleicher & Schuell), precipitated with ethanol and dissolved in 5 m*M* Tris (pH 7.5) and 0.1 m*M* EDTA at a concentration of 2.0 μg/ml. To produce transgenic mice, pronuclei of fertilized CB6 F1 eggs are microinjected with the 3.7-kb fragment at a concentration of 2.0 μg/ml. Surviving embryos are transferred into the oviducts of pseudopregnant ICR mice. By this approach it is possible to obtain AΔ5 transgenic mice in which the ratio of core enzyme to holoenzyme is increased in heart. At day 1 after birth, transgenic mice have an increased heart weight-to-body weight ratio that persists throughout life. End-diastolic and end-systolic dimensions are increased while fractional shortening is decreased. Finally, the thickness of the septum and of the left ventricular posterior wall is reduced.[27]

Protein Phosphatase Activity Measurements

To measure phosphatase activities, total brain extracts are prepared from adult mice with a teflon homogenizer (15 strokes at 100 rpm) in 1x TBS, 1% (v/v) Triton X-100, in the presence of protease inhibitors (Complete™ with EDTA, Roche). This buffer is optimized for PP2A, to inhibit cation-dependent PP2B and PP2C activities. Homogenates are prepared in duplicate and two phosphatase assays are performed with each homogenate using the phosphatase kit V2460 from Promega. Endogenous free phosphate is removed on a Sephadex G-25 column, followed by normalization for protein content. Over a period of 10 min, release of phosphate is measured from a chemically synthesized phosphopeptide (RRA(pT)VA; pT = phosphothreonine).[28] This peptide is a substrate that

[26] R. Ruediger, N. Brewis, K. Ohst, and G. Walter, *Virology* **238**, 432 (1997).
[27] N. Brewis, K. Ohst, K. Fields, A. Rapacciuolo, D. Chou, C. Bloor, W. Dillmann, H. Rockman, and G. Walter, *Am. J. Physiol. Heart Circ. Physiol.* **279**, H1307 (2000).
[28] A. Donella Deana, C. H. Mac Gowan, P. Cohen, F. Marchiori, H. E. Meyer, and L. A. Pinna, *Biochim. Biophys. Acta* **1051**, 199 (1990).

can be dephosphorylated by PP2A, PP2C, and although with substantially lower efficiency, PP2B. PP1, in contrast, does not dephosphorylate peptide substrates at all. The amount of released phosphate is determined by measuring the absorbance of a molybdate : malachite green : phosphate complex at 595 nm. We are able to use this assay to compare phosphatase activities in Dom1 mice with controls. After 10 min of incubation, the assay reveals a reduction in activity of 34% ($n = 6$, SEM = ±3%) in Dom1 mice as compared to control homogenates.[22] A similar decrease of PP2A activity is found in 5 and 12 month-old mice. To further confirm that the measured decrease in phosphatase activity is due to a reduced activity of PP2A, brain homogenates are incubated with okadaic acid (OA), a potent inhibitor of PP2A. Concentrations of 10 n*M* OA induce a half-maximal reduction of phosphatase activity in both wild-type and transgenic brain homogenates, normalized for the respective activities in wild-type and transgenic brain homogenates in the absence of OA. As the ratios remain the same, our data indicate that PP2A, and not another serine/threonine-directed phosphatase, is inhibited in brains of Dom1 mice. Additional assays in the presence of 100 m*M* EGTA have, as compared to standard assay conditions, no influence on the ratio of inhibition, suggesting that PP2B is not a significant contaminant. Together, these data demonstrate that a neuronal, postmitotic expression of Cα L199P is sufficient to induce a chronic, 34% reduction of PP2A activity in brains of transgenic mice.[22]

While the technique described above is well suited for transgenic mice with a generally reduced PP2A activity, as in L199P mutant Dom1 mice, it bears some problems when the total PP2A activity is not affected, and when an altered substrate specificity has to be detected. This is the case for L309A mutant Dom5 mice, since the mutation prevents only the B/PR55 family of regulatory subunits from binding to the core dimer. As a consequence, we expect that in these mice other B subunits are recruited into the dimer that is present at limited amounts. By using the artificial phosphopeptide RRA(pT)VA as substrate, general phosphatase activities are likely to be unaffected. Instead, we expect that B/PR55 subunit-specific substrates, like vimentin, have to be used to monitor changes in substrate-specific PP2A activities in L309A mutant Dom5 mice.

Blastocyst Cultures

PP2A is an essential enzyme as illustrated by the embryonic lethal phenotype of the PP2A Cα null mutant. To further assess PP2A function despite the observed early embryonic lethal phenotype, one may use

embryonic $C\alpha^{-/-}$ stem cells as a source of Cα-deficient cell lines. This can be achieved by three means, either by starting with a heterozygous $C\alpha^{+/-}$ embryonic stem cell line that is transfected with a second targeting construct carrying another selection marker (e.g., hygromycin resistance gene),[29] or by increasing the neomycin concentration to obtain a $C\alpha^{-/-}$ cell line by gene conversation. Alternatively, one can monitor the developmental potential of $C\alpha^{-/-}$ embryos that are derived from $C\alpha^{+/-} \times C\alpha^{+/-}$ matings.[15]

To obtain homozygous $C\alpha^{-/-}$ blastocysts, heterozygous $C\alpha^{+/-}$ female mice are hormonally stimulated with gonadotropins (Veterinaria), and crossed with heterozygous $C\alpha^{+/-}$ male mice. Matings with wild-type male mice are included as controls. Blastocysts are obtained 3.5 days postcoitum by flushing the uterine horns, and are cultured on gelatin-coated plates in DMEM (Gibco BRL) supplemented with 20% fetal calf serum (Eurobio). After 2–4 days, blastocysts lose the zona pellucida, adhere to the culture dishes, and the inner cell mass of the blastocysts becomes visible on top of a layer of trophectodermal cells.

Blastocyst cultures are washed in PBS, fixed with 4% formaldehyde in microtubule stabilization buffer (65 m*M* PIPES, 25 m*M* HEPES, 10 m*M* EGTA, 3 m*M* $MgCl_2$, pH 6.9) for 3.5 hr, washed with 0.1% Triton X-100 in PBS, and incubated three times for 10 min in freshly prepared sodium borohydrate (10 mg/ml). Fixed blastocysts are either dehydrated in 100% methanol for storage at −20°C, or directly processed. For *in situ* immunohistochemistry, blastocyst cultures are fixed in Dent's fixative (Methanol/DMSO = 4 : 1) for 3 hr at 4°C. After blocking with 5% sheep serum (Sigma) and 1% BSA in TBS for 3 hr at room temperature, primary antisera are added in 1% BSA and 0.05% Tween-20 in TBS overnight at 4°C. Following washes in TBS/0.5% Tween-20, the secondary FITC- or Cy5-labeled antisera are added for overnight incubations at 4°C. Labeled blastocysts are washed and mounted in 0.1 *M* Tris–HCl pH 9.5/glycerol (3 : 7) including 50 mg/ml *n*-propyl gallate as anti-fading reagent. Blastocysts are viewed by confocal microscopy to determine the functional consequences of the lack of PP2A Cα.

Advantages and Limitations of the Various Transgenic and Knockout Approaches

The advantages and inherent limitations of the different techniques (Fig. 2) aimed to dissect the function of PP2A *in vivo* are outlined in the following paragraph.

[29] Z. W. Li, G. Stark, J. Gotz, T. Rulicke, U. Muller, and C. Weissmann, *Proc. Natl. Acad. Sci. U.S.A.* **93**, 6158 (1996).

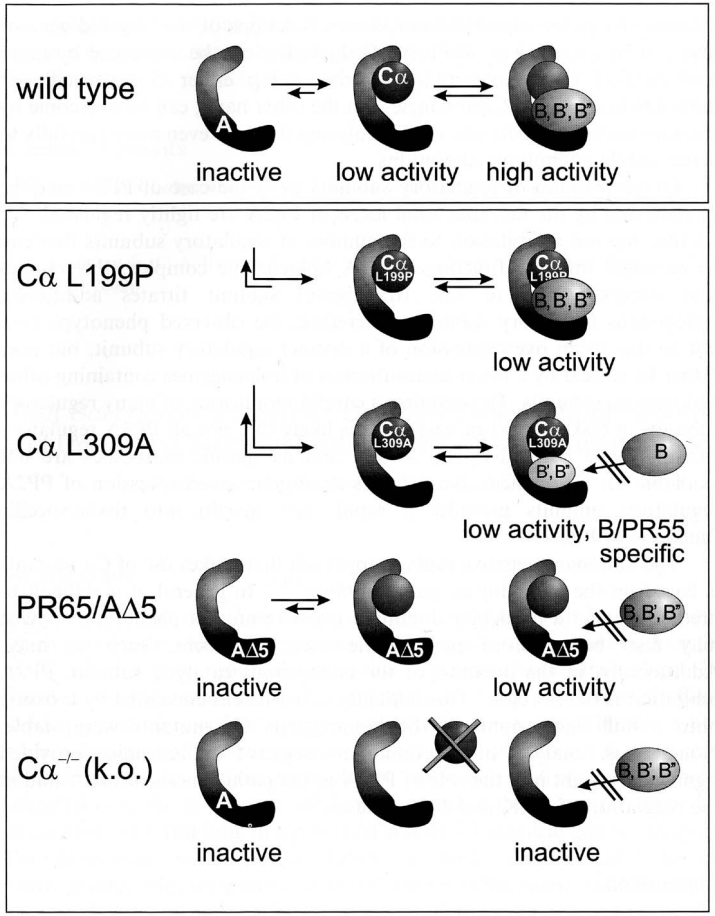

FIG. 2. PP2A subunit composition and activities of the different transgenic and knockout mouse models are summarized.

Knockout approaches in general can have three potential outcomes, either (1) an embryonic or postnatal lethal phenotype (as has been shown for the PP2A Cα knockout[14]), (2) no detectable phenotype due to compensatory mechanisms, or (3) a clear but not life-threatening phenotype

that may be either expected from known functions of the targeted gene or may not be expected at all (Table I). Lethality can be overcome by more sophisticated gene targeting approaches using either tissue-specific or inducible promoters. Redundancies, on the other hand, can be overcome by creating multiple knockouts, or by analyzing the mice even more carefully to detect subtle phenotypic alterations.

Overexpression of regulatory subunits as in the case of PP2A may be complicated by the fact that total levels of PP2A are tightly regulated.[18,30] As this imposes a limitation to the number of regulatory subunits that can be recruited into the functional PP2A holoenzyme complex, this implies that overexpression of one (transgenic) subunit titrates additional, endogenous regulatory subunits. Therefore, the observed phenotype may not be due to an overexpression of a distinct regulatory subunit, but may rather be caused by a lower concentration of holoenzymes containing other endogenous subunits. This requires a careful monitoring of many regulatory subunits, a task that is not easy, as it is likely that not all PP2A regulatory subunits have been identified as yet, and as specific antibodies are not available for all of them. Nonetheless, transgenic overexpression of PP2A regulatory subunits provides a rapid, first insight into tissue-specific functions of PP2A.

The dominant negative mutant approach that makes use of Cα mutants is based on the screening of yeast mutants.[19,23] In general, it is difficult to predict whether a particular dominant negative mutant phenotype in yeast may also be achieved in multiple-tissue organisms, such as mice. Additionally, in the presence of the endogenous catalytic subunit, PP2A inhibition is never 100%. This difficulty could be circumvented by crossing onto a null background, if the homozygous Cα mutants were viable. Nonetheless, analysis of Cα dominant negative mutant mice provided significant insight into the role of PP2A in the pathogenesis of tau,[22] and in the regulation of ERK and JNK kinases.[31]

Conclusion

Considering the putative role of PP2A in the pathogenesis of human diseases, the development of more transgenic and knockout models of PP2A may provide insight into the regulation of PP2A. This may eventually lead to the discovery of therapeutic agents that can specifically counteract PP2A dysfunction. Considering the laborious task of producing and analyzing

[30] S. Wera, A. Fernandez, N. J. Lamb, P. Turowski, M. Hemmings-Mieszczak, R. E. Mayer-Jaekel, and B. A. Hemmings, *J. Biol. Chem.* **270**, 21374 (1995).
[31] S. Kins, P. Kurosinski, R. M. Nitsch, and J. Götz, *Am. J. Pathol.*, in press.

transgenic and knockout mice, the recent advent of RNAi approaches for efficient downregulation of transcription is likely to help in the transgene design, and in the prediction of the expected phenotype.[32]

Acknowledgments

We thank Birgit Ledermann and Jay Tracy for helpful suggestions.

[32] A. M. Silverstein, C. A. Barrow, A. J. Davis, and M. C. Mumby, *Proc. Natl. Acad. Sci. USA* **99**, 4221 (2002).

0076-6879/2003 $35.00

7.2.4 PP2A in learning and memory

Increasing data suggest a role for PP2A and PP1 in hippocampal long-term depression (Bennett et al., 2001; Mulkey et al., 1994; Mulkey et al., 1993; Thiels et al., 2000). Further studies have shown a more direct effect of PP2A on learning and memory. Chronic intraventricular infusion of OA induced spatial memory deficits in rats, associated with PHF-like hyperphosphorylation of tau (Arendt et al., 1995). Deficits in memory retention were found in chicks treated with CA or OA (Bennett et al., 2001), and unilateral microinjection of OA into rat hippocampus induced a transient impairment of spatial memory on an eight-arm radial maze task in rats (He et al., 2001). Not surprisingly therefore, a recent study shows tau hyperphosphorylation and impairment of spatial memory retention after bilateral injection of CA into rat hippocampus (Sun et al., 2003). Yet it is still not clear whether the association of tau hyperphosphorylation and spatial memory loss in rats is a causal one.
Spatial learning and memory need protein phosphorylation and special enzyme participation. It is well known that spatial learning and memory is hippocampus-dependent, and single cells in the hippocampus can encode specific spatial information. However, how each phosphatase functions and the exact mechanism of behavioral abnormalities when the PPs are inhibited still need more consideration.

7.3 Aim of work

As outlined in section 7.2.2 ("PP2A in human diseases"), PP2A could be a cofactor responsible for the development of human neurodegenerative diseases with tau aggregation such as AD. Therefore the aim of my work was to understand in more detail the function of PP2A in brain pathology and its regulation by regulatory B/PR55 subunits.
Previous work in our lab aimed at understanding PP2A function by gene targeting of Cα in mice, which was embryonically lethal (Gotz and Kues, 1999; Gotz et al., 1998; Gotz et al., 2000; Gotz and Schild, 2003). To circumvent lethality and to address PP2A function in brain, we used a dominant negative mutant approach. We expressed the Cα mutant L199P in brain of transgenic mice. PP2A activity was reduced to 66%, causing endogenous tau to be abnormally phosphorylated at the epitopes Ser202/Thr205 and Ser422, and ERK and JNK to be activated (Kins et al., 2001; Kins et al., 2003; p. 28 and Fig. 2 p. 32).
As described in section 7.2.4 ("PP2A in learning and memory"), PP2A deficits are likely to cause impaired LTP, learning and memory. Therefore, the CαL199P mutant mice were tested in a set of behavioral tasks mainly addressing memory deficits through impairment in the hippocampus (Morris water maze), but also the amygdala (fear conditioning). As the L199P mutation is in the catalytic core of Cα, it has been shown *in vitro* to abolish the catalytic activity without affecting holoenzyme assembly (Evans et al., 1999) (but see: (Ogris et al., 1999; Yu et al., 2001)). To elucidate the function of distinct regulatory B subunits in targeting and activating PP2A towards its substrates, the Cα mutant L309A was expressed in transgenic mice using the neuron specific

promoter Thy1.2 (p. 28 and Fig. 2 p. 32). In addition, in collaboration with Dr. B. Hemmings' group at the Friedrich Miescher Institute (FMI) in Basel, gene targeting of several of the PP2A regulatory subunits of the B/PR55 family was initiated. We concentrated on the PR55γ subunit, since its high and almost exclusive expression in brain made it the most interesting PR55 subunit in regard to tau phosphorylation in brain, with a potential involvement in AD and other tauopathies (Schmidt et al., 2002) (see section 8.2 p. 41). The function of B/PR55 regulatory subunits was also addressed by applying the very novel technology of short interfering RNA (siRNA) to stably and specifically knock down mRNA levels in human neuroblastoma and kidney cells.

8 RESULTS

8.1 Behavioral analysis of PP2A/Cα(L199P) transgenic mice

Transgenic mice expressing the dominant negative L199P mutation in the catalytic subunit Cα of PP2A and wild-type (WT) littermates as a control group were tested in spatial learning tasks using two different protocols of the Morris water maze test. Previous experiments with these transgenic mice revealed a 30% reduction of PP2A activity in brain homogenates, together with abnormally phosphorylated endogenous tau that was partly relocated to the somatodendritic compartment. Also these mice were the first transgenic mouse model showing that PP2A is an *in vivo* phosphatase of tau (Kins et al., 2001).

To exclude motor deficits that could disturb the evaluation of learning and memory capacity, L199P and WT mice were tested for their ability to maintain balance on the rotarod at accelerating rotation speeds of up to 40 rpm.

8.1.1 L199P transgenic mice show modest learning deficits

In a first Morris water maze test, the acquisition phase consisted of 4 days with 6 trials each (Figure 7). On the 5th day, the platform was removed and the time every mouse stayed in the target and the opposite quadrant were measured for one minute (called probe trial; Figure 8). After two days of rest, the platform position was changed to the opposite quadrant and the mice had to relearn the new platform position in an acquisition phase consisting of 3 days with 6 trials per day (Figure 7). On day four, the platform was again removed and memory retention was examined in a single 60 sec trial (Figure 8). The time required finding the platform during acquisition and the time spent in quadrants in the probe trial was determined as a measure of learning success.

In the first and second acquisition phases, L199P mice showed a similar performance as WT littermates. Both groups learned to navigate using spatial cues and found the platform on average within 20 s in the last two trials of the first acquisition phase, and in trials 10 to 18 of the second acquisition phase, respectively. While there is no major difference in the learning of the first platform position between transgenics and wild-types, the second acquisition phase with a reversed platform position reveals that the transgenic mice had some difficulties to navigate to the platform in the first trials on the second day (trials 7-9). This effect disappeared in the following trials, in which mice of both groups performed very well.

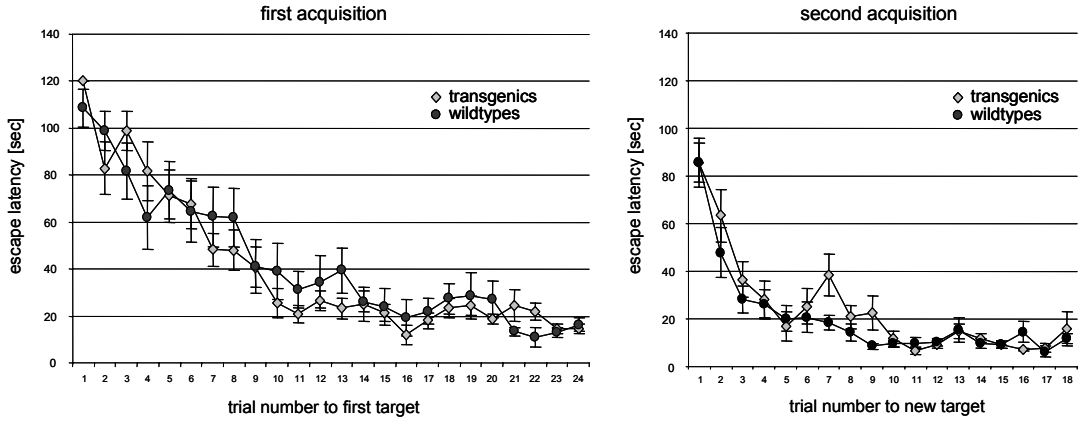

Figure 7: Similar performance of transgenic and WT mice in the acquisition of a target in the Morris water maze. Escape times were measured for each trial, 6 trials per day. The graphs show mean escape latencies of 9 transgenic (light grey) and 18 WT littermates (black). Error bars represent standard errors (SEM).

Two probe trials, one after the acquisition phase for each platform position, were analyzed for the time spent in the target and opposite quadrants. Animals were observed for one minute and the times spent in each quadrant were calculated as per cent (Figure 8). By spending more than 25% of time (chance) in the target quadrant, again both groups of mice showed that they can navigate and have learned the platform position very well. But while WT mice search the platform in the correct quadrant more than 50% of the time in the first probe trial, L199P mice spent significantly less time in the target quadrant (P=0.01). This finding does not project 1:1 to the opposite quadrant (P=0.12), which indicates that the time L199P mice do not search in the target quadrant must be equally spent in all remaining quadrants (Figure 8). The results of the probe trial for the second reversed platform position resemble the ones for the first position. Transgenic mice spent less time in the quadrant of the new platform position (Figure 8). This effect is somewhat less pronounced than in the first probe trial (P=0.05), but on the other hand, in this trial L199P mice spent significantly more time in the opposite quadrant, where the old target had been (P=0.04) (Figure 8). This could indicate that transgenic mice confounded the task of learning a new platform position with the search for the old position, an effect that could have caused the differences observed on day 2 of the second acquisition phase (Figure 7).

To confirm these significant but rather small behavioral differences between L199P and WT mice, I adapted a more sophisticated learning-capacity test for the water maze described by the group of Richard Morris (Chen et al., 2000). The main difference was that each mouse had to search for five different platform positions drawn from a set of 20 possible locations whereas the performance criterion to get a new platform position was three trials in a row with an average escape latency of less than 15 s. The maximum number of trials was 40 for location 1, and 32 trials thereafter, therefore the maximal duration of the test was 21 days.

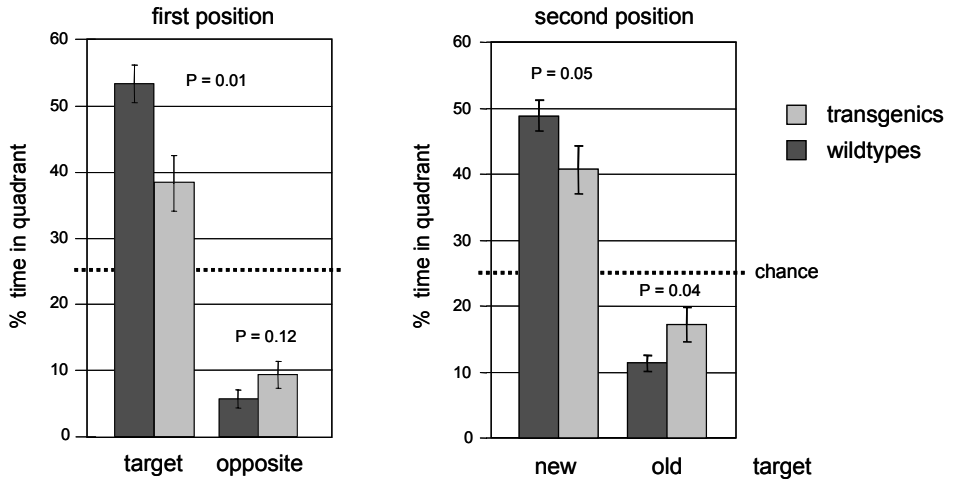

Figure 8: Transgenic mice perform worse in probe trials in the Morris water maze. After acquisition, the time each mouse spent in target and opposite quadrants, and new and old quadrants, respectively during one minute were analyzed. The graphs show the average time per cent 9 transgenic (light grey) and 18 WT littermates (black) spent in quadrants. Error bars represent standard errors (SEM). By spending more than 25% of time (chance) in the target quadrant, both groups showed that they can navigate and have well learned the platform position. But while WT mice search the platform in the correct quadrant more than 50% of the time in the first probe trial, L199P mice spent significantly less time in the target quadrant (P=0.01). In the search of the second reversed platform position, transgenic mice spent less time in the quadrant of the new platform position (P=0.05) and spent significantly more time in the opposite quadrant, where the old target had been (P=0.04).

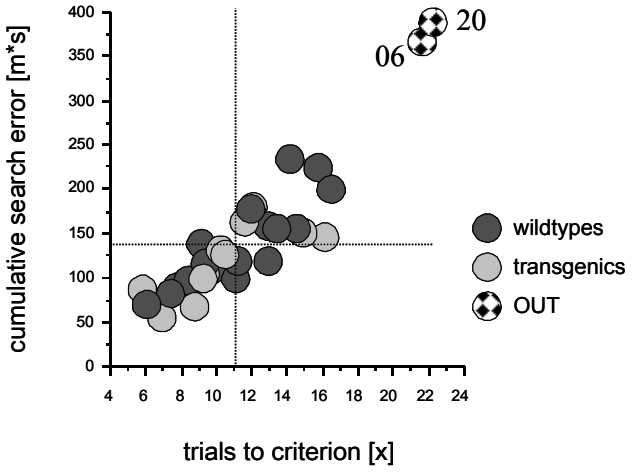

	TTC	CSE
mean	10.94	133.1
STD	2.99	45.7
SEM	0.555	8.49
count	29	29
min.	5.670	56.45
max.	16.40	234.6

Descriptive statistics inclusion criteria

Figure 9: Bivariate scattergram split by groups and descriptive statistics inclusion criteria. Trials to criterion [x] (TTC) of mice numbers 06 and 20 are 3.3 standard deviations (STD) above mean while the cumulative search error [m*s] (CSE) of mice 06 and 20 are 5.3 STD above mean. These two mice (numbers 06 and 20) can therefore be excluded from the analysis. The inclusion criteria for all mice (29, "count") are summarized in the table. SEM, standard error of mean; min., max., minimum and maximum values included. The dotted lines represent the mean values. (in collaboration with Dr. D. Wolfer)

Inclusion criteria were set such that a mouse that performed very badly, as described by the number of trials to criterion and the cumulative search error, was excluded from the analysis (Figure 9). Trials to criterion of mice numbers 06 and 20 were 3.3 standard deviations above mean while their cumulative search errors were 5.3 standard deviations above mean. These two mice were therefore excluded from the analysis. Descriptive statistics inclusion criteria and a bivariate scattergram split by groups for all mice are shown in Figure 9.

The more sophisticated relearning paradigm revealed that transgenic L199P mice navigate less precisely than WT littermates (Figure 10). These effects were statistically significant but small and they were only captured by path geometry directly. They do not translate into a general escape performance and therefore I can say that the navigation problem does not appear to be linked specifically to the continuous relearning situation (Figure 10). I could as well observe that transgenics adapted normally to the test, that thigmotaxis, indicating that a mouse is constantly swimming along the wall of the pool, was not increased, and that the tendency to float was even smaller for L199P mice. In contrast, the average swim speed was significantly increased in transgenics (P=0.04) (Figure 10).

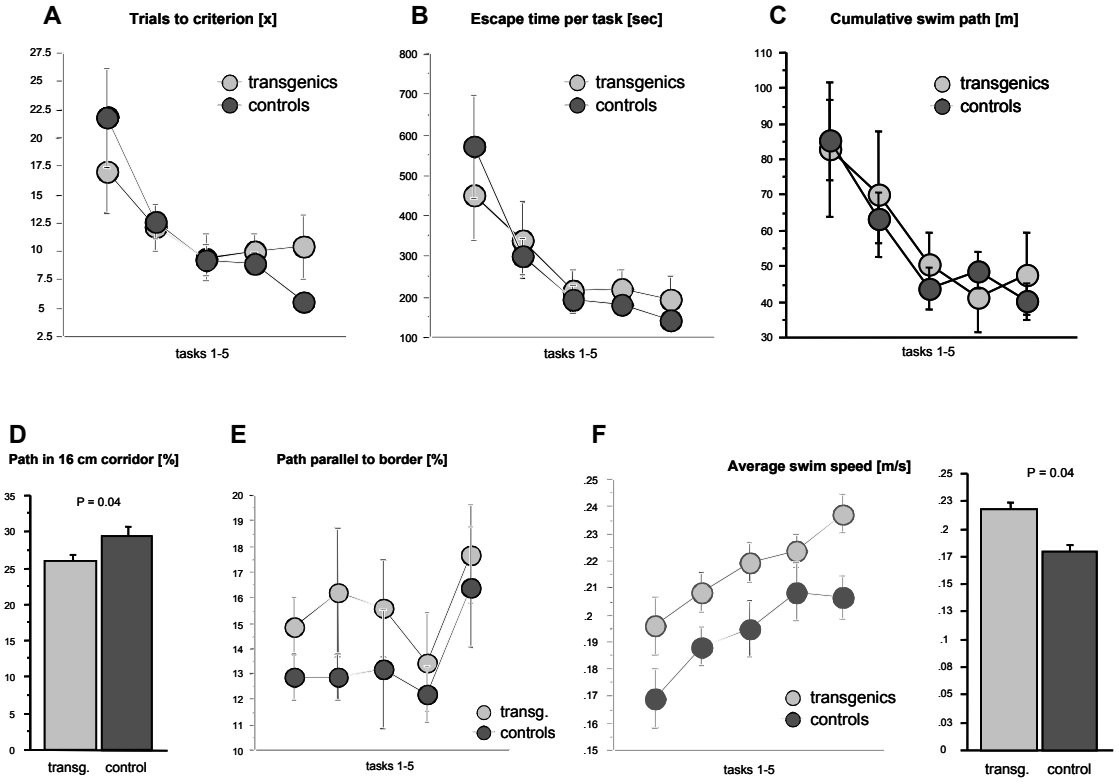

Figure 10: L199P mice navigate less precisely as captured by path geometry. A more sophisticated relearning water maze protocol shows that the general escape performance as measured by the number of trials to criterion (*A*), the escape time per task (*B*), and the cumulative swim path (*C*) was not different in the two groups analyzed. In contrast, parameters describing path geometry as the path in 16 cm corridor (*D*) and the path parallel to border (*E*) revealed that transgenic L199P mice navigate less precisely than WT littermates. These effects were statistically significant but small. The average swim speed increased in both groups over all trials and was significantly increased in transgenics (P=0.04) (*F*). (in collaboration with Dr. D. Wolfer)

Finally L199P and WT mice were analyzed in a fear conditioning test. During fear conditioning, subjects learn to associate a neutral stimulus (CS) or training situation (context) with a coinciding painful stimulus (US). Subsequently, learning performance and fear-related behavior can be analyzed in the conditioned subject. The amygdale has been shown to be required for both the acquisition and expression of a learned fear response to explicit cues or a context (LeDoux, 2000; Repa et al., 2001). The hippocampus is not required to associate a single cue such as a tone with foot shock, provided that the two stimuli overlap temporally, contextual and cued fear conditioning however requires the intact hippocampus (Bach et al., 1995; Chen et al., 1996).

The L199P mice tested did not show any differences in context and emotional learning. This is not particularly surprising since other groups have found largely intact fear conditioning despite severe learning deficits in other tasks (Minichiello et al., 1999).

8.2 PP2A in the wild-type mouse

To increase our understanding of the function of PP2A in the mouse under physiological conditions, the following study was carried out. It was designed to obtain the necessary information to interpret the phenotype in PP2A transgenic and knockout mouse models.

European Journal of Neuroscience, Vol. 16, pp. 2039–2048, 2002

Diversity, developmental regulation and distribution of murine PR55/B subunits of protein phosphatase 2A

Karsten Schmidt,[1,†] Stefan Kins,[2,*,†] Andreas Schild,[2] Roger M. Nitsch,[2] Brian A. Hemmings[1] and Jürgen Götz[2]
[1]Friedrich Miescher Institute, Maul beerstrasse 66, 4058 Basel, Switzerland
[2]Division of Psychiatry Research, University of Zurich, August Forel Str. 1, 8008 Zürich, Switzerland

Keywords: Alzheimer's disease, brain, holoenzyme, spinocerebellar ataxia, splice variant, WD-40 repeat

Abstract

Protein phosphatase (PP2A) 2A is a hetero-trimeric holoenzyme that consists of a core dimer composed of a catalytic subunit that is tightly complexed with the scaffolding subunit PR65/A. This core dimer associates with variable regulatory subunits of the PR55/B, PR61/B′, PR72/B″ and PR93/PR110/B‴ families. As PP2A holoenzymes containing PR55/B have been shown to be involved in the pathogenesis of Alzheimer's disease, we characterized the PR55/B family with particular emphasis on its distribution and expression in the brain. We determined the genomic organization of all members of the PR55/B family and cloned their murine cDNAs. Thereby, two novel splice variants of PR55/Bβ were identified. In addition, Northern blot analysis revealed multiple transcripts for the different PR55 subunits, suggesting a higher variability within the PR55 family. *In situ* hybridization analysis revealed that all PR55/B subunits were widely expressed in the brain. PR55/Bα and Bβ protein expression varies significantly in areas of the brain affected by neurodegenerative diseases such as the hippocampus or cerebellum. At the cellular level, PR55/Bβ protein expression was confined to neurons, whereas PR55/Bα was also expressed in activated astrocytes indicating that the PR55 isoforms confer a different function to the holoenzyme complex. As PP2A dysfunction has been demonstrated to contribute to various human diseases, dissecting the PP2A holoenzyme and its particular function in different cell types will assist in the development of novel therapeutic strategies.

Introduction

Protein phosphatase 2A (PP2A, *PPP2*) is one of the major serine/threonine-specific phosphatases which, together with PP1 (protein phosphatase 1), PP2B (calcineurin), and PP2C, is involved in many diverse cellular processes (Millward *et al*., 1999).

Several holoenzyme complexes of PP2A have been isolated from a variety of tissues and have been extensively characterized. The core enzyme is a dimer, consisting of a highly conserved catalytic subunit (C) and a structural scaffolding subunit (PR65/A) that forms complexes with variable regulatory B subunits. Four families of B subunits have been identified so far, termed PR55/B, PR61/B′, PR72/B″ and PR93/PR110/B‴ (Janssens & Goris, 2001). A striking feature of the regulatory subunits is the lack of sequence similarity between these families, despite the recognition of similar sequence motifs within the A subunit. Due to the expression in mammals of at least two A, two C, four B, at least eight B′, four B″, and two B‴ isoforms, a total of approximately 75 PP2A holoenzymes can be generated. Taking the different splice variants into account, even more holoenzymes can be formed (Janssens & Goris, 2001). This complexity, in addition to post-translational modifications including phosphorylation and methylation of the C subunits, provides a vast variety of possibilities for the regulation of PP2A activity. Many substrates of PP2A have been described, including the microtubule-associated protein tau (Gong *et al*., 1994). Hyperphosphorylated forms of tau form insoluble intracellular deposits in several human neurodegenerative diseases including Alzheimer's disease (AD) (Gotz, 2001). Previous studies have shown that in brain homogenates of AD patients, PP2A activity was 30% lower than in those of control subjects (Gong *et al*., 1995) and, of five subunits analyzed, PP2A Cα, PR55/Bγ and PR61ε mRNA expression was quantitatively decreased in the CA3 region of the hippocampus (Vogelsberg-Ragaglia *et al*., 2001). A role for PP2A in tau dephosphorylation is also supported by the finding that PP2A is localized on microtubules and that it binds directly to tau (Sontag *et al*., 1999). In particular, PP2A holoenzymes containing regulatory subunits of the PR55/B family were shown to bind and dephosphorylate tau very efficiently (Goedert *et al*., 1992; Sontag *et al*., 1999). Recent findings in subjects with spinocerebellar ataxia, in whom an expanded CAG repeat has been identified immediately upstream of the PR55/Bβ gene, indicate that dysregulation of PR55 may have functional consequences in neurodegenerative disorders (Holmes *et al*., 1999).

Genetic approaches in mice will play an integral role in understanding PP2A function *in vivo* (Janssens *et al*., 2001). To provide a framework for the interpretation of phenotypes of mice that either lack PP2A subunits (Gotz *et al*., 1998; Gotz *et al*., 2000) or display an altered PP2A composition or activity (Kins *et al*., 2001; Planel *et al*., 2001), we determined the genomic organization, identified novel splice variants and analyzed the mRNA and protein expression of the PR55/B regulatory subunits of PP2A in different tissues, in particular the brain.

Correspondence: Dr Jürgen Götz, as above.
E-mail: goetz@bli.unizh.ch

**Present address*: Center of Molecular Biology, University of Heidelberg, Im Neuenheimer Feld 282, 69120 Heidelberg, Germany

†K.S. and S.K. contributed equally to this work.

Received 15 May 2002, revised 16 August 2002, accepted 13 September 2002

doi:10.1046/j.1460-9568.2002.02274.x

Materials and methods

PR55 cDNA cloning

Different mouse brain cDNA libraries were screened to isolate cDNA clones of the three PR55/B isoforms that have been previously described in humans (α, β, and γ) (Mayer *et al.*, 1991), and a fourth isoform (σ) that has been identified in the rat (Strack *et al.*, 1999). In addition, the human sequences of the PR55/B isoforms were used to search murine expressed sequence tags (ESTs) in the NCBI nucleotide database. From EST libraries (Incyte Genomics, St. Louis, Missouri, USA and Invitrogen, Paisley, UK), a full-length IMAGE cDNA clone for PR55/Bα (thymus, accession # aa111189) and two splice variants for PR55/Bβ termed PR55/Bβ.1 (testis, EST accession # aa108896, GeneBank accession # AS512670) and PR55/Bβ.2 (lung, EST accession # bi150825, GeneBank accession # AF536771) were obtained. PR55/Bγ was obtained from a λ ZAPII mouse brain library (Stratagene, La Jolla, California, USA) by screening with a human cDNA probe at low stringency. PR55/Bβ and σ cDNAs were isolated by isoform-specific PCR amplification of the Marathon-Ready mouse brain cDNA library (Clontech, Palo Alto, California, USA). Nucleotide sequences were determined by automated sequencing (ABI PRISM 3700, Applied Biosystems, Foster City, California, USA).

BAC genomic clones and chromosomal localization

The cDNAs encoding the PR55/B subunits were used to screen a mouse BAC library constructed from 129/SvJ genomic DNA (Genome Systems, Palo Alto, California, USA). A BAC sublibrary was screened to establish the genomic organization of PR55/Bα. Positive clones were identified by filter hybridization using the corresponding ^{32}P-labelled cDNA fragments. A 20-kb PR55/Bα *Eco*RI fragment covering exons 4–10 was subcloned and sequenced. The complete genomic organization of PR55/Bα, β, and the partial organization of γ and σ was assembled by a Blast screening of the Ensembl murine database. The Ensembl database was also used to determine the chromosomal localization of the four PR55/B genes.

Northern blot analysis

Two micrograms of polyA$^+$ mRNA derived from different tissues of adult 3-month-old Balb/c mice and four embryonic stages of Balb/c mice (Clontech) were prehybridized at 50 °C for 4 h in Express Hybridization buffer (Clontech) complemented with denatured and sonicated salmon sperm DNA (100 mg/mL), and sequentially hybridized with ^{32}P-labelled PR55/B subunit-specific 45 bp-long antisense oligonucleotides

(α: 5′-tatctgcttctgctacgtcatcatctactgctcctttcacctgag-3′,
β 5′-gttgaattctaccgtagagataatgtcagctgtgaagggcttcat-3′,
γ 5′-agtggagatgacgtcagcttctgtcacatagctgtggtcccgcag-3′,
σ 5′-tattggaacccgtagtgccgtaattctaaatgggtctcgaagtcg-3′).

The β antisense probe hybridizes to all PR55/Bβ transcripts including β.1 and β.2. A random-primed 2-kb human β-actin cDNA probe was used for normalization. The blots were washed sequentially using increasingly stringent conditions. The final wash was performed at 60 °C for 30 min in a buffer containing 0.1 × SSC and 0.1% SDS, conditions used previously to differentiate between highly homologous transcripts (Kins *et al.*, 2000; Ramming *et al.*, 2000). Finally, the membranes were exposed to Biomax films (Kodak) for 10–60 h at –70 °C.

In situ *hybridization*

Wild-type mice were anaesthetized with a mixture of 2% Rompun (Xylazinum, Bayer Leverkeusen) and 10% Ketaminal 10 (Vererinaria AG, Zürich, Switzerland), transcardially perfused with PBS containing 4% paraformaldehyde, postfixed overnight at 4 °C, and paraffin embedded. Sections (7 μm) were dried overnight at 42 °C on coated glass slides, dewaxed and permeabilized by acid treatment (0.1 M HCl for 10 min), followed by a proteinase K treatment (10 μg/mL) for 10 min at 37 °C. After acetylation with 0.1 M triethanolamine and 0.4% acetic anhydride (20 min at room temperature), sections were incubated for 1 h at room temperature in hybridization buffer (25% deionized formamide, 4 × SSC, 5 × Denhardt's reagent, 0.25 mg/mL yeast tRNA, 10% dextransulphate, 50 mM dithiothreitol, 1 mM EDTA, 0.5 mg/mL salmon sperm DNA in 50 mM phosphate buffer pH 7). The sections were hybridized overnight at room temperature in hybridization buffer with DIG-labelled 45 bp antisense oligonucleotide probes and the complementary sense probes. Sections were washed at 37 °C in solutions of decreasing salt concentrations (2×, 1×, 0.2 × SSC), blocked with 2% (v/v) normal sheep serum, and incubated with an anti-DIG antibody conjugated to alkaline phosphatase (Roche, Basel, Switzerland) in 100 mM Tris/HCl pH 7.5, 150 mM NaCl, 0.1% Triton X-100, and 1% normal sheep serum. Alkaline phosphatase activity was visualized with staining solution (100 mM Tris/HCl pH 9.5, 100 mM NaCl, 50 mM $MgCl_2$, 1 mM levamisole, 450 ng/μl NBT, and 175 ng/μl BCIP) for 2–14 h. After washing, slides were mounted in Mowiol (Hoechst, Frankfurt, Germany).

Western blot analysis

To determine the specificity of the PR55/B-specific antibodies, COS cells were transfected with constructs encoding HA-tagged PR55/Bα, PR55/Bβ, and PR55/Bγ, and lysates analyzed by Western blotting. To ascertain the tissue distribution of PR55/Bα and PR55/Bβ, murine tissues were homogenized in TBS containing protease inhibitors (Complete® containing EDTA, Roche). Triton X-100 was added to a final concentration of 1%, and the homogenate was mixed in an overhead incubator for 1 h at 4 °C. After centrifugation at 5000 ***g*** for 5 min at 4 °C, the supernatant was used for Western blot analysis. As a control, recombinant PR55/Bα was loaded. For subfractionation, brains were homogenized in 10 mM Tris pH 7.5, 1 mM EGTA, 1 mM EDTA, and 1 mM dithiothreitol in the presence of protease inhibitors. The homogenate was centrifuged at 100 000 ***g*** for 60 min, and the supernatant (S1, cytosolic proteins) was removed. The pellet was rehomogenized in 10 volumes of homogenization buffer plus 1% Triton X-100 and centrifuged as before. The supernatant (S2, membrane fraction) was removed, and the pellet was resuspended in 10 volumes of homogenization buffer (P2, cytoskeletal proteins) (McNeill & Colbran, 1995; Strack *et al.*, 1998). Protein concentrations were determined with the DC-protein assay (Bio-Rad, Hercules, California, USA) following the instructions of the manufacturer. Proteins (40 μg) were separated on 10–20% tricine gradient gels (Novex), and transferred to Hybond ECL membranes. Ponceau stainings of the membranes were included to confirm loading of similar amounts of protein. Blots were developed with the following rabbit antisera: anti-β-actin (Abcam, Cambridge, United Kingdom, 1 : 5000), anti-GAPDH (BioDesign, Saco, Maine, United States, 1 : 500), anti-APP (Amyloid precursor protein, C-terminal, Sigma, 1 : 400), anti-phospho-APP (Thr668 phosphorylated, Cell Signalling, Beverly, MA, USA, 1 : 1000), anti-GFAP (Innogenex, San Ramon, California, USA 1 : 300), anti-PP2A/Bα 14–57 (Calbiochem, 1 : 200), anti-PP2A/Bβ 2–14 (Calbiochem, 1 : 200), anti PP2A/Bγ 53–66 (Calbiochem, 1 : 200), and anti-PP2A/Cα #45 (Gotz & Kues,

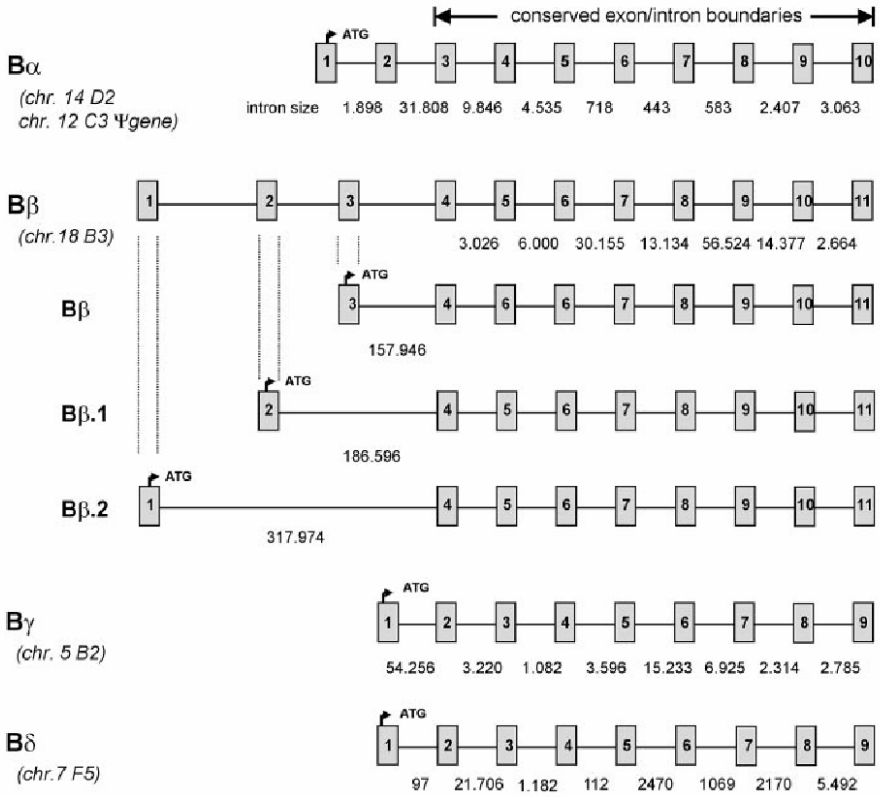

FIG. 1. Genomic structure and chromosomal localization of the four murine PR55/B isoforms including the novel PR55/Bβ.1 and PR55/Bβ.2 splice variants. Exon/intron boundaries of the final eight exons are conserved in each isoform and the PR55/Bβ splice variants. Boxed numbers represent the exons, and the size of the introns is indicated. The first coding exon of each isoform is indicated by an arrow.

1999), and HRP-conjugated secondary antibodies as described (Kins *et al*., 2001).

Immunohistochemistry

Brains from three-month-old wild-type mice were used for immunohistochemical analysis. Animals were anaesthetized as described above and perfused transcardially with 4% paraformaldehyde in sodium phosphate buffer. Sections (40 μm) were cut on a vibratome and permeabilized with 0.1% NP-40 (Calbiochem), using standard published procedures (Gotz *et al*., 1998; Kins *et al*., 2001). Some of the sections were pretreated either with 5 μg/mL proteinase K or 0.1% Triton X-100 in TBS or PBS at 37 °C for 2.5 min for signal enhancement. The PR55/Bα and PR55/Bβ antisera (Calbiochem) were used at 1 : 200 dilutions, anti-GFAP mouse monoclonal (Innogenex, San Ramon, California, USA) at 1 : 1000, and the mouse monoclonal anti-MAP-2 (Chemicon, Temecula, California, USA) at 1 : 200. For peroxidase/DAB stainings, secondary antibodies were obtained from Vector Laboratories (Burlingame, California, USA, Vectastain ABC kits PK-6101 and PK-6102). For immunofluorescence, secondary antibodies were obtained from Molecular Probes (Eugene, Oregon, USA, ALEXA-FLUOR™ series). Sections were dehydrated in an ascending series of ethanol and flat-embedded between glass slides and coverslips in Eukitt (Kindler, Germany).

Results

Cloning of all murine PR55/B subunits and two novel splice variants

Four murine cDNAs encoding the PR55/Bα, β, γ, and σ subunits were identified, as well as two novel splice variants, β.1 and β.2 (Fig. 1). PR55/Bα was obtained as an IMAGE mEST clone (accession # 111189, from thymus). In addition, a PR55/Bα pseudogene was identified in a genomic database with exons 3–10 fused. The nucleotide sequence contained many point mutations, indicating that the pseudogene is not functional. PR55/Bβ was isolated by isoform-specific PCR amplification of a mouse brain cDNA library (Clontech). In addition, two PR55/Bβ splice variants were identified, encoding amino-terminally spliced variants of the β

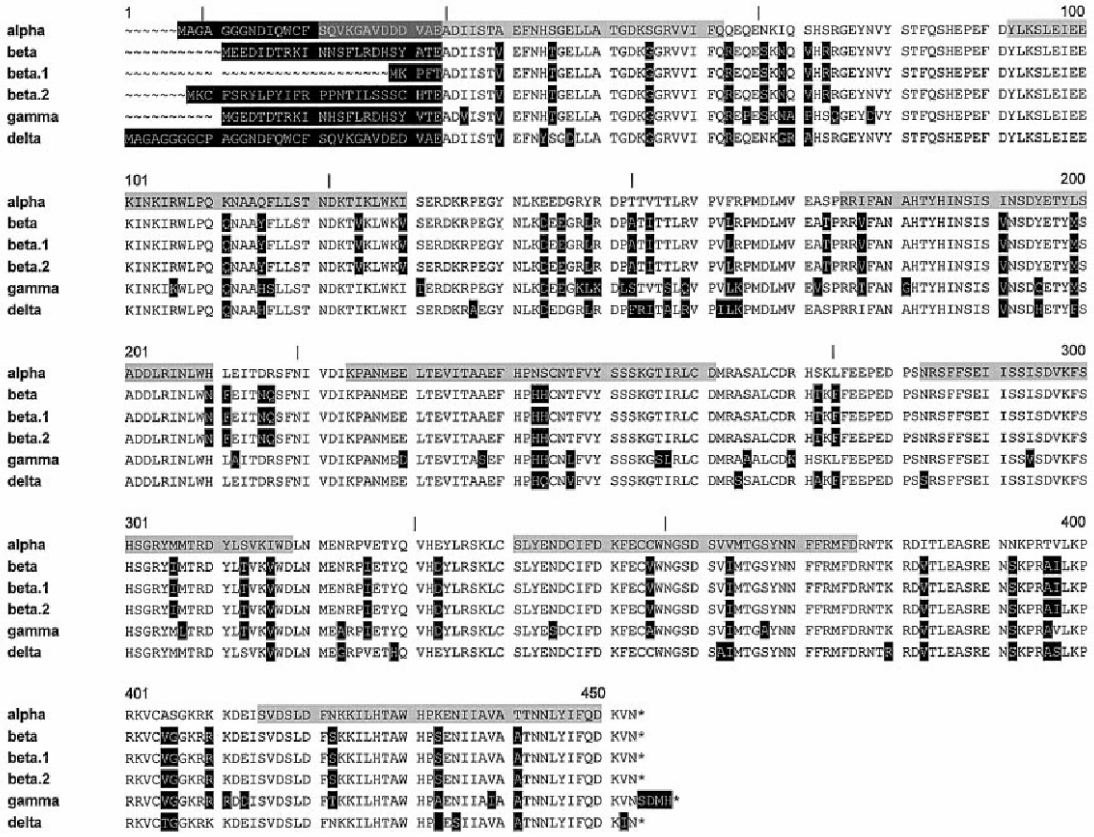

FIG. 2. Alignment of the amino acid sequences of the murine PR55/B isoforms. The highly diverse amino-terminus is highlighted in black. The overall sequence similarity is in the range of 90%, and amino acid differences are highlighted in black using Bα as reference. The WD-40 repeat motifs are shown in light grey whereas the overlap of the PR55/Bα N-terminus with the first WD-40 repeat is highlighted in dark grey. The exon boundaries are indicated with vertical lines for PR55/Bα.

subunit that do not result in a shift of the open reading frame (ORF). PR55/Bγ was isolated from a λ ZAPII mouse brain library (Stratagene), and PR55/Bσ was isolated by tissue-specific PCR from a mouse brain cDNA library (Clontech). All mRNA and corresponding protein sequences were compared to those obtained in other species. Alignment of the murine protein sequences revealed, as for other species, a high degree of sequence conservation of the four subunits, with the exception of a highly diverse amino-terminus (Fig. 2). The overall sequence identity is in the range of 90%, the interspecies conservation of the individual subunits is between 94% (α) and 97% (γ), when compared to the human isoforms.

The genomic organization of PR55/B subunits is highly conserved

Specific cDNA probes were used to screen a mouse BAC library constructed from 129/SvJ genomic DNA. We isolated three PR55/Bα clones, and one each for PR55/Bβ and PR55/Bγ. The genomic organization was established by restriction enzyme analysis and Southern blotting. A 20-kb *Eco*RI fragment of the α isoform containing exons 4–10 was subcloned and sequenced. The genomic maps of the remaining isoforms were partially established *in silico* (Fig. 1). The size of the introns was determined based on publicly available sequence data. Some of the introns are quite large, which is indirectly supported by the finding that the respective genes are not present in their full length on single BAC clones.

PR55/Bα is localized on chromosome 14D2, the likely PR55/Bα pseudogene on chromosome 12C3, PR55/Bβ on chromosome 18B3, PR55/Bγ on chromosome 5B2, and PR55/Bσ on chromosome 7F5.

Alignment of the cDNA and genomic sequences of the PR55/B isoforms revealed that the exon/intron boundaries of the final eight exons are conserved for each isoform, the PR55/Bβ splice variants, and when compared with other species. The *PR55/Bα* gene consists of 10 coding exons, whereas all other isoforms have nine coding exons. The transcription start site for the splice variant PR55/Bβ.2 is

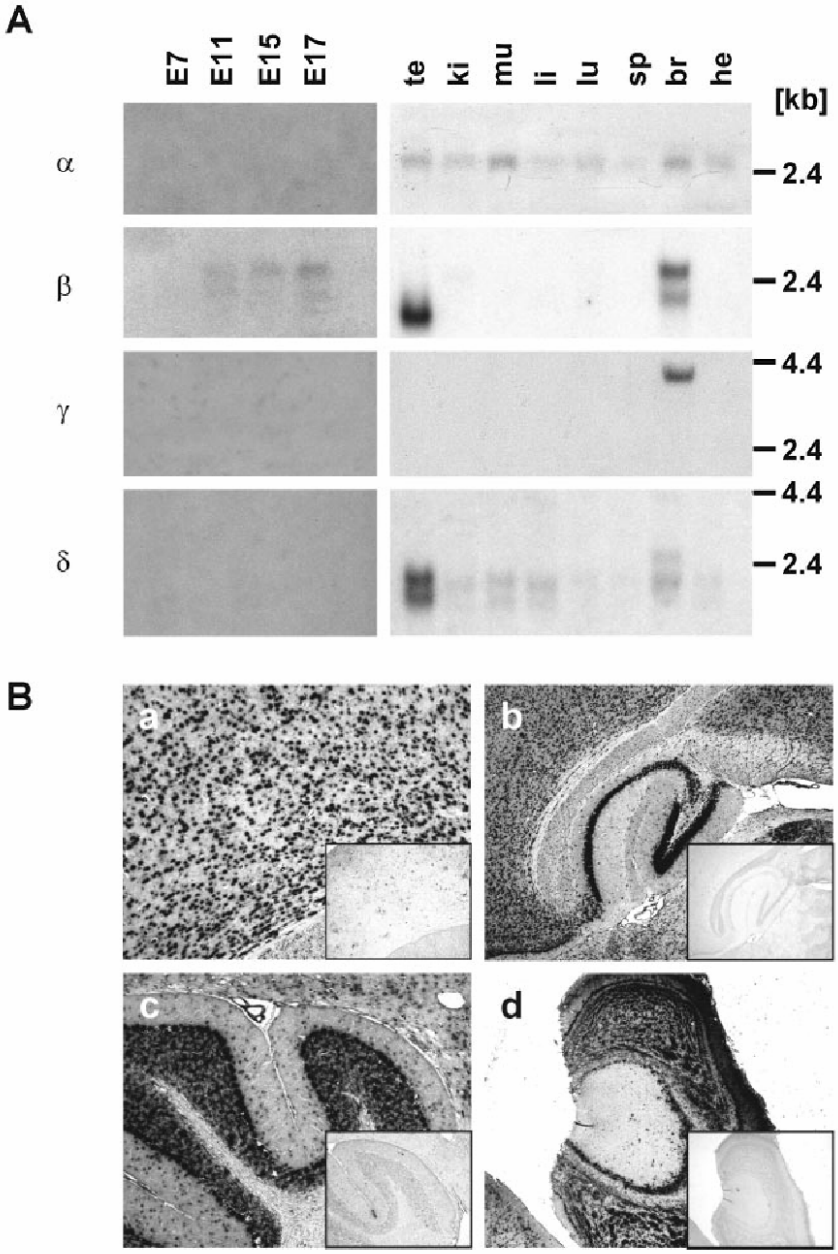

FIG. 3. (A) Embryonic and tissue-specific distribution of murine regulatory PR55/B subunit mRNAs. Blots with mRNA of different embryonic stages or multiple tissues were hybridized with probes directed against PR55/B α, β, γ, and σ subunit transcripts, respectively. E7, embryonic day 7; te, testis; ki, kidney; li, liver; lu, lung; sp., spleen; br, brain; he, heart. (B) The distribution of the PR55/Bα subunit mRNA is shown by *in situ* hybridization analysis of cortex (a), hippocampus (b), cerebellum (c), and olfactory bulb (d). No significant staining was obtained using the corresponding sense probes on adjacent sections (insets).

on exon 1, followed by the start codon for PR55/Bβ.1 on exon 2, and the start codon for PR55/Bβ on exon 3. Alignment of the murine sequences revealed that all isoforms, including the novel PR55/Bβ.1 and PR55/Bb.2 isoforms, contain a structural WD-40 repeat motif of five to seven imperfect repeats, depending on the stringency of the parameters, as in humans (Fig. 2).

High diversity of PR55/B mRNAs

We performed a Northern blot analysis using isoform-specific probes, to determine the mRNA expression of PR55/B (Fig. 3A). The β antisense probe hybridizes to all PR55/Bβ transcripts including β.1 and β.2. No transcripts were detected for α, γ, or σ in mice at embryonic days E7, E11, E15, or E17. In contrast, a 2.5-kb β transcript was detected as early as embryonic day E11, with increasing levels until E17. Hybridization of multiple tissue Northern blots revealed a PR55/Bα transcript of 2.5 kb in all tissues examined, similar to the expression pattern in humans (Mayer *et al.*, 1991). Likewise, PR55/Bσ was expressed in all tissues. In testis, two mRNA species of 2.1 and 2.3 kb were found, whereas in all other tissues 2.0 and 2.2 kb transcripts were present. However, in brain, an additional transcript of 2.5 kb was detected. A major PR55/Bβ transcript of 2.5 kb and a minor transcript of 2.0 kb were found in brain, whereas in testis a 1.8-kb transcript was detected. Upon longer exposure, transcripts were found in additional tissues including lung and spleen. In contrast to PR55/Bβ, the 4.4 kb transcript of PR55/Bγ was solely restricted to brain. Control hybridizations with a probe specific for β-actin revealed that equal amounts of mRNA were loaded (not shown). These results, together with the identification of two novel splice variants of the Bβ subunit, indicate both a high complexity of the PR55/B family and a very fine-tuned regulation of distinct functions of the heterotrimeric PP2A holoenzyme.

In situ *hybridization analysis of brain sections*

To visualize the distribution of PR55/B subunit mRNAs in mouse brain, DIG-labelled antisense oligonucleotide probes specific for all PR55/B subunits were hybridized to parasagittal mouse brain sections. The distribution of the PR55/Bα subunit mRNA is shown in cortex, hippocampus, and cerebellum (Fig. 3B). No significant staining was obtained using the corresponding sense probes on adjacent sections (insets Fig. 3B). All PR55/B subunits were widely distributed in the brain, with a predominant expression by neurons. In general, hybridization was strongest in cell-dense areas such as the

TABLE 1. Distribution of PR55 mRNAs in brain

	PR55/Bα	PR55/Bβ	PR55/Bγ	PR55/Bσ
Hippocampus	+++	+++	+++	++++
Olfactory bulb	++++	++++	++++	++++
Cortex	++	+	+	++
Cerebellum	+++++	+++++	+++	+++++
Striatum	++	++	+++	++
Thalamus	++	+	+	+
Brain stem	+++	++	–	+++
Pons	++	+	+	+

Signal intensities: –, none; +, low; ++, low to intermediate; +++, intermediate; ++++, high; and +++++, very high.

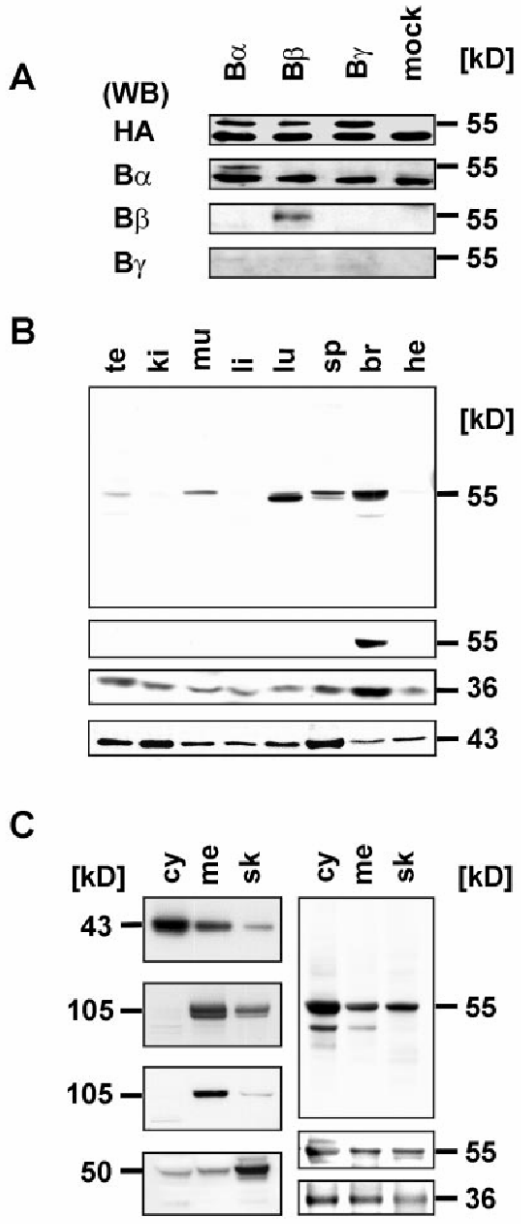

FIG. 4. (A) For detection of PR55/B, commercial antibodies were used that have been shown previously to be specific for the PR55/Bα and Bβ subunits on Western blots and by immunohistochemistry (Strack *et al.*, 1998). The specificity of the above antibodies was determined by transfecting COS cells with constructs encoding HA-tagged PR55/Bα, Bβ, and Bγ, and analysing lysates using Western blot analysis. Whereas the HA-antibody detected all PR55 isoforms, the PR55/Bα- and PR55/Bβ-specific antibodies detected only the respective isoforms. The commercially available Bγ antiserum was not specific as shown previously (Strack *et al.*, 1998) and was therefore excluded from the subsequent analysis. (B) The expression profile of PR55/Bα, PR55/Bβ and PP2A Cα determined by Western blot analysis. Protein was extracted from: te, testis; ki, kidney; li, liver; lu, lung; sp., spleen; br, brain; and he, heart. (C) To determine the subcellular localization, brain homogenates were fractionated into fractions enriched for cytosolic (cy), membranous (me), and cytoskeletal (sk) proteins as confirmed by the staining with antibodies specific for GAPDH (cy, 43 kDa), APP (me, 115 kDa), phosphorylated APP (me, 115 kDa), and GFAP (sk, 50 kDa). Cα was present in all fractions, with slightly lower levels in the cytoskeletal fraction. PR55/Bα and β were present in all fractions, with highest levels in the cytosolic fraction.

cerebellum, hippocampus, and olfactory bulb (Table 1). PR55/Bα and PR55/Bσ showed a similar distribution, and hybridization was more intense in brain stem than in cortex. In the dentate gyrus, the PR55/Bβ probe hybridized strongly to singulate cells, whereas the three other antisense probes hybridized more uniformly. With the exception of PR55/Bγ that was absent in the brain stem, the four PR55/B subunits were transcribed in all brain areas analyzed (Table 1).

Immunoblot analysis of PR55/B subunits

For detection of PR55/B, commercial antibodies were used that have been shown previously to be specific for the PR55/Bα and Bβ subunits on Western blots and by immunohistochemistry (Strack *et al.*, 1998). The commercially available Bγ antiserum has been shown to be cross-reactive (Strack *et al.*, 1998) and was therefore excluded from our analysis of the tissue distribution of PR55 subunits. We confirmed the specificity of the above antibodies by transfecting COS cells with constructs encoding HA-tagged PR55/Bα, Bβ, and Bγ, and analyzed lysates using Western blot analysis. Whereas the HA-antibody detected all PR55 isoforms, the PR55/Bα- and PR55/Bβ-specific antibodies detected only the respective isoforms (Fig. 4A and Strack *et al.*, 1998). To determine the expression profile of PP2A Cα and of the PR55/B subunits, protein extracts were obtained from different tissues (Fig. 4B). A β-actin specific antibody (data not shown) and a GAPDH specific antibody (Fig. 4B) were included as controls. Cα was present in all tissues examined with levels highest in the brain. Next, we determined the tissue distribution of the PR55 subunits. PR55/Bα was ubiquitously present; levels were very low in kidney, liver, and heart, intermediate in testis, muscle, and spleen, and highest in lung and brain, as shown with the commercially available antiserum: similar results were obtained with a second PR55/Bα-specific antiserum. PR55/Bβ was found in brain and testis, consistent with the Northern blot data. Upon longer exposure, Bβ was also detected in additional tissues including lung and spleen (Fig. 4B). The commercially available anti-PR55/Bγ antiserum was not reactive, and anti-PR55/Bσ antisera were not available.

To determine the subcellular localization of the PR55/B subunits, we generated brain homogenate fractions enriched for cytosolic, membranous and cytoskeletal proteins (Fig. 4C). This subfractionation protocol enriches for cytosolic, membraneous and cytoskeletal proteins, but does not completely separate them; the membrane fraction contains *trans*-membrane as well as membrane-associated proteins, and the cytoskeletal fraction contains all proteins that are insoluble in 1% Triton X-100, including RAFTs. Enrichment was

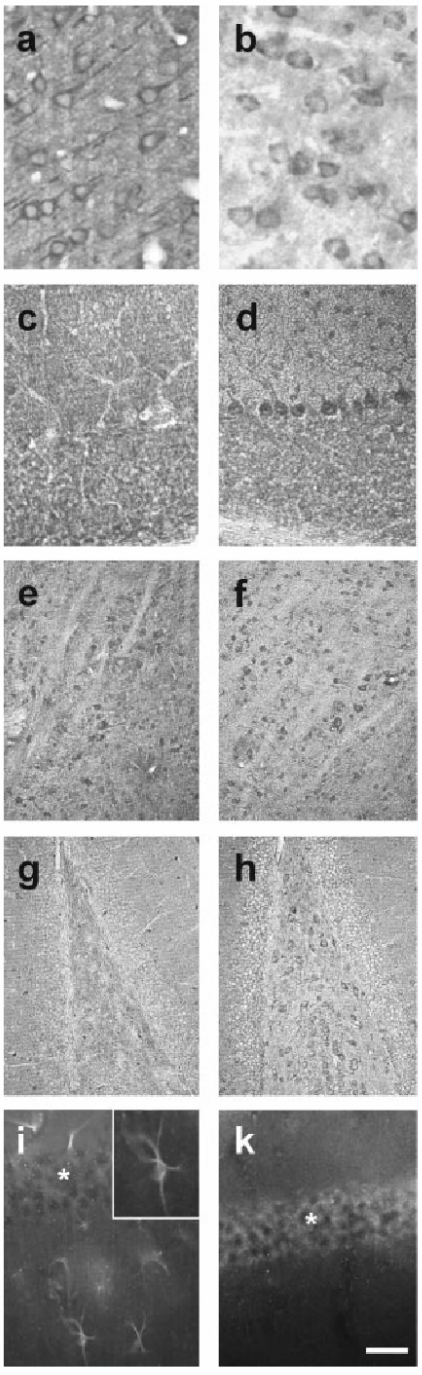

FIG. 5. To determine the distribution of PR55/Bα and Bβ protein in the brain, we analyzed parasagittal sections by immunohistochemistry. Both isoforms are widely expressed. The distribution in cortex, cerebellum, brain stem, in the hilus of the hippocampus, and the CA1 region of the hippocampus is shown for Bα (a, c, e, g and i) and Bβ (b, d, f, h and k). In the cortex (a and b), Bα is present in somata and apical dendrites of pyramidal neurons, whereas Bβ is mainly confined to the soma. In the cerebellum, the anti-Bβ antiserum intensely stains somata and dendrites of Purkinje cells, whereas Bα is present in additional cell types and weakly stains Purkinje cells (c and d). In the brain stem, both subunits are expressed in different cell types, including motor neurons (e and f). While Bβ is stronger in neurons of the hilus of the dentate gyrus, Bα is not detected (g and h); in the CA1 region of the hippocampus (indicated by an asterisk), Bβ is more strongly expressed than α; however, the Bα-specific antiserum strongly stains cells resembling activated astrocytes (see inset in i and Fig. 6). Scale bar, 20 μm (a and b); 30 μm (c, d, i and k); 40 μm (e–h).

demonstrated by Western blot analysis of the three fractions and probing the blot using a GAPDH-specific antibody as cytoplasmic marker, two APP (amyloid precursor protein)-specific antibodies as markers for the membrane fraction, and a GFAP (glial fibrillar acid protein)-specific antibody as marker for the cytoskeletal fraction. The APP-specific antibody revealed a doublet representing the immature and mature form of APP, whereas the phospho-APP-specific antibody detected only the mature and phosphorylated form of APP. Our data are consistent with previous studies in the rat using identical experimental conditions (Strack *et al*., 1998). Cα was present in all fractions, with slightly lower levels in the cytoskeletal fraction. PR55/Bα and β were present in all fractions, with highest levels in the cytosolic fraction.

PR55 subunits are differentially expressed in brain and display a diverse subcellular localization

To determine the distribution of PR55/Bα and β proteins in the brain, we analyzed parasagittal sections using immunohistochemistry (Fig. 5). Both isoforms were widely expressed in the brain; stainings were generally weak in the hippocampus, more intense throughout the cortex and brain stem, and even stronger in the cerebellum. In the cortex, Bα was present in somata and apical dendrites of pyramidal neurons, whereas Bβ was mainly confined to the soma (Fig. 5a and b). In the cerebellum, the anti-Bβ antiserum intensely stained somata and dendrites of Purkinje cells, whereas Bα was present in additional cell types and weakly stained Purkinje cells (Fig. 5c and d). In the brain stem, both subunits were expressed in different cell types, including motor neurons (Fig. 5e and f). PR55/Bβ was stronger in neurons of the hilus of the dentate gyrus, whereas Bα was not detected (Fig. 5g and h); in the CA1 region of the hippocampus, PR55/Bβ was more strongly expressed than PR55/Bα: however, the PR55/Bα-specific antiserum strongly stained cells resembling activated astrocytes (Fig. 5i and k).

Our RNA *in situ* hybridization data indicated a preferential expression of PR55/Bα and β by neurons. To determine neuronal vs. glial expression of PR55/Bα and β proteins, we analyzed parasagittal brain sections using double-immunofluorescence analysis using PR55/Bα- and β-specific antisera together with a MAP-2-specific antibody as a dendritic marker for neurons, and a GFAP-specific antibody as a marker for activated astrocytes, respectively (Fig. 6). PR55/Bα was localized to cell bodies and dendrites of neurons (Fig. 6a–c), whereas PR55/Bβ was mainly confined to the cell body (Fig. 6d–f). In areas of the brain with activated astrocytes, PR55/Bα was expressed by these cells at much higher levels than by neurons, as judged by the fluorescence settings (Fig. 6g–i). In contrast, PR55/Bβ was only expressed at background levels, indicating a distinct role of PR55/Bα during astrocytosis (Fig. 6k–m). Together, as neurons outnumber astrocytes in healthy brain, the number of Bα and Bβ-expressing neurons by far exceeded that of Bα-expressing astrocytes, confirming the findings of our RNA *in situ* hybridization analysis (Fig. 3).

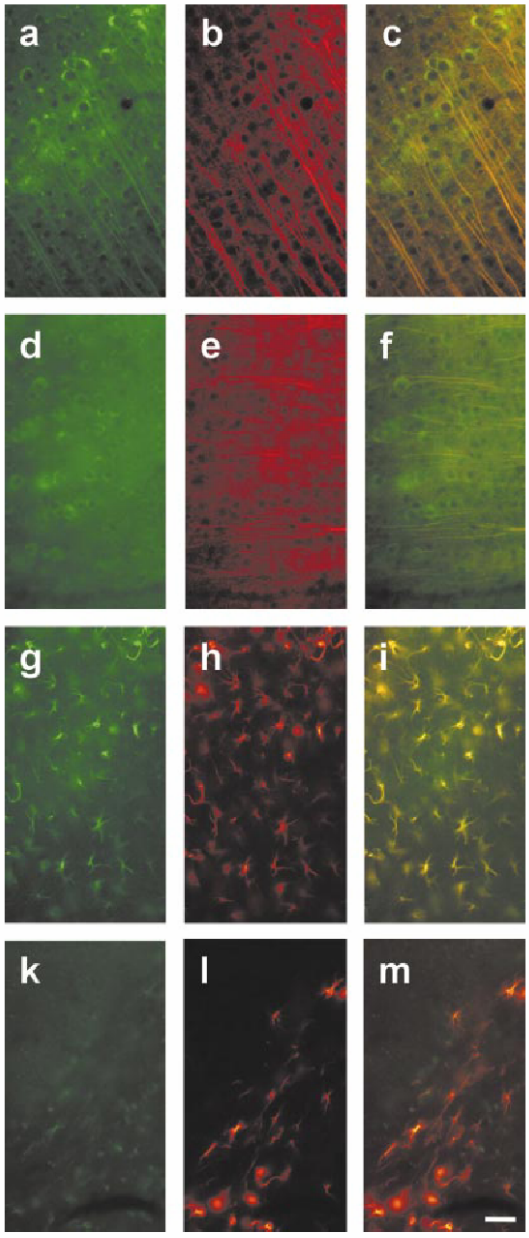

FIG. 6. PR55/Bα is, in addition to neurons, strongly expressed by activated astrocytes. To determine neuronal vs. glial expression of PR55/Bα (a–c, g–i) and Bβ (d–f, k–m) in the cortex, we analyzed parasagittal sections by double-immunofluorescence analysis using PR55-specific antisera together with a MAP-2-specific antibody as dendritic marker for neurons (a–f), and a GFAP-specific antibody as marker for activated astrocytes (g–m), respectively. PR55/Bα is localized to cell bodies and dendrites (a–c; a: Bα/Cy2, b: MAP-2/Cy3, c: merge), whereas PR55/Bβ is mainly confined to the cell body of neurons (d–f: d, Bβ/Cy2; e, MAP-2/Cy3; f, merge). PR55/Bα is expressed by activated astrocytes (g–i: g, Bα/Cy2; h, GFAP/Cy3; i, merge) at much higher levels than by neurons, whereas PR55/Bβ is only expressed at background levels (k–m: k, Bβ/Cy2; l, GFAP/Cy3; m, merge). Neuronal expression of PR55/Bα and PR55/Bβ in (g) and (k) is visible upon longer exposure. Scale bar, 20 μm.

Discussion

In the present study, we performed an analysis of the distribution and developmental regulation of the murine PR55/B subunit family of PP2A, with particular emphasis placed on its role in the brain.

We identified two novel splice variants of the β subunit, PR55/Bβ.1 and Bβ.2, encoding amino-terminally spliced forms of the β isoform that preserve the ORF and result in a protein that has the first 23 amino acids replaced by five and 26 novel amino acids, respectively (Fig. 1). Whereas Bβ and Bβ.2 had a size of roughly 55 kDa, Bβ.1 had a size of 53 kDa. Different PR55/Bβ transcripts were revealed after Northern blot analysis, a major transcript of 2.5 kb and a minor transcript of 2.0 kb in the brain, and a 1.8-kb transcript in the testis. Similarly, for PR55/Bσ, multiple transcripts between 2.0 and 2.5 kb were detected in all tissues examined. However, as no σ-specific antiserum was available, there was no possibility of testing for the presence of this isoform. Together, our data indicate that different PR55/B transcripts are tightly regulated at the transcriptional level in different cell types. For comparison, ribonuclease assays were performed in the rat for all four subunits, precluding the possibility of detecting splice variants (Strack *et al*., 1998; Strack *et al*., 1999). Thus, it appears likely that in mammals the variability of the PR55/B family is even higher than previously thought. For other families of PP2A regulatory subunits, multiple splice variants have also been described (McCright *et al*., 1996; Janssens *et al*., 2001).

No transcripts were detected for the α, γ, and σ subunits in mouse embryos until embryonic day E17, in contrast to a 2.5-kb β transcript that was detected as early as E11, with increasing levels until E17. These data indicate that the β subunits exert a distinct function during development. Previous data in rat have also shown a differential expression of the four subunits during peri- and postnatal development using ribonuclease protection assays. RNA levels were quantified in E18, P1, P7, P14, P21, and adult rat brain. α levels stayed constant throughout all stages of development, β levels were approximately threefold reduced, and γ levels threefold increased when adult brain was compared with E18 brain (Strack *et al*., 1998). RNA levels were determined in eight subdissected brain regions. Differences in RNA levels were generally moderate, with the exception of the β subunit mRNA that was sevenfold higher in the olfactory bulb compared with the cerebellum (Strack *et al*., 1998).

Our Northern blot analysis of adult tissues including testis, kidney, muscle, liver, lung, spleen, brain, and heart revealed that the α and σ subunits were ubiquitously expressed, indicating that these subunits are involved in general cellular processes of adult, but not immature tissues. In contrast to the α and σ subunits, the γ subunit was transcribed exclusively in the brain, and the β subunit was restricted to the brain and testis. This indicates that these subunits confer the PP2A holoenzyme with brain-specific functions. Also, expression of all four subunits in adult tissues indicates a diversification of the function of the four subunits. A tight transcriptional control of the individual PP2A regulatory subunits may be critical for proper cell function, as indicated by the recent finding of a CAG expansion in the 5′ region of PR55/Bβ associated with spinocerebellar ataxia 12, an autosomal dominant neurodegenerative disease (Holmes *et al*., 1999).

The high levels of expression of both PP2AC isoforms in brain (Khew-Goodall & Hemmings, 1988) and the brain-specific expression of some members of the PR55/B (Mayer *et al*., 1991; Zolnierowicz *et al*., 1994; Strack *et al*., 1998) and B′/PR61 (McCright & Virshup, 1995; Csortos *et al*., 1996) subunit families indicate that PP2A has unique functions in neuronal cells (Price & Mumby, 1999). These include the dephosphorylation of neurofilaments (Saito *et al*., 1995; Strack *et al*., 1997) and neuronal-specific microtubule-associated proteins including tau and MAP-2 (Mandelkow *et al*., 1995). Interestingly, the aggregation of hyperphosphorylated tau in neurofibrillary tangles is a pathological hallmark of AD, and hyperphosphorylation of tau has been proposed as a mechanism leading to neuronal degeneration (Lee, 1995; Billingsley & Kincaid, 1997). As mentioned above, a pool of PP2A mainly containing PR55/B subunits associates with microtubules (Sontag *et al*., 1995). In a more recent report, it was shown that only trimeric PP2A forms containing PR55/Bα or PR55/Bβ, but not PR55/Bγ or B′/PR61, associate with neuronal microtubules, and that this interaction depends on an as yet unidentified anchoring factor (Price *et al*., 1999).

Previous studies with rat brain have shown that the α, β, and γ isoforms are transcribed in all brain areas examined (Strack *et al*., 1998). In agreement with these findings, our *in situ* hybridization and immunohistochemical analysis of the murine brains showed that all PR55/B subunits, including σ, were widely distributed in brain with regional differences in expression levels. At the protein level, PR55/Bα and β were differently distributed in the cerebellum. PR55/Bβ was mainly localized to somata and dendrites of Purkinje cells, whereas α was present in additional cell types and present at lower levels in Purkinje cells. As the cerebellum is affected in spinocerebellar ataxia, a disease for which an association with an expanded CAG repeat immediately upstream of the PR55/Bβ gene has been shown, a detailed analysis of the PP2A holoenzyme composition may contribute to the understanding of the pathogenesis (Holmes *et al*., 1999). In the cortex and hippocampus, areas prominently affected in AD brains, the distribution of the two PR55 subunits also varies. Whereas PR55/Bα is present in apical dendrites, β is mainly confined to cell bodies suggesting distinct subcellular substrates. The presence of PR55/Bα in activated astrocytes at staining intensities far exceeding those seen for neurons indicates a pivotal role of PR55/Bα in activated astrocytes. Remarkably, astrocyte activation is an early step in the pathogenesis of AD and related disorders (Kurosinski & Gotz, 2002). Collectively, our data indicate that the individual PR55/B subunits exert specialized functions in different subcellular compartments of neurons and in the course of astrocytic activation, but their widespread distribution in the brain indicates that they are also involved in central functions of both neurons and glial cells. Finally, sequence analysis of all murine PR55/B subunits revealed the presence of five to seven degenerate WD-40 repeats depending on the setting of the search parameters (Fig. 2). WD-40 repeats are minimally conserved sequences of approximately 40 amino acids that typically end in tryptophan–aspartate (WD) and are thought to mediate protein–protein interactions (Neer *et al*., 1994). Insight into the distinct role of PR55/B subunits and their specific interaction partners may emerge from knock-out studies in mice. In *Drosophila*, PR55/B mutant phenotypes have been described; however, in contrast to mice, *Drosophila* only expresses one PR55/B isoform (Gomes *et al*., 1993; Mayer-Jaekel *et al*., 1993; Uemura *et al*., 1993; Mayer-Jaekel *et al*., 1994; Silverstein *et al*., 2002). Considering the putative role of PP2A in the pathogenesis of human diseases, all these studies may eventually lead to the discovery of therapeutic agents that can specifically counteract PP2A dysfunction.

Acknowledgements

We thank Peter Cron and Eva Moritz for excellent technical assistance. This work was supported in part by grants from the Bundesamt für Bildung und Wissenschaft, Bern (BBW Nr. 98.0176) to BAH and from the Bayer

Alzheimer Research Network (BARN) and the Swiss National Science Foundation to JG. The Friedrich Miescher Institute is part of the Novartis Research Foundation.

Abbreviations

AD, Alzheimer's disease; ORF, open reading frame; PBS, phosphate-buffered saline; PP2A, protein phosphatase 2 A; TBS, Tris-buffered saline.

References

Billingsley, M.L. & Kincaid, R.L. (1997) Regulated phosphorylation and dephosphorylation of tau protein: effects on microtubule interaction, intracellular trafficking and neurodegeneration. *Biochem. J.*, **323**, 577–591.

Csortos, C., Zolnierowicz, S., Bako, E., Durbin, S.D. & DePaoli-Roach, A.A. (1996) High complexity in the expression of the B′ subunit of protein phosphatase 2A0. Evidence for the existence of at least seven novel isoforms. *J. Biol. Chem.*, **271**, 2578–2588.

Goedert, M., Cohen, E.S., Jakes, R. & Cohen, P. (1992) p42 MAP kinase phosphorylation sites in microtubule-associated protein tau are dephosphorylated by protein phosphatase 2A1. Implications for Alzheimer's disease. *FEBS Lett.*, **312**, 95–99.

Gomes, R., Karess, R.E., Ohkura, H., Glover, D.M. & Sunkel, C.E. (1993) Abnormal anaphase resolution (aar): a locus required for progression through mitosis in *Drosophila*. *J. Cell Sci.*, **104**, 583–593.

Gong, C.X., Grundke-Iqbal, I., Damuni, Z. & Iqbal, K. (1994) Dephosphorylation of microtubule-associated protein tau by protein phosphatase-1 and -2C and its implication in Alzheimer disease. *FEBS Lett.*, **341**, 94–98.

Gong, C.X., Shaikh, S., Wang, J.Z., Zaidi, T., Grundke-Iqbal, I. & Iqbal, K. (1995) Phosphatase activity toward abnormally phosphorylated tau: decrease in Alzheimer disease brain. *J. Neurochem.*, **65**, 732–738.

Gotz, J. (2001) Tau and transgenic animal models. *Brain Res. Rev.*, **35**, 266–286.

Gotz, J. & Kues, W. (1999) The role of protein phosphatase 2A catalytic subunit Calpha in embryogenesis: evidence from sequence analysis and localization studies. *Biol. Chem.*, **380**, 1117–1120.

Gotz, J., Probst, A., Ehler, E., Hemmings, B. & Kues, W. (1998) Delayed embryonic lethality in mice lacking protein phosphatase 2A catalytic subunit Calpha. *Proc. Natl Acad. Sci. USA*, **95**, 12370–12375.

Gotz, J., Probst, A., Mistl, C., Nitsch, R.M. & Ehler, E. (2000) Distinct role of protein phosphatase 2A subunit calpha in the regulation of E-cadherin and beta-catenin during development. *Mech. Dev.*, **93**, 83–93.

Holmes, S.E., O'Hearn, E.E., McInnis, M.G., Gorelick-Feldman, D.A., Kleiderlein, J.J., Callahan, C., Kwak, N.G., Ingersoll-Ashworth, R.G., Sherr, M., Sumner, A.J., Sharp, A.H., Ananth, U., Seltzer, W.K., Boss, M.A., Vieria-Saecker, A.M., Epplen, J.T., Riess, O., Ross, C.A. & Margolis, R.L. (1999) Expansion of a novel CAG trinucleotide repeat in the 5′ region of PPP2R2B is associated with SCA12. *Nature Genet.*, **23**, 391–392.

Janssens, V. & Goris, J. (2001) Protein phosphatase 2A: a highly regulated family of serine/threonine phosphatases implicated in cell growth and signalling. *Biochem. J.*, **353**, 417–439.

Khew-Goodall, Y. & Hemmings, B.A. (1988) Tissue-specific expression of mRNAs encoding alpha- and beta-catalytic subunits of protein phosphatase 2A. *FEBS Lett.*, **238**, 265–268.

Kins, S., Betz, H. & Kirsch, J. (2000) Collybistin, a newly identified brain-specific GEF, induces submembrane clustering of gephyrin. *Nature Neurosci.*, **3**, 22–29.

Kins, S., Crameri, A., Evans, D.R., Hemmings, B.A., Nitsch, R.M. & Gotz, J. (2001) Reduced PP2A activity induces hyperphosphorylation and altered compartmentalization of tau in transgenic mice. *J. Biol. Chem.*, **276**, 38193–38200.

Kurosinski, P. & Gotz, J. (2002) Glial cells under physiologic and pathological conditions. *Arch. Neurol.*, **59**, 1524–1528.

Lee, V.M. (1995) Disruption of the cytoskeleton in Alzheimer's disease. *Curr. Opin. Neurobiol.*, **5**, 663–668.

Mandelkow, E.M., Biernat, J., Drewes, G., Gustke, N., Trinczek, B. & Mandelkow, E. (1995) Tau domains, phosphorylation, and interactions with microtubules. *Neurobiol. Aging*, **16**, 355–362;discussion 362–353.

Mayer, R.E., Hendrix, P., Cron, P., Matthies, R., Stone, S.R., Goris, J., Merlevede, W., Hofsteenge, J. & Hemmings, B.A. (1991) Structure of the 55-kDa regulatory subunit of protein phosphatase 2A: evidence for a neuronal-specific isoform. *Biochemistry*, **30**, 3589–3597.

Mayer-Jaekel, R.E., Ohkura, H., Ferrigno, P., Andjelkovic, N., Shiomi, K., Uemura, T., Glover, D.M. & Hemmings, B.A. (1994) *Drosophila* mutants in the 55 kDa regulatory subunit of protein phosphatase 2A show strongly reduced ability to dephosphorylate substrates of p34cdc2. *J. Cell Sci.*, **107**, 2609–2616.

Mayer-Jaekel, R.E., Ohkura, H., Gomes, R., Sunkel, C.E., Baumgartner, S., Hemmings, B.A. & Glover, D.M. (1993) The 55 kDa regulatory subunit of *Drosophila* protein phosphatase 2A is required for anaphase. *Cell*, **72**, 621–633.

McCright, B., Rivers, A.M., Audlin, S. & Virshup, D.M. (1996) The B56 family of protein phosphatase 2A (PP2A) regulatory subunits encodes differentiation-induced phosphoproteins that target PP2A to both nucleus and cytoplasm. *J. Biol. Chem.*, **271**, 22081–22089.

McCright, B. & Virshup, D.M. (1995) Identification of a new family of protein phosphatase 2A regulatory subunits. *J. Biol. Chem.*, **270**, 26123–26128.

McNeill, R.B. & Colbran, R.J. (1995) Interaction of autophosphorylated Ca^{2+}/calmodulin-dependent protein kinase II with neuronal cytoskeletal proteins. Characterization of binding to a 190-kDa postsynaptic density protein. *J. Biol. Chem.*, **270**, 10043–10049.

Millward, T.A., Zolnierowicz, S. & Hemmings, B.A. (1999) Regulation of protein kinase cascades by protein phosphatase 2A. *Trends Biochem. Sci.*, **24**, 186–191.

Neer, E.J., Schmidt, C.J., Nambudripad, R. & Smith, T.F. (1994) The ancient regulatory-protein family of WD-repeat proteins. *Nature*, **371**, 297–300.

Planel, E., Yasutake, K., Fujita, S.C. & Ishiguro, K. (2001) Inhibition of protein phosphatase 2A overrides tau protein kinase I/glycogen synthase kinase 3 beta and cyclin-dependent kinase 5 inhibition and results in tau hyperphosphorylation in the hippocampus of starved mouse. *J. Biol. Chem.*, **276**, 34298–34306.

Price, N.E. & Mumby, M.C. (1999) Brain protein serine/threonine phosphatases. *Curr. Opin. Neurobiol.*, **9**, 336–342.

Price, N.E., Wadzinski, B. & Mumby, M.C. (1999) An anchoring factor targets protein phosphatase 2A to brain microtubules. *Mol. Brain Res.*, **73**, 68–77.

Ramming, M., Kins, S., Werner, N., Hermann, A., Betz, H. & Kirsch, J. (2000) Diversity and phylogeny of gephyrin: tissue-specific splice variants, gene structure, and sequence similarities to molybdenum cofactor-synthesizing and cytoskeleton-associated proteins. *Proc. Natl Acad. Sci. USA*, **97**, 10266–10271.

Saito, T., Shima, H., Osawa, Y., Nagao, M., Hemmings, B.A., Kishimoto, T. & Hisanaga, S. (1995) Neurofilament-associated protein phosphatase 2A: its possible role in preserving neurofilaments in filamentous states. *Biochemistry*, **34**, 7376–7384.

Silverstein, A.M., Barrow, C.A., Davis, A.J. & Mumby, M.C. (2002) Actions of PP2A on the MAP kinase pathway and apoptosis are mediated by distinct regulatory subunits. *Proc. Natl Acad. Sci. USA*, **99**, 4221–4226.

Sontag, E., Nunbhakdi-Craig, V., Bloom, G.S. & Mumby, M.C. (1995) A novel pool of protein phosphatase 2A is associated with microtubules and is regulated during the cell cycle. *J. Cell Biol.*, **128**, 1131–1144.

Sontag, E., Nunbhakdi-Craig, V., Lee, G., Brandt, R., Kamibayashi, C., Kuret, J., White, C.L., 3rd, Mumby, M.C. & Bloom, G.S. (1999) Molecular interactions among protein phosphatase 2A, tau, and microtubules. Implications for the regulation of tau phosphorylation and the development of tauopathies. *J. Biol. Chem.*, **274**, 25490–25498.

Strack, S., Chang, D., Zaucha, J.A., Colbran, R.J. & Wadzinski, B.E. (1999) Cloning and characterization of B delta, a novel regulatory subunit of protein phosphatase 2A. *FEBS Lett.*, **460**, 462–466.

Strack, S., Westphal, R.S., Colbran, R.J., Ebner, F.F. & Wadzinski, B.E. (1997) Protein serine/threonine phosphatase 1 and 2A associate with and dephosphorylate neurofilaments. *Brain Res. Mol. Brain Res.*, **49**, 15–28.

Strack, S., Zaucha, J.A., Ebner, F.F., Colbran, R.J. & Wadzinski, B.E. (1998) Brain protein phosphatase 2A: developmental regulation and distinct cellular and subcellular localization by B subunits. *J. Comp. Neurol.*, **392**, 515–527.

Uemura, T., Shiomi, K., Togashi, S. & Takeichi, M. (1993) Mutation of twins encoding a regulator of protein phosphatase 2A leads to pattern duplication in *Drosophila* imaginal discs. *Genes Dev.*, **7**, 429–440.

Vogelsberg-Ragaglia, V., Schuck, T., Trojanowski, J.Q. & Lee, V.M. (2001) PP2A mRNA expression is quantitatively decreased in Alzheimer's disease hippocampus. *Exp. Neurol.*, **168**, 402–412.

Zolnierowicz, S., Csortos, C., Bondor, J., Verin, A., Mumby, M.C. & DePaoli-Roach, A.A. (1994) Diversity in the regulatory B-subunits of protein phosphatase 2A: identification of a novel isoform highly expressed in brain. *Biochemistry*, **33**, 11858–11867.

8.3 B/PR55 levels in undifferentiated and neuronally differentiated cells

Microtubules and microtubule-associated proteins such as tau provide the major mechanical support for the shape of neurites and neurite formation has been shown to be regulated by protein phosphorylation (Chiou and Westhead, 1992; Rogers et al., 1994; Veeranna et al., 1995; Wu and Bradshaw, 1993). Chemical suppression of microtubule elongation, using cytochalasin B and D or latrunculin A to depolymerize actin filaments or colcemid (demecolcine) to disassemble microtubules, as well as treatment with okadaic acid (OA), a potent inhibitor of PP2A, abolished process formation in an immortalized mouse podocyte cell line (Kobayashi et al., 2001). In addition, treatment of PC12 cells with OA revealed a requirement for PP2A in neurite outgrowth by nerve growth factor (NGF) and maintenance of neurites (Chiou and Westhead, 1992). There is evidence that PP2A is mainly responsible for the dephosphorylation of neurofilaments (NFs) (Strack et al., 1997; Veeranna et al., 1995). PP2A thereby produces and preserves filamentous forms of NFs in neurons (Sacher et al., 1992; Sacher et al., 1994; Saito et al., 1995). Thus, PP2A regulates phosphorylation of NFs and the interaction of cytoskeletal proteins during axonal outgrowth.

In a previous study using PC12 like cells, endogenous B/PR55β, B/PR55γ, and B'/PR61β protein expression was shown to be induced during nerve growth factor (NGF)-mediated neuronal differentiation (Strack, 2002). In that study, transient expression of PR55γ, but not PR55α, facilitated neurite outgrowth, irrespective of the presence of NGF. PR55γ specifically promoted long lasting activation of the MAPK cascade (Strack, 2002). This in turn may initiate the gene transcription events required for neuronal differentiation by NGF, as it was suggested in the case of PC12 cells. (Traverse et al., 1992).

These implications of PP2A in neuronal differentiation and neurite stability, together with high expression levels of PP2A subunits in brain compared to peripheral tissues, imply that PP2A may have unique functions in the brain.

Significant insight into PP2A function *in vivo* is expected to be obtained by genetic approaches in mice (Gotz and Schild, 2003; Janssens and Goris, 2001). To provide a framework for the interpretation of phenotypes of mice that either lack PP2A subunits (Gotz et al., 1998; Gotz et al., 2000) or display an altered PP2A composition or activity (Kins et al., 2001; Kins et al., 2003; Planel et al., 2001), we previously determined the genomic organization, identified novel splice variants and analyzed the mRNA and protein expression of the PR55/B regulatory subunits of PP2A in different tissues, in particular the brain (Schmidt et al., 2002). Here, we determined mRNA levels of the four members of the PR55 subunit family in human embryonic kidney (HEK-293) and in undifferentiated and neuronally differentiated human neuroblastoma cells (SH-SY5Y).

8.3.1 High levels of PR55α mRNA compared to PR55β, γ and δ in HEK-293 and undifferentiated SH-SY5Y cells

By multiple tissue Northern blot analysis using isoform-specific probes we have previously shown that PR55α and δ mRNA transcripts were present in all tissues examined in the mouse. PR55β was mainly confined to brain and testis, and at low levels to lung and spleen, whereas PR55γ was restricted to brain. Northern blot analysis of different embryonic stages has revealed transcription of PR55β, whereas transcripts of the remaining three subunits were not detectable (Schmidt et al., 2002). Here, PR55 transcription was addressed in human tissue culture systems with a special emphasis on neuronal differentiation by using two cell-lines, SH-SY5Y neuroblastoma cells (Figure 11*A*) and HEK-293 embryonic kidney cells (Figure 11*B*). The former can be neuronally differentiated in a step-wise manner (Figure 11*C,D*). SH-SY5Y cells were initially derived from the parental SK-N-SH line, which comprises a major neuroblastic (N-type) (Figure 11*A*, arrowhead) and a minor substrate adherent (S-type) species (Figure 11*A*, arrow) (Ross et al., 1983).

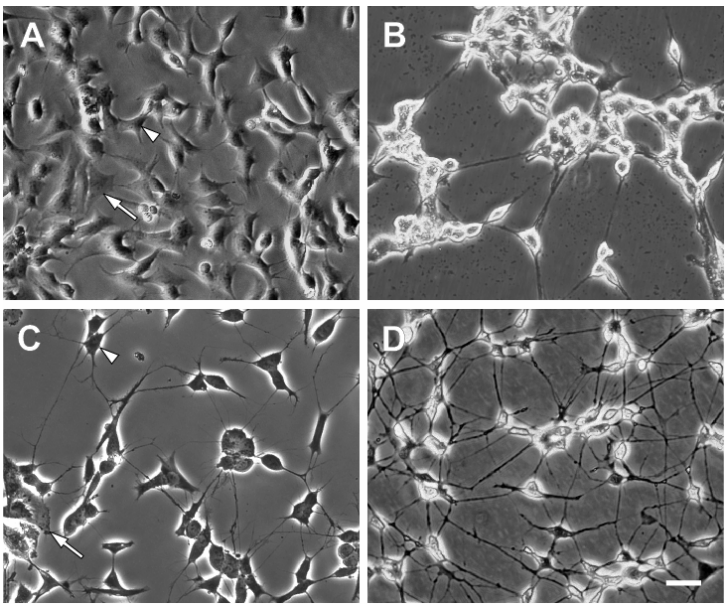

Figure 11: Step-wise neuronal differentiation of human SH-SY5Y neuroblastoma cells. (*A*) SH-SY5Y cells comprise a major neuroblastic (N-type; *arrowhead*) and a minor substrate adherent (S-type; *arrow*) species (Ross et al., 1983). (*B*) Non-neuronal HEK-293 are shown for comparison. (*C*) Upon neuronal differentiation of SH-SY5Y cells with RA for 5 days, a considerable proportion of the neuroblastic cells differentiate into a more neuronal phenotype by extending neuritic processes (*N-R-type*). (*D*) By incubating the cells for additional 5 days with BDNF, S-type cells disappear and basically all cells display a fully mature neuronal phenotype, with a robust network of neuritic processes (*N-R/B-type*). Scale bar: 30 µm.

Steady-state mRNA levels of the four B/PR55 subunits were determined by qRT-PCR for both cell lines. The primers used for this study discriminate the four isoforms, but if PR55β was spliced similar in humans as in mice, they would not detect the two splice variants (Schmidt et al., 2002). I found comparable mRNA levels of the four members of the PR55 family in both HEK-293 and undifferentiated SH-SY5Y cells (Figure 12). PR55α was the major species in both cell-types, with four- to seven-fold higher mRNA levels compared to PR55δ. Amounts of PR55γ mRNA were slightly lower than those of PR55δ. Compared with PR55α, PR55β concentrations

were 62-fold lower in SH-SY5Y cells and barely detectable in HEK-293 cells. This suggests that the PR55β subunit, despite its low relative levels compared to the other three subunits, may perform a distinct function in cells that are capable of neuronal differentiation.

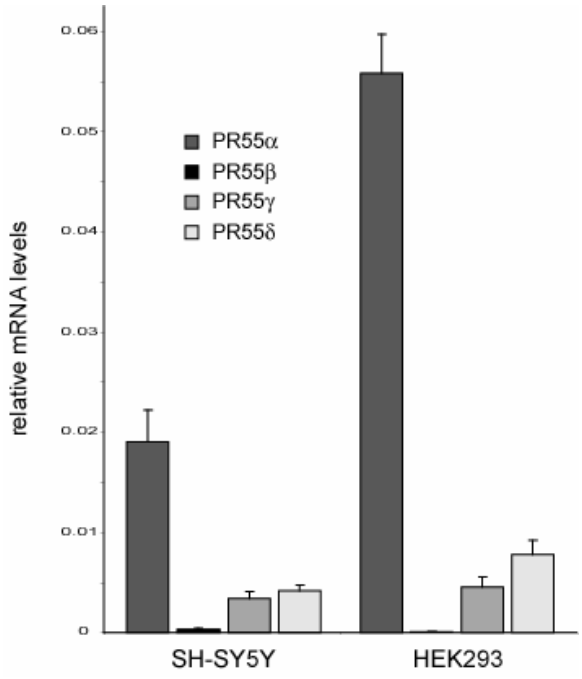

Figure 12: PR55α, β, γ and δ mRNA levels in undifferentiated SH-SY5Y cells and HEK-293 cells as determined by qRT-PCR. mRNA levels of the four members of the PR55 family are comparable in both cell-types. PR55α is the major species, with four- to sevenfold higher levels compared to PR55δ. Levels of PR55γ are slightly lower than those of PR55δ. PR55β levels are very low in SH-SY5Y cells and barely detectable in HEK293 cells. Compared with PR55α, PR55β levels were 62-fold lower in SH-SY5Y cells.

8.3.2 Neuronal differentiation of SH-SY5Y cells causes an increase in PR55β mRNA levels, followed by a rise in PR55γ and PR55δ mRNA, but not PR55α

To determine whether neuronal differentiation would affect PR55 subunit mRNA levels, I sequentially differentiated SH-SY5Y neuroblastoma cells into neuron-like cells. In a first step, cells were incubated with retinoic acid (RA) for 5 days (*N-R-type*, Figure 11C), followed by BDNF treatment for additional 5 days (*N-R/B-type*, Figure 11*D*). RA treatment causes both an inhibited growth rate and an extension of neuritic processes. BDNF enhances the differentiating effects of RA, resulting in a homogeneous population of cells (i.e. lacking S-type cells) with rounded cell bodies and lengthened neuritic processes. The cultures are characterized by neuritic arborization, forming extensive networks and displaying growth cones. When SH-SY5Y cells were differentiated for 5 or 10 days, mRNA levels of PR55β, γ and δ subunit mRNA increased 2.7-, 2.3-, and 1.9-fold, respectively (p=0.013, 0.007, 0.024) (Figure 13*A*). On the contrary, the amount of PR55α mRNA did not change significantly during differentiation (p=0.1) (Figure 13*A*). As there were major differences in absolute mRNA levels for the four subunits under non-differentiated conditions, I set these values at 100% (Figure 13*B*). Moreover, the two

differentiation stages were looked at separately. Upon differentiation into N-R-type cells, the quantity of PR55β mRNA increases 2.8-fold (p=0.048), while PR55α, PR55γ, and PR55δ displayed only non significant increases in mRNA levels (p=0.5, 0.2, and 0.5). When SH-SY5Y cells were further differentiated into N-R/B-type cells, amounts of PR55γ and PR55δ increase 2.9- and 2.6-fold compared to undifferentiated SH-SY5Y cells (p=0.004 for both isoforms). The 2.7-fold increases of PR55β mRNA levels are comparable to those obtained for N-R-type cells. The quantity of PR55α mRNA increased in a linear time dependent manner, but this rise was statistically not significant (p=0.1).

Together, these data show that PR55α is likely to perform more general functions in the cell, which are not associated with neuronal functions, while PR55β seems to be specifically induced during neuronal differentiation.

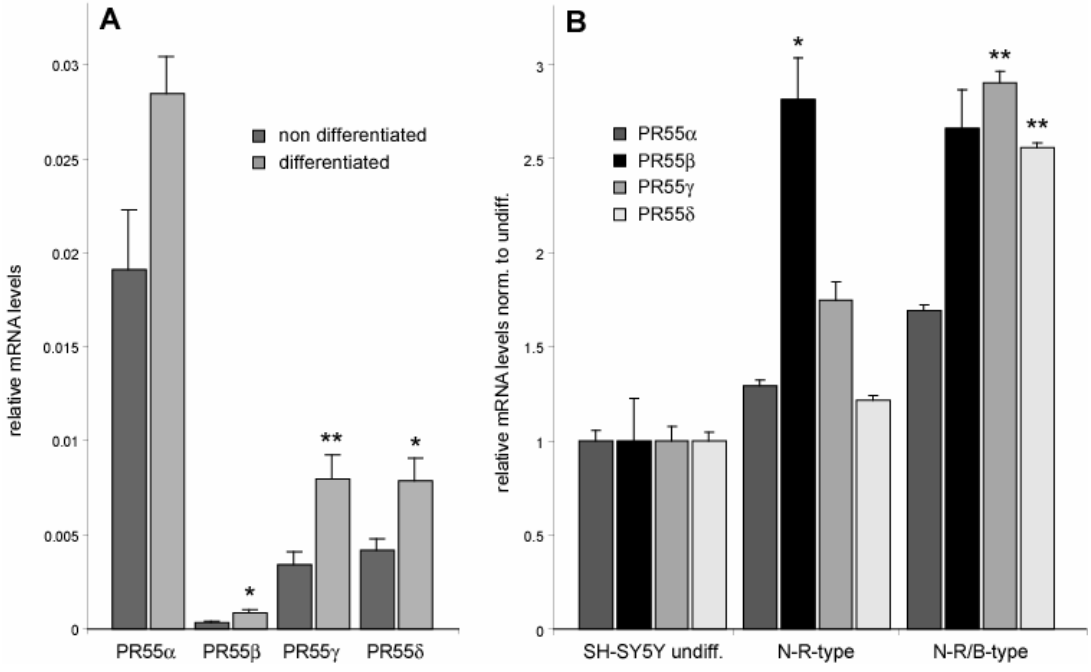

Figure 13: Relative PR55α, β, γ and δ mRNA levels in undifferentiated (n=12) compared to neuronally differentiated (n=6) SH-SY5Y cells as determined by qRT-PCR. (*A*) While the amount of PR55α mRNA does not change significantly during differentiation (p=0.1), levels of PR55β, γ and δ subunit mRNA increase 2.7-, 2.3-, and 1.9-fold, respectively, when differentiated for 5 to 10 days (*, p=0.013, **, 0.007, *, 0.024). (*B*) Levels of the four PR55 subunits in undifferentiated SH-SY5Y cells are set to 100%, while the numbers for N-R-type cells and N-R/B-type cells correspond to the quotients of differentiated normalized to undifferentiated. Error bars therefore show the sum of squared relative errors of the means. Upon differentiation into N-R-type cells, levels of PR55β increase 2.8-fold (*, p=0.048), while PR55α, PR55γ, and PR55δ increase to some extent, although not significantly (p=0.5, 0.2, 0.5). When SH-SY5Y cells are further differentiated into N-R/B-type cells, levels of PR55γ and PR55δ increase 2.9- and 2.6-fold compared to amounts in undifferentiated SH-SY5Y cells (**, p=0.004 for both). The PR55β mRNA levels at 2.7-fold concentrations are comparable to the ones obtained from N-R-type cells. The abundance of PR55α increases in a linear time dependent manner, but this rise is statistically not significant (p=0.1).

8.4 Generation and analysis of transgenic mice expressing the dominant negative mutant form of PP2A Cα, L309A

Recruitment of regulatory subunits into the PP2A complex is determined by post-translational modifications of the C subunit at its highly conserved carboxy-terminus, which contains a DYFL motif at position 306-309 (Ogris et al., 1997). The modifications include tyrosine phosphorylation and methylation of leucine 309 (Tolstykh et al., 2000; Turowski et al., 1995; Yu et al., 2001; Zukerberg et al., 2000). When negatively charged amino acids were introduced at threonine 304 or tyrosine 307 to mimic phosphorylation, the A, but not the B subunits, were bound by mutant C in transfected NIH3T3 cells (Ogris et al., 1997). Similar findings were obtained with mutants Y307F and L309Q, demonstrating the importance of the carboxy-terminal residues for heterotrimer assembly (Chung et al., 1999). More specifically, it was shown that the L309A mutant was defective in binding distinct subunits, such as B/PR55α, *in vitro* (Bryant et al., 1999). Comparable findings were obtained in *S. cerevisiae*. Removal of the carboxy-terminal leucine or substitution by alanine did not inhibit general PP2A activity, but abolished binding of B/PR55. Binding of B'/PR61 was assumed to be retained as judged from a cell growth inhibition assay (Evans and Hemmings, 2000). These data support the notion that B/PR55 and B'/PR61 compete for binding to the core dimer. In the present study, I focused on the role of leucine 309 in PP2A heterotrimer assembly in transgenic mice.

A second aspect addressed is the role of PP2A holoenzymes in the phosphorylation of proteins implicated in human disease. Subunit A, for instance, has been identified as a tumor suppressor. It is mutated in melanomas and in tumor-derived cell lines (Calin et al., 2000; Ruediger et al., 2001; Wang et al., 1998). Further, an expanded CAG repeat was found immediately upstream of the B/PR55β gene in humans with spinocerebellar ataxia (Holmes et al., 1999). Finally, PP2A dysfunction has been implicated in Alzheimer's disease (AD) and frontotemporal dementia, both of which are characterized by neurofibrillary tangles (Gong et al., 1995). These are composed of hyperphosphorylated forms of the microtubule-associated protein tau (Gotz et al., 2004). Tau is a substrate of PP2A, and frontotemporal dementia mutant tau shows reduced binding to PP2A (Goedert et al., 2000; Sontag et al., 1999). In AD brains, PP2A activity was decreased by 30% compared with controls (Gong et al., 1995), and in the hippocampus of AD patients, of five subunits analyzed, Cα, B/PR55γ, and B'/PR61ε mRNA levels were decreased (Vogelsberg-Ragaglia et al., 2001). In addition, reduced amounts of ABαC were found in AD cortex, and PP2A activity was correlated with neurofibrillary tangle load (Sontag et al., 2004). Since hyperphosphorylated tau shows a reduced affinity to microtubules and thereby alters their stability, abnormally phosphorylated tau may affect neuronal viability, intracellular transport and cell adhesion (Gotz et al., 2004).

As the L199P mutation is in the catalytic core of Cα, it abolishes the catalytic activity, possibly without affecting holoenzyme assembly (Evans et al., 1999) (but see: (Ogris et al., 1999; Yu et al., 2001)).

I expressed the Cα mutant L309A under the neuronal promoter Thy1.2 with strong expression in brain, but also the Harderian (lacrimal) gland of transgenic mice. I found an altered recruitment

of regulatory subunits into the PP2A complex, demonstrating the importance of residue L309 in PP2A heterotrimer assembly *in vivo*. The PP2A substrate tau was abnormally phosphorylated in brain. In addition, incubation of vimentin with brain extracts demonstrated a role for distinct PP2A heterotrimers in vimentin dephosphorylation. Moreover, L309A expression in the Harderian gland caused a delayed and degenerative development of the gland. I provide evidence that cadherin/β-catenin-mediated cell adhesion requires a normal PP2A heterotrimer composition.

8.4.1 Expression of the dominant negative mutant form of PP2A Cα, L309A, in brain and Harderian gland

An expression vector with the neuron-specific elements of the mThy1.2 promoter was used to express the human PP2A Cα mutant L309A in mice, which can not be carboxymethylated anymore. Although the expression of transgenes under this promoter is mainly restricted to postmitotic neurons, expression has also been reported in immature neuroblast layers of the CNS, and in several organs and tissues outside the nervous system (Campsall et al., 2002). To facilitate detection of the mutant protein, a haemagglutinin (HA) epitope was fused to the amino-terminus (Evans et al., 1999; Kins et al., 2001). Seven founders transmitted the transgene in a Mendelian fashion, of which three expressed the transgene at high levels (data not shown). Line Dom5/III was chosen for further analysis as expression was strong in the hippocampus and cortex, formations which are degenerating in AD, but also in the thalamus and the Purkinje cells of the cerebellum (Figure 14*A-F*). Moreover, Cα L309A was expressed in the Harderian gland, the major portion of the lacrimal system.

The transgenic mice showed a normal fertility. Gross examination did not reveal any behavioral or neurological impairment, nor was there any evidence for neurodegeneration. Motor functions were unaffected as tested on the rotarod with mice at different ages (data not shown). To determine the expression pattern of the transgene, an HA-specific antibody was used on Western blots. Cα L309A was expressed in brain and Harderian gland (Figure 14*G*). No expression was found in lung, liver, heart, spleen and skeletal muscle of transgenic mice or in any tissue of WT littermate controls (Figure 14*G*). Western blot analysis of brain extracts with antibodies directed against epitopes conserved between human and murine PP2A C revealed that total levels of C were not increased upon expression of the mutant protein (data not shown). This finding is consistent with previous observations in mice (Gotz et al., 1998; Kins et al., 2001), and with tissue culture experiments, which demonstrated that protein levels of C are subject to an effective autoregulatory mechanism keeping total levels constant (Baharians and Schonthal, 1998; Wera et al., 1995).

Staining of L309A brain sections with an HA-specific antibody revealed cytosolic expression in neurons within most brain areas. These included cortical layers III-VI (Figure 14*A*), the CA1 and CA3 fields of the hippocampal formation (Figure 14*C,E*), the thalamus, and the Purkinje cells of the cerebellum (data not shown), whereas no staining was detected in WT brain (Figure 14*B,D,F*).

Together, our data show that the transgene is expressed in brain areas affected by tau pathology and neurodegeneration in AD.

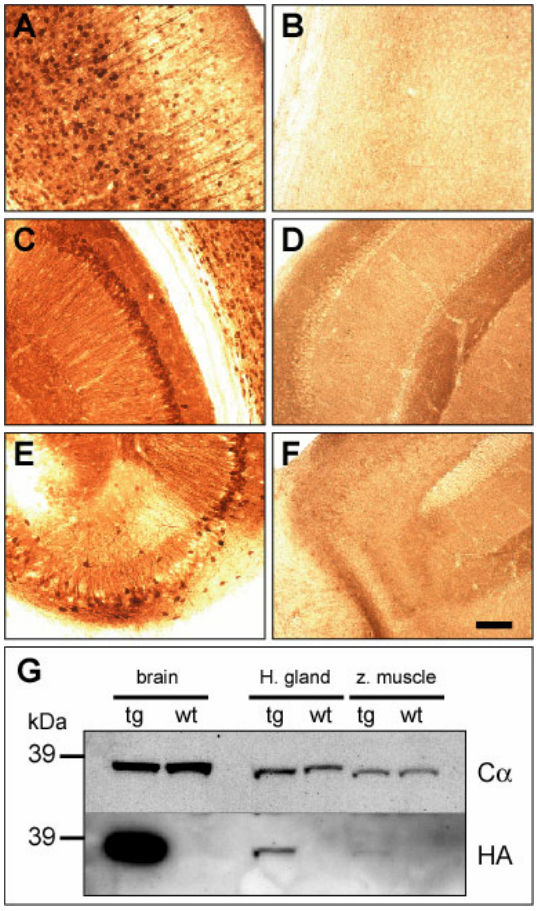

Figure 14:
Expression pattern of Cα L309A in transgenic mice. Immunohistochemical staining of L309A brain sections using an HA-specific antibody reveals neuronal expression within most brain areas. Strong expression is found in cortical layers III-VI (*A*), and the CA1 (*C*) and CA3 (*E*) fields of the hippocampal formation. No staining is detected in corresponding brain areas of WT mice (*B,D,F*). Scale bar: 100 µm. (*G*) Western blotting of tissue homogenates using an HA-specific antibody shows that the transgene is strongly expressed in the brain but also in the Harderian gland of L309A mice (TG). The zygomatic (cheek) muscle was included because of its proximity to the gland and brain. Expression is not detectable in skeletal muscle, lung, liver, heart, and spleen. Similarly, no expression is found in brain and gland of WT controls. An antibody directed against PP2A C (endogenous and mutant) reveals that total levels of C are not increased upon expression of Cα L309A.

8.4.2 Altered recruitment of PP2A regulatory subunits into the PP2A complex in L309A mice

Based on *in vitro* findings that residue L309 regulates the recruitment of regulatory subunits into the PP2A complex, I assessed the heterotrimer composition in L309A mutant brain and Harderian gland. PP2A regulatory subunits were quantified by Western blotting using crude brain homogenates. This serves as an indirect measure for the recruitment of regulatory subunits into the PP2A complex, where they are more stable than in the monomeric unbound form. In L309A mice, our study revealed an altered recruitment of regulatory subunits into the complex (Figure 15*A*). In brain, PR55α and PR61ε were reduced to 49% (n=8 transgenics (TG), 10 WT) and 48% (n=3 TG, 5 WT) (Figure 15*B*). Relative levels of A and C were unaffected in L309A mice, based on normalization with glyceraldehyde-3-phosphate dehydrogenase (GAPDH), hence, levels of regulatory subunits were normalized to A (Figure 15*B*). In the Harderian gland PR55α was reduced to 46% (5 glands pooled) and PR61ε to 38% (2 x 5 glands pooled), whereas

PR61γ and PR59 were increased 2.5- and 3-fold, respectively, compared to WT (2 x 5 glands pooled) (Figure 15*C*). For comparison, B subunit levels were not altered in tissues other than brain and Harderian gland. Even extracts derived from the zygomatic muscle adjacent to the Harderian gland did not reveal altered levels of B subunits (Figure 15*A*). Additional regulatory subunits have not been examined, as for most of them specific antibodies are not available.
Together, our data demonstrate that leucine 309 of Cα controls PP2A regulatory subunit composition *in vivo* and that regulatory subunits are stabilized upon recruitment into the PP2A heterotrimer complex.

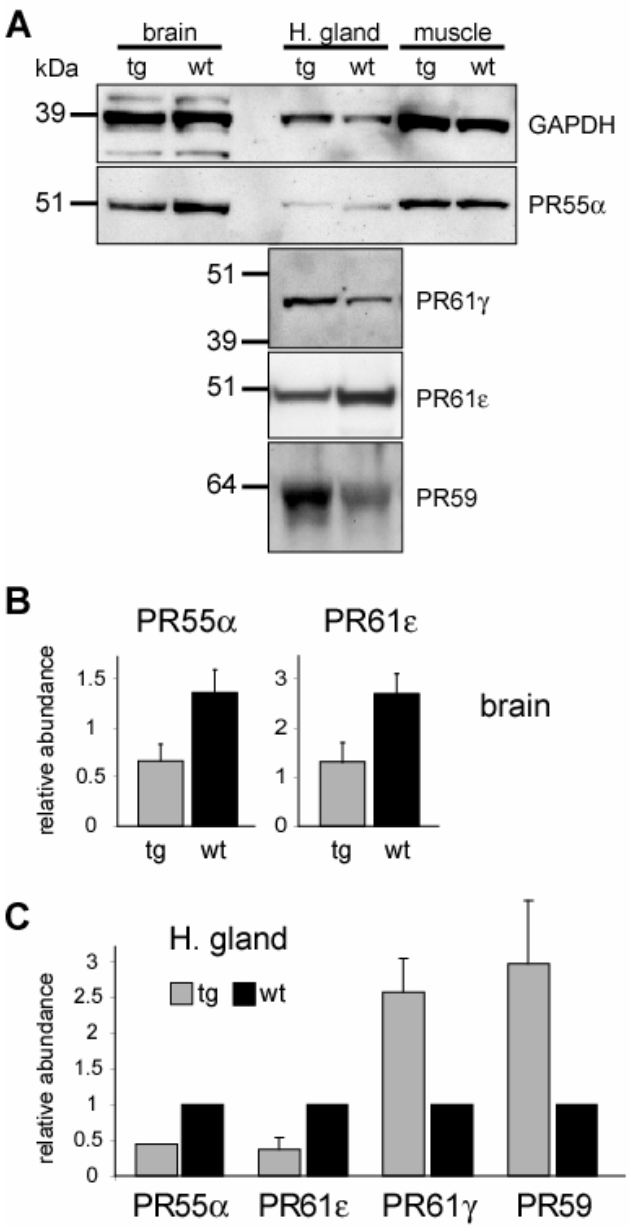

Figure 15:
Altered levels of distinct regulatory subunits in L309A mice. (*A*) Immunoblotting and subsequent quantification of density values. In total brain extracts of L309A (TG) versus WT mice, PR55α and PR61ε are reduced to 49% (8 TG, 10 WT) and 48% (3 TG, 5 WT), respectively, together with a non-significant increase in levels of PR61γ and PR59 (*B*, and data not shown). Relative levels of subunits C and A are unaffected in L309A mice, based on comparison with GAPDH, and therefore, levels of regulatory subunits were normalized to A (*B*). Mean values and standard errors are shown. In total extracts of the Harderian gland (*C*), PR55α is reduced to 46% (5 glands pooled) and PR61ε to 38% (2 x 5 glands), and PR61γ and PR59 levels are increased 2.5- and 3-fold, respectively, when compared with WT controls for which levels were set to 100% (2 x 5 glands). The relative abundance of regulatory subunits is a measure of the degree of recruitment into the PP2A complex, as momomers are stabilized when bound to the core dimer.

8.4.3 Increased phosphorylation of the PP2A substrates tau and vimentin

Altered PP2A subunit composition was expected to affect substrate specificity *in vivo*. Therefore, I stained L309A and WT brain sections with the phosphorylation-dependent anti-tau antibodies S199P, CP13, AT100, AT180, 12E8, AD2, and pS^{422}, directed against tau phosphorylated at S199, S202/T205, T212/S214, T231/S235, S262/S356, S396/S404, and S422, respectively (Buee-Scherrer et al., 1996; Bussiere et al., 1999; Delacourte et al., 1998; Goedert et al., 1994; Hoffmann et al., 1997; Saito et al., 1995; Sergeant et al., 1999; Seubert et al., 1995). These epitopes were previously used to assess tau phosphorylation in human WT and frontotemporal dementia mutant tau transgenic mice (Gotz et al., 2001; Gotz et al., 2001; Gotz et al., 1995; Probst et al., 2000). Antibody CP13 revealed phosphorylated tau in L309A mice throughout the brain, but predominantly in cerebellar Purkinje cells, and in axonal and somatodendritic compartments of cortical and thalamic neurons (Figure 16*A,C,E*). Other epitopes of tau were not phosphorylated at detectable levels. No phospho-tau immunoreactivity was detected in non-transgenic controls (Figure 16*B,D,F*).

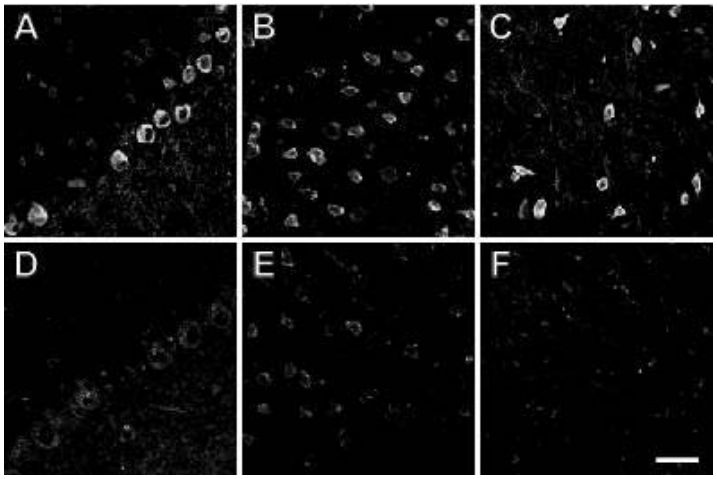

Figure 16:
Tau phosphorylation in the brain of L309A mice. The CP13 antibody directed against tau phosphorylated at Ser-202/Thr-205 reveals immuno-reactive tau throughout the brain of L309A transgenic mice. Staining is prevalent in axonal and somatodendritic compartments of cerebellar Purkinje cells (*A*), and neurons of the frontal cortex (*B*) and thalamus (*C*). Corresponding areas of non-transgenic controls are not stained (*D-F*). Scale bar: 20 µm.

As the cytoskeletal protein vimentin is an *in vitro* substrate of B/PR55 containing PP2A heterotrimers (Turowski et al., 1999), recombinant vimentin was pre-labeled with protein kinase A and [γ-32P]-ATP, and subsequently dephosphorylated with L309A and WT brain extracts. I found that both extracts dephosphorylated vimentin within minutes, however, dephosphorylation of vimentin was more pronounced with WT than with L309A homogenates (Figure 17). Dephosphorylation by WT could be partially inhibited with 30 nM OA, a potent PP2A inhibitor, providing evidence for a PP2A-mediated dephosphorylation of vimentin (Figure 17).
Finally, to assess overall PP2A activity, I analyzed total brain and hippocampal extracts using a commercial assay with the small artificial phosphopeptide RRA(pT)VA as substrate. I found that general PP2A activity was not decreased in L309A mice (data not shown).

Together, our data indicate that vimentin is a substrate of PP2A, and that, as shown for tau, distinct PP2A regulatory subunits regulate vimentin dephosphorylation.

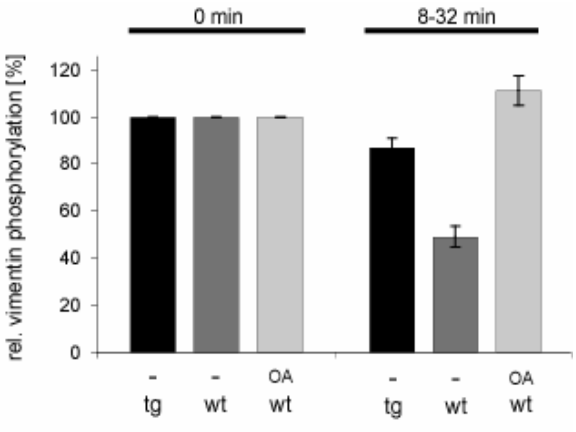

Figure 17: Increased vimentin dephosphorylation with L309A brain homogenates.
Recombinant vimentin was pre-labeled with [γ-^{32}P]-ATP by protein kinase A, followed by dephosphorylation with brain extracts. Dephosphorylation of vimentin is more pronounced with WT than with L309A (TG) brain homogenates. This can be inhibited with 30 nM OA. The extent of vimentin phosphorylation is indicated by relative signal density values which are normalized to the corresponding samples at time 0 (= 100%). Shown are mean values and standard errors (n=3 x 3).

8.4.4 Slit-eye phenotype in L309A mice caused by delayed and impaired development of the Harderian and lacrimal gland

The L309A mice demonstrated a 100% penetrant slit-eye phenotype reminiscent of enophthalmos in man, which became evident at two weeks of age (Figure 18). This phenotype might be caused by small eyes (microphthalmia) due to impaired development or atrophy, by changes of the retroocular structures including lacrimal glands, fatty tissue and muscles, or by defects of the bony orbit itself. Microphthalmia and defects of the bony structures could be excluded as a possible cause implying that altered retroocular structures caused the depression of the eyeball within the orbit (enophthalmos).

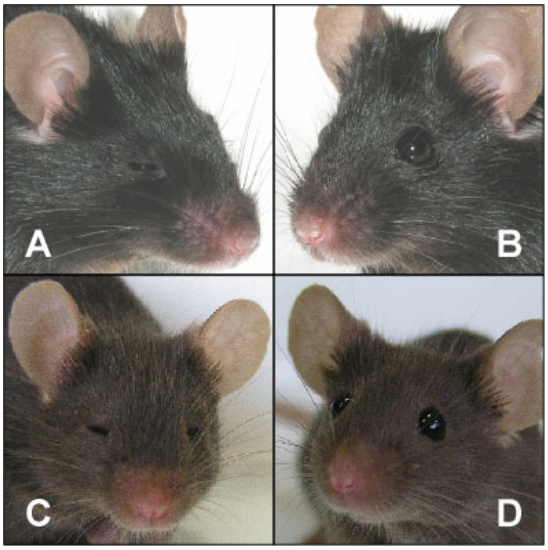

Figure 18:
Slit-eye phenotype of L309A transgenic mice.
In WT mice two weeks postnatally, the eyes bulge and appear large and wide open (*B,D*), whereas in L309A mice (*A,C*), delayed and impaired development of the Harderian and lacrimal glands causes the eyes to sink deeply into the orbits (enophthalmos).

Sagittal sections through the eyes of two and eleven month-old L309A mice revealed a normal structure of the anterior uvea with an intact iris, stroma and pigment epithelium. There was evidence for a slight age-related atrophy of the ciliary body and age-related degeneration of the outer retinal layer (Figure 19). The lens, retinal organization, photoreceptors and Bruch's membrane appeared normal, except for a few old transgenic mice, where cataract was observed. On the contrary, haematoxylin/eosin (HE) stainings of decalcified and paraffin embedded mouse heads showed marked changes in the transgenic Harderian and lacrimal gland, implying that altered retroocular structures caused the enophthalmos.

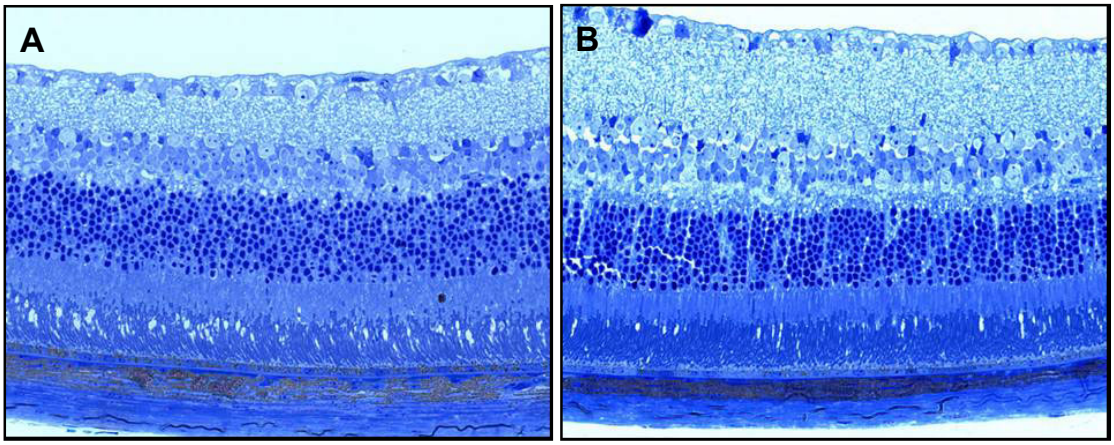

Figure 19: Morphology in L309A mutant eyes. Sagittal sections through the eyes of two and eleven month-old L309A (*A*) and WT (*B*) mice revealed a normal structure of the anterior uvea with an intact iris, stroma and pigment epithelium. There was evidence for a slight age-related atrophy of the ciliary body and age-related degeneration of the outer retinal layer; however the lens, retinal organization, photoreceptors and Bruch's membrane appeared normal, except for a few old transgenic mice, where cataract was observed. Original magnification x 400. (in collaboration with Dr. Ch. Remé)

The Harderian gland was first described in 1694 by the Swiss physician Johann Jacob Harder (1656-1711). It occurs in most terrestrial vertebrates and is located within the orbit where, in some species, especially ungulates and rodents, it is the largest structure. Humans only possess a rudimentary one. The Harderian gland is a large tubular alveolar tissue located within the orbit, on the posterior aspect of the eyeball. It indents the extraorbital lacrimal gland, which is comparably small and located in the anterior orbit. The tubules of the gland are formed of a single layer of columnar epithelial cells surrounded by myoepithelial cells (Payne, 1994). The chief product(s) of the gland varies between different groups of vertebrates, and epithelial cells possess granules or vacuoles whose contents may be mucous, serous or lipid. In rodents, the gland synthesises lipids, porphyrins and indoles. In the case of lipid vacuoles, the gland is unusual in releasing these by an exocytotic mechanism. It is unclear whether the gland can act both as an exocrine and endocrine organ. There is control of gland structure and synthesis through a variety of humoral agents, including gonadal, thyroid and pituitary hormones; in addition there is a rich autonomic innervation and many neuropeptides have been identified. The proposed functions of the gland are remarkably diverse. The lipids are thought to lubricate

the eye and the nictitating membrane (Buzzell, 1996). Secretions coat the eye, and drain down into the nose. Moreover, the Harderian gland has been proposed to play a role in osmoregulation, the immune response, photoprotection and retinal-pineal axis establishment and include the gland being a source of thermoregulatory lipids and growth factors. (Payne, 1994). However, despite more than three centuries of investigation, many features of this gland, including its development and function, are not yet well established (Buzzell, 1996).

Several transgenic approaches have been applied either to gain insight into Harderian gland function or they happened to cause a Harderian phenotype, due to choice of promoter and transgene. Expression of oncogenes such as v-ras caused proliferative alterations ranging from hyperplasia to wide tissue destruction (Sinn et al., 1987; White et al., 1990). In the most advanced situations, these changes were accompanied by a glandular hypertrophy (Coto-Montes et al., 1997). These and related studies demonstrated that the Harderian gland is susceptible to hyperplasia and tumor formation, without providing insight into organogenesis and function. In int-3 transgenic mice incomplete differentiation and the presence of proliferating immature ductule cells were reported demonstrating that expression of the activated Notch-related int-3 gene causes deregulation of normal developmental controls *in vivo* (Jhappan et al., 1992). To address functional aspects, prolactin transgenic mice were compared with prolactin knockout mice. It was found that prolactin is required for porphyrin secretion by the Harderian gland but that it is not playing an essential role in the secretory immune function of the lacrimal gland (McClellan et al., 2001). Furthermore, FGF-10, a member of the fibroblast growth factor family, was shown to be required for both lacrimal and Harderian gland formation (Govindarajan et al., 2000).

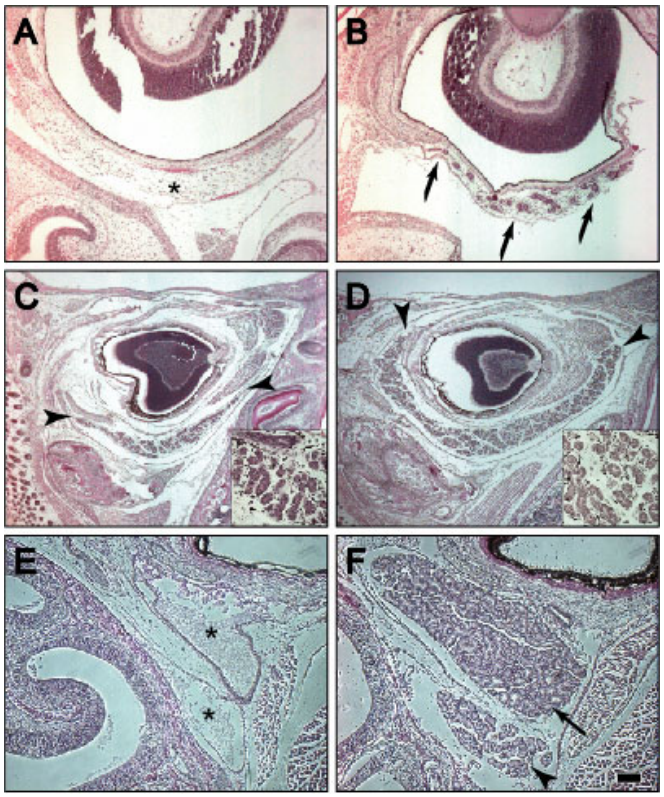

Figure 20:
Delayed and impaired development of L309A Harderian and lacrimal glands. At postnatal day 3 (P3), a Harderian gland (*A*, asterisk) can not be detected on haematoxylin/eosin-stained frontal L309A sections. In contrast, on WT sections acini of the developing gland are visible in the posterior aspect of the eyeball (*B*, arrows). At P10, sagittal sections present a tiny gland in L309A (*C*) compared to WT mice (*D*). While in WT mice, the gland spans more than the total of the posterior aspect of the eyeball (*D*, arrowheads), this extension is much shorter in L309A mice (C, arrowheads). Insets show the gland at higher magnification. At P18, in L309A mice, most portions of the posterior aspect of the eyeball are devoid of glandular tissue (*E*, indicated by an asterisk). An age-matched WT mouse displays a lacrimal system with both the Harderian (arrow) and lacrimal gland (arrowhead) (*F*). Scale bar: *A,B,E,F* (0.10 mm); *C,D* (0.25 mm); insets (46 µm).

While in WT mice the gland starts to develop perinatally, its development was delayed in L309A mice, as shown for postnatal day 3 (P3) (Figure 20*A,B*). WT mice start to develop an intact gland around birth, with secretory tubules and alveoli that grow considerably as the mice become older. The mThy1.2 promoter used for transgene expression is turned on at around embryonic day E16, shortly before the gland becomes visible in WT mice, and reaches maximal levels at P28 (Kollias et al., 1987; Luthi et al., 1997). At P10, the L309A Harderian gland was tiny compared to WT (Figure 20*C,D*). While the two Harderian glands grew rapidly in WT mice at P12, causing the eyes to bulge, the transgene-induced destruction of the Harderian gland in the L309A mice became visible upon external inspection as it caused the eyes to sink deeply into the orbits (Figure 18). A vast deterioration of the Harderian gland was evident in all L309A mice at P18, leaving extra space in the orbit (Figure 20*E,F*). Yet, cell types and the general glandular organization of the tissue were not affected. When 11- to 15-month-old L309A mice were examined, the Harderian gland was almost completely missing, with the average weight of the lacrimal system being reduced from 180 mg to less than a fourth (data not shown).
Nevertheless, when 1, 3, 10 and 18 days old L309A and WT mice were analyzed with a TUNEL (terminal deoxynucleotidyl transferase–mediated dUTP-biotin nick end labeling) assay, similar numbers of apoptotic cells were found (Figure 21). This indicates that Harderian and lacrimal glands are not subject to degeneration but rather to an impaired development.

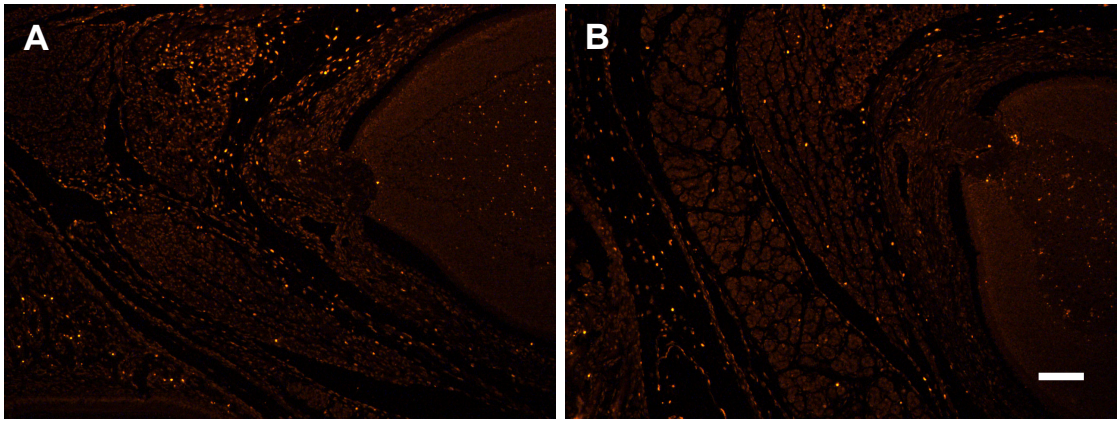

Figure 21: Tiny Harderian and lacrimal glands are not due to apoptosis. Sagittal sections from 10-days-old L309A (*A*) and WT (*B*) mice stained with TUNEL (terminal deoxyribonucleotidyl transferase (TdT)-mediated biotin-16-dUTP nick-end labeling) demonstrated that the tiny glands found in L309A mice are not due to atrophy through apoptosis and degeneration, but rather the result of an aberrant development. Scale bar: 0.2 mm. (in collaboration with Dr. L. Ittner)

To determine whether defective innervation may have contributed to small Harderian glands in L309A mice, sections from 18 days old glands were stained with the neuron-specific antibodies NSE and PGP9.5. These revealed comparable numbers of nerve fibers with similar diameters in both WT and L309A glands (Figure 22).

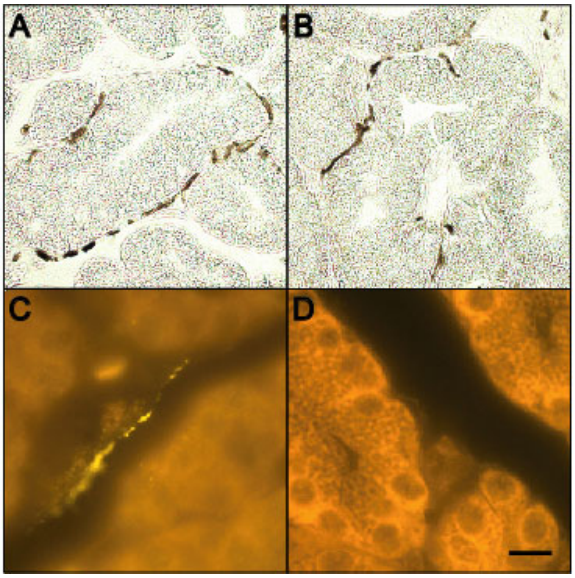

Figure 22:
Intact innervation of the L309A Harderian gland. Parasagittal sections from 18-days-old L309A (*A,C*) and WT (*B*) mice, stained with the neuron-specific antibodies NSE (*A,B*) and PGP9.5 (*C*) reveal comparable numbers of nerve fibers with similar diameters in the Harderian glands at all ages analyzed. As a control, the primary antibody was omitted (*D*). Scale bar: *A,B* (28 µm); *C,D* (20 µm).

Together, these data show that the carboxy-terminal leucine L309 of the catalytic subunit of PP2A determines PP2A heterotrimer composition *in vivo*. Moreover, our findings indicate that PP2A plays a crucial role in regulating cell adhesion *in vivo*, as demonstrated for the Harderian gland, where L309A expression causes a delayed and impaired postnatal development resulting in enophthalmos. Our findings imply that PP2A executes similar functions in other glandular tissues.

8.4.5 Function of L309A mutant eyes

To test whether enophthalmos in L309A mice altered eye function, Ganzfeld electroretinography (ERG) analyses of 10 month-old L309A mice (n=4) and WT littermate controls (n=4) was performed in collaboration with Dr. M. Seeliger and coworkers. This revealed normal retinal function in L309A mice lacking a proper Harderian gland (Figure 23). Moreover, scanning laser ophthalmoscopy after contrast dye injection showed normal blood flow in the eye although a pulsation of larger veins occurred in L309A mice (Figure 24). This venous pulsations in all L309A transgenic mice that underwent SLO imaging (n=4) may indicate altered hemodynamic characteristics due to the different eye position in the orbit.

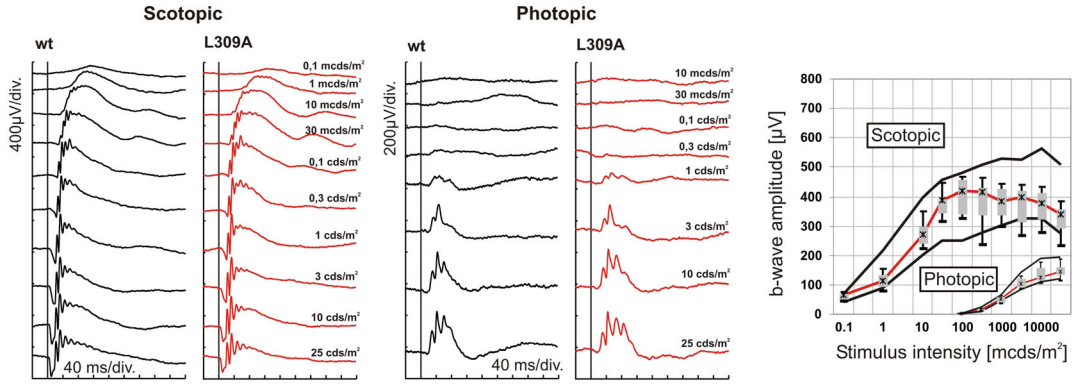

Figure 23: Electrophysiological evaluation of L309A transgenic mice aged 10 months. Left: Scotopic (dark adapted) intensity series. Center: Photopic (light adapted) intensity series. Right: Dark-adapted and light-adapted b-wave amplitudes as a function of the logarithm of the flash intensity. In both graphs, data from the transgenic mice are given as box-and-whisker-plots showing 5% and 95% quantiles (whiskers), 25% and 75% quartiles (box), and the median (marked by a cross). The black lines delimit the range given by the 5 and 95 % quantile of the wt controls. (in collaboration with Dr. M. Seeliger and coworkers)

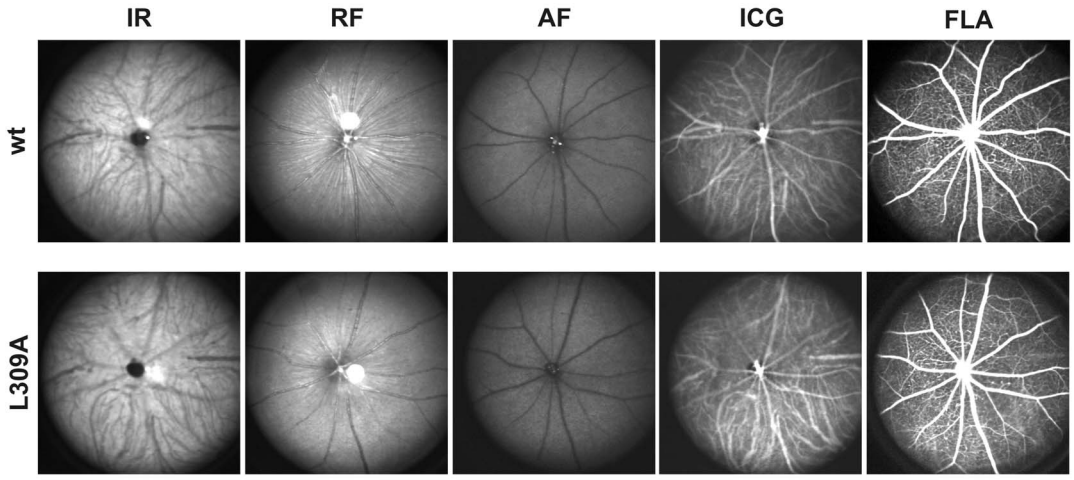

Figure 24: Scanning laser ophthalmoscopy (SLO). *In vivo* imaging of L309 transgenic mouse eyes (bottom row) in comparison to WT (top row). From left to right: Native imaging in infrared (IR, 830 nm), red-free (RF, 514 nm), and autofluorescence mode (AF, 488 nm & barrier at 500 nm). Angiography with indocyanine green (ICG, 795 nm & barrier at 810), and fluorescein (FLA, 488 nm & barrier at 500 nm). There is no apparent difference between the transgenic and the WT mice. (in collaboration with Dr. M. Seeliger and coworkers)

8.4.6 Defective cell adhesion in the L309A Harderian gland

Our group has previously shown defective cell adhesion in PP2A $C\alpha^{-/-}$ embryos, with reduced levels of β-catenin and E-cadherin. Moreover, both proteins were translocated to the cytoplasm, suggesting a role for PP2A in stabilizing the β-catenin/E-cadherin complex at the plasma membrane (Gotz et al., 2000). When I addressed cell adhesion in the L309A mice, cadherins and β-catenin were not significantly affected in brain. However, while both proteins showed prominent membrane localization in WT Harderian glands, they were significantly reduced and more broadly distributed throughout the cytoplasm in the L309A gland (Figure 25 and 26).

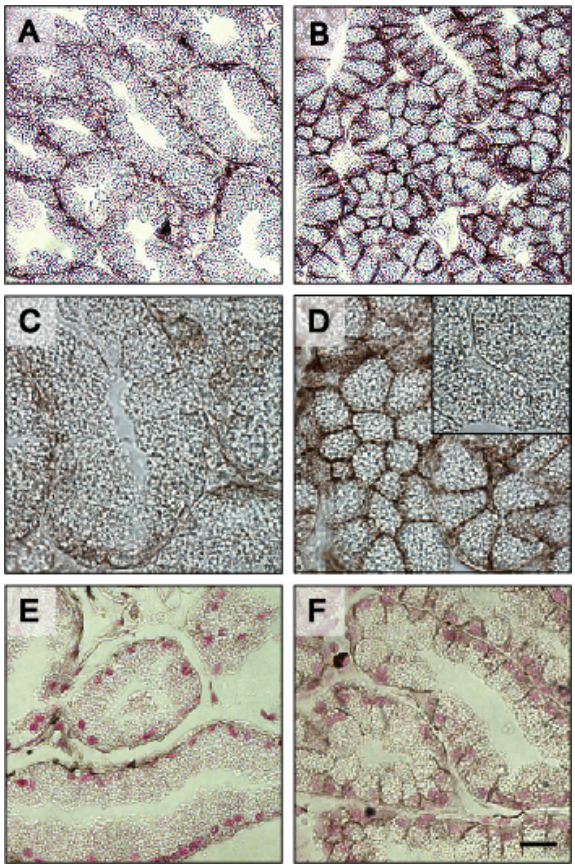

Figure 25:
Cell adhesion in the L309A Harderian gland. Immunohistochemical staining of Harderian glands reveals altered cellular localization and reduced levels of cadherins (*A-D*) and β-catenin (*E,F*). Frontal sections of L309A mice (*A,C,E*) and corresponding WT sections (*B,D,F*) are shown at three magnifications. Both proteins show prominent membrane localization in the WT gland, but are significantly reduced and more broadly distributed throughout the cytosol in the mutant gland (inset in *D* shows control without a primary antibody). Scale bar: *A,B* (11 µm); *C,D* (14 µm); *E,F* (20 µm).

I next performed a Western blot analysis of membrane and cytosolic fractions from brain and gland. To confirm the purity of the fractions, antibodies specific for GAPDH and the carboxy-terminal fragment of the amyloid precursor protein, APP, were used. Cadherins and β-catenin were found almost exclusively in the membrane fraction of both L309A and WT brains (Figure 26). In the WT Harderian gland, both cadherin and β-catenin were found in the cytosolic fraction with levels that were approximately three times lower than in the membrane fraction. In L309A glands, this ratio was preserved for cadherin, however, in both fractions levels were four times lower than in WT. In contrast, levels of β-catenin were reduced threefold in the cytosol of the L309A gland, but ninefold in the membrane fraction. Together this indicates a major reduction of membrane-associated β-catenin in the L309A gland, resulting in similar levels of β-catenin both in the cytosolic and the membrane fraction (Figure 26). β-actin, which is associated with the cadherin-β-catenin complex through α-catenin, was equally abundant in L309A and WT brains, but in contrast to GAPDH, hardly detectable in the cytosolic fraction of the L309A gland (Figure 26). Cα L309A was found at higher levels in the cytosolic than in the membrane fraction in brain and almost exclusively in the cytosolic fraction of the L309A gland (Figure 25).

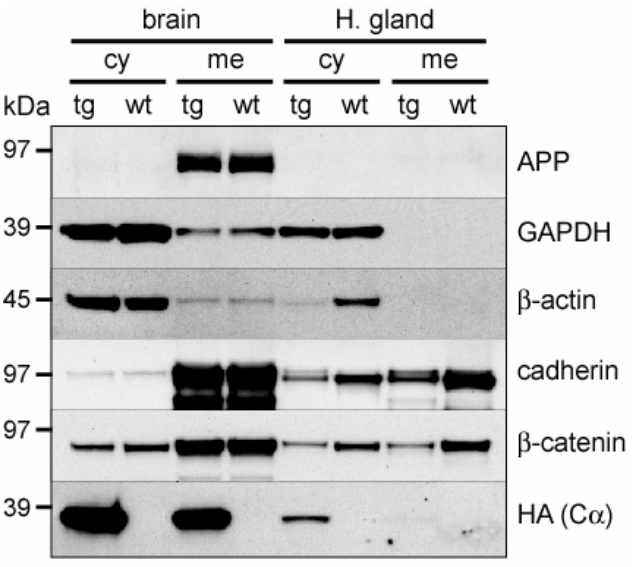

Figure 26:
Major reduction of membrane-associated β-catenin in the L309A (TG) gland.
L309A glands show similar levels of β-catenin in both membrane (me) and cytosolic (cy) fractions, whereas in WT, β-catenin is three times more abundant in the membrane fraction. Levels of cadherins are reduced fourfold in both fractions in the L309A compared to the WT gland. β-Actin is hardly detectable in the cytosolic fraction of the L309A gland, while it is equally abundant in brains of L309A and WT mice. Cα L309A is found at higher levels in the membrane compared to the cytosolic brain fraction, but almost exclusively in the cytosolic fraction of the gland. Purity of the fractions was confirmed with GAPDH- and amyloid precursor protein-specific antibodies.

For cadherin, adhesion has previously been shown to depend on casein kinase 2 (CK2) and glycogen synthase kinase-3β (GSK-3β) mediated phosphorylation (Lickert et al., 2000). Since there are activity-dependent antibodies available for GSK-3β, but not for CK2, I concentrated my analysis on GSK-3β, which is negatively regulated by phosphorylation at Ser-9 (Lau et al., 1999). By immuno-blotting, an increased phosphorylation at Ser-9 of GSK-3β was found in the L309A gland, but not in brain or zygomatic (cheek) muscle (Figure 27). As total levels of GSK-3β were reduced in the L309A gland compared to WT, but not in brain or the zygomatic muscle, relative levels of Ser-9 phosphorylated GSK-3β in the L309A gland are even higher.

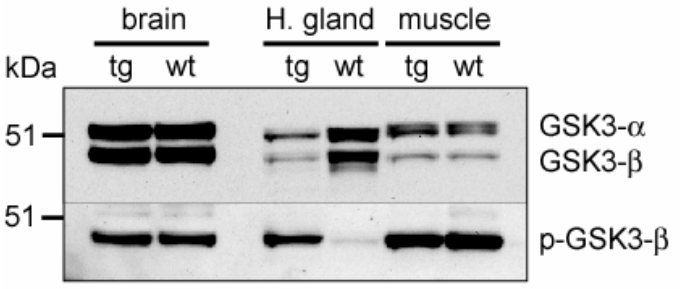

Figure 27: In the TG gland GSK-3β is phosphorylated at Ser-9, which negatively regulates kinase activity. Total levels of GSK-3α and GSK-3β are reduced in the L309A gland, whereas phosphorylation at Ser-9 is increased.

9 DISCUSSION

9.1 Modest learning deficits in L199P transgenic mice

Transgenic mice expressing the dominant negative L199P mutation in the catalytic subunit Cα of PP2A have revealed a 30% reduction of PP2A activity in brain homogenates, together with abnormally phosphorylated endogenous tau that was partly relocated to the somatodendritic compartment. These mice were the first transgenic mouse model showing that PP2A is an *in vivo* phosphatase of tau (Kins et al., 2001).

In two different Morris water maze tests, the "standard" and a more sophisticated protocol, L199P mutant mice showed similar performance as WT littermates in regard to escape latency and the number of trials to criterion. In contrast, in two independent probe trials, one after the acquisition phase and one after the reversal phase (new platform position), L199P mice spent significantly less time in the target quadrant. I speculate that transgenic mice confounded the task of learning a new platform position with the search for the old position, an effect that could have caused the bad performance by L199P mice on day 2 of the reversal phase. The more sophisticated second relearning test revealed that transgenic L199P mice navigate less precisely. The observed effects were statistically significant but small and were only captured by path geometry directly and did not translate into a general escape performance. Since this second test was especially focusing on the relearning, I conclude that the navigation problem does not appear to be linked specifically to the continuous relearning situation. Transgenic mice adapted normally to the test, thigmotaxis was not increased, and the tendency to float was even smaller for L199P mice. Analysis of the same mice on a rotarod revealed no motor deficits in L199P mice. Nevertheless, the average swim speed was significantly increased in transgenics. There is no plausible explanation for this phenomenon except for the widely accepted fact that the overexpression of any transgene causes many transgenic mice to be hyperactive and therefore more active in open field and Y-Maze tests (Holcomb et al., 1999; Moechars et al., 1999; Wong et al., 1997), which could also make them swim faster in a water maze test. Weight differences and size could be another explanation, although this would probably translate into the ability to maintain balance on the rotarod at accelerating rotation speeds, and such differences in performance have never been observed.

Although the behavioral tests using the Morris water maze revealed only modest learning deficits for the L199P mice, these were found several times for different parameters. It is expected that learning deficits would be more pronounced if the PP2A activity in the brain of transgenic mice would be further reduced. This could be achieved by overexpressing the dominant negative mutant form of PP2A/Cα, L199P, by breading our mice to homozygosity. Another approach would be to reduce levels of endogenous PP2A/Cα to increase the dominant negative effect by crossing the L199P mice to the heterozygous Cα knock-out mice. Also interbreeding with AD-transgenic models including tau filament-forming mice, and by a complete knock-out of the brain specific regulatory subunit of PP2A, PR55γ would possibly cause

an increased behavioral phenotype. Finally PP2A activity could be further reduced by using PP2A inhibitors such as OA. This has been done in chicken and rat in the course of our study. Deficits in memory retention were found in chicken treated with calyculin (CA) or OA (Bennett et al., 2001), and unilateral injection of OA into rat hippocampus induced a transient impairment of spatial memory on an eight-arm radial maze task in rats (He et al., 2001). Recently, another group showed tau hyperphosphorylation and impairment of spatial memory retention after bilateral injection of CA into rat hippocampus (Sun et al., 2003). However, by using OA and in particular CA instead of transgenic approaches, these studies do not reveal whether the behavioral findings are due to PP2A inhibition alone and/or to PP1 inhibition. As discussed in section 9.3 (page 69), OA is only specific for PP2A within a specific concentration range, and CA is inhibiting both, PP2A and PP1. Our approach, which for obvious reasons is 100% PP2A specific, revealed an effect of PP2A. Yet, it remains to be established whether the association of tau hyperphosphorylation and spatial memory loss is a causal one. Spatial learning and memory need regulated protein phosphorylation executed by a specific set of enzymes. It is well accepted that spatial learning and memory is hippocampus-dependent, and single cells in the hippocampus can encode specific spatial information. However, how each phosphatase functions and the exact mechanism of behavioral abnormalities caused by PP inhibition are barely understood.

9.2 B/PR55 levels in undifferentiated and neuronally differentiated cells

Steady-state mRNA levels of the four B/PR55 regulatory PP2A subunits were determined by qRT-PCR in both HEK-293 and SH-SY5Y cells. I found comparable mRNA levels of the four members of the PR55 family in both HEK-293 and undifferentiated SH-SY5Y cells. PR55α was the major species in both cell-types, and amounts of PR55γ mRNA were slightly lower than those of PR55δ. PR55β concentrations were very low in SH-SY5Y cells and barely detectable in HEK-293 cells. This suggests that the PR55β subunit, despite its low relative levels compared to the other three subunits, may perform a distinct function in cells that are capable of neuronal differentiation. The finding that PR55γ was transcribed by non-neuronal HEK-293 cells as well, whereas in adult tissue it is restricted to brain, may be related to the relative ease with which HEK-293 cells can acquire neuronal properties upon transfection with genes encoding channel subunits and the like (Abraha et al., 2000).

When SH-SY5Y cells were differentiated, mRNA levels of PR55β, γ and δ subunit mRNA increased significantly. On the contrary, the amount of PR55α mRNA did not change during differentiation.

Our data show that PR55α is likely to perform more general functions in the cell, which are not associated with neuronal functions. In contrast, PR55β seems to be specifically induced during neuronal differentiation. Increased PR55β levels may both be caused by transition from an impure population composed of S- and N-type cells to a pure neuroblastic N-type population (transition of SH-SY5Y cells to N-R-type cells), and by an increased arborization during the

transition from N-R-type to N-R/B-type SH-SY5Y cells. Consistent with my findings, we have preliminary data of an impaired differentiation and a reduced viability in a partial knock-down cell line expressing a siRNA construct targeting PR55β (Dr. K. Schmidt, unpublished data).
Our data, together with the fact that PP2A plays an active role in neurite outgrowth and the maintenance of neurites (see section 8.3), point at specific roles for distinct regulatory B subunits in neuron-like cells.
To gain further insight into PR55 subunit function, short interfering RNA (siRNA)-mediated approaches may be envisaged to down-regulate individual PR55 subunits. However, this approach may be complicated by the fact that the four subunits are highly homologous (Schmidt et al., 2002). In addition, HEK-293 and SH-SY5Y cells are dividing at a pace that causes the immediate dilution of an *in vitro* produced and transfected siRNA construct. Also, down-regulation of one PR55 subunit may cause the compensatory upregulation of other members of the PR55 family or regulatory subunits belonging to other regulatory subunit families. This notion is supported by our finding in L309A mutant PP2A Cα transgenic mice demonstrating that recruitment of distinct regulatory subunits into the PP2A holoenzyme complex occurs at the expense of other subunits (Schild et al., submitted).

9.3 Transgenic mice expressing PP2A Cα, L309A

In WT mice, protein PP2A core dimers, composed of the catalytic subunit C and the structural subunit A, exhibit a low activity and only acquire full activity when the heterotrimer is assembled. The mutation L199P lies within the catalytic core of Cα and our mice therefore represent a transgenic mouse model in which the catalytic activity of PP2A is reduced without affecting holoenzyme assembly. To study PP2A heterotrimer composition in a transgenic mouse model, the dominant negative carboxy-terminal mutation L309A of Cα was expressed, which eliminates or reduces the binding of distinct regulatory subunits of PP2A. In the present study I showed firstly a role for L309 in regulating PP2A subunit composition *in vivo*, secondly a function for PP2A in tau and vimentin phosphorylation in brain, and thirdly a role for PP2A in cell adhesion in the Harderian gland.
This was achieved by expressing the PP2A Cα mutant L309A using an expression vector with the neuron-specific elements of the mThy1.2 promoter. Expression of transgenes using this promoter is mainly limited to postmitotic neurons. Nevertheless, in immature neuroblast layers of the CNS, and in several organs and tissues outside the nervous system, expression under the mThy1.2 promoter has also been reported (Campsall et al., 2002). The mouse line chosen for further analysis showed a strong expression in formations affected by AD, namely hippocampus and cortex, but also in other brain areas and in the Harderian gland, the major portion of the lacrimal system.
That total levels of C were not increased in the brain upon expression of the mutant protein was shown with the antibody PP2A/C and the antiserum 45, both directed against epitopes conserved between human and murine C. This result is consistent with tissue culture

experiments demonstrating that protein levels of C are subject to an effective autoregulatory mechanism keeping total levels constant (Baharians and Schonthal, 1998; Wera et al., 1995), and has also been observed in mutant L199P transgenic and heterozygous Cα knock-out mice (Gotz et al., 1998; Kins et al., 2001).

In vitro data suggest that L309A can alter the binding capacity of individual regulatory subunits to the PP2A dimer. Therefore, I assessed the PP2A heterotrimer composition in L309A mutant brain and Harderian gland by Western blotting using crude brain homogenates. PP2A heterotrimers were also purified by immunoprecipitation using A-specific antibodies, and in addition, microcystin sepharose affinity chromatography was used to enrich for protein phosphatases (Kloeker and Wadzinski, 1999; Meek et al., 1999). Enrichment for heterotrimers by immunoprecipitation revealed the same altered levels of regulatory subunits as for crude extracts and after MC purification (data not shown). This outcome indicates that regulatory subunits, which are not recruited by the AC core dimer, are degraded more rapidly and are therefore less abundant *in vivo*. This result is consistent with a model proposed earlier in which in *Drosophila* Schneider cells, not only was the AC core dimer unstable when not associated with regulatory subunits, but more importantly, knocking out A destabilized B and C, and knocking out C destabilized A and B (Li et al., 2002; Silverstein et al., 2002). The notion that the various regulatory subunits may be produced in abundance and compete for binding to the core dimer is supported by our finding that PR55α and PR61ε were decreased, whereas in the same tissue PR61γ and PR59 were increased. Additional regulatory subunits have not been examined, as for most of them specific antibodies are not available. Interestingly, of five PP2A subunits analyzed, PR61ε mRNA levels have been reported to be reduced in AD brain (Vogelsberg-Ragaglia et al., 2001).

In L309A mice, tau is abnormally phosphorylated at S202/T205, a typical AD phospho-epitope. Other epitopes of tau were not phosphorylated at detectable levels, which could either indicate specificity of regulatory subunits for S202/T205 or limitations in the detection method. Even though hyperphosphorylation of tau was found in brain, there was no sign of neurodegeneration, consistent with findings in WT and mutant tau transgenic mice with an even more pronounced hyperphosphorylation of tau (Goedert et al., 1995).

The cytoskeletal protein vimentin has been shown to be an *in vitro* substrate of B/PR55 containing PP2A heterotrimers (Turowski et al., 1999). I found that dephosphorylation of vimentin was more pronounced with WT than with L309A brain homogenates in an *in vitro* assay, and dephosphorylation by WT homogenates could be partially inhibited with 30 nM OA. Our data indicate that vimentin is a substrate of PP2A, and that distinct PP2A regulatory subunits regulate vimentin dephosphorylation, as shown for tau.

A previous study with fibroblasts suggested that vimentin phosphorylation caused by high (1-2 μM) but not low (10 nM) concentrations of OA was due to inhibition of protein phosphatase 1 (PP1), and not PP2A (Eriksson et al., 1992). However, *in vivo* or in tissue culture, OA has to be 100-fold more concentrated to cross the membrane at a rate comparable to other PP inhibitors such as calyculin A (Favre et al., 1997), whereas in cell extracts, OA inhibits PP2A at about 100-fold lower concentrations than those effective for PP1 (Cohen et al., 1989). Moreover, various

factors such as pH and temperature have an effect on membrane penetration (Namboodiripad and Jennings, 1996). Taking this into account, I conclude that with the OA concentrations used in my assay I can be sure to have inhibited mainly PP2A and can therefore state that vimentin is a substrate of PP2A *in vivo*. This finding is further supported by immunoprecipitation studies demonstrating an association of vimentin with B/PR55 (Turowski et al., 1999). In addition, it was shown *in vitro* that phosphorylation of vimentin was stimulated by PP2A inhibition in a dose-dependent manner, using 35-methyl-OA (Yatsunami et al., 1991).
General PP2A-specific phosphatase activity, as determined with a small artificial phosphopeptide as a substrate, was not decreased in L309A brain. This may indicate that elevated levels of regulatory subunits other than PR55α and PR61ε were able to counterbalance the L309A-mediated reduction in PP2A activity. This outcome is in agreement with findings in *S. cerevisiae*, where PP2A activity remained stable after removal or substitution of the carboxy-terminal leucine (Evans and Hemmings, 2000). To gain further insight, phosphopeptides would be needed that are selectively dephosphorylated by specific PP2A heterotrimers.

In addition to an abnormal dephosphorylation of cytoskeletal proteins in brain, I observed a slit-eye phenotype in L309A mice that was not caused by motor deficits or eye irritations but was rather the consequence of enophthalmos as a result of marked changes in the Harderian gland. I showed that PP2A is required for the integrity of the Harderian gland. Specifically I demonstrated that L309 of PP2A Cα plays a crucial role in regulating PP2A subunit composition and thereby controls cell adhesion in the Harderian gland.
Our findings were obtained by organ-specific expression of the PP2A Cα mutant L309A. Expression of transgenes using the mThy1.2 promoter is mainly but not exclusively confined to postmitotic neurons. It has also been reported in immature neuroblast layers of the CNS and in several organs and tissues outside the nervous system (Campsall et al., 2002).
The transgenic gland displayed a delayed and aberrant development. In 11- to 15-month-old L309A mice, the Harderian gland was almost completely absent. Nevertheless, the remaining glandular structure was intact, with no sign of alterations in cell types. Also, when transgenic glandular tissue was pooled, sufficient material was available to perform biochemical experiments. Reduced tear production due to a defective lacrimal system may be a reason for an opaque cornea occasionally observed in L309A mice. Degeneration of the Harderian gland in our L309A mice strikingly resembles that caused by prenatal exposure to 2,4-dichlorophenyl-p-nitrophenyl ether (nitrofen; NIT) (Gray et al., 1982), where a role of PP2A has been suggested (Arufe et al., 1999; Lazzereschi et al., 1997).
To investigate the nature of PP2A dysfunction responsible for the Harderian gland phenotype, I determined the PP2A subunit composition in the gland in more detail. Based on *in vitro* findings that L309A can alter the binding capacity of individual regulatory subunits to the PP2A dimer, I assessed the PP2A heterotrimer composition in L309A mutant gland by Western blotting using crude protein homogenates. This approach was based on the assumption that regulatory subunits, which are not recruited by the AC core dimer are degraded more rapidly and are therefore less abundant *in vivo*, a model proposed earlier in Drosophila Schneider cells (Li et al., 2002; Silverstein et al., 2002). The notion that the various regulatory subunits may be

produced in abundance and compete for binding to the core dimer is supported by our finding that PR55α and PR61ε were decreased, whereas in the same tissue PR61γ and PR59 were increased.
Impaired development of the lacrimal system is unlikely caused by defective or reduced parasympathetic innervation, as the neuron-specific antibodies NSE and PGP9.5 revealed comparable numbers of nerve fibers with similar diameters in both WT and L309A glands.
The finding that cells in the Harderian gland degenerated whereas those in brain did not, can not be explained by relative expression levels of the transgene. Rather, there may be a greater redundancy of phosphatases in brain as illustrated by the observation in humans that half of all genes were expressed in the brain with many being preferentially expressed in brain compared to peripheral tissues (Colantuoni et al., 2000; Consortium, 2004; Sandberg et al., 2000). In addition, glandular cells form a tight united cell structure, with cadherin and β-catenin playing crucial roles in stabilizing cell-cell contacts, whereas neurons are more loosely organized and form contacts via synapses.

Inhibition of PP2A with OA *in vitro* not only causes demethylation of leucine 309, but interestingly also induces hyperphosphorylation of β-catenin and loss of cell-cell contact in human epidermal cells (Favre et al., 1997; Serres et al., 2000; Serres et al., 1997). Our group has previously shown defective cell adhesion in PP2A $C\alpha^{-/-}$ embryos (Gotz et al., 2000). There, cellular levels of β-catenin and E-cadherin were reduced, and both proteins were translocated to the cytoplasm, suggesting a role for PP2A in stabilizing the E-cadherin/β-catenin complex at the plasma membrane in blastocysts (Gotz et al., 2000). In the L309A mouse model, reduced membrane levels of cadherins and β-catenin may, in part, also be due to altered phosphorylation. However, this is difficult to assess as no phosphosite-specific antibodies are available for those serine and threonine residues that regulate cell adhesion (Lickert et al., 2000). For cadherin, adhesion was shown to depend on casein kinase 2 (CK2) and GSK-3β mediated phosphorylation (Lickert et al., 2000). Treatment of keratinocytes with OA caused a decrease in cadherin phosphorylation, with a shift from the membrane to the cytoplasm and preventing cells from forming aggregates (Serres et al., 2000). In L309A Harderian gland, the altered localization of cadherin could be due to a reduced phosphorylation by GSK-3β, which is negatively regulated by phosphorylation at Ser-9 (Lau et al., 1999). An increased phosphorylation was found at this epitope in the L309A gland. Increased Ser-9 phosphorylation was not found in L309A brain, suggesting a more sophisticated control mechanism for activities of kinases and phosphatases. Also, I did not observe altered β-actin levels in brain, while β-actin was reduced to hardly detectable levels in the cytosolic fraction of the Harderian gland. β-actin may be destabilized due to an impaired interaction with the cadherin-β-catenin complex through α-catenin.

Together, our data show firstly that the carboxy-terminal leucine L309 of the catalytic subunit of PP2A determines PP2A heterotrimer composition *in vivo*. Secondly, I have demonstrated that this affects substrate specificity as shown for tau and vimentin. Thirdly, our findings indicate that PP2A in general and its heterotrimer composition in particular play a crucial role in cell

adhesion *in vivo*, as demonstrated for the Harderian gland where PP2A stabilizes β-catenin and cadherin in the plasma membrane. Reduced recruitment of specific regulatory subunits into the PP2A complex was shown to be associated with increased recruitment of other subunits. Establishing a role for distinct regulatory subunits, however, awaits further studies. Also, because of the observed interference of subunit assembly, B subunit-specific knock-out strains may not necessarily assist in this elucidation.

9.3.1 PP2A deficits in the thalamus of L309A mice may prevent the development of the Harderian gland through thyroid hormones

The metabolic maintenance and functions of Harderian and submandibular glands are regulated by hormones (Hoffman, 1971; Kumegawa et al., 1977). The Harderian gland is a large, orbital, lacrimal-type gland. Although it has been found to produce lubrication, pheromones, and immunoglobulins, its physiological role is not clear (Hoffman, 1971). The observation that L309A transgenic mice were significantly smaller in body mass (Figure 18), together with the undersized Harderian gland, causes us to speculate that the PP2A composition in brain could play a role in the production of thyroid hormones. The weight difference though does not translate into body size measured from the nose to the anus (data not shown), indicating that L309A mice have no altered level of growth hormones but rather of thyroid hormones, which have an impact on metabolic pathways. Also, mediated by altered thyroid hormone levels, PP2A could indirectly affect the development of the Harderian gland. In addition PP2A deficits in the thalamus as revealed by hyperphosphorylated tau in thalamic neurons of L309A mice (Figure 16*E*) could have effects on the brain-pituary-thyroid axis. This hypothesis states that the effects mediated through the L309A mutation are not directly linked to the Harderian gland through expression in the gland itself (Figure 14), but rather through a pathway involving the thalamus, the pineal gland, the thyroid gland and finally thyroid hormone and thyroxine levels (see Figure 29).

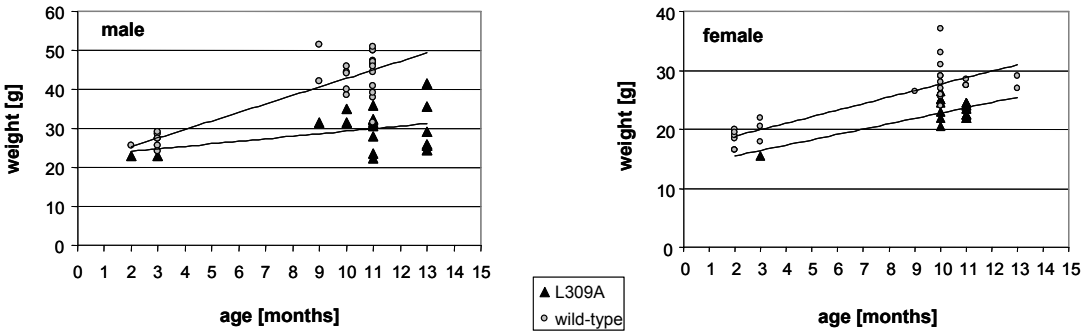

Figure 28: Body weight or L309A mice compared to WT littermates. Male (left) and female (right) mice show an age dependent increase in body weight. This increase is much less pronounced in L309A male mice. In both transgenic males and females, there is a significant overall reduction in body weight for mice older than 9 months. Body weight or mass is not to be confounded with body size which remains equal for both groups (data not shown).

The thyroid gland, which is located in the lower part of the neck, produces and releases two hormones, tetraiodothyronine (thyroxine, T_4) and triiodothyronine (T_3) (LoPresti and Singer, 1997). The gland has two lobes containing follicles filled with a colloid known as thyroglobulin in which the thyroid hormones are stored. The thyroid gland is predominantly a T_4-producing organ. Only about 20% of T_3 is synthesized and released from the thyroid; the remainder is produced by peripheral conversion of T_4 into T_3 by enzymes called deiondinase in the liver and kidney (LoPresti and Singer, 1997; Reed and Pangaro, 1995). Thyroid hormone production is regulated by serum T_4 and T_3 levels, as well as through the hypothalamic–pituitary axis. The hypothalamus stimulates the release of thyrotropin-releasing hormone (TRH). TRH stimulates the pituitary gland to release thyroid-stimulating hormone (thyrotropin, TSH) which, in turn, stimulates the thyroid to increase hormone synthesis. A rise in the thyroid hormone level inhibits the release of TRH and TSH by a negative feedback mechanism.

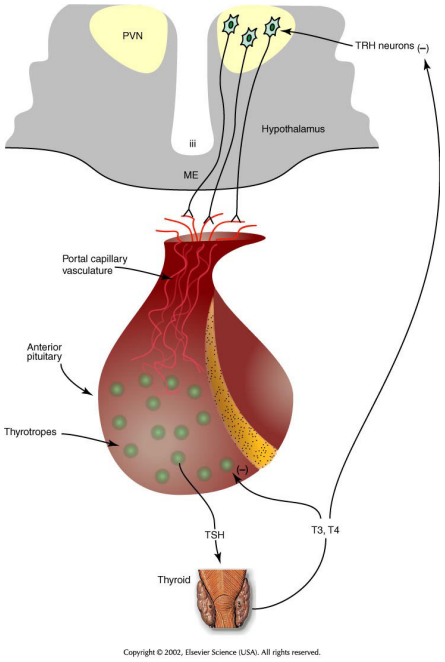

Figure 29: Schematic representation of the brain–pituitary–thyroid axis. TRH neurons in the paraventricular nucleus project their neuroterminals to the external zone of the median eminence. This occurs bilaterally, although only a unilateral projection is shown. TRH travels through the portal vasculature to cause the synthesis and release of TSH from thyrotropes. This molecule acts at the thyroid gland to cause the biosynthesis and release of the thyroid hormones, T_3 and T_4. These are released into the general circulation to affect metabolism and feedback in a negative manner at the thyrotropes of the pituitary and the TRH neurons of the PVN. PVN, paraventricular nucleus; TRH, thyrotropin-releasing hormone; ME, median eminence; iii, third ventricle; TSH, thyroid-stimulating hormone; T_3, triiodothyronine; T_4, thyroxine.

Chemical destruction of the Harderian gland can be achieved in mice by prenatal exposure to the herbicide 2,4-dichlorophenyl-p-nitrophenyl ether (nitrofen; NIT), a human carcinogen no longer manufactured or sold (Gray et al., 1982). The effects on experimental mice by NIT are striking in regard to resemblance to our L309A mice (Gray et al., 1982). Studies on the toxicity of NIT suggest an altered thyroid function (Ambrose et al., 1971), and lowered serum thyroxine levels (Gray and Kavlock, 1983). Earlier reports have revealed that growth of the Harderian glands is correlated with an increase in thyroxine secretion (Dohler et al., 1979), that thyroxine accelerates the development of the gland (Wetterberg et al., 1970), and regression of the Harderian gland was reported in thyroidectomized adult rats (Boas and Scow, 1954). In addition it has been shown that PP2A plays an important role in thyroid cell growth and in the

thyrotropin pathway (Lazzereschi et al., 1997), and observations on sheep thyroid cells indicate that PP2A and PP1 could be important mediators of thyroid hormone production (Arufe et al., 1999).

With this evidence bringing together PP2A and the Harderian gland, I propose that an altered PP2A composition in L309A mice may cause a deterioration of the Harderian glands by lowering thyroxine levels during development and/or throughout life.

Interestingly, the most striking feature of Graves disease, a human diseases involving excessive thyroid hormone (hyperthyroidism), is ophthalmopathy, with the eye changes including abnormal protrusion of the eyeballs from the orbits (Burman, 1995; Ladenson, 1996; O'Donnell and Spaulding, 1997; Streetman and Khanderia, 2003). This exopthalmia (bulging eyes) involving 1 or both eyes is the result of a local accumulation of hydrophilic mucopolysaccharides leading to edema. This in turn is caused by abnormal antibodies that attach to TSH receptor sites on the thyroid gland and cause long-term activation of it. In severe cases, exophthalmia can damage the optic nerve (Burch and Wartofsky, 1993; Streetman and Khanderia, 2003; Weetman, 1992; Weetman, 2003). In a patient with high rates of T_3, T_4 and TSH, physical examination showed bilateral and symmetrical exophtalmia, together with lid lag, increased thyroid volume with irregular surface and hardened consistence (Werneck et al., 2003). The Harderian gland as a direct cause for exopthalmia has been described after tumor formation in mice, where the bulging of the eyes was due to Halderian gland hyperplasia (Radany et al., 1997; Sinn et al., 1987).

Exopthalmia is exactly the opposite of what I observe in the L309A mice, namely enophthalmos. Therefore, as expected, L309A mice did not show any hyperthyroidism, which can be quite easily diagnosed by physical examination. In hyperthyroidism, the thyroid gland is enlarged, soft, and without nodules. This was leaving us with the more probable version of thyroid hormone insufficiency (hypothyroidism). In humans, hypothyroidism can cause severe problems such as sleep apnea, hypothermia, hypoventilation, neuropsychiatric syndromes, peripheral neuropathy, cerebellar ataxia, and coma. A test series of blood sera to answer the question of whether L309A mice have altered T_3, T_4, TSH, and TRH levels is currently being analyzed.

9.4 Targeting of PP2A PR55/B isoforms

In a collaboration with K. Schmidt and B. Hemmings from the Friedrich Miescher institute (FMI) in Basel, our aim was to produce knock-out mice by targeting the PP2A PR55/B isoforms α, β, and γ. The targeting constructs for γ, as outlined in Figure 30, was cloned by A.S. at the Division of Psychiatry Research, Zurich, while the constructs for α and β were produced at the FMI in Basel. The two constructs, α and γ were transformed into embryonic stem (ES) cells at the Institute for lab animal research in Zurich, while the targeting of β and as a repetition also α took place at the FMI. For all isoforms, control constructs with an enlarged short arm were designed and cloned in a way that the PCR to control for positive targeting could be optimized in advance by electroporating the control construct into ES cells. More than 1000 neomycine resistance positive ES cell clones were picked per isoform, lysed and analyzed by PCR. For many

clones, additional restriction enzyme digests and subsequent Southern blots were performed and analyzed. However, only unspecific integration events and some false positives, but no targeting by homologous recombination, were detected for all three constructs. This is particularly striking, since the constructs were designed to target different exon-intron regions and were in part performed at different institutes with diverging methods. How can three independent genes be impossible to target with the techniques applied. It seams as if the extremely high homology of PR55 isoforms in the range of 90% (see page 45, (Schmidt et al., 2002)) makes these target sequences to behave in the same way. Since they belong to different chromosomes and chromosomal regions, it must be the sequence itself rather than the region that makes them inaccessible. The sequence might for example cause the DNA to be particularly packed and therefore not accessible for recombination enzymes. Another possibility is that the high number of PR55 pseudogenes throughout the genome increases the risk for a random recombination. Therefore the number of false positive neomycin resistant clones may have been too high to find the needle, namely the homologous recombinant, in the haystack.

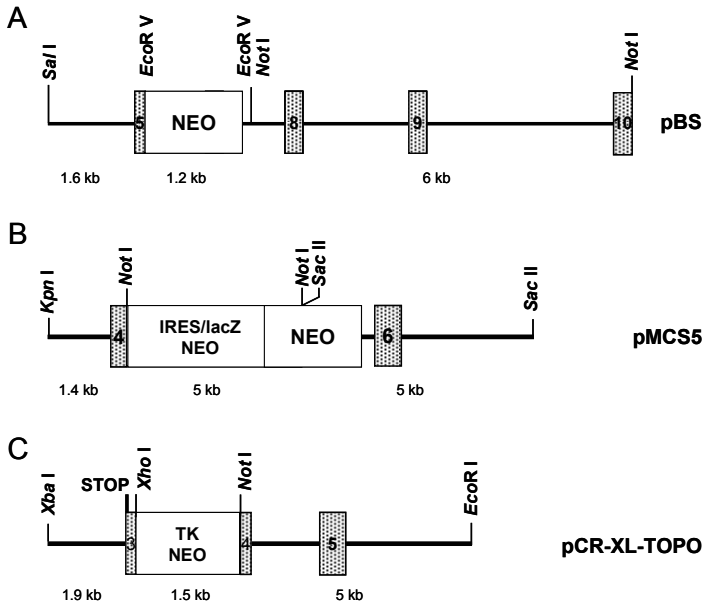

Figure 30:
Targeting strategies for the three PR55/B isoforms α (A), β (B), γ (C). The dotted boxes with numbers represent the corresponding exons. Important restriction enzyme sites are indicated and the final targeting plasmids are noted, namely pBS, pMCS5, and pCR-XL-TOPO. Inserts contained the Neomycin resistance gene (NEO). IRES; internal ribosome entry site to enhance translation. lacZ; lacZ reporter gene encoding ß-galactosidase. TK; thymidine kinase promoter.

Knockout approaches in general can have three potential outcomes, either (1) an embryonic or postnatal lethal phenotype (as has been shown for the PP2A Cα knockout (Gotz et al., 1998)), (2) no detectable phenotype due to compensatory mechanisms, or (3) a obvious but not life-threatening phenotype that may be either expected from known functions of the targeted gene or may not be expected at all. Lethality can be overcome by more sophisticated gene targeting approaches using either tissue-specific or inducible promoters. Redundancies, on the other hand, can be overcome by creating multiple knockouts, or by analyzing the mice even more carefully to detect subtle phenotypic alterations.

9.5 Conclusion and Perspectives

The dominant negative mutant approach that makes use of Cα mutants is based on the screening of yeast mutants (Evans and Hemmings, 2000; Evans et al., 1999). In general, it is difficult to predict whether a particular dominant negative mutant phenotype in yeast may also be achieved in multiple-tissue organisms, such as mice. Additionally, in the presence of the endogenous catalytic subunit, PP2A inhibition is never 100%. This difficulty could be circumvented by crossing onto a null background, if the homozygous Cα mutants were viable. Nonetheless, analysis of Cα dominant negative mutant mice provided significant insight into the role of PP2A in the pathogenesis of tau (Kins et al., 2001) and in the regulation of ERK and JNK kinases (Kins et al., 2003). To complement these results, I have shown that a reduced PP2A activity in the mouse brain causes modest learning deficits in Morris water maze tasks. In addition our data reveal that the carboxy-terminal leucine L309 of the catalytic subunit of PP2A determines heterotrimer composition *in vivo*. This affects substrate specificity as shown for tau and vimentin. I have also shown that PP2A in general and its heterotrimer composition in particular play a crucial role in development and cell adhesion. Increased recruitment of specific regulatory subunits into the PP2A complex was shown to be associated with decreased recruitment of others; however, establishing a role for distinct regulatory subunits awaits further studies. Also, because of the observed interference of subunit assembly, B subunit-specific knockout strains may not necessarily assist in this elucidation.

Overexpression of regulatory PP2A subunits on the other hand may be complicated by the fact that total levels of PP2A are tightly regulated (Baharians and Schonthal, 1998; Wera et al., 1995). As this imposes a limitation to the number of regulatory subunits that can be recruited into the functional PP2A holoenzyme complex, this, in essence, implies that overexpression of one (transgenic) subunit titrates additional, endogenous regulatory subunits. Therefore, the observed phenotype may not be due to an overexpression of a distinct regulatory subunit, but may rather be caused by a lower concentration of holoenzymes containing the other endogenous subunits. This requires a careful monitoring of the many regulatory subunits, a task that is not easy, as it is likely that not all PP2A regulatory subunits have been identified as yet, and because specific antibodies are not available for all of them. Nonetheless, transgenic overexpression of PP2A regulatory subunits provides a rapid, first insight into tissue-specific functions of PP2A.

9.5.1 Relevance for the pathology of AD and FTD

With the two PP2A transgenic mouse lines, L199P and P309A, we could demonstrate that point mutations in important functional sites of the catalytic subunit are sufficient to cause abnormal phosphorylation of the PP2A substrate tau in the brain. As in L199P mice, PP2A deficits also caused discrepancies in learning and memory, whereas these did not seem to be related to tau pathology but rather to regulatory mechanisms of PP2A on long term depression that need to be

further investigated in electrophysiological studies. Considering the putative role of PP2A in the pathogenesis of human diseases, the development of transgenic models of PP2A may provide insight into the regulation of PP2A accelerating pathogenesis. A more detailed understanding of how regulatory subunits of PP2A are recruited into the core dimer shall help us to discover means to control the activity of PP2A in tauopathies like AD and FTD. However, it is unlikey that unspecific inhibitors of PP2A like OA, or activators that need yet to be discovered, would be of any value in the treatment of these diseases. Understanding the regulatory mechanisms of PP2A is therefore crucial in controlling PP2A in a way that specific subunits and consequently substrates will be affected without disturbing the general activity of PP2A. Our P309A mice provide evidence *in vivo* that methylation at the well conserved carboxy-terminus of the catalytic subunit is important for binding regulatory subunits to the PP2A core dimer. The dominant negative mutant PP2AC in these mice demonstrated that PP2A activity towards particular substrates, as shown for tau and vimentin, can be regulated without changing its general activity, as revealed in a non specific phosphatase assay. Since this meets the requirements of a potentially successful therapy for tauopathies, our mouse model may eventually lead to the discovery of therapeutic agents that can specifically counteract PP2A dysfunction. Considering the laborious task of producing and analyzing transgenic and knockout mice, future research in this field should take advantage of recent advents in RNA interference techniques. These approaches for efficient down-regulation of transcription is likely to help in the transgene design, and in the prediction of the expected phenotyp.

10 METHODS

10.1 DNA and bacteria work: Engineering, mutagenesis, cloning, extraction, purification, and analysis

10.1.1 Culturing and storage of Escherichia coli (E. coli)

E. coli were grown in Luria Bertani (LB) medium. After transformation, bacteria were plated on LB agar plates (LB medium containing 15 g/l Bacto agar) supplemented with the appropriate antibiotics for the selection of successfully transformed clones. For long-term storage of transformed *E. coli,* 200 µl of sterile glycerol (100%) were added to 800 µl of o/n bacterial cultures and were kept at -80°C.

- LB medium: 10 g/l Bacto tryptone, 5 g/l Bacto yeast extract, 10 g/l NaCl, pH 7.0.

10.1.2 Preparation and transformation of competent E. coli

10.1.2.1 Chemically competent *E. coli*

Chemically competent cells were used for the transformation with large plasmids. To be able to transform *E. coli,* they have to go through a state of competence during which DNA can enter the cells. Such competence is achieved by treating *E. coli* with Ca^{2+}, which destabilizes the cell membrane. The addition of DNA to the competent cells then leads to the formation of DNA/Ca^{2+} complexes, and subsequent heating of the cell/DNA suspension causes the DNA to enter the cells.

To produce competent cells, cultures of DH5α or XL-10 cells grown in LB-medium o/n at 37°C were diluted to an OD_{600} of 0.01. The bacteria were then incubated until they reached an OD_{600} of 0.4. Cells were pelleted by centrifugation at 4,000 g at 4°C for 15 min, resuspended in 10 ml of a 0.1 M $CaCl_2$ solution and kept on ice for 1 h. Cells were collected by centrifugation at 4,000 g at 4°C, resuspended in 0.1 M $CaCl_2$, 0.02 M $MgCl_2$, 15% (v/v) glycerol. Aliquots of competent cells were immediately frozen in liquid nitrogen and stored at -80°C.

To transform chemically competent cells, diluted circular plasmid DNA or an aliquot of a ligation reaction were added to 50 µl *E. coli*, which have been thawed on ice. This mixture was incubated on ice for 30 min, followed by a heat shock at 42°C for 45 s. Cells were chilled on ice for 2 min to be rescued. After addition of 900 µl LB-medium, prewarmed to 42°C, cells were incubated on a shaker at 225 rpm and 37°C for 1 h. Transformed bacteria were plated onto agarose plates containing the appropriate antibiotic for selection and were incubated at 37°C. The transformation of ligated and digested pSuper vectors (see 10.1.19) gave rise to 300-450 colonies compared to 40 colonies on negative control plates.

10.1.2.2 Electro-competent *E. coli*

To prepare electro-competent *E. coli*, cells were extensively washed with distilled water to remove ions from the solution and thereby weakening cell membranes by osmotic stress: An o/n-culture of DH5α cells was diluted 1:100 in fresh medium and incubated until an OD_{600} of 0.5 was reached. The culture was chilled on ice for 15 min and harvested by centrifugation at 4,000 g for 15 min at 4°C. The pellet was resuspended in ice-cold water and the suspension was centrifuged at 4,000 g for 15 min at 4°C. This step was repeated

once. The cells were then resuspended in 10% (v/v) cold glycerol, centrifuged as above and again resuspended in glycerol, the cell concentration being about 1-3 x 10^{10} cells/ml. Aliquots of electro-competent cells were snap-frozen in liquid nitrogen and stored at -80°C.
For the transformation, electro-competent cells were exposed to an electric field that temporarily destabilizes regions of the cell membrane. In that way small pores are formed through which DNA can enter the bacteria. 50 µl of electro-competent cells were gently thawed on ice and mixed with the plasmid solution (≤100 ng DNA in H_2O or 1-2 µl ligation mixture) and transferred to a chilled electroporation cuvette (0.1 mm). Cells were electroporated in the Gene pulser machine at 25 µF, 1.8 kV and pulse controller at 200 Ω. This produced an electric pulse with a time constant of 4 to 5 msec and field strength of 12.5 kV/cm. Immediately 500 µl LB-medium were added to the cells and they were incubated on a shaker at 225 rpm and 37°C for 30 min. *E.coli* were then plated on agarose plates containing the appropriate antibiotics for the selection of transformed cells.

10.1.3 Preparation of plasmid DNA

To extract plasmids from *E. coli*, Qiagen or Sigma plasmid purification protocols were used. The principle of these kits is based on selective alkaline denaturation, alkaline lysis of the cells in combination with the anionic detergent SDS (Birnboim and Doly, 1979): Cell walls are cracked, and proteins as well as high molecular weight genomic DNA are denatured. In contrast, covalently closed circular DNA remains double-stranded, stays in solution and can be recovered from the supernatant by binding to an anion-exchange resin.
Plasmid DNA was isolated from small scale (1-2 ml), intermediate scale (20-50 ml) and large scale (250 ml) bacterial cultures following the manufacturer's protocols. To determine the yield of a plasmid DNA preparation, the optical density (OD) was measured at 260 nm. Pure DNA shows a ratio of the absorbtion at 260 nm (A_{260}; protein) to the absorbtion at 280 nm (A_{280}; DNA, RNA) of 1.8 to 2.0, the absrobtion at 310 nm being approximately zero.

10.1.4 Phenol-chloroform extraction of DNA

A mixture of phenol:chloroform:isoamylalcohol (25:24:1) is used to remove proteins from nucleic acid solutions. The DNA is recovered from the aqueous phase by precipitation while denatured proteins stay in the organic phase and interphase.
The desired amount of DNA was diluted to 200-300 µl in water, and an equal volume of phenol:chloroform:isoamylalcohol (25:24:1) was added. The combination was mixed well on a vortex, and after centrifugation at 20,000 g for 5 min, the aqueous phase containing the DNA was transferred to a fresh tube. This procedure could be repeated to increase the purity of the DNA preparation. Finally, the DNA in the aqueous phase was precipitated and concentrated using one of the following methods.

10.1.5 Precipitation of DNA by ethanol or isopropanol

To isolate DNA from solution it can be precipitated with ethanol under high-salt condition. The addition of ethanol depletes the hydration shell of the negative charged phosphate groups in the backbone of the DNA. Positively charged ions bind to these groups so that a precipitate can form.
DNA was precipitated from solution by adding 1/10 volume of 3 M NaAc (pH 5.2) and 2.5 volumes of cold 100% ethanol, incubation at -20°C for 30 min and centrifugation at 20,000 g for 20 min at 4°C. After two washes with cold 70% ethanol, the DNA pellet was dried for 5-10 min at RT and resuspended in 10 mM Tris (pH 8.0) or water.

Precipitation of DNA by isopropanol follows the same principle as precipitation by ethanol, nevertheless there are two major differences in the outcome, namely small DNA fragments are not well precipitated but the precipitated DNA is cleaner.
DNA was precipitated from solution by adding 1/10 volume of 3 M NaAc (pH 5.2) and 0.7 volumes of 100 % Isopropanol and centrifugation at 20,000 g for 20 min at RT. The DNA pellet was dried for 5-10 min at RT and resuspended in 10 mM Tris (pH 8.0) or water.

10.1.6 Polymerase Chain Reaction (PCR)

The polymerase chain reaction is a fast method to amplify DNA-sequences of interest (Mullis, 1986). To produce multiple copies of DNA, two specific primers are used that are complementary to one of the two strands and define the sequence to be amplified.
The DNA is denatured at 95°C to separates the two strands. A subsequent decrease in temperature allows the two primers to anneal to their complementary sequences on the template DNA. The optimal annealing temperature for a primer pair is in the range of its melting temperature. In a next step, the heat stable DNA polymerase catalyzes the replication of the DNA at 72°C (elongation temperature). By repeating this temperature cycle, the DNA sequence of interest is amplified in an exponential manner.
1 ng of plasmid DNA or 5 ng cDNA were used as a template for the PCR. For the reaction on a Perkin Elmer 9700 PCR machine, 10 pmol forward primer, 10 pmol reverse primer, 10 mM dNTPs, 2.5 mM $MgCl_2$ and 1 U of polymerase were used. The reaction was started by denaturing the DNA and activating the DNA polymerase for 5-10 min at 95°C followed by 25-40 cycles; Denaturation for 30 sec to 1 min, annealing of primers at 50-65°C for 45 sec to 1.5 min, and elongation at 72°C for 1 to 3 min. The repeated cycles were followed by a final elongation step at 72°C for 7 min. The conditions used depended much on the polymerase, the melting temperature of the primers and the sequence to be amplified. When PCR fragments were used for cloning, a polymerase with proofreading activity was used (eg. Expand High Fidelity PCR System, Roche). More frequently however, AmpliTaq Gold DNA poymerase (Applied Biosystems) and RedTaq genomic DNA polymerase (Sigma) were used.

10.1.7 Site-directed mutagenesis

Site-directed mutagenesis allows us to create point mutations, to switch amino acids, and to delete or insert single or multiple amino acids without the need of subcloning. To produce mutations of 1 to 3 amino acids, mismatch primers were used to amplify both plasmid strands.
The L309A amino acid substitution in PP2A Cα was introduced into the cDNA using the QuickChange site-directed mutagenesis kit (Stratagene) following the manufacturer's protocol. The primers sequences were as follows: sense: 5'-GTCGTACCCCAGACTACTTCGCGTAAGGATCCGGTACCG-3'; antisense: 5'-CGGTACCGGATCC TTACGCGAAGTAGTCTGGGGTACGAC-3'. The construct was sequenced to confirm the absence of randomly introduced mutations (see 10.1.20).

10.1.8 Colony PCR

Colony PCR is a method that allows the screening of a large number of transformed *E. coli* clones for positives directly off the plate, instead of having to isolate plasmids from small scale cultures of these cells.
DNA polymerase, dNTPs, primers, $MgCl_2$ and buffer were mixed in a reaction tube as described in the section PCR above. For colony PCR, RedTaq genomic DNA polymerase (Sigma) and 35 cycles were used. The two primers added to the reaction were specific for the transformed plasmid. Colonies were picked with a sterile pipette tip and dipped into the reaction mixture. To break the cell walls and release plasmid DNA,

the mixture was boiled at 95°C for 5 min prior to the PCR. PCR products were analyzed on an agarose gel to determine which clone contained the plasmid of interest.
To grow positive clones in culture for the preparation of plasmid DNA, the corresponding pipette tip was incubated in LB-medium containing the appropriate antibiotic for selection on a shaker at 37°C o/n.

10.1.9 Colony hybridization

Colony hybridization was used for a rapid colony screening after the transfection of *E. coli* with ligation mixtures including empty vectors and therefore conferring antibiotic resistance to many negative clones. The procedure, in which bacteria are lysed and DNA is fixed to membranes, makes simply use of a microwave oven (Foster et al., 1997).
A transfected ligation reaction was plated on two separate agar plates and colonies grown o/n. Turbo-lifts were prepared on pure nitrocellulose transfer membrane filters (0.45 µm, BioTrace). Filters were laid in contact with bacteria, keyed with three syringe pinholes, and removed to be placed colony side up on Whatman no. 1 filters soaked in 2 x SSC plus 5% SDS for about 2 min. The filters were placed in a microwave oven and treated on a rotating turntable for 2.5 min at full setting. Immediately after microwaving, the filters were prehybridized at 65°C with 3 x SSC 0.1% SDS, 10 x Denhardt's solution and 250 µg/m1 denatured salmon sperm DNA for 30 min. The DNA probe with homology to the gene of interest was [α-32P]dCTP labeled with the Rediprime II Random Prime Labeling System (Amersham) and subsequently purified with the nucleotide removal kit (Quiagen). The [α-32P]dCTP labeled probe was then hybridized for about 4 h at 65°C in the prehybridization solution. Washes were at 65°C using 0.1 x SSC. 0.1% SDS. Kodak Bio-Max films were exposed to the membrane for 1 to 3 days. The Bacterial colonies, which are diminished by the lifting onto the filters, were regrown by incubation at 37°C so that they were ready for picking when identified as positive.

10.1.10 Cutting DNA with restriction endonucleases

For DNA cloning tasks or for the analysis of plasmid or genomic DNA, restriction endonucleases of type II were used, which recognize and cut DNA at palindrome sequences.
Cutting 0.2 - 1.0 µg DNA with restriction endonucleases were usually performed for 1 to 4 h with 1 U of restriction enzyme under buffer and temperature conditions as recommended by the manufacturers. If necessary double digests were performed sequentially, with purification steps in between. Cleavage efficiency was observed by agarose gel electrophoresis, with 200 ng of plasmid DNA for analytical purposes and 1 µg for preparative gels.

10.1.11 Forming blunt ends by fill-in and removal of overhangs

To ligate sticky DNA ends of different origin, blunt ends need to be formed before ligation can take place. Klenow fragment, a large fragment of DNA polymerase I that retains polymerization and 3'→ 5' exonuclease activity of the holoenzyme without degrading 5' termini, was used to fill–in 5' overhangs and remove 3' overhangs to form blunt ends.
The reaction to form blunt ends was performed for 15 min at RT in EcoPol buffer (New England Biolabs), supplemented with 1 mM DTT and 1 mM dNTPs (each) and 1 U of Klenow fragment per µg of DNA.

10.1.12 Hybridization of DNA oligonucleotides

Introduction of short DNA sequences (tags) to gene sequences or additional restriction sites into plasmids can be achieved by one cloning step with cassette cloning. These cassettes are short double-stranded oligonucleotides sequences with sticky ends to be introduced into the target sequence.
The DNA oligonucleotides were mixed in equi-molar concentrations in 10 mM Tris (pH 8.0) or water. After denaturation for 5 min at 95°C a slow temperature decrease allowed the hybridization of the complementary oligonucleotide strands.

10.1.13 Purification of DNA fragments

PCR products, oligonucleotides and fragments of any enzymatic DNA digestion were either purified by recovering the DNA from agarose gels (see 10.1.15) or by using the so called PCR purification kit (Qiagen or Sigma) following the manufacturer's instructions.

10.1.14 Agarose gel electrophoresis

Agarose gel electrophoresis was used to determine the size of DNA fragments or to isolate the fragment of interest from a DNA mixture. Because of the negatively charged phosphate groups in the backbone of nucleic acids, DNA and RNA migrate towards the positive anode when exposed to an electric field. The migration rate of DNA is proportional to the inverse log10 number of base pairs (Helling et al., 1974) and depends to some extent on the conformation of the DNA. DNA was visualized either by ethidium bromide (Sigma) or the more sensitive CYBR green I nucleic acid gel stain (Molecular Probes) for analysis under UV-light, or by crystal violet (Sigma), which is visible in daylight and was preferred for isolating DNA fragments without harming them with UV-light (Dutt, 1980). The length of the observed DNA fragments can be determined by comparison with a DNA ladder as marker. Depending on the size range of linear DNA to be resolved, 0.4 to 2.0% (w/v) agarose was dissolved in 1x TAE buffer by heating:

% agarose	DNA size range (bp)
0.40	2000 – 30,000
0.75	1000 – 15,000
1.00	500 – 10,000
1.25	300 – 5000
1.50	200 – 4000
2.00	100 – 2500

When cooled down to 50°C, the gel was complemented with 1 µg/ml ethidium bromide. All samples were loaded with 1x DNA loading buffer.

- TAE (Tris-acetate) buffer: 40 mM Tris-acetate (pH 7.6), 1 mM Na_2EDTA.
- DNA loading buffer 6x: 0.25% (w/v) bromphenol blue, 0.25% (w/v) xylene cyanol, 30% (v/v) glycerol.

10.1.15 Recovery of DNA fragments from agarose gels

After having resolved DNA fragments by electrophoresis the band containing the DNA of interest was cut out from the gel using a scalpel. Crystal violet was preferred over ethidium bromide to visualize DNA for the recovery; Bands are visible as they separate and can be cut out as soon as they are sufficiently resolved, and more importantly the DNA is not exposed to the damaging effects of UV light. Nevertheless if ethidium bromide had to be used because crystal violet was too week, the gel was cut on a table with UV-light at

302 nm. If sensitive enzymatic reactions followed the DNA recovery, TAE buffer with only 0.1 mM Na_2EDTA was used to avoid interference of high EDTA concentrations with enzyme activity. Finally, to recover DNA from the agarose gel, the gel extraction kit by Qiagen was used according to manufacturer's instructions.

10.1.16 Dephosphorylation of plasmid DNA

Digested plasmid DNA containing complementary cohesive ends or blunt ends tend to self-ligate producing empty vectors. In order to suppress such self-ligation and therefore decrease the vector background in cloning strategies, alkaline phosphatase, either shrimp (SAP, Roche) or calf intestinal (CIP, New England Biolabs), were used to remove terminal 5' phosphate groups from DNA.
For the hydrolysis of 5'-phosphate groups 1 µg DNA and 1-3 U of SAP or CIP were incubated at 37°C for 1 h in the appropriate buffer according to the manufacturers.
Before ligation, vectors were purified with the GenElute PCR clean up kit (Sigma) and eluted in 50 µl H_2O.

10.1.17 Annealing of oligonucleotides

Oligonucleotides of 64 bases used for the expression of siRNA constructs (Elbashir et al., 2001; Elbashir et al., 2001) (see section 11.2.4 p. 103) were annealed by mixing sense and antisense single stranded DNA, heating to 95°C and slowly cooling down to 4°C. In detail, 100 pmol of each oligonucleotide (sense and antisense) in 120 µl H_2O were incubated at 95°C for 5 min, followed by 20 min at 70°C. The mixture was then cooled down to 4°C as slowly as possible in a water bath.

10.1.18 Phosphorylation of DNA at 5' ends

Annealed oligonucleotides have to be phosphorylated at the 5' hydroxy termini to allow subsequent ligation. 40 pmol annealed oligonucleotides (49 µl) were incubated with 50 units of T4 polynucleotide kinase (5 µl) in 1x T4 ligation buffer (containing ATP, New England Biolabs) at 37°C for 40 min. Enzymes were heat inactivated at 65°C for 20 min, then samples were put back on ice. Annealed phosphorylated oligos were at 0.7 pmol/ul.

10.1.19 Ligation of DNA fragments

PCR products, double stranded oligonucleotides or other DNA fragments can be ligated to linearized plasmid DNA in an ATP consuming enzymatic process. The E. coli T4 DNA ligase catalyzes the ligation of two DNA strands at the 5' phosphate and the 3' hydroxy groups.
Depending on the size of the vector and insert, the molar ratio between vector and insert was varied. In the case of the pSUPER-GFP vector, approximately 0.3 pmol (300 ng) were mixed with 3 pmol of inserts. This mixture was incubated with 400 units of T4 DNA ligase in 1 x T4 ligation buffer (New England Biolabs) at 4°C overnight.
In the case of pSUPER, the inserts were designed such that the restriction site BglII was destroyed upon correct ligation. This gave the option to digest the ligation mix with BglII to better select positive clones after the ligation.

10.1.20 DNA sequencing

To confirm DNA sequences after cloning or site-directed mutagenesis, constructs were sequenced using DNA cycle sequencing based on the chain-terminator method (dideoxy method) (Sanger et al., 1977). In this

technique, the DNA to be sequenced is incubated with the Klenow fragment of DNA polymerase I, a suitable primer, and a small amount of all four 2',3'-dideoxynucleoside triphosphates (ddNTPs) labeled with different dyes together with an excess of unlabeled deoxynucleoside triphosphates (dNTPs) of the four bases. When the dideoxy analog is incorporated in the growing polynucleotide, chain growth is terminated because of the absence of a 3'-OH group. The products, a series of truncated chains, are electrophoretically separated in a capillary according to molecular weight and are detected by exciting the different dyes coupled to ddNTPs at the corresponding wavelengths with a laser.
The Big Dye terminator v1.1 Cycle Sequencing kit provides buffer, nucleotides and the polymerase.
1 µg plasmid DNA, 10 pmol primer and 4 µl reaction Ready Mix were mixed in a total reaction volume of 10 µl. The DNA amplification reaction was carried out using the following parameters on the GeneAmp PCR System 9700 (Applied Biosystems): 25 cycles of 15 s at 96°C, 30 s at 96°C, 30 s at 50°C, and 4 min at 60°C. The samples were then kept at 4°C, DNA was precipitated with ethanol and washed with 70% (v/v) ethanol. The DNA pellet was resuspended in 20 µl HPLC-grade water and was analyzed with the ABI Prism 310 Genetic Analyzer and ABI Prism 7700 Sequence Detector (Applied Biosystems). Sequence readouts of 200-400 bp by the Sequence detection software 1.9.1 (Applied Biosystems) were transformed to and computationally analyzed with the programs SeqMan II and MegAlign 4.00 (DNASTAR).

10.1.21 Southern blotting of genomic DNA

Southern blotting after restriction digestion of genomic DNA was used to screen ES-cells for the event of homologous recombination of the targeting knockout construct.
10 µg of genomic DNA were digested by the appropriate restriction endonucleases for 12 h. The digest was separated on a 0.5% agarose gel using TAE or TBE buffers, whereas TBE gave less background. The gel was run slowly for 12 h. Transfer of DNA to a nitrocellulose membrane was as follows: a Hybond N+ membrane (Amersham Biosciences) was presoaked in 0.4 M NaOH and the transfer was performed in 0.4 M NaOH using capillary blot technique. After 12 h of transfer, the membrane was treated with 2x SSC, let dry and was crosslinked with UV-light. To label a DNA probe with [α-32P]dCTP, the Rediprime II Random Prime Labelling System (Amersham) and QIAGEN nucleotide removal kit were used. The membrane was prehybridized in hybridization buffer containing 0.5 M NaP (pH 7.2), 1% BSA, 0.25 mM EDTA, 15% deionized formamide, and 7% SDS for 1 h at 65°C in a roller tube and hybridized with the labeled probe for 3 h at the same conditions. The membrane was washed with 2x SSC, 1% SDS for 30 min, then twice with 0.2x SSC, 1% SDS for 15 min at 65°C. The α-32P-labeled and hybridized probes were then detected by a Phosphor-Imager screen and read with the STORM 860 Phosphor-Imager (Molecular Dynamics), or by X-ray films for several days at -80°C.

10.2 RNA work: Extraction, purification, and analysis

Since RNA is much more prone to degradation than DNA, special care had to be taken to avoid break down of RNA by RNases. All solutions were treated with Diethylpyrocarbonate (DEPC) and autoclaved or sterile filtered. The working area and pipettes were treated with RNase away (Catalys).

10.2.1 Total RNA extraction from eukaryotic cells

10.2.1.1 Trizol method

Total RNA was extracted from eukaryotic cells by using a technique described by Chomczynski (Chomczynski, 1993). A monophasic chaotropic lysis reagent is used to lyse eukaryotic cells. Addition of chloroform to the lysate generates an organic phase to which DNA and proteins are extracted, while RNA stays in the aqueous supernatant. The RNA is precipitated from the supernatant with isopropanol, resuspended in DEPC treated water and stored in aliquots at -80°C.
Total RNA was extracted from eukaryotic cells by mechanical shearing in Trizol reagent (Invitrogen) directly on the culture dish, passing the lysate several times through a 26G needle. RNA was then purified from proteins and DNA by chloroform extraction and isopropanol precipitation. This procedure does not require any DNase treatment.

10.2.1.2 RNeasy kit with optional DNase treatment

The procedure of the RNeasy kit (Qiagen) for purest RNA longer than 200 nucleotides combines lysis of the cells with highly denaturing guanidine isothiocyanate buffer and a silica gel based membrane.
A maximum of 10 x 10^6 mammalian cells were lysed in the denaturing RLT buffer (Qiagen). The lysate was then filtered through a QiaShredder for proper homogenization. After 1:1 dilution with 100% ethanol, the cell-homogenate was loaded onto a silica membrane. If necessary, any residual DNA could be degraded with a compatible RNase free DNAse kit (Qiagen) after the first washing step In general, the kits were used as described in the supplier's protocols.
RNA concentration was determined by measuring the absorbance at 260 nm in a capillary spectrophotometer (Eppendorf), where an absorbance of 1 unit at 260 nm corresponds to 40 µg RNA per ml. The purity of RNA can be estimated by dividing the absorbance at 260 nm through the one at 280 nm (A_{260}/A_{280}). Pure RNA has an A_{260}/A_{280} ratio of 1.9 – 2.1

10.2.2 Quality assessment of total RNA

The purity, integrity and size distribution of total RNA can be checked by agarose gel electrophoresis (or the Agilent 2100 Bioanalyzer). The 18S and 28S ribosomal RNA from eukaryotic sources should appear as sharp bands whereas the 28S ribosomal RNA band should be approximately twice as intense as that of the 18S RNA band.
2 µg total RNA were resuspended in RNA sample buffer, heated to 95°C for 5 min and chilled on ice, before it was loaded on a 1% agarose gel, together with 2 µl (0.5 µg) RNA 6000 ladder (Ambion), and run in TAE buffer at 20 V overnight. The gel was then put in an ethidium bromide bath for 30 min and washed well in H_2O. The gel was examined on a UV transilluminator to visualize the RNA whereas 28S RNA corresponds to 4.7 kb and 18S RNA to 1.9 kb.

- 2x RNA sample buffer (NEB): 2x TBE (pH 8.3), 13% ficoll (w/v), 0.01% bromophenol blue and 7 M urea.

10.2.3 Quantitative real-time PCR (qRT-PCR)

The method of relative quantification of mRNA in quantitative real-time PCR (qRT-PCR) is based on direct monitoring of PCR products by measuring the increase in fluorescence caused by the binding of SYBR Green to double stranded (ds) cDNA. The template is the cDNA generated from a reverse transcription reaction.
Total RNA from cells was isolated (section 10.2.1), RNA concentration was measured in a photometer and 4 µg were used for reverse transcription. The cDNA was generated using the SuperScript First-Strand

Synthesis System for RT-PCR and random hexamers as primers (Invitrogen) following manufacturer's instructions. Specific reverse transcription of mRNA was achieved by using oligo(dT) primers, which bind specifically to the poly(A) tails of eukaryotic mRNA. The cDNA was diluted 1:20 in H2O for the qRT-PCR.
For the detection of mRNA during qRT-PCR, the following gene specific HPLC-purified primers (Metabion) were designed to amplify 70-90 bp at the 5' end of the open reading frame (ORF) using the primer design software Primer Express 1.5 (Applied Biosystems):

PR55α [forward: 5'-GTTCAGGAAGCGGAGACCC-3', reverse: 5'-TCCAGCTCCTGCCATGTTG-3'],
PR55β [forward: 5'-CCCGCAAAATCAA-CAACAGTT-3' and 5'-GCAGCCTCGCAGAACCC-3',
reverse: 5'-CCGTGTG-GTTGAATTCTACCG-3' and 5'-CCATGGTCCGAGCCTGAG-3'],
PR55γ [forward: 5'-GCTGACATCATCTCTACCGTTGAG-3', reverse: 5'-GCCGCCCT-TGTCACCTG-3'],
PR55δ [forward: 5'-GCTTCTCGCAGGTCAAGGG-3' and 5'-GACGAGGACGTGGCCG-3',
rev.: 5'-AAACTCAACGGTGGAAATGATGT-3' and 5'-TGTTGCAAGAAGATCTCCAGAGTAA-3'].

The cDNA was amplified on an ABI Prism 7700 Sequence Detector System using SYBR Green PCR core reagents (Applied Biosystems).
The amplification reaction in a total of 25 µl included the following:

10 x SYBR Green PCR buffer	2.5 µl	1 x
25 mM $MgCl_2$	3.0 µl	3 mM
dNTPs	2.5 µl	1.25 mM
Amp.Erase	0.25 µl	0.25 U
Ampli Taq Gold	0.15 µl	0.75 U
primers, 5 µM each	4.0 µl	0.8 µM
H_2O	2.6 µl	
template DNA (1:20)	10 µl	approx. 0.8 ng/µl

For signal detection, the ABI Prism 7700 Sequence Detector System was programmed with an initial sterilization step of 2 min at 50°C, followed by 10 min denaturation and polymerase activation at 95°C and 40 temperature cycles for 15 s at 95°C and 1 min at 60°C. To normalize for fluorescence fluctuations, the passive reference dye ROX is used.
The Sequence Detection Software 1.9.1 (Applied Biosystems) was used for the analysis of raw data and ΔCt values (cycle threshold values) were determined using the standard curve method according to the manufacturer's guidelines (Applied Biosystems). ΔCt values of the mRNAs of interest were put in relation to ΔCt values of one or several of the following stable human reference genes as internal controls (Chen et al., 2004; Hoerndli et al., 2004):

GAPD [forward: 5'-TGGGCTACACTGAGCACCAG-3', reverse: 5'-CAGCGTCAAAGGTGGAGGAG-3']
POLR2F [forward: 5'-CCCGAAAGATCCCCATCAT-3', reverse: 5'-CACCCCCCAGTCTTCATAGC-3']
PGK [forward: 5'-TGAAGGACTGTGTAGGCCCAG-3', reverse: 5'-TTCTTCCTCCACATGAAAGCG-3']

P-values were calculated with the Mann-Whitney nonparametric test. The specificity of the PCR amplification was confirmed on an agarose gel.

10.2.4 Short interfering RNA (siRNA)

10.2.4.1 Stable expression of siRNA by pSUPER vector

Post transcriptional gene silencing or RNA interference can be used in mammalian cells and even mice to study gene function (Elbashir et al., 2001) Long double-stranded RNA (dsRNA) is processed by a specific ribonuclease, called dicer, to a short dsRNA containing 3' overhangs of 2 nucleotides and a 5' phosphate

(Ketting et al., 2001). This short interfering RNA (siRNA) associates with the RNA-induced silencing complex (RISC) that guides siRNA to its corresponding target mRNA (Hammond et al., 2001). Once the siRNA is associated with its mRNA target, nucleases within RISC cleave and inactivate the mRNA (Tuschl et al., 1999; Zamore et al., 2000).
Apropriate target sequences for silencing were designed following the siRNA user guide (Oct. 2002) by Tuschl and coworkers (www.rockefeller.edu/labheads/tuschl/sirna) and recommendations by Ambion (www.ambion.com/techlib/tb/tb_506). 19 nucleotide target sequences, which should be flanked in the mRNA with AA at the 5' and TT at the 3' end were chosen 100 bp from start and termination of translation. To verify sequence specificity of a siRNA towards its target, a database search was performed at www.ncbi.nlm.nih.gov/BLAST. For the stable expression and production of siRNA in mammalian cells, DNA constructs were designed and cloned into the expression vector pSUPER (OligoEngine), such that a hairpin-loop RNA is formed that can be processed into a functional siRNA. For that, two oligonucleotides were designed, which when annealed form a HindIII and a mutated BglII site and contain the target sequence in sense and anti-sense orientation, separated by a 9 bp spacer (loop). Such oligonucleotides (Microsynth) were annealed and cloned into pSUPER, which has been modified to express GFP for positive selection. pSUPER was then stably transfected into HEK-293 and SH-SY5Y cells (see 10.4.2).

10.2.4.2 *In vitro* generated siRNA for transient transfection

For transient transfection of mammalian cells with siRNA constructs, 29-mer oligonucleotides were designed such that transcribing them *in vitro* gave rise to double-stranded functional siRNA. For the *in vitro* transcription, the Silencer siRNA construction kit (Ambion) was used and oligonucleotides were designed following the manufacturer's instructions. siRNA was quantified by diluting it 1:25 in 10 mM Tris-HCl, pH 8.0, 1 mM EDTA, followed by measuring the absorbance at 260 nm in the spectrophotometer (Eppendorf). A_{260} = siRNA in ng/ml. This number divided by 14 corresponds to siRNA concentration in nM. Transfection into mammalian cells was performed as described in chapter 10.4.2.

10.3 Protein work: Extraction, fractionation, immunoprecipitation and analysis

10.3.1 Protein extraction from mouse tissue

For immunoblotting, extracts were prepared with a acetat homogenizer in a buffer containing 70 mM Tris, 150 mM NaCl, pH 8, and 1% (v/v) Triton X-100 in the presence of protease inhibitors (Complete™ with EDTA, Roche). Brains and other mouse tissues were quickly removed from the sacrificed mouse and immediately put in chilled lysis buffer on ice. Homogenates were centrifuged for 5 min at 5,000 g, the supernatant was rotated overhead at 4°C for 30 min followed by centrifugation for 30 min at 20,000 g and 4°C. Supernatants were kept at -20°C.
As a faster technique used for expression analysis in mouse brains, the tissue was homogenized by passage through a 16G and 26G needle on ice in 1.5 ml of extraction buffer per brain. The samples were incubated on ice for 30 min followed by a centrifugation for 10 min at full speed.
For purer protein preparations, supernatants were dialyzed overnight at 4°C on a membrane in contact with an appropriate dialysis buffer.

10.3.2 Cell fractionation

For cell fractionation, a buffer containing 20 mM Tris-HCl, pH 7.4, 250 mM sucrose, 1 mM DTT and protease inhibitors was used. Lysates were centrifuged for 45 min at 100,000 g to separate the cytosolic fraction. The pellet was resuspended with 0.5% Triton X-100 and 5 mM EGTA in lysis buffer and centrifuged for 30 min at 100,000 g. The supernatant was taken as membrane fraction.

10.3.3 Measurement of protein concentration

Protein concentrations of cell or tissue extracts were measured as described by Lowry et al. (Lowry et al., 1951) using the DC protein assay (BioRad). Proteins react with an alkaline copper tartrate solution and reduce folin reagent. The reduced folin species have a characteristic blue color with an absorption maximum at 750 nm. Following the instruction manual, protein concentrations were calculated based on the absorptions of a standard curve. The standard curve was recorded with different dilutions of a protein standard (BSA) from 0.25 mg/ml to about 1.5 mg/ml in the corresponding solution.

10.3.4 Immunoblotting of proteins

Immunoblotting is a method to identify a protein of interest and determine its size in a protein extract. Proteins are separated by SDS-PAGE and electrophoratically transferred from the gel to a nitrocellulose membrane where they are immobilized and can be detected by specific antibodies.

10.3.4.1 SDS polyacrylamide gel electrophoresis (PAGE)

Separation of proteins was carried out by SDS PAGE (Laemmli, 1970) on NuPAGE Novex Bis-Tris gels (Invitrogen). Proteins were dissociated into their polypeptide subunits using the anionic detergent SDS in combination with β-mercaptoethanol as a reducing agent of disulfide bonds and heat. SDS with its high negative charge and hydrophobic tail that interacts strongly with hydrophobic regions of polypeptide chains binds quantitatively to proteins, giving them linearity and uniform charge, so that they can be separated solely on the basis if their size. Within a homogenous electric field, the migration speed of an SDS covered polypeptide is inversely proportional to the logarithm of its molecular mass.
Depending on the task, 10% or 4-12% gels were used and usually run at RT and 90 V for 2-3 h.

- 4x Sample buffer: 100 mM Tris-Base, 100mM Tris-HCl, 8 % (w/v) LDS, 4% (v/v) ß-mercaptoethanol, 40% (v/v) glycerol, 0.08 % (w/v) serva blueG250, 0.025 phenol red, 0.6‰ EDTA, 1.92 M glycine.
- 20x NuPage running buffer: 1M MOPS, 1M Tris-Base, 69.3 mM SDS, 20.5mM EDTA.

10.3.4.2 Transfer of proteins

Following SDS-PAGE the stacking gel was removed and the resolving gel was equilibrated in transfer buffer for 3 min on a shaker platform. Whatman papers and nitrocellulose membranes were cut to the size of the gel and soaked in transfer buffer. The gel and the membrane were sandwiched between soaked pieces of a sponge, Whatman paper and perforated plastic plates. Blotting was carried out in a blotting tank (Novex) for 2 h at 300 mA at 4°C or overnight at 20 mA at 4°C.

- Transfer buffer: 1 x MOPS NuPage, 20 % (v/v) methanol

10.3.4.3 Ponceau S staining of immobilized proteins

Proteins that are immobilized on a membrane can be reversibly stained using Ponceau S dye. This method can serve as a tool to evaluate the efficiency of protein transfer to the membrane, to estimate the amount of proteins loaded or even to directly determine the size of proteins.
Nitrocellulose membranes were washed well in water before they were incubated in Ponceau S for a few min. Membranes were then destained by washing them well in water.

- Ponceau S solution: 0.2% (w/v) Ponceau S red, 3% (w/v) sulfonic acid, 0.1% (v/v) glacial acid.

10.3.4.4 Coomassie brilliant blue staining of immobilized proteins

Coomassie brilliant blue is a dye that is used to detect unlabeled proteins that are separated by SDS-PAGE. Proteins are visualized as discreet blue bands by nonspecific binding of the dye to the positively charged amino groups of polypeptides.
The gel was stained for 1 h on a shaking platform and de-stained until discrete blue bands were visible.

- staining solution: 0.16% (w/v) Coomassie Brilliant Blue R250, 40% (v/v) methanol, 10% (v/v) acetic acid)
- destaining solution: 45% (v/v) methanol, 10% (v/v) glacial acetic acid

10.3.4.5 Western blotting

After the transfer of proteins from the SDS gel to the nitrocellulose membrane, the membrane was blocked for at least 1 h in TBST/10% (w/v) milk to prevent unspecific binding of antibodies. The primary antibody was diluted in TBST to an appropriate concentration (see section 10.8 p. 100) and the blot was incubated at RT for 2 h or overnight at 4°C. To remove all traces of unspecifically bound primary antibodies the membrane was washed 3 x for 5 min in TBST. Incubation of the blot with the secondary antibody conjugated to horseradish peroxidase was carried out for 1 h at RT. After the addition of ECL reagent (Amersham) or SuperSignal West femto (Pierce) as a chemifluorescent substrate for the peroxidase enzyme, bands were visualized by using X-omat LS films and the Kodak X-OMAT 2000 Processor. Density values were calculated with the ImageJ software (Wayne Rasband, NIH, USA).

- 10 x TBST: 0.2 M Tris, 2.5 M NaCl, 1% (v/v) Tween 20

10.3.5 Immunoprecipitation

Immunoprecipitation is a technique to separate, enrich and purify a specific protein and its interaction partners from a mixture of various proteins. Immunoprecipitated proteins can subsequently be analyzed by Immunoblotting.
As described by (Lin et al., 1998), the monoclonal antibody 5H4 directed against the Aα subunit of PP2A immunoprecipitates free A subunit and the core enzyme, but not holoenzymes, whereas the monoclonal antibody 6F9 directed against Aα immunoprecipitates all three species. Using these two antibodies, we isolated PP2A heterotrimers. Goat anti-rat IgM (μ chain specific, 1:15) was bound to protein G sepharose (1:3) (Amersham Biosciences) in 20 mM sodium phosphate, pH 7.0, before the antibody 5H4 (rat IgM, 1:10) could be linked. 5H4 binds repeat 1 near the amino-terminus of A and only precipitates core dimers and A monomers. The flowthrough was added to a Sepharose G-6F9 complex. 6F9 recognizes the amino-terminal eleven amino acids of A and precipitates the remaining PP2A heterotrimers (Lin et al., 1998). For microcystin (MC) precipitation, 50 µl of 50% MC-agarose (Upstate, Lake Placid, NY) was incubated with 3 mg protein extract at 4°C overnight.The flowthrough was then brought together with the antibody 6F9 (rat $IgG_{2a,}$ 1:10) bound to Sepharose G. 6F9 recognizes the amino-terminal 11 amino acids of A and therefore precipitates the

remaining PP2A heterotrimers. All other proteins should have been removed with the flowthrough. The protein G-sepharose slurry with antibodies was incubated overnight at 4°C on a head-over-end shaker and all wash steps were repeated 3 times with exess sodium phosphate, 20 mM, pH 7.0. Proteins bound to the sepharose were eluted from the beads by incubation with SDS gel sample buffer and incubation at 90°C for 5 min. The eluted trimers were run on an SDS polyacrylamide gel and blotted to a nitrocellulose membrane for detection of PP2A subunits.

10.3.6 Protein phosphatase assays

One µg of recombinant vimentin (Cytoskeleton, Denver, CO) was labeled with 50 pmol γ-P^{32}-ATP and 0.8 U PKA in a buffer containing 0.1 mM dATP, 8 mM $MgCl_2$, 20 mM Tris-HCl pH 7.5, 1 mM benzamidine, 3 mM DTT, 10 mM NaF, 2 mM vanadate, and Complete™ without EDTA at 30°C for 3.5 h. Labeled vimentin was purified on SigmaSpin columns (Sigma-Aldrich). Total brain extracts were prepared in TBS in the presence of protease inhibitors. Then, 40 ng of labeled vimentin was added to 300 µg brain extract in 50 mM imidazole (pH 7.2), 0.2 mM EGTA, 0.02% β-mercaptoethanol, and 0.1 mg/ml BSA. Reactions were stopped with β-mercaptoethanol-containing sample buffer and boiling for 5 min followed by SDS-PAGE. General phosphatase activity was measured with a Ser/Thr phosphatase assay according to the manufacturer's recommendations (Promega, Madison, WI). Brain homogenates were also incubated with OA (Calbiochem).

10.4 Mammalian cells in culture

10.4.1 Cultivation and storage of cell lines

The following neuronal and non-neuronal mammalian cell lines have been used; Human embryonic kidney HEK-293 cells (DSMZ # ACC 305), and human neuroblastoma SH-SY5Y cells (DSMZ # ACC 209).

10.4.1.1 HEK-293 cells

HEK-293 cells were cultivated at 37°C/ 5% CO_2/ 95% humidity in the following medium:

- Cultivation Medium: Dulbecco's Modified Eagle Medium (DMEM), 10 % (v/v) Foetal Bovine Serum (FCS), Penicillin-Streptomycin
- Freezing Medium: 90 % (v/v) FCS, 10 % DMSO

Confluent layers of cells were washed with PBS, released from the dish by incubation with trypsin/EDTA for 3 min, and split to new plates at ratios of 1:20 to 1:5, depending on the purpose.

For storage of HEK-293 cells, they were trypsinised and resuspended in culture medium, pelleted by centrifugation at 1,000 g for 5 min and resuspended in freezing medium. Cell aliquots were immediately chilled on ice and frozen at -80°C in a □cetate□m box. After one day at -80°C the aliquots were transferred to liquid nitrogen and kept for long time storage.

To recultivate frozen cells, cell aliquots were thawed quickly in a water-bath at 37°C, and before the thawing process was complete, cells were resuspended in excess of medium in order to dilute the DMSO. Cells were pelleted by centrifugation, resuspended, and plated on dishes at a seeding density corresponding to approximately 30% confluency.

10.4.1.2 SH-SY5Y cells

SH-SY5Y cells were cultivated at 37°C/ 5% CO_2/ 95% humidity in the following cultivation medium:

- Cultivation medium: DMEM/ Nutrient Mixture F-12 (DMEM/F-12) 1:1 mixture, supplemented with 15% (v/v) FCS, and 2 mM L-glutamine.

Confluent layers of cells were washed with PBS, released from the dish by incubation with trypsin/EDTA for 3 min, and split to new plates at a ratio of less than 1:5.

SH-SY5Y cells be triggered to differentiate to a neuronal-like phenotype (Encinas et al., 2000). For differentiation, SH-SY5Y cells were seeded on collagen type I coated dishes at a density of 0.3 – 2.0 x 10^4 cells/cm^2. To induce neuronal differentiation, cells were incubated in medium containing retinoic acid (RA) for five days, followed by an additional five days in serum free medium supplemented with brain-derived neurotrophic factor (BDNF).

- Differentiation medium I (days 1-5): DMEM/F-12, 2 % FCS, 2 mM L-glutamine, 20 µM all-trans retinoic acid (RA).
- Differentiation medium II (days 5-10): DMEM/F-12, 2 mM L-glutamine, 50 ng/ml BDNF.

Long time storage of SH-SY5Y cells was achieved as follows: Cells were trypsinised and resuspended in culture medium, pelleted by centrifugation at 1,000 g for 5 min and resuspended in freezing medium. Cell aliquots were immediately chilled on ice and frozen at -80°C in a polystyrene box. After one day at -80°C the aliquots were transferred to liquid nitrogen and kept for long time storage.

To recultivate frozen cells, cell aliquots were thawed quickly in a water-bath at 37°C, and cells were immediately resuspended in cultivation medium and pelleted by centrifugation. After resuspension, cells were plated on dishes at a seeding density corresponding to more than 50% confluency.

- Freezing medium: 90% (v/v) cultivation medium, 10% (v/v) dimethylsulfoxide (DMSO).

10.4.2 Transient and stable transfection of cultured mammalian cells

Eukaryotic cells can be transiently or stably transfected with circular DNA. Transient transfection is used to obtain temporary high levels of expression in a cell line. The DNA is not necessarily integrated into the chromosome and consequently no selection marker is used. Cells are harvested and analyzed two days after transfection. In contrast, in stable transfection the DNA is integrated in the host genome and non-transfected cells are eliminated by selection with antibiotics such as geneticin (G418) or hygromycin.

For the transfection of cultured mammalian cells, a technique was applied that makes use of the fact that cationic lipids can create artificial membrane vesicles (liposomes) which can then serve as a DNA carrier. The DNA/lipid complex adheres and fuses with the cell membrane and the DNA is released into the cytoplasm.

Cells were grown to 70 – 80% confluency at the day of transfection. 30 min before adding the transfection reagent cells were washed with PBS and fresh medium without penicillin/streptomycin was added. For a 60-mm dish, 10 µg of DNA were diluted into 0.5 ml OPTI-MEM I. 30 µl of lipofectamine 2000 (LF2000) reagent were diluted in 0.5 ml OPTI-MEM I and incubated at RT for 5 min. The diluted LF2000 reagent and DNA were combined and incubated at RT for 20 min, allowing DNA/LF2000 complexes to from. The complexes were then added to the cultured cells. 6 to 12 h later, the medium containing transfection reagent was replaced by fresh culture medium. Experiments with transient expression were started 48 h after transfection.

A similar procedure was used to transfect DNA for stable expression, but in contrast, cells were passaged at a 1:5 to 1:10 dilution into fresh growth medium containing penicillin/streptomycin 24 h after transfection. The next day, selective medium (including G418) for the antibiotic resistance gene transfected (neomycin) was added and selection pressure was kept-up for at least 10 days.

To generate a clonal cell line or to select for GFP expression rather than neomycin expression, cells were seeded at extremely low density and let grown for a few days. Positive single clone colonies were manually picked under a fluorescence microscope.

10.5 Transgenic and knock-out mice

10.5.1 DNA constructs and transgenic mice

A 978 bp cDNA fragment encoding human PP2A C was fused to a haemagglutinin epitope located immediately downstream of the start codon. The L309A amino acid substitution was introduced into the cDNA using the QuickChange site-directed mutagenesis kit (Stratagene). The mutated fragment was subcloned into the neuron-specific mThy1.2 expression vector (Luthi et al., 1997). For pronuclear injection, vector sequences were removed and the DNA was purified with PrepAGene (Bio-Rad) and Millipore Ultrafree-MC 0.22 µm filter units.
Transgenic mice were produced by microinjection of B6D2F1 x B6D2F1 embryos (Gotz et al., 1995). Founders were identified by PCR analysis of tail lysates using oligonucleotides Thy1.2 (5'-AAGTCACC CAGCAGGGAGGTGCTC-3') and PP2ACα (5'-TCTCGCAGAGGCTCTTGACCTGGGAC-3'), and intercrossed with C57BL/6 mice to establish lines.

10.5.2 Immunohistochemistry

10.5.2.1 Tissue preparation

In order to preserve the brain tissue from degradation, mice are perfused transcardially under deep anesthesia (with an overdose of Rompun (Bayer)/Etaminol10 (Veterinaria)) using a peristaltic pump connected to two reservoirs containing saline and fixative solution, respectively. A cut along the sternum is made in order to expose the end of the sternum, then, with sharp scissors, a cut is made through the skin, diaphragm and laterally on both sides upward across the ribs and parallel to the lungs; the cannula is then inserted through the left ventricle into the ascending aorta. Immediately, the right auricle must be punctured with forceps, to allow the escape of return circulation. Perfusion is performed with phosphate buffered saline (PBS, pH 7.4) for 10 min at room temperature, followed by 4% paraformaldehyde in PBS on ice. Brains were removed and immersion-fixed in the same fixative overnight at 4°C. Immunohistochemistry was performed either on thick (40 µm) vibratome sections or on thin (4 µm) paraffin sections. For vibratome sections, the tissue was cut directly in PBS after fixation. In contrast, for paraffin sections, tissue was first dehydrated in an ascending series of ethanol and xylol prior to paraffin embedding.

10.5.2.2 Immunostaining of vibratome sections

40 µm vibratome sections were stained free-floating. They were permeabilized with They were permeabilized with methanol at –20 °C for 5 min and were blocked for at least 2 h at RT in a PBS blocking solution containing 5% goat serum, 5% BSA, and 0.1% Triton-X100. Primary antibodies were added for an overnight incubation at 4°C in the same blocking buffer. After several washing steps, secondary antibodies were added and incubated in blocking buffer but without Triton-X100 for 2 h at RT. Washing in PBS at RT

consisted of three repetitions for 20 min at RT on a rocking platform. Sections were mounted with Mowiol (Hoechst) or were dehydrated and flat-embedded between glass slides and coverslips in Eukitt (Kindler).

10.5.2.3 Immunostaining of paraffin sections

To allow antibodies to penetrate fixed tissue embedded in paraffin, it has to be dewaxed and rehydrated. To detect an antigen, specific primary antibodies and secondary antibodies (conjugated to fluorescent dyes or biotin) are used. For immunofluorescence, 4 µm paraffin-sections were dewaxed in xylol and rehydrated in graded ethanol. They were washed well in PBS (fluorescence) or TBS (DAB) and permeabilized by either pretreating the sections with 15 min of microwave at 95°C in citric acid buffer, pH 5.8, or with methanol at –20 °C for 5 min. Depending on the antibodies used, some sections were pretreated with 5 µg/ml proteinase K or 0.1% Triton X-100 in TBS (TBST) for 2.5 min at 37°C for signal enhancement. Sections were then blocked for 30 min in PBS or TBS containing 10% normal serum and 4% milk. Depending on the secondary antibody used, the serum was adjusted or a mix of goat and horse were applied. Sections were then incubated with the primary antibody diluted in PBS or TBS containing 5% normal serum and 2% milk overnight at 4°C or for 1 h at RT. Sections were washed three times with PBS or TBS, were incubated with the secondary antibody for 30 min at RT, and were washed again. The fluorescence stained sections were mounted directly with Moviol (Hoechst) while vectastain ABC reagent (Vector Laboratories) was added to the DAB labeled sections for 30 min. These sections were washed again and were incubated with peroxidase substrate solution (DAB) (Pierce) for 10 min. After washing in TBS, sections can be counterstained with Nuclear Fast Red (Fluka), rinsed with water followed by dehydration in graded ethanol and xylene. Sections were then embedded with in Eukitt (Kindler).

10.5.3 TUNEL assay

TUNEL (terminal deoxynucleotidyl transferase–mediated dUTP-biotin nick end labeling) staining of 4 µm paraffin-sections were performed using the TUNEL kit by Boehringer-Mannheim Biochemica with minor modifications (Gavrieli et al., 1992; Gotz et al., 2001).

10.5.4 Decalcification and haematoxylin/eosin (HE) staining of heads

After perfusion with 4% paraformaldehyde, mouse heads were washed in PBS followed by H_2O. Then they were decalcified at room temperature for 3-4 days in a solution of 0.15 M EDTA and 70 mM HCl, pH 6.5. After washing with H_2O, the heads were dehydrated and embedded in paraffin. 4 µm sections were incubated in haematoxylin for 15 min, hydrated, differentiated in 0.25% HCl in 50% ethanol, rehydrated, and rinsed in 96% ethanol. Sections were incubated in eosin for 5 sec, rinsed in 70% ethanol, dehydrated, and mounted in Eukitt (Kindler).

10.5.5 *In situ* hybridization

WT mice were anaesthetized with a mixture of 2% Rompun (Xylazinum, Bayer) and 10% Ketaminal 10 (Vererinaria), transcardially perfused with PBS containing 4% paraformaldehyde, postfixed overnight at 4 °C, and paraffin embedded. Sections (7 µm) were dried overnight at 42 °C on coated glass slides, dewaxed and permeabilized by acid treatment (0.1 m HCl for 10 min), followed by a proteinase K treatment (10 µg/mL) for 10 min at 37 °C. After acetylation with 0.1 m triethanolamine and 0.4% acetic anhydride (20 min at room temperature), sections were incubated for 1 h at room temperature in hybridization buffer (25% deionized formamide, 4× SSC, 5× Denhardt's reagent, 0.25 mg/mL yeast tRNA, 10% dextransulphate,

50 mM DTT, 1 mM EDTA, 0.5 mg/mL salmon sperm DNA in 50 mM phosphate buffer pH 7). The sections were hybridized overnight at room temperature in hybridization buffer with DIG-labelled 45 bp antisense oligonucleotide probes and the complementary sense probes (see materials, page 103). Approximately 30 ng of DIG labeled oligonucleotide in 30 µl hybridization buffer were used per section. Three negative controls were included: (1) a DIG labeled sense probe, (2) a 1:300 diluted DIG labeled antisense probe in unlabeled antisense probe, and (3) prehybridization buffer without probe. All samples were incubated for 20 hours at 37°C. Sections were then washed at 37°C in solutions of decreasing salt concentrations (2x, 1x, 0.2x SSC), incubated in buffer 1 (100 mM TrisCl (pH7.5) 150 mM NaCl) for 10 min followed by blocking in buffer 1 supplemented with 2% (v/v) normal sheep serum and 0.05% Triton-X100, for 30 minutes. Immunostaining was then achieved by incubating the sections with an anti-DIG antibody conjugated to alkaline phosphatase (Roche) at 1:200 in buffer 1 (100 mm Tris/HCl pH 7.5, 150 mm NaCl, 0.1% Triton X-100, and 1% normal sheep serum) for 4 hours at room temperature. Sections were washed twice in buffer 1 and buffer 2 (100 mM TrisCl (pH9.5), 100 mM NaCl, and 50 mM $MgCl_2$) for 10 minutes each. Alkaline phosphatase activity was visualized with staining solution (100 mM Tris/HCl pH 9.5, 100 mM NaCl, 50 mM MgCl2, 1 mM levamisol, 0.3% NBT, 0.35% BCIP) for 2-14 h in the dark, until the color developed. The reaction was stopped with buffer 3 (10 mM Tris Cl (pH8.1) and 1 mM EDTA). After washing, slides were mounted in Mowiol (Hoechst).

All oligonucleotides were labeled with digoxigenin-dUTP using the DIG Oligonucleotide Tailing kit (Roche Molecular Biochemicals) following the manufacturer's instructions. 100 pmol of each oligonucleotide was initially used. The yield for each digoxigenin-dUTP labeled oligonucleotide was approximately 4 pmol/µl (about 50 ng/µl), as determined by dot blotting onto a Nylon membrane and detected by anti-digoxigenin-AP conjugates (Roche Molecular Biochemicals) using the CSPD developing system (Roche Molecular Biochemicals).

10.5.6 Extraction of genomic DNA from mouse tails

Mouse tail was lysed and genomic DNA was isolated by precipitation with isopropanol or with the Dneasy (Qiagen) or GenElute mammalian genomic DNA kits (Sigma). Depending on the size of the tail and the protocol used, the total yield of genomic DNA ranged between 10 and 30 µg. The kits were used according to manufacturer's protocols. Isolated genomic DNA was stored at 4°C.

10.5.6.1 Simplified mammalian DNA isolation with isopropanol precipitation

4-8 mm mouse tail was lysed at 55°C overnight in 500 µl lysis buffer containing 100 mM Tris-HCl (pH 8.5), 5 mM EDTA, 0.2 % (w/v) SDS, 200 mM NaCl, 100 µg proteinase K/ml (Laird et al., 1991). After centrifugation for 5 min at 22,800 g, 300 µl of the supernatant were transferred into a clean tube. One volume of isopropanol was added and the samples were mixed until the precipitation of the genomic DNA was complete. Using a pipette tip the precipitate was recovered from the solution and was washed once with 300 µl of 70% ethanol. The genomic DNA was dissolved in 200 to 500 µl of TE buffer and stored at 4°C.

10.5.7 Ganzfeld electroretinography (ERG)

Electroretinograms were obtained according to procedures previously described (Seeliger et al., 2001). In summary, mice were dark-adapted overnight and their pupils dilated prior to the experiments. The animals were anesthetized by subcutaneous injection of ketamine (66.7 mg/kg) and xylazine (11.7 mg/kg). ERGs were binocularly recorded from the corneal surface by means of gold wire ring electrodes, and silver needle electrodes served as reference (forehead) and ground (tail). The ERG equipment consisted of a Ganzfeld

bowl, a DC amplifier, and a PC-based control and recording unit (Toennies Multiliner Vision, Jaeger/Toennies, Höchberg, Germany). Bandpass filter cut-off frequencies were 0.1 and 3000 Hz. Single flash recordings were obtained both under dark-adapted (scotopic) and light-adapted (photopic) conditions. The light adapted part was performed with a background illumination of 30 cd/m2 that started 10 minutes before the first recording. Stimuli were presented with increasing intensities from 10^{-4} cd*s/m^2 to 25 cd*s/m^2, divided into ten steps of 0.5 and 1 log cd*s/m^2. Ten responses were averaged with an inter-stimulus interval (ISI) of 5s or 17s (for 1, 3, 10, 25 cd*s/m^2).

10.5.8 Scanning laser ophthalmoscopy (SLO)

Imaging was performed with a Heidelberg Retina Angiograph (HRA1, Heidelberg Engineering GmbH, Dossenheim, Germany), a confocal scanning-laser ophthalmoscope providing two laser wavelengths for fundus visualization (Argon green, 514 nm, and infrared, 835 nm), and two laser wavelengths for angiography (Argon blue, 488 nm (barrier 500 nm) for fluorescence angiography, and infrared, 795 nm (barrier 810 nm) for indocyanine green (ICG) angiography).

Fluoresceine angiography was performed following a s.c. injection of 1.5 mg fluorescein-Na (University pharmacy, University of Tuebingen), and ICG angiography following a s.c. injection of 1 mg ICG (ICG-Pulsion, Pulsion Medical Systems AG, Munich, Germany).

10.6 Behavioral tests; learning and locomotor activity

10.6.1 Learning-capacity tests in the water maze

The design of the apparatus followed the description given by Morris (Morris, 1984). It consisted of a white Plexiglas circular pool of 150 cm diameter and 50 cm height, filled with water (15 cm deep, 24-26°C) made opaque by the addition of milk. Distant visual cues for navigation were provided by numerous black and white symbols on the walls. A wire mesh platform (14 × 14 cm) was placed 0.5 cm below the water surface, with its centre 35 cm from the side of the pool. Every day, animals were adapted to the test room for at least 30 min before testing. To avoid visual orientation prior to release, the mice were transferred from their cages to the pool in a white plastic cup from which they glided into the water, with the opening of the plastic cup toward the wall of the pool. Mice were released from eight symmetrically placed positions on the pool perimeter in a predetermined, but not sequential order. They were left swimming either until they found the platform or until 120 s (protocol 1) or 90 s (protocol 2) had elapsed. Finding the platform was defined as staying on the grid for at least 3 s. After staying on the platform for about 10 s, the mice were given the opportunity to climb on to a wire mesh grid attached to a stick, which was also used to pick up swimming animals not having found the target. If mice did cross the platform without stopping (jumping immediately into the water), they were left swimming until they met the criteria above. Between trials, the animals were placed under infrared lamps and allowed to warm up and dry off. Intertrial times were 10 min (protocol 2) and varied from 30 to 60 min (protocol 1). The swim paths of the mice were recorded by means of a video camera suspended above the centre of the pool and fed to an electronic imaging system (ASBA Wild & Leitz) which extracted and stored X-Y coordinates at a frequency of 4.2 Hz, and with 256 × 256 pixels of spatial resolution (Noldus). Swim paths were recorded and could be used to calculate a wide range of parameters,

the most important being the time required to find the platform during acquisition and reversal phases, and the time spent in quadrants in the probe trial. These were determined as a measure of learning success.

10.6.1.1 Protocol 1 "The simple"

Animals were trained on four consecutive days with six up to 120 s trials daily to find a platform (acquisition phase). The position of the hidden platform remained fixed for the acquisition phase. On the 5th day, the platform was removed and the time every mouse stayed in the target and the opposite quadrant were measured for one minute (called probe trial). After two days of rest the platform position was changed to the opposite quadrant and the mice had to relearn the new platform position during three days with 6 trials per day (reversal phase). On day four, the platform was again removed and memory retention was examined in a single 60 s trial (Wolfer et al., 2001).

10.6.1.2 Protocol 2 "The sophisticated"

This water maze test is based on the same principle as protocol 1 with the major difference that once the individual mouse has learned the platform position, it will immediately get a new position and therefore will have to relearn several times. It was described and used by the group of Richard Morris (Chen et al., 2000) and was adapted to our apparatus (Morris, 1984) as described above.
Since all mice have performed in the water maze protocol 1 before, there was no need for a cued training-to-criterion. For the learning-capacity test the platform was moved between different locations drawn from a set of 20 possible locations. Each mouse swam eight trials per day with a maximal trial duration of 90 s and an interval between trials of 10 min. Mice had to search for five different platform positions whereas the performance criterion to get a new platform position was three trials in a row with an average escape latency of less than 15 s. The maximum number of trials was 40 for location 1, and 32 trials thereafter, therefore the maximal duration of the test was 21 days.

10.6.2 Rotarod test (motor coordination)

Motor coordination was measured using an accelerating rotarod device (Ugo Basile, Italy) which consists of a rotating drum with a diameter of 3 cm covered with knurled Perspex to provide an adequate grip, and accelerating speed from 4 rpm up to 40 rpm. The performance on the Rotarod was recorded by the time spent (in s) and the maximal speed reached (in rpm). Each mouse was accustomed to the task 3 times, with a maximal time of 300 s, whereas 40 rpm was reached after 270 s. Mice were left at rest for 2 hours, and were then tested twice with the same accerlerating speed, the maximal time being 300 s.

10.6.3 Fear conditioning

During fear conditioning subjects learn to associate a neutral stimulus (CS) or training situation (context) with a coinciding painful stimulus (US). Subsequently, learning performance and fear-related behavior can be analyzed in the conditioned subject. Six transgenic L199P mice and six WT littermates were tested for their response to a conditioned fear stimulus Both contextual and auditory cued fear conditioning were studied with a 4-day test protocol. After two adaptation sessions on day1 ('neutral context', i.e. a plastic cage, 12 × 20 cm, in a soundproof test box, with dim light and a fan providing background noise), animals were trained in an altered context ('shock context': 25 × 25 cm cm, grid floor, strong light, peppermint smell, fan off) on day 2. Animals received three CS-US pairings in 1-min intervals (CS, 4 kHz, 75 dB for 10 s; US, 0.7 mA foot shock, delivered during the last second of the CS). A control group (n=3 per genotype)

received the same training stimuli without temporal coincidence. On day 3, tone-specific memory of both experimental and control mice was tested in the neutral context. As behavioral indicator of fear, occurrence of freezing was determined by the experimenter every 10 s for 2 min without the CS, then for 2 min with the CS (twice 30 s duration with 30 s pause). At the same time suppression of locomotor activity was measured using an infrared photobeam activity monitoring system (SCANET). On day 4, experimental animals were tested for their context-specific memory over a period of 2 min in the shock context in the same way.

10.7 Microscopy

Visual assessment of cell viability in culture and counting of cell density in solution were performed on an upright Nikon TMS F light microscope. Manual clonal picking of single cells and counting of transfection rate were performed on a Nikon Eclipse TE300 using corresponding fluorescence filters. Analysis of haematoxylin/eosin (HE) and immunohistochemical stainings was performed on the fluorescence microscopes Eclipse E800 (Nikon) and the inverted DM IRE2 (Leica). The latter captures pictures with the digital unit DFC 480 (Leica) directly into the Photoshop 6.0 software (Adobe) while the two other microscopes capture pictures with the TV lens C- 0.6 x (Nikon) and the Kappa ImageBase 2.2-Control software (Kappa opto-electronics).

10.8 Antibodies

Antibodies used for Western blot (WB) analysis, immunohistochemistry (IH), or immunoprecipitation (IP) were: HA (Roche, Basel, Switzerland, IH 1:200, WB 1:1000); antiserum 45 (Dr. B. Hemmings, Basel, Switzerland, anti-Cα; directed against the first 20 amino acids of Cα, WB 1:100) (Gotz et al., 1998); PP2A/C (Oncogene Research Products, Cambridge, MA, WB 1:100); PP2A/A, 6G3 (Covance, Berkeley, CA, WB 1:1000); PP2A/A, 6F9 and 5H4 (BabCO, Richmond, CA, IP 1:150); PP2A/Bα (Calbiochem, San Diego, CA, WB 1:500); PR61γ and PR61ε (Dr. B. Hemmings, WB 1:300); β-actin (Abcam, Cambridge, MA, WB 1:5000); β-catenin (Biodesign International, Saco, ME, IH 1:100, WB 1:500); GAPDH (Biodesign International, WB 1:1000); NSE (DakoCytomation, Glostrup, Denmark, IH 1:200); PGP9.5 (Abcam, WB 1:2000); Pan cadherin (Lab Vision, Fremont, CA, IH 1:100, WB 1:500); GSK-3β (Santa Cruz Biotechnology, Santa Cruz, CA, WB 1:500); p-GSK-3β (Ser 9) (Santa Cruz Biotechnology, WB 1:500); APP C-terminal (Sigma-Aldrich, St. Louis, MO, WB 1:4000). The rabbit anti-PR59 antiserum Δ1-113 (WB: 1:5000) was raised against a fusion protein containing a 6xHIS-tag fused to amino acids 114-521 of murine PR59. The following phosphotau-specific antibodies were used: CP13 (Dr. P. Davies, Bronx, NY, IH 1:500); AT100 and AT180 (Innogenetics, Gent, Belgium, IH 1:100) (Goedert et al., 1994); 12E8 (Dr. P. Seubert, Elan Pharmaceuticals, South San Francisco, CA, IH 1:100) (Seubert et al., 1995); AD2 (Dr. C. Mourton-Gilles, Lille, France, IH 1:500) (Buee-Scherrer et al., 1996); pS^{422} (Biosource, Camarillo, CA, IH 1:50); and S199P (Dr. A. Delacourte; Lille, France, IH 1:1000) (Delacourte et al., 1998; Sergeant et al., 1999). For immunofluorescence, secondary antibodies were obtained from Molecular Probes (Alexa-Fluor series, Eugene, OR), and for immunoblotting, HRP-conjugated secondary antibodies (Vector Laboratories, Burlingame, CA) were used. For more details on secondary antibodies see the Materials section 11.8.2 on page 110.

11 Materials

11.1 Plasmids

pBluescript II KS+	Stratagene
pcDNA 3, pcDNA 3.1	Invitrogen
pCR-XL-TOPO	Invitrogen
pCR-II-TOPO	Invitrogen
pEGFP-N1	BD Biosciences, Clontech
pEX12	Dr. H. van der Putten (Luthi et al., 1997)
pSUPER	OligoEngine

11.2 DNA oligonucleotides

11.2.1 Primers for qRT-PCR

Gene	Sequence 5' – 3', forward	Sequence 5' – 3', reverse
PR55α	GTTCAGGAAGCGGAGACCC	TCCAGCTCCTGCCATGTTG
PR55β(I)	CCCGCAAAATCAACAACAGTT	CCGTGTGGTTGAATTCTACCG
PR55β(II)	GCAGCCTCGCAGAACCC	CCATGGTCCGAGCCTGAG
PR55γ	GCTGACATCATCTCTACCGTTGAG	GCCGCCCTTGTCACCTG
PR55δ(I)	GCTTCTCGCAGGTCAAGGG	AAACTCAACGGTGGAAATGATGT
PR55δ(II)	GACGAGGACGTGGCCG	TGTTGCAAGAAGATCTCCAGAGTAA
PP2A Cα	TATCAGATCACTTGATCGCCTACA	CATCTGGATCTGACCACAGCAA
PR61ε	CCGGTGATATTGACAATAGGAGAGA	TGCCAGAGCCACCTTTCG
PR65/Aα	TCTTCTCCCAGCATTGCCC	TTTCCTGTCAGACTGCGGC
GAPD (X01677)	TGGGCTACACTGAGCACCAG	CAGCGTCAAAGGTGGAGGAG
POLR2F (Z27113)	CCCGAAAGATCCCCATCAT	CACCCCCCAGTCTTCATAGC
PGK	TGAAGGACTGTGTAGGCCCAG	TTCTTCCTCCACATGAAAGCG

11.2.2 Primers for PCR and sequencing (selection)

Name of gene/construct	Use	F; forward R; reverse	Sequence 5' – 3'
Thy1.2-PP2A/Cα	genotyping	F (Thy1.2)	AAGTCACCCAGCAGGGAGGTGCTC
		R (PP2A/Cα)	TCTCGCAGAGGCTCTTGACCTGGGAC
pSUPER	Sequencing of insert	F	CTCACTATAGGGCGAATTGGA
		R	TGTGGAATTGTGAGCGGATA

11.2.3 Oligonucleotide templates for siRNA (*in situ* synthesis)

Gene	S; sense A; antisense	Sequence 5′ – 3′
PR55α (A)	S	AAAGATGACAACTCTACCACCCCTGTCTC
	A	AAGGTGGTAGAGTTGTCATCTCCTGTCTC
PR55α (B)	S	AACCACCTAATTTTATTGATCCCTGTCTC
	A	AAGATCAATAAAATTAGGTGGCCTGTCTC
PR55α (C)	S	AAATGACCTGTTACTGGGATCCCTGTCTC
	A	AAGATCCCAGTAACAGGTCATCCTGTCTC
PR55α (D)	S	AACTAAGCAGGAAGTGGGTTCCCTGTCTC
	A	AAGAACCCACTTCCTGCTTAGCCTGTCTC
PR55β (A)	S	AATATTACAACCCGACCCCCCCCTGTCTC
	A	AAGGGGGGTCGGGTTGTAATACCTGTCTC
PR55β (C)	S	AAATGATCTGTTGCTTGGATCCCTGTCTC
	A	AAGATCCAAGCAACAGATCATCCTGTCTC
PR55β (E)	S	AAAAACTTATCTCTTTTCTCCCCTGTCTC
	A	AAGGAGAAAAGAGATAAGTTTCCTGTCTC
PR55γ (A)	S	AAGATGACGACCCGGCCGCCCCCTGTCTC
	A	AAGGGCGGCCGGGTCGTCATCCCTGTCTC
PR55γ (F)	S	AACGGTAGAGATGATGTCAGCCCTGTCTC
	A	AAGCTGACATCATCTCTACCGCCTGTCTC
PR55γ (G)	S	AACTTGTCGAAAATGCAGTCGCCTGTCTC
	A	AACGACTGCATTTTCGACAAGCCTGTCTC
PR55γ (X)	S	AAAGGTCATGTCGGGGATGACCCTGTCTC
	A	AAGTCATCCCCGACATGACCTCCTGTCTC
PR55δ (A)	S	AAAATAACAACTCTGCCGCCCCCTGTCTC
	A	AAGGGCGGCAGAGTTGTTATTCCTGTCTC
PR55δ (F)	S	AACGGTGGAAATGATGTCCGCCCTGTCTC
	A	AAGCGGACATCATTTCCACCGCCTGTCTC
PR55δ (H)	S	AAAAATTCGCCGTGGACTCGCCCTGTCTC
	A	AAGCGAGTCCACGGCGAATTTCCTGTCTC

11.2.4 Oligonucleotide templates for siRNA (pSUPER expression)

Gene	S; sense A; antisense	Sequence 5′ – 3′
PR55α	S	GATCCCC**TCCAGTCTCATAGCAGAGGRRCAAGAGACCTCTGCTATGAGACTG GA**TTTTTGGAAA
	A	AGCTTTTCCAAAAA**TCCAGTCTCATAGCAGAGGTCTCTTGAACCTCTGCTATGA GACTGGA**GGG
PR55β	S	GATCCCC**TCAGGTTCATCGTAGGGGTTTCAAGAGAACCCCTACGATGAACCT GA**TTTTTGGAAA
	A	AGCTTTTCCAAAAA**TCAGGTTCATCGTAGGGGTTCTCTTGAAACCCCTACGATG AACCTGA**GGG
PR55γ	S	GATCCCC**TGCGCCCCACAGCCAGGGCTTCAAGAGAGCCCTGGCTGTGGGGCG CA**TTTTTGGAAA
	A	AGCTTTTCCAAAAA**TGCGCCCCACAGCCAGGGCTCTCTTGAAGCCCTGGCTGT GGGGCGCA**GGG
PR55δ	S	GATCCCC**GCGGACATCATTTCCACCG**TTCAAGAGA**CGGTGGAAATGATGTCCG C**TTTTTGGAAA
	A	AGCTTTTCCAAAAA**GCGGACATCATTTCCACCG**TCTCTTGAA**CGGTGGAAATGA TGTCCGC**GGG

11.2.5 Oligonucleotide templates for *in situ* hybridization

Gene	S; sense A; antisense	Sequence 5′ – 3′
PR55α	S (control)	CTCAGGTGAAAGGAGCAGTAGATGATGACGTAGCAGAAGCAGATA
	A	TATCTGCTTCTGCTACGTCATCATCTACTGCTCCTTTCACCTGAG
PR55β (I)	S (control)	ATGAAGCCCTTCACAGCTGACATTATCTCTACGGTAGAATTCAAC
	A	GTTGAATTCTACCGTAGAGATAATGTCAGCTGTGAAGGGCTTCAT
PR55β (II)	S (control)	CGGCTCCGGGATCCTGCCACCATCACAACCCTGCGGGTGCCTGTC
	A	GACAGGCACCCGCAGGGTTGTGATGGTGGCAGGATCCCGGAGCCG
PR55γ	S (control)	CTGCGGGACCACAGCTATGTGACAGAAGCTGACGTCATCTCCACT
	A	AGTGGAGATGACGTCAGCTTCTGTCACATAGCTGTGGTCCCGCAG
PR55δ (I)	S (control)	AGCTGGAGGCGGCGGCTGCCCGGCGGGCGGCAACGACTTCCAGTG
	A	CACTGGAAGTCGTTGCCGCCCGCCGGGCAGCCGCCGCCTCCAGCT
PR55δ (II)	S (control)	CGACTTCGAGACCCATTTAGAATTACGGCACTACGGGTTCCAATA
	A	TATTGGAACCCGTAGTGCCGTAATTCTAAATGGGTCTCGAAGTCG

11.3 Buffers, solutions, media

Designation	Composition
Blocking solution (*in situ*)	1× Buffer 1 supplemented with 0.1% Triton X-100 and 2% normal sheep serum
Buffer 1, 10× (*in situ*)	100 mM Tris HCl, pH 7.5, 150 mM NaCl:
Buffer 2 (*in situ*)	100 mM Tris-HCl, pH 9.5, 100 mM NaCl, 50 mM $MgCl_2$
Buffer 3, stop solution (*in situ*)	10 mM Tris-HCl, pH 8.1, 1 mM EDTA
Coomassie staining solution	0.16% (w/v) Coomassie Brilliant Blue R250, 40% (v/v) methanol, 10% (v/v) acetic acid
Coomassie destaining solution	(45% (v/v) methanol, 10% (v/v) glacial acetic acid).
Dennhard's solution, 50x	Ficoll, polyvinylpyrrolidone, BSA, H_2O
DNA sample buffer	0.25%(w/v) bromphenol blue, 0.25% (w/v) xylene cyanol FF, 30% (w/v) glycerol
Hydrolysis buffer (*in situ*)	1 M DTT, 1 M $NaHCO_3$, 1 M Na_2CO_3, H_2O
LB agar	LB medium, 15 g/l Bacto Agar
LB medium	10 g/l Bacto Tryptone, 5 g/l Bacto yeast extract, 10 g/l NaCl, pH 7.0
MOPS buffer, 10x	0.2 M MOPS [3-(N-morpholino)-propanesulfonic acid], pH7.2, 0.5 M sodium acetate, 0.01 M EDTA
Neutralizing buffer (*in situ*)	1 M DTT (1.52 g in 10 ml H_2O), 1 M NaAc (29.4 g in 100 ml H_2O), H_2O
Paraformaldehyd (PFA) 4% in PBS	heat PBS in microwave to 75°C, add 4 g PFA (stirring under hood) and NaOH dropwise until clear
PBS, 10x	1.4 M NaCl, 0.027 M KCL, 0.1 M Na_2HPO_4 x 2 H_20, 0.018 M KH_2PO_4
Ponceau S solution	0.2% (w/v) Poinceau-S red, 3% (w/v) sulfonic acid, 0.1% (v/v) glacial acid
Prehybridization and hybridization solutions	500 mg/50 ml formamide (deionised with ion exchanger amberlite MB-3), SSC, Denhardt's, salmon sperm DNA, yeast RNA, dextransulfate, DTT, PBS, EDTA (pH 8)
Protein sample buffer, 2x	450 mM Tris-HCl pH 8.45, 12% (v/v) Glycerol, 4% (w/v) SDS, 7.5‰ Coomassie brilliant Blue, 2.5‰ Phenol Red
RNA sample buffer, 6x	10 mM EDTA, pH 8.0, 0.25% (w/v) bromphenol blue, 0.25% (w/v) xylenecyanol, 50% (v/v) glycerol

Sodium acetate, 3 M, pH 5.2	Sodium acetate × 3 H_2O, acetic acid to pH 5.2
SSC, 20x	3 M NaCl, 300 mM sodiumcitrate (acetate), pH 7.5
Staining solution (*in situ*)	Buffer 2, NBT (100 mg NBT/ml in 70% dimethylformamide), BCIP (50 mg/ml in 100% dimethylformamide), 1 M levamisol
TAE buffer	40 mM Tris-acetate, 1 mM EDTA
TBS, 10x	0.84 M Tris-HCL, 0.16 M Tris-Base, 1.5 M NaCl

11.4 Kits, systems, assays

Name	**Order nr.**	**Supplier**
Big Dye Terminator v1.1 Cycle Sequencing	4336776	Applied Biosystems
DC protein assay	500-0113/4/5	BioRad
CSPD developing system	1 755 633	Roche Molecular Biochemicals
DIG Oligonucleotide Tailing	1 417 231	Roche Molecular Biochemicals
ECL Western Blotting Detection Reagents	RPN 2106	Amersham Biosciences
Gene Elute Gel Extraction	NA1111	Sigma
Gene Elute Miniprep	PLN-350	Sigma
Gene Elute PCR Clean-up	NA1020	Sigma
Gene Elute Plasmid Maxiprep	PLX-50	Sigma
QIAGEN Nucleotide Removal		Qiagen
QIAGEN Plasmid Maxi	12165	Qiagen
QIAGEN Plasmid Mini	12125	Qiagen
QIAGEN Rneasy	74104	Qiagen
QIAquick Gel Extraction	28706	Qiagen
QIAquick PCR Purification	28106	Qiagen
QIAshredder	79656	Qiagen
Quick-change site-directed mutagenesis	200518	Stratagene
Rediprime II Random Prime Labelling System	RPN 1633	Amersham
Rnase free DNAse	79254	Qiagen
Ser/Thr phosphatase assay system	V2460	Promega
Silencer siRNA construction	1620	Ambion
Silencer siRNA labeling	1632	Ambion

Superscript first strand synthesis system for RT-PCR	11904-018	Life Technologies
SuperSignal West Femto Maximum Sensitivity Substrate	34095	Pierce
SYBR Green PCR Core Reagents	4304886	Applied Biosystems
TOPO-XL PCR Cloning	45-0008	Invitrogen
Tunnel stain	1684 817	Roche
Vectastain ABC (rabbit, mouse, goat)	PK-6101/2/5	Vector Laboratories

11.5 Chemicals and laboratory commodities

[α-32P]dCTP	Hartmann Analytic
[γ-32P]dATP	Hartmann Analytic
Acetic acid, glacial	Merck
Acetic anhydride	Fluka
Agarose	Invitrogen
Amberlite	Merck
Ampicillin	Sigma
AmpliTaq Gold polymerase	Applied Biosystems
β-mercaptoethanol	Sigma
Bacto agar	Becton Dickinson
Bacto tryptone	Becton Dickinson
Bacto yeast	Becton Dickinson
BDNF	Peprotech
Biomax MR film	Kodak
Bovine Serum Albumin (BSA)	Sigma
Bromo-Chloro-Indolyl Phosphate (BCIP)	Boehringer-Roche
Bromphenol blue	Sigma
BSA	Sigma
BSA, acetylated	Invitrogen
$CaCl_2$	Sigma
Chromatography Paper (3MM Chr)	Whatmann
Cell culture dishes	TTP
Cell culture media	Invitrogen
Chloroform	Sigma
Collagen Type I	Sigma
Complete protease inhibitor	Roche
Coomassie Brillant Blue	Merck
Crystal violet	Sigma
Culture slides	Falcon
DAB/Metal Concentrate (10 x)	Pierce
DAPT	Calbiochem
DC Protein Assay	BioRAD
DEPC H_20	Ambion
DEPC	Sigma
Dextransulfate	Sigma
DH5α *E.coli*	Life Technologies
DMEM/F12	Life Technologies
DMEM	Life Technologies
DMSO	Sigma
DNA ladder 50 bp	Invitrogen
DNA ladders (100 bp, 1 kb and 2-Log)	New England Biolabs
DNA Polymerase 1 (Klenow fragment)	New England Biolabs

dNTPs	Sigma
DTT	Sigma
E. coli tRNA	Sigma
E.coli T4 DNA ligase	New England Biolabs
E.coli T4 polynucleotide kinase	New England Biolabs
EDTA 0.5M solution	Sigma
EGTA	Fluka
Ethanol	Merck
Ethidium bromide	Sigma
Eukitt	Kindler, Freiburg, Germany
Fetal calf serum (FCS)	Life Technologies
Ficoll Typ 400	Sigma
Formaldehyde	Fluka
Formamide	Calbiochem, Merck
Formic acid	Merck
Gene Pulser cuvette (0.1 cm)	BioRad
Geneticin G418	Life Technologies
Glacial acetic acid	Merck
Glycerol	Sigma
Glycine	Merck
Goat Serum	Vector Laboratories
HCl	Riedel-de Haën
HEK-293 cells	Deutsche Sammlung von Mikroorganismen und Zellkulturen #305
HEPES	Sigma
Horse Serum	Vector Laboratories
HPLC-grade H_20	Aldrich
Isoamylalcohol	Merk
Isopropanol	Sigma
Kanamycin	Sigma
KCl	Sigma
Ketaminal	Vererinaria, Zürich, Switzerland
KH_2PO_4	Sigma
KOAc	Sigma
KOH	Sigma
Levamisol	Fluka
Lipofectamine (LF2000)	Life Technologies
L-Glutamine	Life Technologies
LiCl	Merck
MES Hydrate	Sigma
MES sodium salt	Sigma
Methanol	Merck
$MgCl_2$	Merck
MgOAc	Sigma
Microscope slides "SuperFrost Plus"	Menzel-Gläser, Germany
Microtome blades S35 type	Feather
Milk/milk powder	Coop
Mowiol	Hoechst, Germany
N2 supplement	Life Technologies
Na_2CO_3	Fluka
Na_2HPO_4	Merck
NaAc	Merck
NaCl 5M	Ambion
NaCl	Sigma
NaHCO3	Sigma
NaOH	Sigma
needle 26GA 5/8 (sterile)	Becton Dickinson
NH_4Oac	Sigma
Nitrocellulose-membrane 0.1 µm	Schleicher & Schuell
Nitrocellulose membrane 0.45 µm	BioRad
Nitrocellulose membrane Hybond-ECL	Amersham Biosciences
Nitrocellulose membrane Hybond-N+	Amersham Biosciences

Nitroblue-Tetrazolium (NBT)	Boehringer-Roche
Normal sheep serum	Sigma
NT3	Juro
Nuclear Fast Red (Kernechtrot)	Fluka
Nu Page polyacrylamide gel, 10%	Invitrogen
Okadaic Acid, Sodium Salt	Calbiochem
Oligonucleotides	Metabion/Microsynth
Optical 96 well Reaction plate	Applied Biosystems
Optical adhesive covers	Applied Biosystems
Optical caps (8 stripes)	Applied Biosystems
Opti-MEM I	Life Technologies
Paraformaldehyde	Electron Micr. Sciences
Pfu Turbo DNA polymerase	Stratagene
Phenol	Merck
Phenolred	Sigma
Pipes	Sigma
Ponceau-S	Merck
Polyornithine	Sigma
Polyvinylpyrrolidone	Sigma
Proteinase K	Roche
Protein A Sepharose	Amersham Pharmacia
Protein G Sepharose	Amersham Pharmacia
Protein gel marker	Invitrogen
RedTaq genomic DNA polymerase	Sigma
Restricition endonucleases	New England Biolabs
Retinoic Acid	Sigma
RNA 6000 ladder	Ambion
Rnase away	Catalys
RNAse free Proteinase K	Boehringer-Roche
Rompun (Xylazinum)	Bayer
Salmon sperm DNA	Roche
SDS	Sigma
SeeBlue Plus2 pre-stained protein standard	Invitrogen
Shrimp alkaline phosphatase	Roche
SH-SY5Y neuroblastoma cells	Deutsche Sammlung von Mikroorganismen und Zellkulturen #209
SigmaSpin post reaction purification columns	Sigma
Simply Blue Safe stain	Life Technologies
Sodium acetate	Sigma
Sodium citrate	Merck
SPARE quartz capillaries	Biochrom
Sucrose	Sigma
Sulfuric acid	Merck
SYBR Green I nucleic acid gel stain	Molecular Probes
Syringe 1 ml	Becton Dickinson
Tissue freezing medium	Jung
Tricine	Sigma
Triethanolamine	Fluka
Triton X-100	Sigma
Trizma acetate	Sigma
Trizma base	Sigma
Trizma hydrochloride	Sigma
Trizol	Life Technologies
Trypsin/EDTA	Invitrogen
Tween 20	Sigma
Ultra pure salmon sperm DNA	Invitrogen
Uvette disposable cuvettes	Eppendorf
Vimentin (recombinant Syrian hamster)	Cytoskeleton
X-Omat LS film	Kodak
Xylenecyanol	Merck
Yeast extract	Becton Dickinson
Yeast RNA from Brewers yeast	Boehringer-Roche

11.6 Laboratory devices

ABI Prism 310 Genetic Analyzer	Applied Biosystems,
ABI Prism 7700 Sequence Detector	Applied Biosystems
Agilent 2000 Bioanalyzer	Agilent Technologies
Bio Photometer	Eppendorf
Blotting Tank	BioRad
C25 Incubatorshaker	Fisher Scientific
Centrifuge 5417C	Eppendorf
Centrifuge 5417R	Eppendorf
Centrifuge 5804R	Eppendorf
Concentrator 5301 speedvac	Eppendorf
Cryotome Leica CM 1900	Leica
Electrophoresis powersupply consort E865	Witec AG
Gene Pulser II Electroporation System	BioRad
Gene Quant Pro (Photometer)	Amersham Pharmacia
GeneAmp PCR System 9700	Applied Biosystems
EasyCast Electrophoresis System	Owl
Kodak X-OMAT 2000 Processor	Kodak
Memmert waterbath	Fisher Scientific
Microtome Leica RM 2135	Leica
MP 220 pH meter	Mettler Toledo
Nikon Eclipse E800	Nikon
Nikon Eclipse TE300	Nikon
Nikon TMS F	Nikon
NUAIRE Autoflow CO_2 jacked Incubator	Inotech
Rota-Rod 7650	Ugo Basile, Comerio, Italy
Rotor GSA	Sorvall
Rotor SS34	Sorvall
Scaltec SBC 31 Balance	Vaudaux
Scaltec SBC 51 Balance	Vaudaux
SKAN VSE-2000-120 sterilhood	Skan
Sorvall RC 26 Plus	Kendro
STORM 860 Phosphor-Imager	Molecular Dynamics
Thermomixer	Eppendorf
Universal 32 Hettich centrifuge	Fisher scientific
UV Stratalinker 1800	Stratagene
Vacuum Pump OME28 C/H	Alcatel
Vibratome Leica VT 1000S	Leica
WTB Cabinincubator	Faust

11.7 Software

Adobe Illustrater 9.0.1	Adobe
Adobe Photoshop 6.0	Adobe
Endnote 8, reference manager	Endnote
ImageJ quantification software	Wayne Rasband, NIH, USA
Microsoft Excel, Powerpoint, Word (2002)	Microsoft
Primer Expresss 1.5	Applied Biosystems
SeqMan II and MegAlign 4.00	DNASTAR
Sequence detection software 1.9.1	Applied Biosystems

11.8 Antibodies

11.8.1 Primary antibodies

See in the Methods section 10.8 on page 100.

11.8.2 Secondary antibodies

Antibody	Origin	Dilution	Order Nr	Supplier
anti-digoxigenin-AP conjugates	mouse	1:500	1 093 274	Roche Molecular Biochemicals
anti-goat HRP	donkey	1:5000	705 035 147	Jackson
anti-mouse Cy3	donkey	1:250	715 165 151	Jackson
anti-mouse HRP	goat	1:2000	1858413	Pierce
anti-rabbit Cy3	donkey	1:250	711 165 152	Jackson
anti-rabbit HRP	goat	1:2000	1858415	Pierce
anti-rat Cy3	donkey	1:250	712 165 153	Jackson
anti-rat HRP	goat	1:5000	NA 935 V	Amersham
anti-streptavidin biotinyl.	goat		BA-0500	Reactolab

12 Abbreviations

A	Adenosine
A_{260}	Absorption 260 nm
A_{280}	Absorption at 280 nm
aa	amino acids
AD	Alzheimer's disease
AP	Alkaline phosphatase
ApoE	Apolipoproteine E
APP	β-amyloid precursor protein
APP_S-α	soluble β-APP cut by α-sec
APP_S-β	soluble β-APP cut by β-sec
APPswe	APP double mutation, K595N and M596L
α-sec	α-secretase
ATP	Adenosine triphosphate
Aβ	β-amyloid peptide
$Aβ_{40}$	β-amyloid peptide of 40 aa
$Aβ_{42}$	β-amyloid peptide of 42 aa
BACE	β-site APP cleavage enzyme (β-secretase)
β-APP	APP cut by β-sec
BDNF	Brain-derived neurotrophic factor
BLAST	Basic local alignment search tool
bp	base pairs
BSA	Bovine serum albumine
β-sec	β-secretase, BACE
C	Cytosine
CA	Calyculin
CaMKII	Calmodulin-dependent protein kinase II
cDNA	complemetary desoxyribonucleic acid
Chr	Chromosome
C_T	Threshold cycle
C-ter	C-terminal
CTF	C-terminal fragment
CTF-α	membrane tethered C-ter fragment generated by α-sec
CTF-β	membrane tethered C-ter fragment generated by β-sec
Cdk	cyclin-dependent kinase
dATP	desoxy ATP
dCTP	desoxy CTP
DEPC	Diethylpyrocarbonate
dGTP	desoxy GTP
DIG	Digoxigenin
DMEM	Dulbeccos' modified Eagle Medium
DMEM/F12	DMEM/Nutrient Mixture F-12
DMSO	Dimethylsulfoxide
DNA	Desoxyribonucleic acid
DNase	Desoxyribonuclease
dNTP	desoxy nucleotide triphosphate
ds-cDNA	double stranded cDNA
DSMZ	Deutsches Zentrum für molekularbiologische Sammlungen
dsRNA	double stranded ribonucleic acid
DTT	Dithiothreitol
E. coli	*Escherichia coli*
ECL	Enhanced chemiluminescence
EDTA	Ethylen-diamin-tetraacetic acid
EGTA	Ethylene-glycol-bis(2-aminoethyl)-tetraacetic acid
ERG	Ganzfeld electroretinography
ERK	Extracellular signal-related kinase
F	Farad constante
FAD	Familial form of Alzheimer's disease

FCS	Fetal calf serum
FTD	Frontotemporal dementia
g	gravitational force
G	Guanidine
GAPDH	glyceraldehyde-3-phosphate dehydrogenase
GFAP	glial fibrillary acidic protein
GFP	Green fluorescent protein
γ-sec	γ-secretase (protein complex)
GSK-3	Glycogen synthase kinase 3
HA	Haemagglutinin
HEK-293	Human embryonic kidney cells
HEPES	N-[2-Hydroxyethyl]piperazine-N'-[2-ethanesulfonic acid]
HPLC	High performance liquid chromatography
HRP	Horseradish peroxidase
IP	Immunoprecipitation
JNK	c-Jun N-terminal kinase
kb	kilobase
kDa	kilodalton
LB	Luria Bertani
LF2000	Lipofectamine 2000
M	Molar
MAP	mitogen-activated protein
MAPK	mitogen-activated protein kinase
MC	Microcystin
MKP	MAP kinase phosphatase
MOPS	3-N-morpholinpropansulfonic acid
MT	microtubule
mRNA	messenger ribonucleic acid
NF	neurofilament
NFT	Neurofibrillary tangles
NGF	Nerve growth factor
NT3	neurotropic factor Neurotrophin-3
OA	Okadaic acid
OD	Optical density
Oligo	Oligonucleotide
o/n	overnight
ORF	Open reading frame
PBS	Phosphate buffered saline
PBGD	Porphobilinogen-Deaminase
PCR	Polymerase chain reaction
PFA	Paraformaldehyde
PGK	Phosphoglycerate kinase
PHF	Paired helical filaments
PKA	Protein kinase A
PKC	Protein kinase C
POLR2F	polymerase (RNA) II (DNA directed) polypeptide F
poly-dT	desoxy thymidine polymer
PP	Protein phosphatase
PP2A	Protein phosphatase 2A
PS	Presenilin
PSEN1	gene encoding Presenilin isoform1
PSEN2	gene encoding Presenilin isoform 2
PSP	Progressive supranuclear palsy
PTB	phosphotyrosine interacting/ binding domain
qRT-PCR	quantitative real-time PCR
RA	Retinoic acid
RISC	RNA induced silencing complex
RNA	Ribonucleic acid
RNase	Ribonuclease
rpm	rotations per minute
RT	Room temperature
SAD	Sporadic Alzheimer’s Disease

SAP	Shrimp alkaline phosphatase
SD	Standard deviation
SDS	Sodium dodecyl sulfate
SEM	standard error of the mean
SH-SY5Y	Human neuroblastoma cell line
siRNA	short interfering RNA
SLO	scanning laser ophthalmoscopy
T	Thymidine
T_3	triiodothyronine
T_4	thyroxine
TAE	Tris acetate EDTA buffer
tauP301L	Tau protein with the mutation P301L
TBS	Tris buffered saline
TEA	Triethanolamine
TSH	thyroid-stimulating hormone
TUNEL	terminal deoxyribonucleotidyl transferase (TdT)-mediated biotin-16-dUTP nick-end labeling
U	Unit
UV	Ultra-violett
V	Volt
v/v	volume per volume
w/v	weight per volume
WB	Western blotting
WT	wild-type

13 References

Abraha, A., Ghoshal, N., Gamblin, T.C., Cryns, V., Berry, R.W., Kuret, J. and Binder, L.I. (2000) C-terminal inhibition of tau assembly in vitro and in Alzheimer's disease. *J Cell Sci*, **113**, 3737-3745.

Aitken, A. (1996) 14-3-3 and its possible role in co-ordinating multiple signalling pathways. *Trends Cell Biol*, **6**, 341-347.

Alessi, D.R., Gomez, N., Moorhead, G., Lewis, T., Keyse, S.M. and Cohen, P. (1995) Inactivation of p42 MAP kinase by protein phosphatase 2A and a protein tyrosine phosphatase, but not CL100, in various cell lines. *Curr Biol*, **5**, 283-295.

Allen, B., Ingram, E., Takao, M., Smith, M.J., Jakes, R., Virdee, K., Yoshida, H., Holzer, M., Craxton, M., Emson, P.C., Atzori, C., Migheli, A., Crowther, R.A., Ghetti, B., Spillantini, M.G. and Goedert, M. (2002) Abundant tau filaments and nonapoptotic neurodegeneration in transgenic mice expressing human P301S tau protein. *J Neurosci*, **22**, 9340-9351.

Alvarez, G., Munoz-Montano, J.R., Satrustegui, J., Avila, J., Bogonez, E. and Diaz-Nido, J. (1999) Lithium protects cultured neurons against beta-amyloid-induced neurodegeneration. *FEBS Lett*, **453**, 260-264.

Alzheimer, A. (1907) Über eine eigenartige Erkrankung der Hirnrinde. *Zentralblatt für Nervenheilkunde und Psychiatrie*, **30**, 177-179.

Ambrose, A.M., Larson, P.S., Borzelleca, J.F., Smith, R.B., Jr. and Hennigar, G.R., Jr. (1971) Toxicologic studies on 2,4-dichlorophenyl-p-nitrophenyl ether. *Toxicol Appl Pharmacol*, **19**, 263-275.

Anderson, N.G., Maller, J.L., Tonks, N.K. and Sturgill, T.W. (1990) Requirement for integration of signals from two distinct phosphorylation pathways for activation of MAP kinase. *Nature*, **343**, 651-653.

Andersson, L. and Porath, J. (1986) Isolation of phosphoproteins by immobilized metal (Fe3+) affinity chromatography. *Anal Biochem*, **154**, 250-254.

Anderton, B.H., Betts, J., Blackstock, W.P., Brion, J.P., Chapman, S., Connell, J., Dayanandan, R., Gallo, J.M., Gibb, G., Hanger, D.P., Hutton, M., Kardalinou, E., Leroy, K., Lovestone, S., Mack, T., Reynolds, C.H. and Van Slegtenhorst, M. (2001) Sites of phosphorylation in tau and factors affecting their regulation. *Biochem Soc Symp*, 73-80.

Andrade, M.A. and Bork, P. (1995) HEAT repeats in the Huntington's disease protein. *Nat Genet*, **11**, 115-116.

Arendt, T. (2003) Synaptic plasticity and cell cycle activation in neurons are alternative effector pathways: the 'Dr. Jekyll and Mr. Hyde concept' of Alzheimer's disease or the yin and yang of neuroplasticity. *Prog Neurobiol*, **71**, 83-248.

Arendt, T., Holzer, M., Fruth, R., Bruckner, M.K. and Gartner, U. (1995) Paired helical filament-like phosphorylation of tau, deposition of beta/A4-amyloid and memory impairment in rat induced by chronic inhibition of phosphatase 1 and 2A. *Neuroscience*, **69**, 691-698.

Arendt, T., Holzer, M., Fruth, R., Bruckner, M.K. and Gartner, U. (1998) Phosphorylation of tau, Abeta-formation, and apoptosis after in vivo inhibition of PP-1 and PP-2A. *Neurobiol Aging*, **19**, 3-13.

Arendt, T., Holzer, M., Stobe, A., Gartner, U., Luth, H.J., Bruckner, M.K. and Ueberham, U. (2000) Activated mitogenic signaling induces a process of dedifferentiation in Alzheimer's disease that eventually results in cell death. *Ann N Y Acad Sci*, **920**, 249-255.

Arriagada, P.V., Growdon, J.H., Hedley-Whyte, E.T. and Hyman, B.T. (1992) Neurofibrillary tangles but not senile plaques parallel duration and severity of Alzheimer's disease. *Neurology*, **42**, 631-639.

Arufe, M.C., Beckett, G.J., Duran, R. and Alfonso, M. (1999) Effect of okadaic acid and calyculin-A, two protein phosphatase inhibitors, on thyrotropin-stimulated triiodothyronine secretion in cultured sheep thyroid cells. *Endocrine*, **11**, 235-240.

Asami-Odaka, A., Ishibashi, Y., Kikuchi, T., Kitada, C. and Suzuki, N. (1995) Long amyloid beta-protein secreted from wild-type human neuroblastoma IMR-32 cells. *Biochemistry*, **34**, 10272-10278.

Bach, M.E., Hawkins, R.D., Osman, M., Kandel, E.R. and Mayford, M. (1995) Impairment of spatial but not contextual memory in CaMKII mutant mice with a selective loss of hippocampal LTP in the range of the theta frequency. *Cell*, **81**, 905-915.

Baharians, Z. and Schonthal, A.H. (1998) Autoregulation of protein phosphatase type 2A expression. *J Biol Chem*, **273**, 19019-19024.

Baker, M., Kwok, J.B., Kucera, S., Crook, R., Farrer, M., Houlden, H., Isaacs, A., Lincoln, S., Onstead, L., Hardy, J., Wittenberg, L., Dodd, P., Webb, S., Hayward, N., Tannenberg, T., Andreadis, A., Hallupp, M., Schofield, P., Dark, F. and Hutton, M. (1997) Localization of frontotemporal dementia with parkinsonism in an Australian kindred to chromosome 17q21-22. *Ann Neurol*, **42**, 794-798.

Barford, D. (1996) Molecular mechanisms of the protein serine/threonine phosphatases. *Trends Biochem Sci*, **21**, 407-412.

Barford, D., Das, A.K. and Egloff, M.P. (1998) The structure and mechanism of protein phosphatases: insights into catalysis and regulation. *Annu Rev Biophys Biomol Struct*, **27**, 133-164.

Barghorn, S., Zheng-Fischhofer, Q., Ackmann, M., Biernat, J., von Bergen, M., Mandelkow, E.M. and Mandelkow, E. (2000) Structure, microtubule interactions, and paired helical filament aggregation by tau mutants of frontotemporal dementias. *Biochemistry*, **39**, 11714-11721.

Bassett, C.N. and Montine, T.J. (2003) Lipoproteins and lipid peroxidation in Alzheimer's disease. *J Nutr Health Aging*, **7**, 24-29.

Baumann, K., Mandelkow, E.M., Biernat, J., Piwnica-Worms, H. and Mandelkow, E. (1993) Abnormal Alzheimer-like phosphorylation of tau-protein by cyclin-dependent kinases cdk2 and cdk5. *FEBS Lett*, **336**, 417-424.

Bennecib, M., Gong, C.X., Grundke-Iqbal, I. and Iqbal, K. (2000) Role of protein phosphatase-2A and -1 in the regulation of GSK-3, cdk5 and cdc2 and the phosphorylation of tau in rat forebrain. *FEBS Lett*, **485**, 87-93.

Bennecib, M., Gong, C.X., Grundke-Iqbal, I. and Iqbal, K. (2001) Inhibition of PP-2A upregulates CaMKII in rat forebrain and induces hyperphosphorylation of tau at Ser 262/356. *FEBS Lett*, **490**, 15-22.

Bennett, P.C., Zhao, W. and Ng, K.T. (2001) Concentration-dependent effects of protein phosphatase (PP) inhibitors implicate PP1 and PP2A in different stages of memory formation. *Neurobiol Learn Mem*, **75**, 91-110.

Bertram, L. and Tanzi, R.E. (2004) Alzheimer's disease: one disorder, too many genes? *Hum Mol Genet*, **13 Spec No 1**, R135-141.

Bierer, L.M., Hof, P.R., Purohit, D.P., Carlin, L., Schmeidler, J., Davis, K.L. and Perl, D.P. (1995) Neocortical neurofibrillary tangles correlate with dementia severity in Alzheimer's disease. *Arch Neurol*, **52**, 81-88.

Birnboim, H.C. and Doly, J. (1979) A rapid alkaline extraction procedure for screening recombinant plasmid DNA. *Nucleic Acids Res*, **7**, 1513-1523.

Boas, N.F. and Scow, R.O. (1954) Apparent exophthalmos in the rat following cortisone treatment or thyroidectomy. *Endocrinology*, **55**, 148-155.

Bowser, R. and Smith, M.A. (2002) Cell cycle proteins in Alzheimer's disease: plenty of wheels but no cycle. *J Alzheimers Dis*, **4**, 249-254.

Braak, E., Griffing, K., Arai, K., Bohl, J., Bratzke, H. and Braak, H. (1999) Neuropathology of Alzheimer's disease: what is new since A. Alzheimer? *Eur Arch Psychiatry Clin Neurosci*, **249 Suppl 3**, 14-22.

Braak, H. and Braak, E. (1991) Neuropathological stageing of Alzheimer-related changes. *Acta Neuropathol (Berl)*, **82**, 239-259.

Braak, H. and Braak, E. (1995) Staging of Alzheimer's disease-related neurofibrillary changes. *Neurobiol Aging*, **16**, 271-278; discussion 278-284.

Braak, H., Braak, E., Bohl, J. and Reintjes, R. (1996) Age, neurofibrillary changes, A beta-amyloid and the onset of Alzheimer's disease. *Neurosci Lett*, **210**, 87-90.

Brondello, J.M., Pouyssegur, J. and McKenzie, F.R. (1999) Reduced MAP kinase phosphatase-1 degradation after p42/p44MAPK-dependent phosphorylation. *Science*, **286**, 2514-2517.

Bryant, J.C., Westphal, R.S. and Wadzinski, B.E. (1999) Methylated C-terminal leucine residue of PP2A catalytic subunit is important for binding of regulatory Balpha subunit. *Biochem J*, **339 (Pt 2)**, 241-246.

Buee-Scherrer, V., Condamines, O., Mourton-Gilles, C., Jakes, R., Goedert, M., Pau, B. and Delacourte, A. (1996) AD2, a phosphorylation-dependent monoclonal antibody directed against tau proteins found in Alzheimer's disease. *Brain Res Mol Brain Res*, **39**, 79-88.

Buee, L. and Delacourte, A. (1999) Comparative biochemistry of tau in progressive supranuclear palsy, corticobasal degeneration, FTDP-17 and Pick's disease. *Brain Pathol*, **9**, 681-693.

Bugiani, O., Murrell, J.R., Giaccone, G., Hasegawa, M., Ghigo, G., Tabaton, M., Morbin, M., Primavera, A., Carella, F., Solaro, C., Grisoli, M., Savoiardo, M., Spillantini, M.G., Tagliavini, F., Goedert, M. and Ghetti, B. (1999) Frontotemporal dementia and corticobasal degeneration in a family with a P301S mutation in tau. *J Neuropathol Exp Neurol*, **58**, 667-677.

Burch, H.B. and Wartofsky, L. (1993) Graves' ophthalmopathy: current concepts regarding pathogenesis and management. *Endocr Rev*, **14**, 747-793.

Burman, K.D. (1995) Hyperthyroidism. In: Becker KL, ed. Principles and practice of endocrinology and metabolism. *2nd ed. Philadelphia: JB Lippincott*, 367-385.

Bussiere, T., Gold, G., Kovari, E., Giannakopoulos, P., Bouras, C., Perl, D.P., Morrison, J.H. and Hof, P.R. (2003) Stereologic analysis of neurofibrillary tangle formation in prefrontal cortex area 9 in aging and Alzheimer's disease. *Neuroscience*, **117**, 577-592.

Bussiere, T., Hof, P.R., Mailliot, C., Brown, C.D., Caillet-Boudin, M.L., Perl, D.P., Buee, L. and Delacourte, A. (1999) Phosphorylated serine422 on tau proteins is a pathological epitope found in several diseases with neurofibrillary degeneration. *Acta Neuropathol (Berl)*, **97**, 221-230.

Buzzell, G.R. (1996) The Harderian gland: perspectives. *Microsc Res Tech*, **34**, 2-5.

Cai, H., Wang, Y., McCarthy, D., Wen, H., Borchelt, D.R., Price, D.L. and Wong, P.C. (2001) BACE1 is the major beta-secretase for generation of Abeta peptides by neurons. *Nat Neurosci*, **4**, 233-234.

Calin, G.A., di Iasio, M.G., Caprini, E., Vorechovsky, I., Natali, P.G., Sozzi, G., Croce, C.M., Barbanti-Brodano, G., Russo, G. and Negrini, M. (2000) Low frequency of alterations of the alpha (PPP2R1A) and beta (PPP2R1B) isoforms of the subunit A of the serine-threonine phosphatase 2A in human neoplasms. *Oncogene*, **19**, 1191-1195.

Campsall, K.D., Mazerolle, C.J., De Repentingy, Y., Kothary, R. and Wallace, V.A. (2002) Characterization of transgene expression and Cre recombinase activity in a panel of Thy-1 promoter-Cre transgenic mice. *Dev Dyn*, **224**, 135-143.

Chen, C., Kim, J.J., Thompson, R.F. and Tonegawa, S. (1996) Hippocampal lesions impair contextual fear conditioning in two strains of mice. *Behav Neurosci*, **110**, 1177-1180.

Chen, F., David, D., Ferrari, A. and Gotz, J. (2004) Posttranslational modifications of tau - Role in human tauopathies and modeling in transgenic animals. *Curr Alz Res*.

Chen, G., Chen, K.S., Knox, J., Inglis, J., Bernard, A., Martin, S.J., Justice, A., McConlogue, L., Games, D., Freedman, S.B. and Morris, R.G. (2000) A learning deficit related to age and beta-amyloid plaques in a mouse model of Alzheimer's disease. *Nature*, **408**, 975-979.

Chen, Y., Wollmer, M.A., Hoerndli, F., Münch, G., Kuhla, B., Rogaev, E.I., Tsolaki, M., Papassotiropoulos, A. and Gotz, J. (2004) Role for glyoxalase I in Alzheimer's disease. *Proc Natl Acad Sci U S A*, **101**, 7687-7692.

Cherny, R.A., Atwood, C.S., Xilinas, M.E., Gray, D.N., Jones, W.D., McLean, C.A., Barnham, K.J., Volitakis, I., Fraser, F.W., Kim, Y., Huang, X., Goldstein, L.E., Moir, R.D., Lim, J.T., Beyreuther, K., Zheng, H., Tanzi, R.E., Masters, C.L. and Bush, A.I. (2001) Treatment with a copper-zinc chelator markedly and rapidly inhibits beta-amyloid accumulation in Alzheimer's disease transgenic mice. *Neuron*, **30**, 665-676.

Chevallet, M., Wagner, E., Luche, S., van Dorsselaer, A., Leize-Wagner, E. and Rabilloud, T. (2003) Regeneration of peroxiredoxins during recovery after oxidative stress: only some overoxidized peroxiredoxins can be reduced during recovery after oxidative stress. *J Biol Chem*, **278**, 37146-37153.

Chiou, J.Y. and Westhead, E.W. (1992) Okadaic acid, a protein phosphatase inhibitor, inhibits nerve growth factor-directed neurite outgrowth in PC12 cells. *J Neurochem*, **59**, 1963-1966.

Chomczynski, P. (1993) A reagent for the single-step simultaneous isolation of RNA, DNA and proteins from cell and tissue samples. *Biotechniques*, **15**, 532-534, 536-537.

Chung, H. and Brautigan, D.L. (1999) Protein phosphatase 2A suppresses MAP kinase signalling and ectopic protein expression. *Cell Signal*, **11**, 575-580.

Chung, H., Nairn, A.C., Murata, K. and Brautigan, D.L. (1999) Mutation of Tyr307 and Leu309 in the protein phosphatase 2A catalytic subunit favors association with the alpha 4 subunit which promotes dephosphorylation of elongation factor-2. *Biochemistry*, **38**, 10371-10376.

Citron, M., Vigo-Pelfrey, C., Teplow, D.B., Miller, C., Schenk, D., Johnston, J., Winblad, B., Venizelos, N., Lannfelt, L. and Selkoe, D.J. (1994) Excessive production of amyloid beta-protein by peripheral cells of symptomatic and presymptomatic patients carrying the Swedish familial Alzheimer disease mutation. *Proc Natl Acad Sci U S A*, **91**, 11993-11997.

Cohen, P. (2000) The regulation of protein function by multisite phosphorylation--a 25 year update. *Trends Biochem Sci*, **25**, 596-601.

Cohen, P., Klumpp, S. and Schelling, D.L. (1989) An improved procedure for identifying and quantitating protein phosphatases in mammalian tissues. *FEBS Lett*, **250**, 596-600.

Colantuoni, C., Purcell, A.E., Bouton, C.M. and Pevsner, J. (2000) High throughput analysis of gene expression in the human brain. *J Neurosci Res*, **59**, 1-10.

Consortium, I.H.G.S. (2004) Finishing the euchromatic sequence of the human genome. *Nature*, **431**, 931-945.

Coto-Montes, A., Rodriguez-Colunga, M.J., Tolivia, D. and Sanchez-Barcelo, E. (1997) Histopathological features of the Harderian glands in transgenic mice carrying MMTV/N-ras protooncogene. *Microsc Res Tech*, **38**, 311-314.

Coulson, E.J., Paliga, K., Beyreuther, K. and Masters, C.L. (2000) What the evolution of the amyloid protein precursor supergene family tells us about its function. *Neurochem Int*, **36**, 175-184.

Crystal, H., Dickson, D., Fuld, P., Masur, D., Scott, R., Mehler, M., Masdeu, J., Kawas, C., Aronson, M. and Wolfson, L. (1988) Clinico-pathologic studies in dementia: nondemented subjects with pathologically confirmed Alzheimer's disease. *Neurology*, **38**, 1682-1687.

Csortos, C., Zolnierowicz, S., Bako, E., Durbin, S.D. and DePaoli-Roach, A.A. (1996) High complexity in the expression of the B' subunit of protein phosphatase 2A0. Evidence for the existence of at least seven novel isoforms. *J Biol Chem*, **271**, 2578-2588.

Cummings, J.L., Vinters, H.V., Cole, G.M. and Khachaturian, Z.S. (1998) Alzheimer's disease: etiologies, pathophysiology, cognitive reserve, and treatment opportunities. *Neurology*, **51**, S2-17; discussion S65-17.

Davies, L., Wolska, B., Hilbich, C., Multhaup, G., Martins, R., Simms, G., Beyreuther, K. and Masters, C.L. (1988) A4 amyloid protein deposition and the diagnosis of Alzheimer's disease: prevalence in aged brains determined by immunocytochemistry compared with conventional neuropathologic techniques. *Neurology*, **38**, 1688-1693.

De Strooper, B. and Annaert, W. (2000) Proteolytic processing and cell biological functions of the amyloid precursor protein. *J Cell Sci*, **113 (Pt 11)**, 1857-1870.

Delacourte, A., Sergeant, N., Champain, D., Wattez, A., Maurage, C.A., Lebert, F., Pasquier, F. and David, J.P. (2002) Nonoverlapping but synergetic tau and APP pathologies in sporadic Alzheimer's disease. *Neurology*, **59**, 398-407.

Delacourte, A., Sergeant, N., Wattez, A., Gauvreau, D. and Robitaille, Y. (1998) Vulnerable neuronal subsets in Alzheimer's and Pick's disease are distinguished by their tau isoform distribution and phosphorylation. *Ann Neurol*, **43**, 193-204.

Denu, J.M., Stuckey, J.A., Saper, M.A. and Dixon, J.E. (1996) Form and function in protein dephosphorylation. *Cell*, **87**, 361-364.

Depaoli-Roach, A.A., Park, I.K., Cerovsky, V., Csortos, C., Durbin, S.D., Kuntz, M.J., Sitikov, A., Tang, P.M., Verin, A. and Zolnierowicz, S. (1994) Serine/threonine protein phosphatases in the control of cell function. Adv Enzyme Regul, **34**, 199-224.

DeTure, M., Ko, L.W., Yen, S., Nacharaju, P., Easson, C., Lewis, J., van Slegtenhorst, M., Hutton, M. and Yen, S.H. (2000) Missense tau mutations identified in FTDP-17 have a small effect on tau-microtubule interactions. *Brain Res*, **853**, 5-14.

Di Paolo, G., Antonsson, B., Kassel, D., Riederer, B.M. and Grenningloh, G. (1997) Phosphorylation regulates the microtubule-destabilizing activity of stathmin and its interaction with tubulin. *FEBS Lett*, **416**, 149-152.

Di Rosa, G., Odrijin, T., Nixon, R.A. and Arancio, O. (2002) Calpain inhibitors: a treatment for Alzheimer's disease. *J Mol Neurosci*, **19**, 135-141.

Dohler, K.D., Wong, C.C. and von zur Muhlen, A. (1979) The rat as model for the study of drug effects on thyroid function: consideration of methodological problems. *Pharmacol Ther [B]*, **5**, 305-318.

Durocher, D., Taylor, I.A., Sarbassova, D., Haire, L.F., Westcott, S.L., Jackson, S.P., Smerdon, S.J. and Yaffe, M.B. (2000) The molecular basis of FHA domain:phosphopeptide binding specificity and implications for phospho-dependent signaling mechanisms. *Mol Cell*, **6**, 1169-1182.

Dutt, M.K. (1980) Staining of depolymerised DNA in mammalian tissues with methyl violet 6B and crystal violet. *Folia Histochem Cytochem (Krakow)*, **18**, 79-83.

Egloff, M.P., Cohen, P.T., Reinemer, P. and Barford, D. (1995) Crystal structure of the catalytic subunit of human protein phosphatase 1 and its complex with tungstate. *J Mol Biol*, **254**, 942-959.

Elbashir, S.M., Harborth, J., Lendeckel, W., Yalcin, A., Weber, K. and Tuschl, T. (2001) Duplexes of 21-nucleotide RNAs mediate RNA interference in cultured mammalian cells. *Nature*, **411**, 494-498.

Elbashir, S.M., Lendeckel, W. and Tuschl, T. (2001) RNA interference is mediated by 21- and 22-nucleotide RNAs. *Genes Dev*, **15**, 188-200.

Encinas, M., Iglesias, M., Liu, Y., Wang, H., Muhaisen, A., Cena, V., Gallego, C. and Comella, J.X. (2000) Sequential treatment of SH-SY5Y cells with retinoic acid and brain-derived neurotrophic factor gives rise to fully differentiated, neurotrophic factor-dependent, human neuron-like cells. *J Neurochem*, **75**, 991-1003.

Eriksson, J.E., Brautigan, D.L., Vallee, R., Olmsted, J., Fujiki, H. and Goldman, R.D. (1992) Cytoskeletal integrity in interphase cells requires protein phosphatase activity. *Proc Natl Acad Sci U S A*, **89**, 11093-11097.

Esch, F.S., Keim, P.S., Beattie, E.C., Blacher, R.W., Culwell, A.R., Oltersdorf, T., McClure, D. and Ward, P.J. (1990) Cleavage of amyloid beta peptide during constitutive processing of its precursor. *Science*, **248**, 1122-1124.

Evans, D.A., Funkenstein, H.H., Albert, M.S., Scherr, P.A., Cook, N.R., Chown, M.J., Hebert, L.E., Hennekens, C.H. and Taylor, J.O. (1989) Prevalence of Alzheimer's disease in a community population of older persons. Higher than previously reported. *Jama*, **262**, 2551-2556.

Evans, D.R. and Hemmings, B.A. (2000) Mutation of the C-terminal leucine residue of PP2Ac inhibits PR55/B subunit binding and confers supersensitivity to microtubule destabilization in Saccharomyces cerevisiae. *Mol Gen Genet*, **264**, 425-432.

Evans, D.R., Myles, T., Hofsteenge, J. and Hemmings, B.A. (1999) Functional expression of human PP2Ac in yeast permits the identification of novel C-terminal and dominant-negative mutant forms. *J Biol Chem*, **274**, 24038-24046.

Everett, A.D., Kamibayashi, C. and Brautigan, D.L. (2002) Transgenic expression of protein phosphatase 2A regulatory subunit B56gamma disrupts distal lung differentiation. *Am J Physiol Lung Cell Mol Physiol*, **282**, L1266-1271.

Ewbank, D.C. (1999) Deaths attributable to Alzheimer's disease in the United States. *Am J Public Health*, **89**, 90-92.

Favre, B., Turowski, P. and Hemmings, B.A. (1997) Differential inhibition and posttranslational modification of protein phosphatase 1 and 2A in MCF7 cells treated with calyculin-A, okadaic acid, and tautomycin. *J Biol Chem*, **272**, 13856-13863.

Ferrari, A., Hoerndli, F., Baechi, T., Nitsch, R.M. and Gotz, J. (2003) beta-Amyloid induces paired helical filament-like tau filaments in tissue culture. *J Biol Chem*, **278**, 40162-40168.

Ferrer, I., Blanco, R., Carmona, M. and Puig, B. (2001) Phosphorylated mitogen-activated protein kinase (MAPK/ERK-P), protein kinase of 38 kDa (p38-P), stress-activated protein kinase (SAPK/JNK-P), and calcium/calmodulin-dependent kinase II (CaM kinase II) are differentially expressed in tau deposits in neurons and glial cells in tauopathies. *J Neural Transm*, **108**, 1397-1415.

Fischer, E.H. and Krebs, E.G. (1955) Conversion of phosphorylase b to phosphorylase a in muscle extracts. *J Biol Chem*, **216**, 121-132.

Foster, N.L., Wilhelmsen, K., Sima, A.A., Jones, M.Z., D'Amato, C.J. and Gilman, S. (1997) Frontotemporal dementia and parkinsonism linked to chromosome 17: a consensus conference. Conference Participants. *Ann Neurol*, **41**, 706-715.

Gavrieli, Y., Sherman, Y. and Ben-Sasson, S.A. (1992) Identification of programmed cell death in situ via specific labeling of nuclear DNA fragmentation. *J Cell Biol*, **119**, 493-501.

Geula, C. (1998) Abnormalities of neural circuitry in Alzheimer's disease: hippocampus and cortical cholinergic innervation. *Neurology*, **51**, S18-29; discussion S65-17.

Giannakopoulos, P., Herrmann, F.R., Bussiere, T., Bouras, C., Kovari, E., Perl, D.P., Morrison, J.H., Gold, G. and Hof, P.R. (2003) Tangle and neuron numbers, but not amyloid load, predict cognitive status in Alzheimer's disease. *Neurology*, **60**, 1495-1500.

Glenner, G.G. and Wong, C.W. (1984) Alzheimer's disease: initial report of the purification and characterization of a novel cerebrovascular amyloid protein. *Biochem Biophys Res Commun*, **120**, 885-890.

Goate, A., Chartier-Harlin, M.C., Mullan, M., Brown, J., Crawford, F., Fidani, L., Giuffra, L., Haynes, A., Irving, N. and James, L. (1991) Segregation of a missense mutation in the amyloid precursor protein gene with familial Alzheimer's disease. *Nature*, **349**, 704-706.

Goedert, M., Cohen, E.S., Jakes, R. and Cohen, P. (1992) p42 MAP kinase phosphorylation sites in microtubule-associated protein tau are dephosphorylated by protein phosphatase 2A1. Implications for Alzheimer's disease [corrected] [published erratum appears in FEBS Lett 1992 Nov 23;313(2):203]. *FEBS Lett*, **312**, 95-99.

Goedert, M., Crowther, R.A. and Spillantini, M.G. (1998) Tau mutations cause frontotemporal dementias. *Neuron*, **21**, 955-958.

Goedert, M., Jakes, R., Crowther, R.A., Cohen, P., Vanmechelen, E., Vandermeeren, M. and Cras, P. (1994) Epitope mapping of monoclonal antibodies to the paired helical filaments of Alzheimer's disease: identification of phosphorylation sites in tau protein. *Biochem J*, **301**, 871-877.

Goedert, M., Jakes, R., Qi, Z., Wang, J.H. and Cohen, P. (1995) Protein phosphatase 2A is the major enzyme in brain that dephosphorylates tau protein phosphorylated by proline-directed protein kinases or cyclic AMP-dependent protein kinase. *J Neurochem*, **65**, 2804-2807.

Goedert, M., Jakes, R., Spillantini, M.G., Crowther, R.A., Cohen, P., Vanmechelen, E., Probst, A., Gotz, J. and Burki, K. (1995) Tau protein in Alzheimer's disease. *Biochem Soc Trans*, **23**, 80-85.

Goedert, M., Satumtira, S., Jakes, R., Smith, M.J., Kamibayashi, C., White, C.L., 3rd and Sontag, E. (2000) Reduced binding of protein phosphatase 2A to tau protein with frontotemporal dementia and parkinsonism linked to chromosome 17 mutations. *J Neurochem*, **75**, 2155-2162.

Goedert, M., Spillantini, M.G., Jakes, R., Crowther, R.A., Vanmechelen, E., Probst, A., Gotz, J., Burki, K. and Cohen, P. (1995) Molecular dissection of the paired helical filament. *Neurobiol Aging*, **16**, 325-334.

Goldberg, Y. (1999) Protein phosphatase 2A: who shall regulate the regulator? *Biochem Pharmacol*, **57**, 321-328.

Gomez-Isla, T., Hollister, R., West, H., Mui, S., Growdon, J.H., Petersen, R.C., Parisi, J.E. and Hyman, B.T. (1997) Neuronal loss correlates with but exceeds neurofibrillary tangles in Alzheimer's disease. *Ann Neurol*, **41**, 17-24.

Gomez, N. and Cohen, P. (1991) Dissection of the protein kinase cascade by which nerve growth factor activates MAP kinases. *Nature*, **353**, 170-173.

Gomez-Ramos, A., Diaz-Nido, J., Smith, M.A., Perry, G. and Avila, J. (2003) Effect of the lipid peroxidation product acrolein on tau phosphorylation in neural cells. *J Neurosci Res*, **71**, 863-870.

Gong, C.X., Grundke-Iqbal, I. and Iqbal, K. (1994) Dephosphorylation of Alzheimer's disease abnormally phosphorylated tau by protein phosphatase-2A. *Neuroscience*, **61**, 765-772.

Gong, C.X., Lidsky, T., Wegiel, J., Grundke-Iqbal, I. and Iqbal, K. (2001) Metabolically active rat brain slices as a model to study the regulation of protein phosphorylation in mammalian brain. *Brain Res Brain Res Protoc*, **6**, 134-140.

Gong, C.X., Lidsky, T., Wegiel, J., Zuck, L., Grundke-Iqbal, I. and Iqbal, K. (2000) Phosphorylation of microtubule-associated protein tau is regulated by protein phosphatase 2A in mammalian brain. Implications for neurofibrillary degeneration in Alzheimer's disease. *J Biol Chem*, **275**, 5535-5544.

Gong, C.X., Shaikh, S., Wang, J.Z., Zaidi, T., Grundke-Iqbal, I. and Iqbal, K. (1995) Phosphatase activity toward abnormally phosphorylated tau: decrease in Alzheimer disease brain. *J Neurochem*, **65**, 732-738.

Gong, C.X., Singh, T.J., Grundke-Iqbal, I. and Iqbal, K. (1993) Phosphoprotein phosphatase activities in Alzheimer disease brain. *J Neurochem*, **61**, 921-927.

Gong, C.X., Wegiel, J., Lidsky, T., Zuck, L., Avila, J., Wisniewski, H.M., Grundke-Iqbal, I. and Iqbal, K. (2000) Regulation of phosphorylation of neuronal microtubule-associated proteins MAP1b and MAP2 by protein phosphatase-2A and -2B in rat brain. *Brain Res*, **853**, 299-309.

Gotz, J. (2001) Tau and transgenic animal models. *Brain Res Brain Res Rev*, **35**, 266-286.

Gotz, J., Barmettler, R., Ferrari, A., Goedert, M., Probst, A. and Nitsch, R.M. (2000) In vivo analysis of wild-type and FTDP-17 tau transgenic mice. *Ann N Y Acad Sci*, **920**, 126-133.

Gotz, J., Chen, F., Barmettler, R. and Nitsch, R.M. (2001) Tau Filament Formation in Transgenic Mice Expressing P301L Tau. *J Biol Chem*, **276**, 529-534.

Gotz, J., Chen, F., van Dorpe, J. and Nitsch, R.M. (2001) Formation of neurofibrillary tangles in P301L tau transgenic mice induced by Abeta 42 fibrils. *Science*, **293**, 1491-1495.

Gotz, J. and Kues, W. (1999) The role of protein phosphatase 2A catalytic subunit Calpha in embryogenesis: evidence from sequence analysis and localization studies. *Biol Chem*, **380**, 1117-1120.

Gotz, J., Probst, A., Ehler, E., Hemmings, B. and Kues, W. (1998) Delayed embryonic lethality in mice lacking protein phosphatase 2A catalytic subunit Calpha. *Proc Natl Acad Sci U S A*, **95**, 12370-12375.

Gotz, J., Probst, A., Mistl, C., Nitsch, R.M. and Ehler, E. (2000) Distinct role of protein phosphatase 2A subunit calpha in the regulation of E-cadherin and beta-catenin during development. *Mech Dev*, **93**, 83-93.

Gotz, J., Probst, A., Spillantini, M.G., Schafer, T., Jakes, R., Burki, K. and Goedert, M. (1995) Somatodendritic localization and hyperphosphorylation of tau protein in transgenic mice expressing the longest human brain tau isoform. *Embo J*, **14**, 1304-1313.

Gotz, J. and Schild, A. (2003) Transgenic and knockout models of PP2A. *Methods Enzymol*, **366**, 390-403.

Gotz, J., Schild, A., Hoerndli, F. and Pennanen, L. (2004) Amyloid-induced neurofibrillary tangle formation in Alzheimer's disease: insight from transgenic mouse and tissue-culture models. *Int J Dev Neurosci*, **22**, 453-465.

Gotz, J., Streffer, J.R., David, D., Schild, A., Hoerndli, F., Pennanen, L., Kurosinski, P. and Chen, F. (2004) Transgenic animal models of Alzheimer's disease and related disorders: histopathology, behavior and therapy. *Mol Psychiatry*, **9**, 664-683.

Goux, W.J., Rodriguez, S. and Sparkman, D.R. (1995) Analysis of the core components of Alzheimer paired helical filaments. A gas chromatography/mass spectrometry characterization of fatty acids, carbohydrates and long-chain bases. *FEBS Lett*, **366**, 81-85.

Govindarajan, V., Ito, M., Makarenkova, H.P., Lang, R.A. and Overbeek, P.A. (2000) Endogenous and ectopic gland induction by FGF-10. *Dev Biol*, **225**, 188-200.

Gray, L.E., Jr. and Kavlock, R.J. (1983) The effects of the herbicide 2,4-dichlorophenyl-p-nitrophenyl ether (NIT) on serum thyroid hormones in adult female mice. *Toxicol Lett*, **15**, 231-235.

Gray, L.E., Jr., Kavlock, R.J., Chernoff, N., Ferrell, J., McLamb, J. and Ostby, J. (1982) Prenatal exposure to the herbicide 2,4-dichlorophenyl-p-nitrophenyl ether destroys the rodent Harderian gland. *Science*, **215**, 293-294.

Griswold-Prenner, I., Kamibayashi, C., Maruoka, E.M., Mumby, M.C. and Derynck, R. (1998) Physical and functional interactions between type I transforming growth factor beta receptors and Balpha, a WD-40 repeat subunit of phosphatase 2A. *Mol Cell Biol*, **18**, 6595-6604.

Grover, A., Houlden, H., Baker, M., Adamson, J., Lewis, J., Prihar, G., Pickering-Brown, S., Duff, K. and Hutton, M. (1999) 5' splice site mutations in tau associated with the inherited dementia FTDP-17 affect a stem-loop structure that regulates alternative splicing of exon 10. *J Biol Chem*, **274**, 15134-15143.

Groves, M.R., Hanlon, N., Turowski, P., Hemmings, B.A. and Barford, D. (1999) The structure of the protein phosphatase 2A PR65/A subunit reveals the conformation of its 15 tandemly repeated HEAT motifs. *Cell*, **96**, 99-110.

Grundke-Iqbal, I., Iqbal, K., Quinlan, M., Tung, Y.C., Zaidi, M.S. and Wisniewski, H.M. (1986) Microtubule-associated protein tau. A component of Alzheimer paired helical filaments. *J Biol Chem*, **261**, 6084-6089.

Grundke-Iqbal, I., Iqbal, K., Tung, Y.C., Quinlan, M., Wisniewski, H.M. and Binder, L.I. (1986) Abnormal phosphorylation of the microtubule-associated protein tau (tau) in Alzheimer cytoskeletal pathology. *Proc Natl Acad Sci U S A*, **83**, 4913-4917.

Guan, K.L. and Butch, E. (1995) Isolation and characterization of a novel dual specific phosphatase, HVH2, which selectively dephosphorylates the mitogen-activated protein kinase. *J Biol Chem*, **270**, 7197-7203.

Haass, C., Hung, A.Y. and Selkoe, D.J. (1991) Processing of beta-amyloid precursor protein in microglia and astrocytes favors an internal localization over constitutive secretion. *J Neurosci*, **11**, 3783-3793.

Haass, C., Schlossmacher, M.G., Hung, A.Y., Vigo-Pelfrey, C., Mellon, A., Ostaszewski, B.L., Lieberburg, I., Koo, E.H., Schenk, D. and Teplow, D.B. (1992) Amyloid beta-peptide is produced by cultured cells during normal metabolism. *Nature*, **359**, 322-325.

Hammond, S.M., Caudy, A.A. and Hannon, G.J. (2001) Post-transcriptional gene silencing by double-stranded RNA. *Nat Rev Genet*, **2**, 110-119.

Hardy, J.A. and Higgins, G.A. (1992) Alzheimer's disease: the amyloid cascade hypothesis. *Science*, **256**, 184-185.

Hartzler, A.W., Zhu, X., Siedlak, S.L., Castellani, R.J., Avila, J., Perry, G. and Smith, M.A. (2002) The p38 pathway is activated in Pick disease and progressive supranuclear palsy: a mechanistic link between mitogenic pathways, oxidative stress, and tau. *Neurobiol Aging*, **23**, 855-859.

Hasegawa, M., Smith, M.J. and Goedert, M. (1998) Tau proteins with FTDP-17 mutations have a reduced ability to promote microtubule assembly. *FEBS Lett*, **437**, 207-210.

He, J., Yamada, K., Zou, L.B. and Nabeshima, T. (2001) Spatial memory deficit and neurodegeneration induced by the direct injection of okadaic acid into the hippocampus in rats. *J Neural Transm*, **108**, 1435-1443.

Helling, R.B., Goodman, H.M. and Boyer, H.W. (1974) Analysis of endonuclease R-EcoRI fragments of DNA from lambdoid bacteriophages and other viruses by agarose-gel electrophoresis. *J Virol*, **14**, 1235-1244.

Hemmings, B.A., Adams-Pearson, C., Maurer, F., Muller, P., Goris, J., Merlevede, W., Hofsteenge, J. and Stone, S.R. (1990) alpha- and beta-forms of the 65-kDa subunit of protein phosphatase 2A have a similar 39 amino acid repeating structure. *Biochemistry*, **29**, 3166-3173.

Hendrix, P., Mayer-Jackel, R.E., Cron, P., Goris, J., Hofsteenge, J., Merlevede, W. and Hemmings, B.A. (1993) Structure and expression of a 72-kDa regulatory subunit of protein phosphatase 2A. Evidence for different size forms produced by alternative splicing. *J Biol Chem*, **268**, 15267-15276.

Hensley, K., Floyd, R.A., Zheng, N.Y., Nael, R., Robinson, K.A., Nguyen, X., Pye, Q.N., Stewart, C.A., Geddes, J., Markesbery, W.R., Patel, E., Johnson, G.V. and Bing, G. (1999) p38 kinase is activated in the Alzheimer's disease brain. *J Neurochem*, **72**, 2053-2058.

Higuchi, M., Ishihara, T., Zhang, B., Hong, M., Andreadis, A., Trojanowski, J. and Lee, V.M. (2002) Transgenic mouse model of tauopathies with glial pathology and nervous system degeneration. *Neuron*, **35**, 433-446.

Hilbich, C., Kisters-Woike, B., Reed, J., Masters, C.L. and Beyreuther, K. (1991) Aggregation and secondary structure of synthetic amyloid beta A4 peptides of Alzheimer's disease. *J Mol Biol*, **218**, 149-163.

Hirano, A., Nakano, I., Kurland, L.T., Mulder, D.W., Holley, P.W. and Saccomanno, G. (1984) Fine structural study of neurofibrillary changes in a family with amyotrophic lateral sclerosis. *J Neuropathol Exp Neurol*, **43**, 471-480.

Hirsch, D.D. and Stork, P.J. (1997) Mitogen-activated protein kinase phosphatases inactivate stress-activated protein kinase pathways in vivo. *J Biol Chem*, **272**, 4568-4575.

Hoerndli, F.J., Toigo, M., Schild, A., Gotz, J. and Day, P.J. (2004) Reference genes identified in SH-SY5Y cells using custom-made gene arrays with validation by quantitative polymerase chain reaction. *Anal Biochem*, **335**, 30-41.

Hoffman, R.A. (1971) Influence of some endocrine glands, hormones and blinding on the histology and porphyrins of the Harderian glands of golden hamsters. *Am J Anat*, **132**, 463-478.

Hoffmann, R., Lee, V.M., Leight, S., Varga, I. and Otvos, L., Jr. (1997) Unique Alzheimer's disease paired helical filament specific epitopes involve double phosphorylation at specific sites. *Biochemistry*, **36**, 8114-8124.

Holcomb, L.A., Gordon, M.N., Jantzen, P., Hsiao, K., Duff, K. and Morgan, D. (1999) Behavioral changes in transgenic mice expressing both amyloid precursor protein and presenilin-1 mutations: lack of association with amyloid deposits. *Behav Genet*, **29**, 177-185.

Holmes, S.E., O'Hearn, E.E., McInnis, M.G., Gorelick-Feldman, D.A., Kleiderlein, J.J., Callahan, C., Kwak, N.G., Ingersoll-Ashworth, R.G., Sherr, M., Sumner, A.J., Sharp, A.H., Ananth, U., Seltzer, W.K., Boss, M.A., Vieria-Saecker, A.M., Epplen, J.T., Riess, O., Ross, C.A. and Margolis, R.L. (1999) Expansion of a novel CAG trinucleotide repeat in the 5' region of PPP2R2B is associated with SCA12. *Nat Genet*, **23**, 391-392.

Holness, M.J., Langdown, M.L. and Sugden, M.C. (2000) Early-life programming of susceptibility to dysregulation of glucose metabolism and the development of Type 2 diabetes mellitus. *Biochem J*, **349 Pt 3**, 657-665.

Hong, M., Chen, D.C., Klein, P.S. and Lee, V.M. (1997) Lithium reduces tau phosphorylation by inhibition of glycogen synthase kinase-3. *J Biol Chem*, **272**, 25326-25332.

Hoyer, S. (2002) The brain insulin signal transduction system and sporadic (type II) Alzheimer disease: an update. *J Neural Transm*, **109**, 341-360.

Hsiao, K., Chapman, P., Nilsen, S., Eckman, C., Harigaya, Y., Younkin, S., Yang, F. and Cole, G. (1996) Correlative memory deficits, Abeta elevation, and amyloid plaques in transgenic mice [see comments]. *Science*, **274**, 99-102.

Irizarry, M.C., Deng, A., Lleo, A., Berezovska, O., Von Arnim, C.A., Martin-Rehrmann, M., Manelli, A., LaDu, M.J., Hyman, B.T. and Rebeck, G.W. (2004) Apolipoprotein E modulates gamma-secretase cleavage of the amyloid precursor protein. *J Neurochem*, **90**, 1132-1143.

Ishihara, T., Hong, M., Zhang, B., Nakagawa, Y., Lee, M.K., Trojanowski, J.Q. and Lee, V.M. (1999) Age-dependent emergence and progression of a tauopathy in transgenic mice overexpressing the shortest human tau isoform. *Neuron*, **24**, 751-762.

Ishihara, T., Zhang, B., Higuchi, M., Yoshiyama, Y., Trojanowski, J.Q. and Lee, V.M. (2001) Age-Dependent Induction of Congophilic Neurofibrillary Tau Inclusions in Tau Transgenic Mice. *Am J Pathol*, **158**, 555-562.

Itagaki, S., McGeer, P.L., Akiyama, H., Zhu, S. and Selkoe, D. (1989) Relationship of microglia and astrocytes to amyloid deposits of Alzheimer disease. *J Neuroimmunol*, **24**, 173-182.

Jans, D.A. (1995) The regulation of protein transport to the nucleus by phosphorylation. *Biochem J*, **311 (Pt 3)**, 705-716.

Janssens, V. and Goris, J. (2001) Protein phosphatase 2A: a highly regulated family of serine/threonine phosphatases implicated in cell growth and signalling. *Biochem J*, **353**, 417-439.

Jarrett, J.T. and Lansbury, P.T., Jr. (1993) Seeding "one-dimensional crystallization" of amyloid: a pathogenic mechanism in Alzheimer's disease and scrapie? *Cell*, **73**, 1055-1058.

Jensen, M., Basun, H. and Lannfelt, L. (1995) Increased cerebrospinal fluid tau in patients with Alzheimer's disease. *Neurosci Lett*, **186**, 189-191.

Jhappan, C., Gallahan, D., Stahle, C., Chu, E., Smith, G.H., Merlino, G. and Callahan, R. (1992) Expression of an activated Notch-related int-3 transgene interferes with cell differentiation and induces neoplastic transformation in mammary and salivary glands. *Genes Dev*, **6**, 345-355.

Jiang, C.H., Tsien, J.Z., Schultz, P.G. and Hu, Y. (2001) The effects of aging on gene expression in the hypothalamus and cortex of mice. *Proc Natl Acad Sci U S A*, **98**, 1930-1934.Kamibayashi, C., Lickteig, R.L., Estes, R., Walter, G. and Mumby, M.C. (1992) Expression of the A subunit of protein phosphatase 2A and characterization of its interactions with the catalytic and regulatory subunits. *J Biol Chem*, **267**, 21864-21872.

Kang, D.E., Pietrzik, C.U., Baum, L., Chevallier, N., Merriam, D.E., Kounnas, M.Z., Wagner, S.L., Troncoso, J.C., Kawas, C.H., Katzman, R. and Koo, E.H. (2000) Modulation of amyloid beta-protein clearance and Alzheimer's disease susceptibility by the LDL receptor-related protein pathway. *J Clin Invest*, **106**, 1159-1166.

Kang, J., Lemaire, H.G., Unterbeck, A., Salbaum, J.M., Masters, C.L., Grzeschik, K.H., Multhaup, G., Beyreuther, K. and Muller-Hill, B. (1987) The precursor of Alzheimer's disease amyloid A4 protein resembles a cell-surface receptor. *Nature*, **325**, 733-736.

Kann, M., Sodeik, B., Vlachou, A., Gerlich, W.H. and Helenius, A. (1999) Phosphorylation-dependent binding of hepatitis B virus core particles to the nuclear pore complex. *J Cell Biol*, **145**, 45-55.

Ketting, R.F., Fischer, S.E., Bernstein, E., Sijen, T., Hannon, G.J. and Plasterk, R.H. (2001) Dicer functions in RNA interference and in synthesis of small RNA involved in developmental timing in C. elegans. *Genes Dev*, **15**, 2654-2659.

Khew-Goodall, Y. and Hemmings, B.A. (1988) Tissue-specific expression of mRNAs encoding alpha- and beta-catalytic subunits of protein phosphatase 2A. *FEBS Lett*, **238**, 265-268.

Kienlen-Campard, P., Miolet, S., Tasiaux, B. and Octave, J.N. (2002) Intracellular amyloid-beta 1-42, but not extracellular soluble amyloid-beta peptides, induces neuronal apoptosis. *J Biol Chem*, **277**, 15666-15670.

Kim, D., Su, J. and Cotman, C.W. (1999) Sequence of neurodegeneration and accumulation of phosphorylated tau in cultured neurons after okadaic acid treatment. *Brain Res*, **839**, 253-262.
Kimberly, W.T., Zheng, J.B., Guenette, S.Y. and Selkoe, D.J. (2001) The intracellular domain of the beta-amyloid precursor protein is stabilized by Fe65 and translocates to the nucleus in a notch-like manner. *J Biol Chem*, **276**, 40288-40292.
Kinoshita, N., Ohkura, H. and Yanagida, M. (1990) Distinct, essential roles of type 1 and 2A protein phosphatases in the control of the fission yeast cell division cycle. *Cell*, **63**, 405-415.
Kins, S., Crameri, A., Evans, D.R., Hemmings, B.A., Nitsch, R.M. and Gotz, J. (2001) Reduced PP2A activity induces hyperphosphorylation and altered compartmentalization of tau in transgenic mice. *J Biol Chem*, **276**, 38193-38200.
Kins, S., Kurosinski, P., Nitsch, R.M. and Gotz, J. (2003) Activation of the ERK and JNK signaling pathways caused by neuron specific inhibition of PP2A in transgenic mice. *Am J Pathol*, **163**, 833-843.
Kloeker, S. and Wadzinski, B.E. (1999) Purification and identification of a novel subunit of protein serine/threonine phosphatase 4. *J Biol Chem*, **274**, 5339-5347.
Ko, L.W., Ko, E.C., Nacharaju, P., Liu, W.K., Chang, E., Kenessey, A. and Yen, S.H. (1999) An immunochemical study on tau glycation in paired helical filaments. *Brain Res*, **830**, 301-313.
Kobayashi, N., Reiser, J., Schwarz, K., Sakai, T., Kriz, W. and Mundel, P. (2001) Process formation of podocytes: morphogenetic activity of microtubules and regulation by protein serine/threonine phosphatase PP2A. *Histochem Cell Biol*, **115**, 255-266.
Kollias, G., Spanopoulou, E., Grosveld, F., Ritter, M., Beech, J. and Morris, R. (1987) Differential regulation of a Thy-1 gene in transgenic mice. *Proc Natl Acad Sci U S A*, **84**, 1492-1496.
Kopke, E., Tung, Y.C., Shaikh, S., Alonso, A.C., Iqbal, K. and Grundke-Iqbal, I. (1993) Microtubule-associated protein tau. Abnormal phosphorylation of a non-paired helical filament pool in Alzheimer disease. *J Biol Chem*, **268**, 24374-24384.
Kremmer, E., Ohst, K., Kiefer, J., Brewis, N. and Walter, G. (1997) Separation of PP2A core enzyme and holoenzyme with monoclonal antibodies against the regulatory A subunit: abundant expression of both forms in cells. *Mol Cell Biol*, **17**, 1692-1701.
Kumegawa, M., Takuma, T. and Takagi, Y. (1977) Precocious induction of secretory granules by hormones in convoluted tubules of mouse submandibular glands. *Am J Anat*, **149**, 111-114.
Ladenson, P.W. (1996) Diagnosis of thyrotoxicosis. In: Braverman LE, Utiger RD, eds. Werner and Ingbar's the thyroid. 7th ed. Philadelphia: Lippincott-Raven. 708 -711.
Laemmli, U.K. (1970) Cleavage of structural proteins during the assembly of the head of bacteriophage T4. *Nature*, **227**, 680-685.
Laird, P.W., Zijderveld, A., Linders, K., Rudnicki, M.A., Jaenisch, R. and Berns, A. (1991) Simplified mammalian DNA isolation procedure. *Nucleic Acids Res*, **19**, 4293.
Lamb, B.T., Sisodia, S.S., Lawler, A.M., Slunt, H.H., Kitt, C.A., Kearns, W.G., Pearson, P.L., Price, D.L. and Gearhart, J.D. (1993) Introduction and expression of the 400 kilobase amyloid precursor protein gene in transgenic mice [corrected]. *Nat Genet*, **5**, 22-30.
Lashuel, H.A., Hartley, D., Petre, B.M., Walz, T. and Lansbury, P.T., Jr. (2002) Neurodegenerative disease: amyloid pores from pathogenic mutations. *Nature*, **418**, 291.
Lau, K.F., Miller, C.C., Anderton, B.H. and Shaw, P.C. (1999) Molecular cloning and characterization of the human glycogen synthase kinase-3beta promoter. *Genomics*, **60**, 121-128.
Lazzereschi, D., Coppa, A., Minicione, G., Lavitrano, M., Fragomele, F. and Colletta, G. (1997) The phosphatase inhibitor okadaic acid stimulates the TSH-induced G1-S phase transition in thyroid cells. *Exp Cell Res*, **234**, 425-433.
LeDoux, J.E. (2000) Emotion circuits in the brain. *Annu Rev Neurosci*, **23**, 155-184.
Lee, J., Hong, H., Im, J., Byun, H. and Kim, D. (2000) The formation of PHF-1 and SMI-31 positive dystrophic neurites in rat hippocampus following acute injection of okadaic acid. *Neurosci Lett*, **282**, 49-52.
Lewis, J., Dickson, D.W., Lin, W.L., Chisholm, L., Corral, A., Jones, G., Yen, S.H., Sahara, N., Skipper, L., Yager, D., Eckman, C., Hardy, J., Hutton, M. and McGowan, E. (2001) Enhanced neurofibrillary degeneration in transgenic mice expressing mutant tau and APP. *Science*, **293**, 1487-1491.
Li, X., Scuderi, A., Letsou, A. and Virshup, D.M. (2002) B56-associated protein phosphatase 2A is required for survival and protects from apoptosis in Drosophila melanogaster. *Mol Cell Biol*, **22**, 3674-3684.
Liao, H., Li, Y., Brautigan, D.L. and Gundersen, G.G. (1998) Protein phosphatase 1 is targeted to microtubules by the microtubule-associated protein Tau. *J Biol Chem*, **273**, 21901-21908.
Lickert, H., Bauer, A., Kemler, R. and Stappert, J. (2000) Casein kinase II phosphorylation of E-cadherin increases E-cadherin/beta-catenin interaction and strengthens cell-cell adhesion. *J Biol Chem*, **275**, 5090-5095.
Lin, X.H., Walter, J., Scheidtmann, K., Ohst, K., Newport, J. and Walter, G. (1998) Protein phosphatase 2A is required for the initiation of chromosomal DNA replication. *Proc Natl Acad Sci U S A*, **95**, 14693-14698.
Lobo, A., Launer, L.J., Fratiglioni, L., Andersen, K., Di Carlo, A., Breteler, M.M., Copeland, J.R., Dartigues, J.F., Jagger, C., Martinez-Lage, J., Soininen, H. and Hofman, A. (2000) Prevalence of dementia and major subtypes in Europe: A collaborative study of population-based cohorts. Neurologic Diseases in the Elderly Research Group. *Neurology*, **54**, S4-9.
Longin, S., Jordens, J., Martens, E., Stevens, I., Janssens, V., Rondelez, E., De Baere, I., Derua, R., Waelkens, E., Goris, J. and Van Hoof, C. (2004) An inactive protein phosphatase 2A population is associated with methylesterase and can be re-activated by the phosphotyrosyl phosphatase activator. Biochem J, **380**, 111-119.

LoPresti, J.S. and Singer, P.A. (1997) Physiology of thyroid hormone synthesis, secretion, and transport. In: Falk SA, ed. Thyroid disease: endocrinology, surgery, nuclear medicine, and radiotherapy. *2nd ed. Philadelphia: Lippincott-Raven*, 29 -40.

Loring, J.F., Wen, X., Lee, J.M., Seilhamer, J. and Somogyi, R. (2001) A gene expression profile of Alzheimer's disease. *DNA Cell Biol*, **20**, 683-695.

Lovell, M.A., Xie, C. and Markesbery, W.R. (2001) Acrolein is increased in Alzheimer's disease brain and is toxic to primary hippocampal cultures. *Neurobiol Aging*, **22**, 187-194.

Lowry, O.H., Rosebrough, N.J., Farr, A.L. and Randall, R.J. (1951) Protein measurement with the Folin phenol reagent. *J Biol Chem*, **193**, 265-275.

Lu, P.J., Wulf, G., Zhou, X.Z., Davies, P. and Lu, K.P. (1999) The prolyl isomerase Pin1 restores the function of Alzheimer-associated phosphorylated tau protein. *Nature*, **399**, 784-788.

Luthi, A., Putten, H., Botteri, F.M., Mansuy, I.M., Meins, M., Frey, U., Sansig, G., Portet, C., Schmutz, M., Schroder, M., Nitsch, C., Laurent, J.P. and Monard, D. (1997) Endogenous serine protease inhibitor modulates epileptic activity and hippocampal long-term potentiation. *J Neurosci*, **17**, 4688-4699.

MacKintosh, R.W., Haycox, G., Hardie, D.G. and Cohen, P.T. (1990) Identification by molecular cloning of two cDNA sequences from the plant Brassica napus which are very similar to mammalian protein phosphatases-1 and -2A. *FEBS Lett*, **276**, 156-160.

Malchiodi-Albedi, F., Petrucci, T.C., Picconi, B., Iosi, F. and Falchi, M. (1997) Protein phosphatase inhibitors induce modification of synapse structure and tau hyperphosphorylation in cultured rat hippocampal neurons. *J Neurosci Res*, **48**, 425-438.

Martens, E., Stevens, S., Janssens, J., Gotz, J., Goris, J. and van Hoof, C. (2004) Genomic organisation, chromosomal localisation, tissue distribution and developmental regulation of the PR61/B' regulatory subunits of protein phosphatase 2A in mice. *J Mol Biol*, **336**, 971-986.

Masters, C.L., Simms, G., Weinman, N.A., Multhaup, G., McDonald, B.L. and Beyreuther, K. (1985) Amyloid plaque core protein in Alzheimer disease and Down syndrome. *Proc Natl Acad Sci U S A*, **82**, 4245-4249.

Mattson, M.P., Fu, W., Waeg, G. and Uchida, K. (1997) 4-Hydroxynonenal, a product of lipid peroxidation, inhibits dephosphorylation of the microtubule-associated protein tau. *Neuroreport*, **8**, 2275-2281.

Mayer-Jaekel, R.E. and Hemmings, B.A. (1994) Protein phosphatase 2A--a 'menage a trois'. *Trends Cell Biol*, **4**, 287-291.

Mayer, R.E., Hendrix, P., Cron, P., Matthies, R., Stone, S.R., Goris, J., Merlevede, W., Hofsteenge, J. and Hemmings, B.A. (1991) Structure of the 55-kDa regulatory subunit of protein phosphatase 2A: evidence for a neuronal-specific isoform. *Biochemistry*, **30**, 3589-3597.

McClellan, K.A., Robertson, F.G., Kindblom, J., Wennbo, H., Tornell, J., Bouchard, B., Kelly, P.A. and Ormandy, C.J. (2001) Investigation of the role of prolactin in the development and function of the lacrimal and harderian glands using genetically modified mice. *Invest Ophthalmol Vis Sci*, **42**, 23-30.

McCright, B., Rivers, A.M., Audlin, S. and Virshup, D.M. (1996) The B56 family of protein phosphatase 2A (PP2A) regulatory subunits encodes differentiation-induced phosphoproteins that target PP2A to both nucleus and cytoplasm. *J Biol Chem*, **271**, 22081-22089.

McCright, B. and Virshup, D.M. (1995) Identification of a new family of protein phosphatase 2A regulatory subunits. *J Biol Chem*, **270**, 26123-26128.

Meek, S., Morrice, N. and MacKintosh, C. (1999) Microcystin affinity purification of plant protein phosphatases: PP1C, PP5 and a regulatory A-subunit of PP2A. *FEBS Lett*, **457**, 494-498.

Mehta, P.D., Pirttila, T. and Wisniewski, H.M. (1996) Biological test to confirm the diagnosis of Alzheimer's disease in the cognitively impaired patients. A fact or fiction? In V, K. and C, E. (eds.), *Advances in the Diagnosis and Treatment of Alzheimer's Disease*. Springer Publishing Company New York.

Merrick, S.E., Trojanowski, J.Q. and Lee, V.M. (1997) Selective destruction of stable microtubules and axons by inhibitors of protein serine/threonine phosphatases in cultured human neurons. *J Neurosci*, **17**, 5726-5737.

Millward, T.A., Zolnierowicz, S. and Hemmings, B.A. (1999) Regulation of protein kinase cascades by protein phosphatase 2A. *Trends Biochem Sci*, **24**, 186-191.

Minichiello, L., Korte, M., Wolfer, D., Kuhn, R., Unsicker, K., Cestari, V., Rossi-Arnaud, C., Lipp, H.P., Bonhoeffer, T. and Klein, R. (1999) Essential role for TrkB receptors in hippocampus-mediated learning. *Neuron*, **24**, 401-414.

Moechars, D., Dewachter, I., Lorent, K., Reverse, D., Baekelandt, V., Naidu, A., Tesseur, I., Spittaels, K., Haute, C.V., Checler, F., Godaux, E., Cordell, B. and Van Leuven, F. (1999) Early phenotypic changes in transgenic mice that overexpress different mutants of amyloid precursor protein in brain. *J Biol Chem*, **274**, 6483-6492.

Moreno, C.S., Park, S., Nelson, K., Ashby, D., Hubalek, F., Lane, W.S. and Pallas, D.C. (2000) WD40 repeat proteins striatin and S/G(2) nuclear autoantigen are members of a novel family of calmodulin-binding proteins that associate with protein phosphatase 2A. *J Biol Chem*, **275**, 5257-5263.

Mori, H., Hosoda, K., Matsubara, E., Nakamoto, T., Furiya, Y., Endoh, R., Usami, M., Shoji, M., Maruyama, S. and Hirai, S. (1995) Tau in cerebrospinal fluids: establishment of the sandwich ELISA with antibody specific to the repeat sequence in tau. *Neurosci Lett*, **186**, 181-183.

Mori, H., Kondo, J. and Ihara, Y. (1987) Ubiquitin is a component of paired helical filaments in Alzheimer's disease. *Science*, **235**, 1641-1644.

Morris, R. (1984) Developments of a water-maze procedure for studying spatial learning in the rat. *J Neurosci Methods*, **11**, 47-60.

Morrison, J.H. and Hof, P.R. (1997) Life and death of neurons in the aging brain. *Science*, **278**, 412-419.

Mudher, A.K., Woolley, S.T., Perry, V.H. and Greene, J.R. (1999) Induction of hyperphosphorylated tau in living slices of rat hippocampal formation and subsequent detection using an ELISA. *J Neurosci Methods*, **88**, 15-25.

Mulkey, R.M., Endo, S., Shenolikar, S. and Malenka, R.C. (1994) Involvement of a calcineurin/inhibitor-1 phosphatase cascade in hippocampal long-term depression. *Nature*, **369**, 486-488.

Mulkey, R.M., Herron, C.E. and Malenka, R.C. (1993) An essential role for protein phosphatases in hippocampal long-term depression. *Science*, **261**, 1051-1055.

Mullan, M., Crawford, F., Axelman, K., Houlden, H., Lilius, L., Winblad, B. and Lannfelt, L. (1992) A pathogenic mutation for probable Alzheimer's disease in the APP gene at the N-terminus of beta-amyloid. *Nat Genet*, **1**, 345-347.

Mullis. (1986) *Specific enzymatic amplification of DNA in vitro: the polymerase chain reaction*.

Munoz, D.G., Greene, C., Perl, D.P. and Selkoe, D.J. (1988) Accumulation of phosphorylated neurofilaments in anterior horn motoneurons of amyotrophic lateral sclerosis patients. *J Neuropathol Exp Neurol*, **47**, 9-18.

Nagy, Z., Jobst, K.A., Esiri, M.M., Morris, J.H., King, E.M., MacDonald, B., Litchfield, S., Barnetson, L. and Smith, A.D. (1996) Hippocampal pathology reflects memory deficit and brain imaging measurements in Alzheimer's disease: clinicopathologic correlations using three sets of pathologic diagnostic criteria. *Dementia*, **7**, 76-81.

Namboodiripad, A.N. and Jennings, M.L. (1996) Permeability characteristics of erythrocyte membrane to okadaic acid and calyculin A. *Am J Physiol*, **270**, C449-456.

Neer, E.J., Schmidt, C.J., Nambudripad, R. and Smith, T.F. (1994) The ancient regulatory-protein family of WD-repeat proteins. *Nature*, **371**, 297-300.

Nishito, Y., Usui, H., Shinzawa-Itoh, K., Inoue, R., Tanabe, O., Nagase, T., Murakami, T. and Takeda, M. (1999) Direct metal analyses of Mn2+-dependent and -independent protein phosphatase 2A from human erythrocytes detect zinc and iron only in the Mn2+-independent one. *FEBS Lett*, **447**, 29-33.

Nishito, Y., Usui, H., Tanabe, O., Shimizu, M. and Takeda, M. (1999) Interconversion of Mn(2+)-dependent and -independent protein phosphatase 2A from human erythrocytes: role of Zn(2+) and Fe(2+) in protein phosphatase 2A. *J Biochem (Tokyo)*, **126**, 632-638.

Nosworthy, N.J., Peterkofsky, A., Konig, S., Seok, Y.J., Szczepanowski, R.H. and Ginsburg, A. (1998) Phosphorylation destabilizes the amino-terminal domain of enzyme I of the Escherichia coli phosphoenolpyruvate:sugar phosphotransferase system. *Biochemistry*, **37**, 6718-6726.

Nunomura, A., Perry, G., Aliev, G., Hirai, K., Takeda, A., Balraj, E.K., Jones, P.K., Ghanbari, H., Wataya, T., Shimohama, S., Chiba, S., Atwood, C.S., Petersen, R.B. and Smith, M.A. (2001) Oxidative damage is the earliest event in Alzheimer disease. *J Neuropathol Exp Neurol*, **60**, 759-767.

O'Donnell, A.L. and Spaulding, S.W. (1997) Hyperthyroidism: systemic effects and differential diagnosis. In: Falk S, ed. Thyroid disease: endocrinology, surgery, nuclear medicine, and radiotherap. *2nd ed. Philadelphia: Lippincott-Raven*, 241 -251.

Oddo, S., Billings, L., Kesslak, J.P., Cribbs, D.H. and LaFerla, F.M. (2004) Abeta immunotherapy leads to clearance of early, but not late, hyperphosphorylated tau aggregates via the proteasome. *Neuron*, **43**, 321-332.

Oddo, S., Caccamo, A., Shepherd, J.D., Murphy, M.P., Golde, T.E., Kayed, R., Metherate, R., Mattson, M.P., Akbari, Y. and LaFerla, F.M. (2003) Triple-transgenic model of Alzheimer's disease with plaques and tangles. Intracellular abeta and synaptic dysfunction. *Neuron*, **39**, 409-421.

Odetti, P., Garibaldi, S., Norese, R., Angelini, G., Marinelli, L., Valentini, S., Menini, S., Traverso, N., Zaccheo, D., Siedlak, S., Perry, G., Smith, M.A. and Tabaton, M. (2000) Lipoperoxidation is selectively involved in progressive supranuclear palsy. *J Neuropathol Exp Neurol*, **59**, 393-397.

Ogris, E., Gibson, D.M. and Pallas, D.C. (1997) Protein phosphatase 2A subunit assembly: the catalytic subunit carboxy terminus is important for binding cellular B subunit but not polyomavirus middle tumor antigen. *Oncogene*, **15**, 911-917.

Ogris, E., Mudrak, I., Mak, E., Gibson, D. and Pallas, D.C. (1999) Catalytically inactive protein phosphatase 2A can bind to polyomavirus middle tumor antigen and support complex formation with pp60(c-src). *J Virol*, **73**, 7390-7398.

Orgad, S., Brewis, N.D., Alphey, L., Axton, J.M., Dudai, Y. and Cohen, P.T. (1990) The structure of protein phosphatase 2A is as highly conserved as that of protein phosphatase 1. *FEBS Lett*, **275**, 44-48.

Payne, A.P. (1994) The harderian gland: a tercentennial review. *J Anat*, **185 (Pt 1)**, 1-49.

Perez-Callejon, E., Casamayor, A., Pujol, G., Camps, M., Ferrer, A. and Arino, J. (1998) Molecular cloning and characterization of two phosphatase 2A catalytic subunit genes from Arabidopsis thaliana. *Gene*, **209**, 105-112.

Perez, M., Cuadros, R., Smith, M.A., Perry, G. and Avila, J. (2000) Phosphorylated, but not native, tau protein assembles following reaction with the lipid peroxidation product, 4-hydroxy-2-nonenal. *FEBS Lett*, **486**, 270-274.

Perez, M., Hernandez, F., Gomez-Ramos, A., Smith, M., Perry, G. and Avila, J. (2002) Formation of aberrant phosphotau fibrillar polymers in neural cultured cells. *Eur J Biochem*, **269**, 1484-1489.

Perez, M., Ribe, E., Rubio, A., Lim, F., Moran, M.A., Ramos, P.G., Ferrer, I., Isla, M.T. and Avila, J. (2005) Characterization of a double (amyloid precursor protein-tau) transgenic: Tau phosphorylation and aggregation. *Neuroscience*, **130**, 339-347.

Petersen, B.O., Lukas, J., Sorensen, C.S., Bartek, J. and Helin, K. (1999) Phosphorylation of mammalian CDC6 by cyclin A/CDK2 regulates its subcellular localization. *Embo J*, **18**, 396-410.

Pike, C.J., Burdick, D., Walencewicz, A.J., Glabe, C.G. and Cotman, C.W. (1993) Neurodegeneration induced by beta-amyloid peptides in vitro: the role of peptide assembly state. *J Neurosci*, **13**, 1676-1687.

Pike, C.J., Walencewicz, A.J., Glabe, C.G. and Cotman, C.W. (1991) In vitro aging of beta-amyloid protein causes peptide aggregation and neurotoxicity. *Brain Res*, **563**, 311-314.

Planel, E., Yasutake, K., Fujita, S.C. and Ishiguro, K. (2001) Inhibition of protein phosphatase 2A overrides tau protein kinase I/glycogen synthase kinase 3 beta and cyclin-dependent kinase 5 inhibition and results in tau hyperphosphorylation in the hippocampus of starved mouse. *J Biol Chem*, **276**, 34298-34306.

Poirier, J. (2003) Apolipoprotein E and cholesterol metabolism in the pathogenesis and treatment of Alzheimer's disease. *Trends Mol Med*, **9**, 94-101.

Pratico, D. (2002) Alzheimer's disease and oxygen radicals: new insights. *Biochem Pharmacol*, **63**, 563-567.

Price, D.L. and Sisodia, S.S. (1998) Mutant genes in familial Alzheimer's disease and transgenic models. *Annu Rev Neurosci*, **21**, 479-505.

Probst, A., Gotz, J., Wiederhold, K.H., Tolnay, M., Mistl, C., Jaton, A.L., Hong, M., Ishihara, T., Lee, V.M., Trojanowski, J.Q., Jakes, R., Crowther, R.A., Spillantini, M.G., Burki, K. and Goedert, M. (2000) Axonopathy and amyotrophy in mice transgenic for human four-repeat tau protein. *Acta Neuropathol (Berl)*, **99**, 469-481.

Radany, E.H., Hong, K., Kesharvarzi, S., Lander, E.S. and Bishop, J.M. (1997) Mouse mammary tumor virus/v-Ha-ras transgene-induced mammary tumors exhibit strain-specific allelic loss on mouse chromosome 4. *Proc Natl Acad Sci U S A*, **94**, 8664-8669.

Reed, L. and Pangaro, L.N. (1995) Physiology of the thyroid gland I: synthesis and release, iodine metabolism, and binding and transport. In: Becker KL, ed. Principles and practice of endocrinology and metabolism. *2nd ed. Philadelphia: JB Lippincott*, 285 -291.

Repa, J.C., Muller, J., Apergis, J., Desrochers, T.M., Zhou, Y. and LeDoux, J.E. (2001) Two different lateral amygdala cell populations contribute to the initiation and storage of memory. *Nat Neurosci*, **4**, 724-731.

Robakis, N.K., Wisniewski, H.M., Jenkins, E.C., Devine-Gage, E.A., Houck, G.E., Yao, X.L., Ramakrishna, N., Wolfe, G., Silverman, W.P. and Brown, W.T. (1987) Chromosome 21q21 sublocalisation of gene encoding beta-amyloid peptide in cerebral vessels and neuritic (senile) plaques of people with Alzheimer disease and Down syndrome. *Lancet*, **1**, 384-385.

Rocchi, A., Pellegrini, S., Siciliano, G. and Murri, L. (2003) Causative and susceptibility genes for Alzheimer's disease: a review. *Brain Res Bull*, **61**, 1-24.

Roder, H.M. and Ingram, V.M. (1991) Two novel kinases phosphorylate tau and the KSP site of heavy neurofilament subunits in high stoichiometric ratios. *J Neurosci*, **11**, 3325-3343.

Rogers, M.V., Buensuceso, C., Montague, F. and Mahadevan, L. (1994) Vanadate stimulates differentiation and neurite outgrowth in rat pheochromocytoma PC12 cells and neurite extension in human neuroblastoma SH-SY5Y cells. *Neuroscience*, **60**, 479-494.

Ross, R.A., Spengler, B.A. and Biedler, J.L. (1983) Coordinate morphological and biochemical interconversion of human neuroblastoma cells. *J Natl Cancer Inst*, **71**, 741-747.

Rossor, M.N., Fox, N.C., Freeborough, P.A. and Harvey, R.J. (1996) Clinical features of sporadic and familial Alzheimer's disease. *Neurodegeneration*, **5**, 393-397.

Rouleau, G.A., Clark, A.W., Rooke, K., Pramatarova, A., Krizus, A., Suchowersky, O., Julien, J.P. and Figlewicz, D. (1996) SOD1 mutation is associated with accumulation of neurofilaments in amyotrophic lateral sclerosis. *Ann Neurol*, **39**, 128-131.

Roush, W. (1995) Protein studies try to puzzle out Alzheimer's tangles. *Science*, **267**, 793-794.

Rubin, G.M., Yandell, M.D., Wortman, J.R., Gabor Miklos, G.L., Nelson, C.R., Hariharan, I.K., Fortini, M.E., Li, P.W., Apweiler, R., Fleischmann, W., Cherry, J.M., Henikoff, S., Skupski, M.P., Misra, S., Ashburner, M., Birney, E., Boguski, M.S., Brody, T., Brokstein, P., Celniker, S.E., Chervitz, S.A., Coates, D., Cravchik, A., Gabrielian, A., Galle, R.F., Gelbart, W.M., George, R.A., Goldstein, L.S., Gong, F., Guan, P., Harris, N.L., Hay, B.A., Hoskins, R.A., Li, J., Li, Z., Hynes, R.O., Jones, S.J., Kuehl, P.M., Lemaitre, B., Littleton, J.T., Morrison, D.K., Mungall, C., O'Farrell, P.H., Pickeral, O.K., Shue, C., Vosshall, L.B., Zhang, J., Zhao, Q., Zheng, X.H. and Lewis, S. (2000) Comparative genomics of the eukaryotes. *Science*, **287**, 2204-2215.

Ruediger, R., Pham, H.T. and Walter, G. (2001) Disruption of protein phosphatase 2A subunit interaction in human cancers with mutations in the A alpha subunit gene. *Oncogene*, **20**, 10-15.

Sacher, M.G., Athlan, E.S. and Mushynski, W.E. (1992) Okadaic acid induces the rapid and reversible disruption of the neurofilament network in rat dorsal root ganglion neurons. *Biochem Biophys Res Commun*, **186**, 524-530.

Sacher, M.G., Athlan, E.S. and Mushynski, W.E. (1994) Increased phosphorylation of the amino-terminal domain of the low molecular weight neurofilament subunit in okadaic acid-treated neurons. *J Biol Chem*, **269**, 18480-18484.

Saito, T., Ishiguro, K., Uchida, T., Miyamoto, E., Kishimoto, T. and Hisanaga, S. (1995) In situ dephosphorylation of tau by protein phosphatase 2A and 2B in fetal rat primary cultured neurons. *FEBS Lett*, **376**, 238-242.

Saito, T., Shima, H., Osawa, Y., Nagao, M., Hemmings, B.A., Kishimoto, T. and Hisanaga, S. (1995) Neurofilament-associated protein phosphatase 2A: its possible role in preserving neurofilaments in filamentous states. *Biochemistry*, **34**, 7376-7384.

Salehi, A., Heyn, S., Gonatas, N.K. and Swaab, D.F. (1995) Decreased protein synthetic activity of the hypothalamic tuberomamillary nucleus in Alzheimer's disease as suggested by smaller Golgi apparatus. *Neurosci Lett*, **193**, 29-32.

Salehi, A., Lucassen, P.J., Pool, C.W., Gonatas, N.K., Ravid, R. and Swaab, D.F. (1994) Decreased neuronal activity in the nucleus basalis of Meynert in Alzheimer's disease as suggested by the size of the Golgi apparatus. *Neuroscience*, **59**, 871-880.
Salehi, A., Verhaagen, J., Dijkhuizen, P.A. and Swaab, D.F. (1996) Co-localization of high-affinity neurotrophin receptors in nucleus basalis of Meynert neurons and their differential reduction in Alzheimer's disease. *Neuroscience*, **75**, 373-387.
Sandberg, R., Yasuda, R., Pankratz, D.G., Carter, T.A., Del Rio, J.A., Wodicka, L., Mayford, M., Lockhart, D.J. and Barlow, C. (2000) Regional and strain-specific gene expression mapping in the adult mouse brain. *Proc Natl Acad Sci U S A*, **97**, 11038-11043.
Sanger, F., Nicklen, S. and Coulson, A.R. (1977) DNA sequencing with chain-terminating inhibitors. *Proc Natl Acad Sci U S A*, **74**, 5463-5467.
Sayre, L.M., Zelasko, D.A., Harris, P.L., Perry, G., Salomon, R.G. and Smith, M.A. (1997) 4-Hydroxynonenal-derived advanced lipid peroxidation end products are increased in Alzheimer's disease. *J Neurochem*, **68**, 2092-2097.
Schaffhausen, B. (1995) SH2 domain structure and function. *Biochim Biophys Acta*, **1242**, 61-75.
Schmidt, K., Kins, S., Schild, A., Nitsch, R.M., Hemmings, B.A. and Gotz, J. (2002) Diversity, developmental regulation and distribution of murine PR55/B subunits of protein phosphatase 2A. *Eur J Neurosci*, **16**, 2039-2048.
Schubert, D., Jin, L.W., Saitoh, T. and Cole, G. (1989) The regulation of amyloid beta protein precursor secretion and its modulatory role in cell adhesion. *Neuron*, **3**, 689-694.
Seeliger, M.W., Grimm, C., Stahlberg, F., Friedburg, C., Jaissle, G., Zrenner, E., Guo, H., Reme, C.E., Humphries, P., Hofmann, F., Biel, M., Fariss, R.N., Redmond, T.M. and Wenzel, A. (2001) New views on RPE65 deficiency: the rod system is the source of vision in a mouse model of Leber congenital amaurosis. *Nat Genet*, **29**, 70-74.
Sergeant, N., Wattez, A. and Delacourte, A. (1999) Neurofibrillary degeneration in progressive supranuclear palsy and corticobasal degeneration: tau pathologies with exclusively "exon 10" isoforms. *J Neurochem*, **72**, 1243-1249.
Sergeant, N., Wattez, A. and Delacourte, A. (1999) Neurofibrillary degeneration in progressive supranuclear palsy and corticobasal degeneration: tau pathologies with exclusively exon 10 isoforms. *J Neurochem*, **72**, 1243-1249.
Serres, M., Filhol, O., Lickert, H., Grangeasse, C., Chambaz, E.M., Stappert, J., Vincent, C. and Schmitt, D. (2000) The disruption of adherens junctions is associated with a decrease of E-cadherin phosphorylation by protein kinase CK2. *Exp Cell Res*, **257**, 255-264.
Serres, M., Grangeasse, C., Haftek, M., Durocher, Y., Duclos, B. and Schmitt, D. (1997) Hyperphosphorylation of beta-catenin on serine-threonine residues and loss of cell-cell contacts induced by calyculin A and okadaic acid in human epidermal cells. *Exp Cell Res*, **231**, 163-172.
Seubert, P., Mawal-Dewan, M., Barbour, R., Jakes, R., Goedert, M., Johnson, G.V., Litersky, J.M., Schenk, D., Lieberburg, I., Trojanowski, J.Q. and et al. (1995) Detection of phosphorylated Ser262 in fetal tau, adult tau, and paired helical filament tau. *J Biol Chem*, **270**, 18917-18922.
Seubert, P., Vigo-Pelfrey, C., Esch, F., Lee, M., Dovey, H., Davis, D., Sinha, S., Schlossmacher, M., Whaley, J. and Swindlehurst, C. (1992) Isolation and quantification of soluble Alzheimer's beta-peptide from biological fluids. *Nature*, **359**, 325-327.
Shanley, T.P., Vasi, N., Denenberg, A. and Wong, H.R. (2001) The serine/threonine phosphatase, PP2A: endogenous regulator of inflammatory cell signaling. *J Immunol*, **166**, 966-972.
Shibasaki, F., Price, E.R., Milan, D. and McKeon, F. (1996) Role of kinases and the phosphatase calcineurin in the nuclear shuttling of transcription factor NF-AT4. *Nature*, **382**, 370-373.
Silverstein, A.M., Barrow, C.A., Davis, A.J. and Mumby, M.C. (2002) Actions of PP2A on the MAP kinase pathway and apoptosis are mediated by distinct regulatory subunits. *Proc Natl Acad Sci U S A*, **99**, 4221-4226.
Sinn, E., Muller, W., Pattengale, P., Tepler, I., Wallace, R. and Leder, P. (1987) Coexpression of MMTV/v-Ha-ras and MMTV/c-myc genes in transgenic mice: synergistic action of oncogenes in vivo. *Cell*, **49**, 465-475.
Smith, M.A., Perry, G., Richey, P.L., Sayre, L.M., Anderson, V.E., Beal, M.F. and Kowall, N. (1996) Oxidative damage in Alzheimer's. *Nature*, **382**, 120-121.
Smith, T.F., Gaitatzes, C., Saxena, K. and Neer, E.J. (1999) The WD repeat: a common architecture for diverse functions. *Trends Biochem Sci*, **24**, 181-185.
Sneddon, A.A., Cohen, P.T. and Stark, M.J. (1990) Saccharomyces cerevisiae protein phosphatase 2A performs an essential cellular function and is encoded by two genes. *Embo J*, **9**, 4339-4346.
Sobrido, M.J., Miller, B.L., Havlioglu, N., Zhukareva, V., Jiang, Z., Nasreddine, Z.S., Lee, V.M., Chow, T.W., Wilhelmsen, K.C., Cummings, J.L., Wu, J.Y. and Geschwind, D.H. (2003) Novel tau polymorphisms, tau haplotypes, and splicing in familial and sporadic frontotemporal dementia. *Arch Neurol*, **60**, 698-702.
Song, H., Hanlon, N., Brown, N.R., Noble, M.E., Johnson, L.N. and Barford, D. (2001) Phosphoprotein-protein interactions revealed by the crystal structure of kinase-associated phosphatase in complex with phosphoCDK2. *Mol Cell*, **7**, 615-626.
Sonoda, Y., Kasahara, T., Yamaguchi, Y., Kuno, K., Matsushima, K. and Mukaida, N. (1997) Stimulation of interleukin-8 production by okadaic acid and vanadate in a human promyelocyte cell line, an HL-60 subline. Possible role of mitogen-activated protein kinase on the okadaic acid-induced NF-kappaB activation. *J Biol Chem*, **272**, 15366-15372.
Sontag, E. (2001) Protein phosphatase 2A: the Trojan Horse of cellular signaling. *Cell Signal*, **13**, 7-16.

Sontag, E., Luangpirom, A., Hladik, C., Mudrak, I., Ogris, E., Speciale, S. and White, C.L., 3rd. (2004) Altered expression levels of the protein phosphatase 2A ABalphaC enzyme are associated with Alzheimer disease pathology. *J Neuropathol Exp Neurol*, **63**, 287-301.

Sontag, E., Nunbhakdi-Craig, V., Lee, G., Bloom, G.S. and Mumby, M.C. (1996) Regulation of the phosphorylation state and microtubule-binding activity of Tau by protein phosphatase 2A. *Neuron*, **17**, 1201-1207.

Sontag, E., Nunbhakdi-Craig, V., Lee, G., Brandt, R., Kamibayashi, C., Kuret, J., White, C.L., 3rd, Mumby, M.C. and Bloom, G.S. (1999) Molecular interactions among protein phosphatase 2A, tau, and microtubules. Implications for the regulation of tau phosphorylation and the development of tauopathies. *J Biol Chem*, **274**, 25490-25498.

Spittaels, K., Van Den Haute, C., Van Dorpe, J., Geerts, H., Mercken, M., Bruynseels, K., Lasrado, R., Vandezande, K., Laenen, I., Boon, T., Van Lint, J., Vandenheede, J., Moechars, D., Loos, R. and Van Leuven, F. (2000) Glycogen synthase kinase-3beta phosphorylates protein tau and rescues the axonopathy in the central nervous system of human four-repeat tau transgenic mice. *J Biol Chem*, **275**, 41340-41349.

Squire, L.R. and Zola, S.M. (1998) Episodic memory, semantic memory, and amnesia. *Hippocampus*, **8**, 205-211.

Steegenga, W.T., van der Eb, A.J. and Jochemsen, A.G. (1996) How phosphorylation regulates the activity of p53. *J Mol Biol*, **263**, 103-113.

Steiner, H., Capell, A., Leimer, U. and Haass, C. (1999) Genes and mechanisms involved in beta-amyloid generation and Alzheimer's disease. *Eur Arch Psychiatry Clin Neurosci*, **249**, 266-270.

Stone, S.R., Hofsteenge, J. and Hemmings, B.A. (1987) Molecular cloning of cDNAs encoding two isoforms of the catalytic subunit of protein phosphatase 2A. *Biochemistry*, **26**, 7215-7220.

Strack, S. (2002) Overexpression of the protein phosphatase 2A regulatory subunit Bgamma promotes neuronal differentiation by activating the MAP kinase (MAPK) cascade. *J Biol Chem*, **277**, 41525-41532.

Strack, S., Chang, D., Zaucha, J.A., Colbran, R.J. and Wadzinski, B.E. (1999) Cloning and characterization of B delta, a novel regulatory subunit of protein phosphatase 2A. *FEBS Lett*, **460**, 462-466.

Strack, S., Westphal, R.S., Colbran, R.J., Ebner, F.F. and Wadzinski, B.E. (1997) Protein serine/threonine phosphatase 1 and 2A associate with and dephosphorylate neurofilaments. *Brain Res Mol Brain Res*, **49**, 15-28.

Strack, S., Zaucha, J.A., Ebner, F.F., Colbran, R.J. and Wadzinski, B.E. (1998) Brain protein phosphatase 2A: developmental regulation and distinct cellular and subcellular localization by B subunits. *J Comp Neurol*, **392**, 515-527.

Streetman, D.D. and Khanderia, U. (2003) Diagnosis and treatment of Graves disease. *Ann Pharmacother*, **37**, 1100-1109.

Sun, L., Liu, S.Y., Zhou, X.W., Wang, X.C., Liu, R., Wang, Q. and Wang, J.Z. (2003) Inhibition of protein phosphatase 2A- and protein phosphatase 1-induced tau hyperphosphorylation and impairment of spatial memory retention in rats. *Neuroscience*, **118**, 1175-1182.

Sutherland, E.W., Jr. and Wosilait, W.D. (1955) Inactivation and activation of liver phosphorylase. *Nature*, **175**, 169-170.

Suzuki, N., Cheung, T.T., Cai, X.D., Odaka, A., Otvos, L., Jr., Eckman, C., Golde, T.E. and Younkin, S.G. (1994) An increased percentage of long amyloid beta protein secreted by familial amyloid beta protein precursor (beta APP717) mutants. *Science*, **264**, 1336-1340.

Swaab, D.F., Lucassen, P.J., Salehi, A., Scherder, E.J., van Someren, E.J. and Verwer, R.W. (1998) Reduced neuronal activity and reactivation in Alzheimer's disease. *Prog Brain Res*, **117**, 343-377.

Szilak, L., Moitra, J., Krylov, D. and Vinson, C. (1997) Phosphorylation destabilizes alpha-helices. *Nat Struct Biol*, **4**, 112-114.

Taborsky, G. (1991) On the interaction of phosvitins with ferric ion: solubility of the Fe(III)-phosphoprotein complex under acidic conditions is a function of the iron/phosphate ratio and the degree of phosvitin phosphorylation. *J Inorg Biochem*, **44**, 65-77.

Takeda, A., Smith, M.A., Avila, J., Nunomura, A., Siedlak, S.L., Zhu, X., Perry, G. and Sayre, L.M. (2000) In Alzheimer's disease, heme oxygenase is coincident with Alz50, an epitope of tau induced by 4-hydroxy-2-nonenal modification. *J Neurochem*, **75**, 1234-1241.

Tanaka, T., Zhong, J., Iqbal, K., Trenkner, E. and Grundke-Iqbal, I. (1998) The regulation of phosphorylation of tau in SY5Y neuroblastoma cells: the role of protein phosphatases. *FEBS Lett*, **426**, 248-254.

Tanemura, K., Akagi, T., Murayama, M., Kikuchi, N., Murayama, O., Hashikawa, T., Yoshiike, Y., Park, J.M., Matsuda, K., Nakao, S., Sun, X., Sato, S., Yamaguchi, H. and Takashima, A. (2001) Formation of filamentous tau aggregations in transgenic mice expressing V337M human tau. *Neurobiol Dis*, **8**, 1036-1045.

Tapia, R., Pena, F. and Arias, C. (1999) Neurotoxic and synaptic effects of okadaic acid, an inhibitor of protein phosphatases. *Neurochem Res*, **24**, 1423-1430.

Tatebayashi, Y., Miyasaka, T., Chui, D.H., Akagi, T., Mishima, K., Iwasaki, K., Fujiwara, M., Tanemura, K., Murayama, M., Ishiguro, K., Planel, E., Sato, S., Hashikawa, T. and Takashima, A. (2002) Tau filament formation and associative memory deficit in aged mice expressing mutant (R406W) human tau. *Proc Natl Acad Sci U S A*, **99**, 13896-13901.

Tehrani, M.A., Mumby, M.C. and Kamibayashi, C. (1996) Identification of a novel protein phosphatase 2A regulatory subunit highly expressed in muscle. *J Biol Chem*, **271**, 5164-5170.

Terry, R.D. (1996) The pathogenesis of Alzheimer disease: an alternative to the amyloid hypothesis [see comments]. *J Neuropathol Exp Neurol*, **55**, 1023-1025.
Thiels, E., Kanterewicz, B.I., Knapp, L.T., Barrionuevo, G. and Klann, E. (2000) Protein Phosphatase-Mediated Regulation of Protein Kinase C during Long-Term Depression in the Adult Hippocampus In Vivo. *J Neurosci*, **20**, 7199-7207.
Tolstykh, T., Lee, J., Vafai, S. and Stock, J.B. (2000) Carboxyl methylation regulates phosphoprotein phosphatase 2A by controlling the association of regulatory B subunits. *Embo J*, **19**, 5682-5691.
Traverse, S., Gomez, N., Paterson, H., Marshall, C. and Cohen, P. (1992) Sustained activation of the mitogen-activated protein (MAP) kinase cascade may be required for differentiation of PC12 cells. Comparison of the effects of nerve growth factor and epidermal growth factor. *Biochem J*, **288 (Pt 2)**, 351-355.
Trojanowski, J.Q. and Lee, V.M. (1995) Phosphorylation of paired helical filament tau in Alzheimer's disease neurofibrillary lesions: focusing on phosphatases. *Faseb J*, **9**, 1570-1576.
Turowski, P., Favre, B., Campbell, K.S., Lamb, N.J. and Hemmings, B.A. (1997) Modulation of the enzymatic properties of protein phosphatase 2A catalytic subunit by the recombinant 65-kDa regulatory subunit PR65alpha. *Eur J Biochem*, **248**, 200-208.
Turowski, P., Fernandez, A., Favre, B., Lamb, N.J. and Hemmings, B.A. (1995) Differential methylation and altered conformation of cytoplasmic and nuclear forms of protein phosphatase 2A during cell cycle progression. *J Cell Biol*, **129**, 397-410.
Turowski, P., Myles, T., Hemmings, B.A., Fernandez, A. and Lamb, N.J. (1999) Vimentin dephosphorylation by protein phosphatase 2A is modulated by the targeting subunit B55. *Mol Biol Cell*, **10**, 1997-2015.
Tuschl, T., Zamore, P.D., Lehmann, R., Bartel, D.P. and Sharp, P.A. (1999) Targeted mRNA degradation by double-stranded RNA in vitro. *Genes Dev*, **13**, 3191-3197.
Uchida, K., Kanematsu, M., Sakai, K., Matsuda, T., Hattori, N., Mizuno, Y., Suzuki, D., Miyata, T., Noguchi, N., Niki, E. and Osawa, T. (1998) Protein-bound acrolein: potential markers for oxidative stress. *Proc Natl Acad Sci U S A*, **95**, 4882-4887.
Vafai, S.B. and Stock, J.B. (2002) Protein phosphatase 2A methylation: a link between elevated plasma homocysteine and Alzheimer's Disease. *FEBS Lett*, **518**, 1-4.
Van Hoof, C., Ingels, F., Cayla, X., Stevens, I., Merlevede, W. and Goris, J. (1995) Molecular cloning and developmental regulation of expression of two isoforms of the catalytic subunit of protein phosphatase 2A from Xenopus laevis. *Biochem Biophys Res Commun*, **215**, 666-673.
Van Hoof, C., Janssens, V., De Baere, I., de Winde, J.H., Winderickx, J., Dumortier, F., Thevelein, J.M., Merlevede, W. and Goris, J. (2000) The Saccharomyces cerevisiae homologue YPA1 of the mammalian phosphotyrosyl phosphatase activator of protein phosphatase 2A controls progression through the G1 phase of the yeast cell cycle. *J Mol Biol*, **302**, 103-120.
Veeranna, Shetty, K.T., Link, W.T., Jaffe, H., Wang, J. and Pant, H.C. (1995) Neuronal cyclin-dependent kinase-5 phosphorylation sites in neurofilament protein (NF-H) are dephosphorylated by protein phosphatase 2A. *J Neurochem*, **64**, 2681-2690.
Verdier, Y. and Penke, B. (2004) Binding Sites of Amyloid beta-Peptide in Cell Plasma Membrane and Implications for Alzheimer's Disease. *Curr Protein Pept Sci*, **5**, 19-31.
Vickers, J.C., Delacourte, A. and Morrison, J.H. (1992) Progressive transformation of the cytoskeleton associated with normal aging and Alzheimer's disease. *Brain Res*, **594**, 273-278.
Virshup, D.M. (2000) Protein phosphatase 2A: a panoply of enzymes. *Curr Opin Cell Biol*, **12**, 180-185.
Vogelsberg-Ragaglia, V., Schuck, T., Trojanowski, J.Q. and Lee, V.M. (2001) PP2A mRNA expression is quantitatively decreased in Alzheimer's disease hippocampus. *Exp Neurol*, **168**, 402-412.
Voorhoeve, P.M., Hijmans, E.M. and Bernards, R. (1999) Functional interaction between a novel protein phosphatase 2A regulatory subunit, PR59, and the retinoblastoma-related p107 protein. *Oncogene*, **18**, 515-524.
Wang, J.Z., Gong, C.X., Zaidi, T., Grundke-Iqbal, I. and Iqbal, K. (1995) Dephosphorylation of Alzheimer paired helical filaments by protein phosphatase-2A and -2B. *J Biol Chem*, **270**, 4854-4860.
Wang, J.Z., Wu, Q., Smith, A., Grundke-Iqbal, I. and Iqbal, K. (1998) Tau is phosphorylated by GSK-3 at several sites found in Alzheimer disease and its biological activity markedly inhibited only after it is prephosphorylated by A-kinase. *FEBS Lett*, **436**, 28-34.
Weetman, A.P. (1992) Thyroid-associated ophthalmopathy. *Autoimmunity*, **12**, 215-222.
Weetman, A.P. (2003) Grave's disease 1835-2002. *Horm Res*, **59 Suppl 1**, 114-118.
Wera, S., Fernandez, A., Lamb, N.J., Turowski, P., Hemmings-Mieszczak, M., Mayer-Jaekel, R.E. and Hemmings, B.A. (1995) Deregulation of translational control of the 65-kDa regulatory subunit (PR65 alpha) of protein phosphatase 2A leads to multinucleated cells. *J Biol Chem*, **270**, 21374-21381.
Wera, S. and Hemmings, B.A. (1995) Serine/threonine protein phosphatases. *Biochem J*, **311 (Pt 1)**, 17-29.
Werneck, A.L., Gurgel, L.C., de Mello, L.M. and de Albuquerque, G.Q. (2003) Sudden sensorineural hearing loss: a case report supporting the immunologic theory. *Arq Neuropsiquiatr*, **61**, 1018-1022.
Wetterberg, L., Yuwiler, A., Geller, E. and Schapiro, S. (1970) Harderian gland: development and influence of early hormonal treatment on porphyrin content. *Science*, **168**, 996-998.
White, V., Sinn, E. and Albert, D.M. (1990) Harderian gland pathology in transgenic mice carrying the MMTV/v-Ha-ras gene. *Invest Ophthalmol Vis Sci*, **31**, 577-581.
Wolfer, D.P., Madani, R., Valenti, P. and Lipp, H.P. (2001) Extended analysis of path data from mutant mice using the public domain software Wintrack. *Physiol Behav*, **73**, 745-753.

Wong, R., Vasilyev, V.V., Ting, Y.T., Kutler, D.I., Willingham, M.C., Weintraub, B.D. and Cheng, S. (1997) Transgenic mice bearing a human mutant thyroid hormone beta 1 receptor manifest thyroid function anomalies, weight reduction, and hyperactivity. *Mol Med*, **3**, 303-314.

Wu, J., Tolstykh, T., Lee, J., Boyd, K., Stock, J.B. and Broach, J.R. (2000) Carboxyl methylation of the phosphoprotein phosphatase 2A catalytic subunit promotes its functional association with regulatory subunits in vivo. Embo J, **19**, 5672-5681.

Wu, Y.Y. and Bradshaw, R.A. (1993) Effect of nerve growth factor and fibroblast growth factor on PC12 cells: inhibition by orthovanadate. *J Cell Biol*, **121**, 409-422.

Xie, L., Helmerhorst, E., Taddei, K., Plewright, B., Van Bronswijk, W. and Martins, R. (2002) Alzheimer's beta-amyloid peptides compete for insulin binding to the insulin receptor. *J Neurosci*, **22**, RC221.

Yaffe, M.B. and Cantley, L.C. (1999) Signal transduction. Grabbing phosphoproteins. *Nature*, **402**, 30-31.

Yaffe, M.B. and Elia, A.E. (2001) Phosphoserine/threonine-binding domains. *Curr Opin Cell Biol*, **13**, 131-138.

Yaffe, M.B., Rittinger, K., Volinia, S., Caron, P.R., Aitken, A., Leffers, H., Gamblin, S.J., Smerdon, S.J. and Cantley, L.C. (1997) The structural basis for 14-3-3:phosphopeptide binding specificity. *Cell*, **91**, 961-971.

Yamamoto, H., Hasegawa, M., Ono, T., Tashima, K., Ihara, Y. and Miyamoto, E. (1995) Dephosphorylation of fetal-tau and paired helical filaments-tau by protein phosphatases 1 and 2A and calcineurin. *J Biochem (Tokyo)*, **118**, 1224-1231.

Yankner, B.A. (1996) New clues to Alzheimer's disease: unraveling the roles of amyloid and tau. *Nat Med*, **2**, 850-852.

Yan, Z., Fedorov, S.A., Mumby, M.C. and Williams, R.S. (2000) PR48, a novel regulatory subunit of protein phosphatase 2A, interacts with Cdc6 and modulates DNA replication in human cells. *Mol Cell Biol*, **20**, 1021-1029.

Yatsunami, J., Fujiki, H., Suganuma, M., Yoshizawa, S., Eriksson, J.E., Olson, M.O. and Goldman, R.D. (1991) Vimentin is hyperphosphorylated in primary human fibroblasts treated with okadaic acid. *Biochem Biophys Res Commun*, **177**, 1165-1170.

Yu, X.X., Du, X., Moreno, C.S., Green, R.E., Ogris, E., Feng, Q., Chou, L., McQuoid, M.J. and Pallas, D.C. (2001) Methylation of the protein phosphatase 2A catalytic subunit is essential for association of Balpha regulatory subunit but not SG2NA, striatin, or polyomavirus middle tumor antigen. *Mol Biol Cell*, **12**, 185-199.

Zamore, P.D., Tuschl, T., Sharp, P.A. and Bartel, D.P. (2000) RNAi: double-stranded RNA directs the ATP-dependent cleavage of mRNA at 21 to 23 nucleotide intervals. *Cell*, **101**, 25-33.

Zhu, X., Rottkamp, C.A., Boux, H., Takeda, A., Perry, G. and Smith, M.A. (2000) Activation of p38 kinase links tau phosphorylation, oxidative stress, and cell cycle-related events in Alzheimer disease. *J Neuropathol Exp Neurol*, **59**, 880-888.

Zirlinger, M., Kreiman, G. and Anderson, D.J. (2001) Amygdala-enriched genes identified by microarray technology are restricted to specific amygdaloid subnuclei. *Proc Natl Acad Sci U S A*, **98**, 5270-5275.

Zolnierowicz, S. (2000) Type 2A protein phosphatase, the complex regulator of numerous signaling pathways. *Biochem Pharmacol*, **60**, 1225-1235.

Zolnierowicz, S., Csortos, C., Bondor, J., Verin, A., Mumby, M.C. and DePaoli-Roach, A.A. (1994) Diversity in the regulatory B-subunits of protein phosphatase 2A: identification of a novel isoform highly expressed in brain. *Biochemistry*, **33**, 11858-11867.

Zolnierowicz, S., Van Hoof, C., Andjelkovic, N., Cron, P., Stevens, I., Merlevede, W., Goris, J. and Hemmings, B.A. (1996) The variable subunit associated with protein phosphatase 2A0 defines a novel multimember family of regulatory subunits. *Biochem J*, **317 (Pt 1)**, 187-194.

Zukerberg, L.R., Patrick, G.N., Nikolic, M., Humbert, S., Wu, C.L., Lanier, L.M., Gertler, F.B., Vidal, M., Van Etten, R.A. and Tsai, L.H. (2000) Cables links Cdk5 and c-Abl and facilitates Cdk5 tyrosine phosphorylation, kinase upregulation, and neurite outgrowth. *Neuron*, **26**, 633-646.